THE UNIVERSITY OF
SYDNEY

THE UNIVERSITY OF SYDNEY

Immune-Mediated Drug Induced Liver Injury

A Multidisciplinary Approach

Samuel Ho

Thesis submitted in fulfilment of the requirements for the degree of
Doctor of Philosophy

Faculty of Pharmacy
The University of Sydney

March 2016

Declaration

This research has been carried out through the Faculty of Pharmacy, University of Sydney, under the supervision of Professor David E. Hibbs.

Appropriate ethical approval had been obtained where required.

This research, to the best of my knowledge, is original and is entirely the product of my own scholarly work. Full acknowledgement has been made where the work of others has been cited or used.

The research presented in this thesis has not been submitted wholly or in part toward the award of another degree at another institution.

_____

Samuel Ho

Acknowledgements

I have been blessed by the kindness and wisdom of my supervisors Dr. Romano A. Fois and Prof. David E. Hibbs. They have granted me much guidance and support throughout the entire research process, modelling to me through their life and work how to be a respected and successful member of the academic community even while balancing family and social commitments. I am particularly struck by their humbleness and the desire to pass on their infectious love for research to future generations of students such as myself.

I am sincerely grateful to A/Prof. Timothy Chen and Prof. Andrew McLachlan for their support through my candidature. I am particularly grateful for their words of encouragement and timely advice to steer me out of troublesome situations.

I would like to thank Prof. Alaina Ammit for her assistance in designing the *in vitro* experimental setup described in this thesis and Nowshin Rumzhum for her help in carrying out the experiments. Thanks also to Dr. Ashley Mansell for his collaboration and advice with Toll-Like Receptor 7 stimulation experiments.

I would also like to thank Australia's Therapeutic Goods Administration for provision of the Adverse Drug Reaction data used in this thesis. I also gratefully acknowledge the financial support provided by the Australian Postgraduate Award scholarship administered through The University of Sydney.

During my candidature I developed many long lasting friendships. I would like to express my appreciation and thanks to those with whom I have shared my research journey with, in particular: Carmen, Woroud, Moawiah, Zechariah, our friends on Level 5 and the other research students at the Faculty of Pharmacy.

Many thanks to my family; my wife, parents and sister for their love and ongoing support.

Finally, all glory and praise be to the God and Father of my Lord Jesus Christ, without whom I would not be who I am today.

Thesis Abstract

This thesis presents an approach to expose relationships between immune-mediated drug induced liver injury (IMDILI) and the three-dimensional structural features of toxic drug molecules and their metabolites. The series of analyses in the following chapters test the hypothesis that drugs (or their metabolites) which produce similar patterns of toxicity interact with targets within common toxicological pathways and that activation of the underlying mechanisms depends on structural similarity among toxic molecules.

Chapter 1 provides an introduction to the vast and multifaceted literature surrounding drug induced liver injuries (DILI). It provides an overview of idiosyncratic DILI, including its classification and risk factors. The key mechanistic theories of DILI and the experimental approaches that have been undertaken in its study are also discussed, exposing the need for a multidisciplinary approach to the study for DILI.

Chapter 2 describes the identification of a probe set of drugs with which to facilitate the study of IMDILI. Cases of IMDILI were identified from spontaneous adverse drug reaction (ADR) reports collected by Australia's Therapeutic Goods Administration (TGA). Multivariate logistic regression was used to quantify the association between the occurrence of IMDILI and exposure to drugs of interest. 18 drugs were found to be significantly associated with IMDILI ($P<0.00015$, Bonferroni-adjusted limit for significance).

By comparing the known and predicted interactions with each of the IMDILI probe drugs and examining the interactions that are common between the drugs, it should be possible to identify potential toxicity targets involved in the pathogenesis of IMDILI. **Chapter 3** describes the use of the network map tools SLAP (1) and STITCH (2) for this purpose. There were substantial differences in the results obtained from each search tool; hence it was difficult to ascertain whether any of the known and predicted proteins associated with the IMDILI probe set of drugs are potential toxicity targets involved in the pathogenesis of IMDILI.

In **Chapter 4** the IMDILI probe set of drugs, along with known and proposed metabolites were used as a training set for the development of a pharmacophore model. A 4-point pharmacophore hypothesis consisting of 2 hydrogen-bond acceptors, 1 hydrogen-bond donor and 1 ring moiety was found to be the best representation of structural similarities

within the training set. In external validation the model was able to differentiate between molecules in the Active and Inactive Test sets with sensitivity and specificity of 75% and 92%, respectively.

Chapter 5 describes a number of analyses in which the pharmacophore hypothesis derived in Chapter 4 is used as the starting point for identifying other drugs implicated in IMDILI as well as potential toxicity targets for IMDILI. Pharmacophore screening results demonstrated similarities between the probe IMDILI set of drugs and Toll-Like Receptor 7 (TLR7) agonists, suggesting TLR7 as a potential toxicity target. Similarly, molecular docking results suggested a potential role for the adaptive immune system protein HLA-B*5701 in the pathogenesis of IMDILI.

Chapter 6 presents an experimental attempt to test whether or not the probe IMDILI set of drugs are able to activate TLR7 *in vitro*. A published experimental procedure (3) was adopted to assay for TLR7 activity. However, despite multiple attempts, the published results were not able to be replicated in the lab. Further work is required to develop a viable experimental setup.

The series of studies that encompass this thesis highlights the potential for multidisciplinary approaches in the study of complex diseases. Importantly, linking information from clinical and chemical databases with knowledge from biological pathway and gene-association datasets can reveal potential mechanisms behind idiosyncratic drug reactions. Multidisciplinary approaches are particularly helpful for rare diseases where little knowledge is available, and may provide key insights into mechanisms of toxicity that cannot be gleaned from a single disciplinary study.

Abbreviations

2D	Two dimensional
3D	Three dimensional
ABC transporter	ATP-binding cassette transporter
ADR	Adverse Drug Reaction
ALP	Alkaline phosphatase
ALT	Alanine transaminase
APCs	Antigen Presenting Cells
ASP	Aspartate aminotransferase
BDDCS	Biopharmaceutical Drug Disposition and Classification System
BSA	Bovine Serum Albumin
CER	Comparisonwise Error Rate
CI	Confidence Interval
CoMFA	Comparative Molecular Field Analysis
CoMMA	Comparative Molecular Moment Analysis
CoMSIA	Comparative Molecular Similarity Indices
COSTART	Coding Symbols for a Thesaurus of Adverse Reaction Terms
DAEN	Database of Adverse Event Notifications
DAMPs	Danger-Associated Molecular Patterns
DILI	Drug induced liver injury
DILIN	Drug Induced Liver Injury Network
DISCO	DIStance Comparison
DTT	Dithiothreitol
EER	Experimentwise Error Rate
FAERS	FDA Adverse Event Reporting System
FDA	Food and Drug Administration
GLDH	Glutamate dehydrogenase
GRIND	Grid-Independent Descriptors
GSH	Glutathione
HGLT	Higher Level Group Term
HLA-B	Human Leukocyte Antigen, class I, B
HLT	Higher Level Term
HMGB1	High mobility group box-1
HQSAR	Hologram Quantitative Structure Activity Relationship
HTML	Hyper Text Markup Language
IC	Information Component
ICH	International Conference on Harmonisation of Technical Requirements for Registration of Pharmaceuticals for Human Use
iDILI	Idiosyncratic Drug Induced Liver Injury
IDMT	Intersite Distance Matching Tolerance
IgE	Immunoglobulin E
IMDILI	Immune-Mediated Drug Induced Liver Injury
IRI	International Resource Identifier
IκB	Inhibitor of kappa B
K18	Keratin-18
KEGG	Kyoto Encyclopaedia of Genes and Genomes

LC-MS	Liquid Chromatography-Mass Spectrometry
LLT	Lower Level Term
LPS	Lipopolysaccharides
MAP kinases	Mitogen-Activated Protein kinases
MCMM/LMOD	Mixed Monte-Carlo Multiple Minimum/Low Mode
MedDRA	Medical Dictionary for Regulatory Authorities
MEER	Maximum Experimentwise Error Rate
miRNA	Micro ribonucleic acid
MyD88	Myeloid differentiation primary response gene 88
NAPQI	N-acetyl-p-benzoquinone imine
NFκB	Nuclear Factor kappa-light-chain-enhancer of activated B cells
NIDDK	US National Institute of Diabetes and Digestive and Kidney Diseases
NMR	Nuclear Magnetic Resonance
OMIM	Online Mendelian Inheritance in Man
OSVM	Oren-Spedicato Variable Metric
OWL	Web Ontology Language
PAMPs	Pathogen-Associated Molecular Patterns
PBS	Phosphate-buffered saline
PDB	Protein Data Bank
p-i hypothesis	Pharmacological interaction hypothesis
pIκB	Phosphorylated Inhibitor of kappa B
PPR	Proportional Reporting Ratio
PRCG	Polak-Ribierer Conjugate Gradient
PRR	Pattern Recognition Receptors
PT	Preferred Term
PVDF	Polyvinylidene fluoride
QSAR	Quantitative Structure Activity Relationship
RCSB	Research Collaboratory for Structural Bioinformatics
RDF	Resource Description Framework
RMSD	Root Mean Square Deviation
ROR	Reporting Odds Ratio
SDF	Simple Data Format
SDS	Sodium Dodecyl Sulfate
SLAP	Semantic Link for Association Prediction
SMARTS	Smiles ARbitary Target Specification
SMILES	Simplified Molecular Input Line Entry System
SOC	System Organ Class
ssRNA	Single stranded ribonucleic acid
STITCH	Search Tool for InTeracting Chemicals
TBST	Tris Buffered Saline with Tween ®
TGA	Therapeutic Goods Administration
TLRs	Toll-Like Receptors
TNFα	Tumour Necrosis Factor alpha
WHIM	Weighted Holistic Invariant Molecular

Peer Reviewed Scientific Publications arising from this thesis

Ho SS, McLachlan AJ, Chen TF, Hibbs DE, Fois RA. Relationships Between Pharmacovigilance, Molecular, Structural, and Pathway Data: Revealing Mechanisms for Immune-Mediated Drug-Induced Liver Injury. CPT Pharmacometrics Syst Pharmacol. 2015 Jul;4(7):426-41. doi: 10.1002/psp4.56. Epub 2015 Jun 18. ISSN: 2163-8306

Wong CK, **Ho SS**, Saini B, Hibbs DE, Fois RA. Standardisation of the FEARS database: a systematic approach to manually recoding drug name variants. Pharmacoepidemiol Drug Saf. 2015;24:731–7. ISSN: 1099-1557

Conference Presentations

Ho, S., McLachlan, A., Chen, T., Hibbs, D., Fois, R. (2014) Idiosyncratic Drug Induced Liver Injury: From population to molecular target. *5th FIP Pharmaceutical Sciences World Congress*, Melbourne Convention and Exhibition Centre, Melbourne Australia.

Ho, S., McLachlan, A., Chen, T., Hibbs, D., Fois, R. (2012) Structure toxicity studies of drugs implicated in immune-mediated idiosyncratic hepatotoxicity. *Joint ASCEPT-APSA*, Sydney Convention and Exhibition Centre, Sydney Australia.

Ho, S., Wong, C., Hibbs, D., Chen, T., McLachlan, A., Chebib, M., Hanrahan, J., Fois, R. (2012) Exploring Structure-Toxicity Relationships in Idiosyncratic Adverse Drug-Reactions. *3rd Lhasa symposium*, Downing College, Cambridge United Kingdom.

Ho, S., McLachlan, A., Chen, T., Hibbs, D., Fois, R. (2015) Immune-Mediated Drug Induced Liver Injury: A Multidisciplinary Approach. *C9&Go8 PhD Forum: Perspectives on Big Data*, Nanjing University, Nanjing China.

Table of Contents

Chapter 1: Drug Induced Liver Injury

Drug induced liver injury (DILI) is an enigmatic problem that has continued to frustrate drug development and researchers despite many years of research. DILI is multifaceted, with consequences ranging far beyond the liver itself. The clinical significance of DILI can range from asymptomatic increases in liver enzyme activities to fulminant liver failure and death (4). Importantly, DILI is a leading cause for both the withdrawal of drugs from marketing, and the failure of drugs in preclinical trials (5). A multitude of risk factors have been identified, but the mechanisms of DILI remain unclear. In recent years there have been renewed efforts to provide new insights into DILI with some success. This chapter provides an overview of DILI and identifies key insights into risk factors and mechanisms of hepatotoxicity.

1.1 Classification

Two broad classifications of DILI have been identified, based on the incidence rate and predictability. Paracetamol (acetaminophen) hepatotoxicity is the best known example of *predictable* DILI. The majority of people who exceed the dose threshold will manifest hepatotoxicity and the mechanism of toxicity is well established (6). Paracetamol is metabolised to an electrophilic metabolite NAPQI (*N*-acetyl-p-benzoquinone imine). The body detoxifies this metabolite by conjugating it with glutathione (GSH). When hepatic GSH is depleted, NAPQI binds to other proteins, leading to mitochondrial oxidant stress and apoptosis of liver cells (6).

Some drugs exhibit what is termed *idiosyncratic* DILI (iDILI), where the mechanism of toxicity is poorly understood and hepatotoxicity occurs within the therapeutic dose range. These drugs are usually well tolerated by the majority of the population, with hepatotoxicity manifesting in an unpredictable minority (7). A prospective study carried out in Iceland reported a crude incidence for iDILI at 19.1 cases per 100,000 inhabitants (0.019%), occurring in 1 in 9480 patients taking diclofenac (0.011%), 1 in 133 patients taking azathioprine (0.75%) and 1 in 2350 (0.043%) of patients exposed to amoxicillin/clavulanic acid, one of the most commonly prescribed antibiotics (8). Other figures have estimated the prevalence of DILI due to amoxicillin/clavulanic acid to be 1 in 7143 patients (0.014%) (9).

A subset of iDILI is observed to occur with features of an immune reaction, with 20-30% of iDILI cases presenting with fever, rash and/or eosinophilia (10). Furthermore, genetic associations with immune system proteins have also been identified for some drugs (*e.g.* flucloxacillin DILI and *HLA-B*5701* (11)). This led to iDILI being further divided into immune-mediated DILI (IMDILI), where hepatotoxicity is associated with the immune response, and metabolic idiosyncrasy, which covers all other iDILI not seen to be immune mediated (12,13) (Figure 1.1).

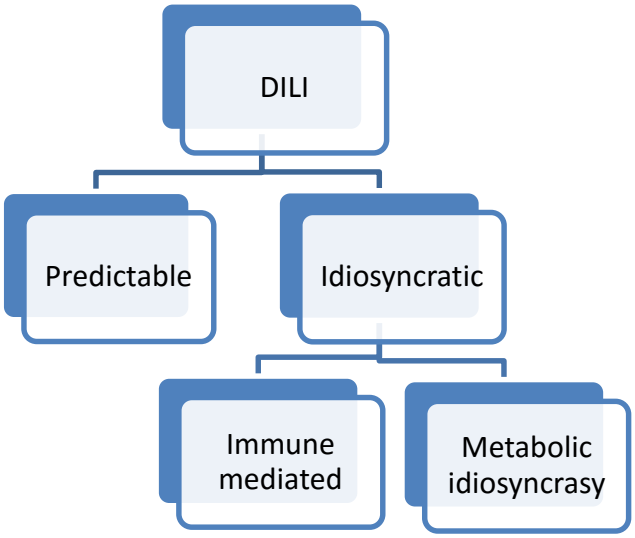

Figure 1.1 Classification of Drug Induced Liver Injury (DILI).

Since the sub classification of iDILI is based on observed characteristics of the clinical presentation rather than any substantial knowledge of the underlying pathophysiology, some have questioned the usefulness of the distinction between IMDILI and metabolic idiosyncrasy (14). Indeed, some presentations of iDILI do not the display signs and symptoms of an immune reaction, but are nevertheless thought to be immune mediated from what is known regarding the mechanism of toxicity. For example, the now withdrawn first-in-class oral anticoagulant ximelagatran has been shown to cause increased alanine transaminase (ALT) activity with no indication of an immune mediated mechanism (15). However, genome-wide association studies revealed a link with proteins of the adaptive immune system thereby suggesting that the ximelagatran related hepatotoxicity is, in fact, immune mediated (16). Other examples include isoniazid DILI which is not typically associated with immunogenic components such as fever or rash, but for which recent evidence for the immune hypothesis has emerged, with the detection of antibodies to

isoniazid and cytochrome P450 enzymes in affected patients (17). However, whether this finding points conclusively towards an immune mediated mechanism is still unclear (18).

1.1.1 Clinical manifestations

IDILI covers all liver injuries that can be attributed to any drug; hence it is understandably an extremely broad end point. Differential diagnosis is extremely difficult since the clinical and laboratory manifestations of iDILI can vary from drug to drug (19) and mimic other forms of liver disease (20), including viral hepatitis and autoimmune liver disease (21). Currently, diagnosis is still dependent on the exclusion of all other possible causes and confounders (22). It is worth noting, however, that the presence of confounders does not exclude iDILI. For example, the interaction of the drug with an existing underlying disease could precipitate DILI which would otherwise not have manifested.

There is a wide spectrum of severity, ranging from asymptomatic elevations in liver transaminase activity to fulminant liver failure and death (4). The timeframe from exposure to clinical signs of DILI is also quite varied, ranging from days (*e.g.* fluconazole DILI (23)) to weeks (*e.g.* rivaroxaban DILI (24)) and months (*e.g.* troglitazone DILI (25)). Typically, delayed onset is a sign of immune involvement, due to the time the immune system needs to coordinate a response (26). However this is not always the case, since some iDILI may involve the interaction of a drug with a precipitating event that transpires sometime during drug therapy.

1.2 Biomarkers

Currently, the main biomarkers of hepatic injury are serum total bilirubin concentration, and the activity of the enzymes alkaline phosphatase (ALP), alanine aminotransferase (ALT) and aspartate aminotransferase (AST). AST is found in a variety of organs, including liver, heart, kidney, muscle and brain, while ALT is more localised to the liver, although still not exclusively. Likewise, ALP can become elevated in hyperthyroidism, malignancy or bone disease (27). Hence, these are not exclusive biomarkers for DILI. Significant increases in enzyme activity can also occur in a number of liver diseases that are unrelated to DILI (*e.g.* due to a hepatic viral infection).

In addition to the lack of specificity, elevations in ALT and AST activity occur after liver injury has already manifested; hence these biomarkers are of limited value in screening for, and

preventing, DILI. To complicate matters further, DILI can also occur without significant elevation in ALT and AST activities (28).

Understandably then, the gold standard status of ALT and AST activity as identifiers of the risk of DILI has been challenged (29). Indeed, a recent study found the common clinical liver function tests to be highly variable in measuring hepatocellular injury of known hepatotoxins when cultured with human hepatocytes (28). There is an urgent need to develop novel, specific biomarkers able to provide an early signal to identify iDILI before acute liver injury occurs. A number of novel biomarkers for DILI are currently under development, including glutamate dehydrogenase (GLDH), High mobility group box-1 (HMGB1) and Keratin-18 (K18) (27). Other possibilities under consideration include cytokines and profiling based on data from *omics* approaches (30).

MicroRNAs (miRNA) are also under development as potential biomarkers for DILI. These small, single stranded RNA (ssRNA) molecules are important in gene regulation (31). Some studies have shown that circulating miRNAs that had emerged from the liver due to cell damage had increased sensitivity to DILI when compared to ALT and AST activity (30). Microarrays have been developed for global miRNA profiling, and preliminary results in the use of miRNA as biomarkers for DILI are promising (32).

Despite these advances many challenges still remain. Since none of these new biomarkers have been extensively validated in the clinical setting they are currently of limited practical value in detecting and preventing DILI (30). Also of concern is the translational ability of biomarkers for DILI from preclinical animal studies into human investigations (27).

1.3 Associations & Risk Factors for iDILI

There are a multitude of factors that have been associated with an increased risk of iDILI (Figure 1.2). These range from sex (33) and level of exercise (34) to metabolic enzymes, including cytochrome P450 and Phase 2 conjugation enzymes (35) and drug transporters (36,37). Examples include erythromycin DILI, which has been associated with genetic variation in ATP-binding cassette transporter (ABC transporter) expression, and sulindac DILI, which is thought to be due to the inhibition of hepatic biliary reuptake (38). Associations have also been drawn with genes encoding immune system proteins, such as Human Leukocyte Antigens (HLA) and interleukins (35).

Unfortunately it is still unclear the extents to which these risk factors interact, if at all, in contributing to the risk of DILI (39). Given the complexity and rarity of iDILI, systems level mapping of the risk factors may be required to deduce the critical elements of the toxicological pathway involved in this form of liver injury (40).

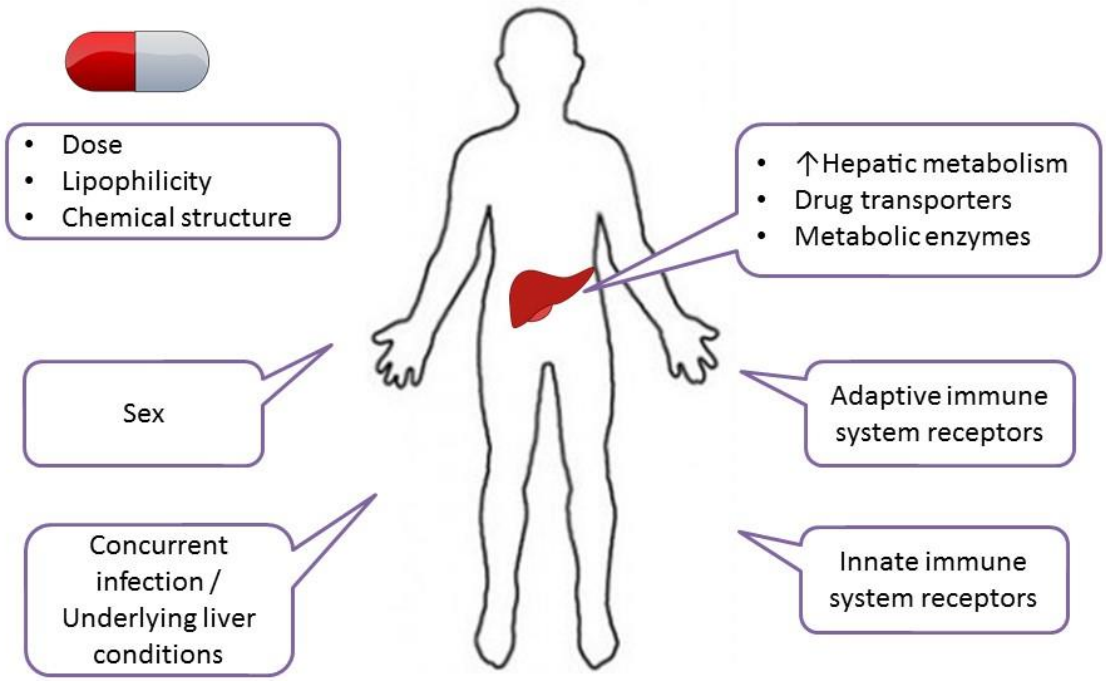

Figure 1.2 Summary of associations and risk factors for idiosyncratic Drug Induced Liver Injury (iDILI). Part of the figure sourced from http://www.clker.com/; http://en.wikipedia.org/.

1.3.1 Characteristics of medications

Traditionally, iDILI has been thought to be independent of the dose of the causative drug, since these reactions lack the dose-toxicity response that is typical of direct hepatotoxins. Moreover, liver injury often only occurs in a small minority of people, with incidence rates thought to be between 2-20 per 100,000 patient-years (41), meaning that the causative drug is usually well tolerated by a majority of the exposed population over the spectrum of approved dose regimens. This also means that iDILI is not often revealed during clinical trial testing in drug development but is identified once the medicine is approved for marketing and taken by a substantially larger and clinically diverse patient cohort.

Nevertheless, the pharmacological basis of drug action confirms there must be some level of dose-response relationship, since intuitively the offending drugs and/or their metabolites must be present in sufficient quantities to initiate the toxicity reaction. In pursuit of this hypothesis, Lambert *et al.* discovered that drugs with daily doses greater than 50 mg are more likely to be associated with DILI, while drugs with daily doses less than 10 mg are less likely to be associated with hepatotoxicity (42). These researchers also noted a relationship between dose and prognosis, where DILI caused by drugs taken at higher daily doses were associated with poorer outcomes, such as death or liver transplantation (42).

Subsequently, it was noted that in addition to high daily dose, hepatic metabolism and lipophilicity of the drug are also associated with an increased risk of DILI (43,44). Increasing lipophilicity is associated with greater permeability into hepatocytes, and is consistent with the hypothesis that increasing hepatic uptake and drug concentrations within the liver leads to an increased risk of DILI.

Vuppalanchi *et al.* further investigated the relationship between drug properties and DILI phenotype, by grouping drugs into their Biopharmaceutical Drug Disposition and Classification System (BDDCS) class (45), which takes into account properties such as solubility and gastrointestinal permeability. This is an improvement upon the associations drawn with daily dose alone, since the daily dose, typically measured in milligrams, does not account for differences in the molecular weights of drugs. These authors found that, while drugs with high solubility and extensive metabolism were associated with selected aspects of the DILI phenotype (*e.g.* longer latency period and higher proportion of hepatocellular injury), the severity and clinical outcomes were unrelated to the drug's BDDCS class. Instead, the outcomes of DILI may more likely be due to host-related factors, such as variations in the immune response and/or the ability to detoxify reactive intermediates, rather than directly attributable to the molecular and biopharmaceutical characteristics of the drug. The authors noted that this finding is contrary to that of Lambert *et al.*, and suggested that this may be due to an inadequate sample size, and/or differences in the DILI registries studied (45). Nevertheless, given the current lack of mechanistic understanding behind DILI it is possible that characteristics of both the drug and host are important, and that toxicity occurs when susceptible individuals are exposed to drugs exhibiting particular molecular and biopharmaceutical properties.

The pharmacokinetic (*e.g.* metabolism) and physicochemical characteristics (*e.g.* lipophilicity, solubility) of drugs are ultimately dependent on the drug's molecular structure, and so it comes as no surprise that links have also been drawn between structural features of drugs and DILI (46). A number of structural alerts have also been developed, designed to allow for the identification of potentially hepatotoxic compounds early in the drug discovery process (47). For example, a recent study by Liu *et al.* identified 12 SMiles ARbitrary Target Specification (SMARTS) notations that were significantly associated with DILI and largely absent from non-hepatotoxic compounds (48). However, if used alone for toxicity screening, structural alerts can result in a high false positive rate, leading to the unnecessary culling of potentially viable compounds for further development (49).

1.3.2 Immune system involvement

There is now a substantial body of evidence to suggest that many DILI are mediated by the immune system. Around 25% of DILI present with hypersensitivity features of fever, rash, eosinophilia and cytopaenia (10). The extent of immune system involvement may also be under reported, since many reactions are mild and resolve spontaneously. Even for cases of mild liver injury, unless transaminase activities are continuously monitored, asymptomatic increases in ALT and AST activity are likely to pass undetected.

While the pattern of liver injury may be different, there is some evidence that the severity and duration of hepatotoxicity is related to the hypersensitivity phenotype (50). This suggests the immune reaction is mediating the hepatotoxicity, rather than acting in response to liver injury caused by other means. However, in some cases (*e.g.* abacavir (51), β-lactam antibiotics and antiepileptic drugs among others (52)), DILI appears in the context of a generalised hypersensitivity syndrome. This confounds attempts to determine whether drug exposure initiated an immune response which subsequently resulted in liver injury or vice versa. Without the mechanistic knowledge of how toxicity pathways are initiated it will be profoundly difficult to develop *in vitro* or indeed any kind of predictive model to screen for potentially hepatotoxic compounds early in drug development, or to identify patients who are at risk.

1.3.2.1 Adaptive immune system

Since some DILI occurs in the context of a generalised hypersensitivity syndrome, in cases where the association is drawn between HLA and drug induced hypersensitivity syndrome rather than explicitly regarding DILI, it may be difficult to judge whether the hepatotoxicity is immune-mediated, and whether the DILI is associated with that particular HLA genotype. For example, the FDA's Livertox database (51) notes that raised liver transaminases can occur in up to 6% of patients exposed to abacavir, and that the DILI usually occurs in the context of a generalised hypersensitivity syndrome. Although it is known that abacavir hypersensitivity is associated with *HLA-B*5701* (53), it is unclear whether this association extends to abacavir DILI.

The adaptive immune system has two arms – cell mediated and humoral immune responses. There is evidence for the involvement of both arms of the adaptive immune system in DILI. For example, flucloxacillin DILI is thought to be mediated by T-cells (54), while for other drugs such as isoniazid, there are findings of anti-drug or auto antibodies against metabolising enzymes (55).

Whether for cell mediated or humoral responses, initiation of the adaptive immune system requires antigen presentation and activation of T-cells. HLA reside on antigen-presenting cells (APCs) and mediate the interaction between the APC and the T cell receptor (56).

Genome wide association studies have linked various adverse drug reactions, including a number of iDILI with particular HLA genotypes (57). Well known examples of HLA associations include: flucloxacillin DILI and *HLA-B*5701*; carbamazepine hypersensitivity and *HLA-A*3101* (58); amoxicillin-clavulanic acid DILI and HLA class II (59); abacavir hypersensitivity and *HLA-B*5701* (60). These associations suggest that either the drug is causing DILI by a non-immune mechanism and preferentially evoking an immune response in people with certain HLA genotypes, or that the adaptive immune system is mediating the toxicity.

1.3.2.2 Innate immune system

The role of the innate immune system in contributing to DILI is often overlooked. It is increasingly recognised that the adaptive system does not work in isolation, and that the

important interplay between innate and adaptive immunity in the defence of the body is also important in mediating DILI (61,62).

1.3.3 Pattern Recognition Receptors

Pattern Recognition Receptors (PRRs) are the effectors of the innate immune system. They detect highly conserved pathogen-associated molecular patterns (PAMPs) often associated with bacterial products (*e.g.* lipopolysaccharides). In addition to PAMPs, PRRs also recognise endogenous damage-associated molecular patterns (DAMPs), activating inflammatory processes in response to cell damage.

1.3.3.1 Toll-like receptors

Toll-like receptors (TLRs) are the classic PRRs that are found in mammals and their role in liver disease has been extensively studied and reviewed (63,64). The liver is the first organ exposed to high levels of pathogens and drugs entering the body from the gastrointestinal tract *via* the hepatic portal vein. Understandably then, the liver has a high concentration of immune cells which remove pathogens and antigens before they can enter the systemic circulation. Kupffer cells are specialised macrophages which line the sinusoids and engulf dead red blood cells and bacteria. Both Kupffer cells and hepatocytes are among the numerous cells within the liver that have been found to express TLRs and have demonstrated responses to TLR ligands (63).

TLR4 was the first mammalian TLR to be characterised and specifically responds to lipopolysaccharides (LPS) from Gram negative bacteria (65,66). The toxicity of LPS appears to be dose dependent, with larger LPS doses resulting in a strong inflammatory response (67). Moderate doses are non-toxic alone, but can result in liver injury when co-administered with drugs – they are commonly used for this purpose in the development of animal models of DILI (68–70). Low LPS doses, ironically, have been shown to have a protective effect against toxicity induced by paracetamol's highly reactive metabolite and chemicals such as carbon tetrachloride and concanavalin-A (71,72). Again, this highlights the complex mechanisms behind DILI and the difficulties in identifying the biological targets and pathways responsible for toxicity.

TLR9 appears to be critical in mediating acetaminophen DILI in mice (73), and TLR7 and TLR3 have been associated with hypersensitivity reactions and are known to enhance the response mounted by the adaptive immune system (74,75).

1.4 Mechanistic theories of IMDILI

Over the years a number of theories have been proposed to explain the mechanisms behind IMDILI. The major hypotheses are summarised in Figure 1.3 and are discussed in the following sections.

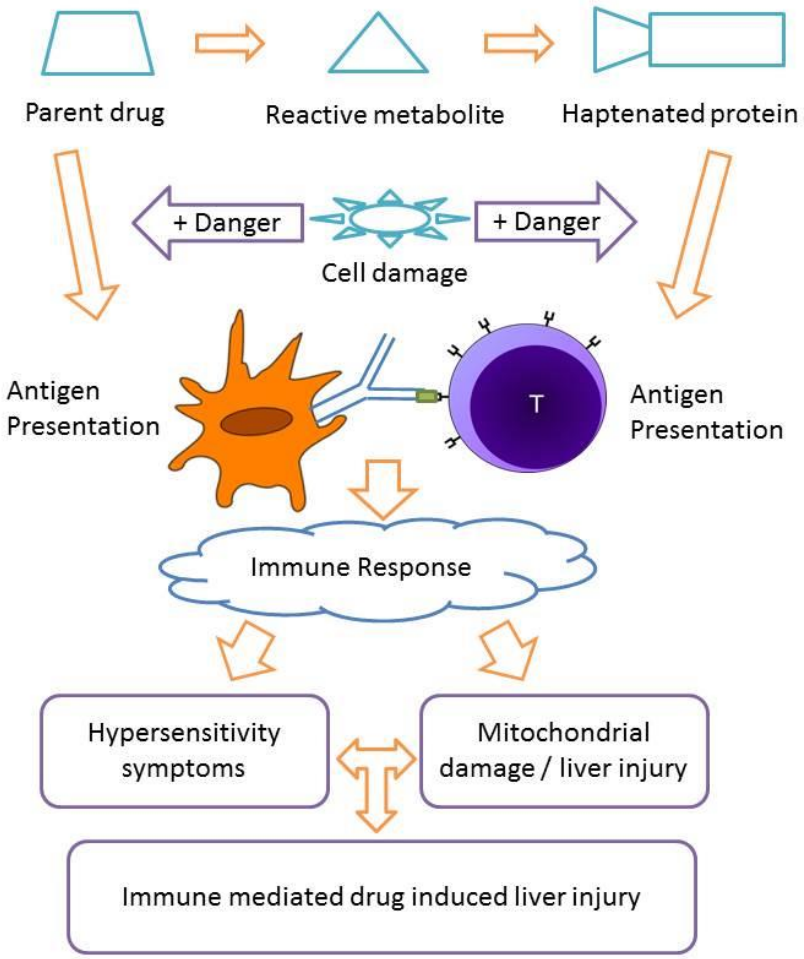

Figure 1.3 Summary of the major mechanistic theories of iDILI. Parent drugs may be metabolised into reactive metabolites. These metabolites act as haptens, covalently binding to cellular proteins. These dysfunctional proteins are identified as 'foreign' and presented by antigen presenting cells (APCs) to T cells to initiate an adaptive immune response. Alternatively, the parent drug may reversibly bind at the immunologic synapse between APCs and T cells to initiate the immune response with a pharmacological interaction (p-i). The danger hypothesis proposes that in addition to antigen presentation, a secondary 'danger' signal is required for immune activation – antigen presentation without this secondary signal results in tolerance. The danger signal may be the result of mild direct toxicity from the drug, or from an underlying condition, such as alcohol induced liver injury or a concomitant bacterial or viral infection. Part of the figure sourced from http://www.clker.com/.

1.4.1 Mitochondria

Mitochondria mediate many important processes within cells, ranging from energy production to apoptosis and necrosis (76). It comes as no surprise then that mitochondria also play a central role in DILI (77). Mitochondrial toxicity offers an alternative to the immune-mediated hypotheses described below.

Drugs and metabolites are known to impair mitochondrial function in a variety of ways, including the direct inhibition of β-oxidation leading to steatosis; inhibition of mitochondrial DNA transcription and protein synthesis, as well the disruption of mitochondrial membranes leading to cell death (77).

Valproic acid resembles medium chain fatty acids and can compete with fatty acids in mitochondria during the β-oxidation process (77). Other drugs (*e.g.* troglitazone) damage mitochondrial DNA leading to apoptosis (78).

Since all pro-apopotic signals are thought to converge on mitochondria (77), it can be difficult to determine whether mitochondrial toxicity is the cause of DILI, or whether mitochondria are merely mediating the toxicity due to another mechanism. This uncertainty means that the mitochondrial hypothesis is not an exclusivist theory; it may hold in conjunction with the hapten, danger, and pharmacological interaction (p-i) hypotheses described below.

1.4.2 Hapten hypothesis

Drugs with a molecular weight smaller than 1000 Daltons are thought to be too small to act as an antigen and elicit an immune response since they may not be able to activate T cells *via* antigen presentation (26). Rather, low molecular weight drugs can be metabolised into reactive intermediates which subsequently bind to cellular proteins, such as the metabolising enzyme that formed them. The body then mounts an immune response against these dysfunctional proteins, resulting in inflammation and organ injury. This is the basis of the hapten hypothesis (26).

There is a large amount of circumstantial evidence for the hapten hypothesis. Pencillin based antibiotics have a chemically reactive β-lactam ring which can form covalent bonds with proteins. The body then mounts a humoral immune response, creating

immunoglobulin E (IgE) which mediates the hypersensitivity reaction (79). Similarly, halothane is metabolised into the reactive metabolite trifluroacetyl chloride, which then covalently binds to cellular proteins (14).

One complication regarding the hapten hypothesis is that drugs implicated in DILI do not always form reactive metabolites. Hence, while the hapten hypothesis may explain the DILI of some drugs, it is by no means the only possible mechanism of hepatotoxicity.

1.4.3 Danger hypothesis

The danger concept, proposed by Matzinger in 1994, challenged the traditional view of immunology where the immune system is tolerant towards 'self', and hostile against 'non-self' (80). Instead, the immune system activates in response to danger, regardless of its origin. Matzinger argues that for the traditional view to hold, a mechanism must exist to induce tolerance to tissue specific antigens on organs (*e.g.* liver and kidneys), and yet still allow for an immune response to tissue specific viruses. Such a mechanism, if it exists, must necessarily be very complex, and must allow the immune system to develop tolerance to a huge number of self-proteins (80), let alone that of symbiotic micro flora. The problem is much simplified if the immune system simply responds to 'danger' (*e.g.* exposure to hydrophobic regions of proteins signalling tissue damage (81)).

For IMDILI, the danger hypothesis postulates that, in addition to the presence of foreign antigen, a second, so-called 'danger signal', signifying cellular toxicity, is required for the activation of the adaptive immune response (62). A danger signal may result from mild cellular damage caused by a drug's direct toxicity. This leads to the release of DAMPs, with subsequent activation of the adaptive immune system to potentiate and exacerbate the reaction.

1.4.4 Pharmacological interaction (p-i) hypothesis

Based on the observation that some drugs are able to stimulate an immune response in the absence of chemical reactivity or metabolite formation, Pichler proposed the pharmacological interaction (p-i) hypothesis as an alternative to the hapten and pro-hapten hypotheses (82). The p-i concept is a modification of the hapten hypothesis where, rather than reactive metabolites, it is the parent drug itself that bridges the junction between antigen presenting cells and T-cell receptors to initiate the adaptive immune response.

The p-i hypothesis may be important in mediating the toxicity of ximelagatran, since its chemical structure resembles that of a peptide and may be able to bind directly to HLA (83). Recent evidence also suggests that some flucloxacillin DILI may be mediated through a p-i mechanism (84).

1.5 Study methodologies

Given the complexity of DILI and the length of time it has been an active field of research, it comes as no surprise that each research group has tackled the problem differently, according to their area of expertise and availability of resources. Many methodological approaches have been utilised in the study of iDILI, ranging from *in vitro* studies on cell lines (6) to the use of microfluidic liver biochips (85), *in vivo* animal models (*e.g.* zebra-fish (86) and rabbits (87)), bioinformatics approaches (88) and epidemiological approaches (89) (Figure 1.4).

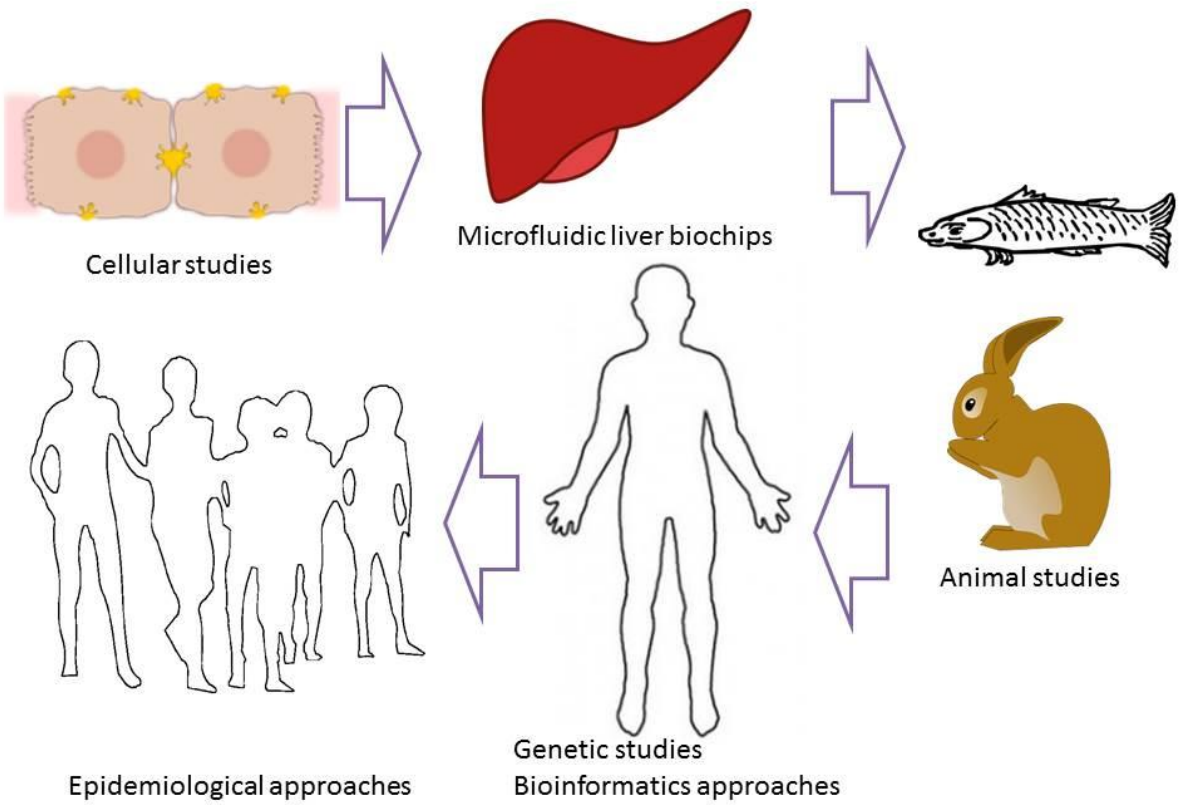

Figure 1.4 Idiosyncratic Drug Induced Liver Injury (iDILI) has been studied through a multitude of methodologies, yet many mysteries remain regarding the mechanisms of toxicity and the bioloical targets and pathways involved. Part of the figure sourced from http://www.clker.com/; http://en.wikipedia.org/.

1.5.1 Models of hepatotoxicity

While *in vitro* and *in vivo* models of iDILI exist, they are far from perfect (90). Unless models are able to capture and account for the large number of risk factors and proteins associated with iDILI, it is likely that a generalizable, predictive model of iDILI will remain elusive.

Hartung recently described the frustrations associated with translating *in vitro* and animal studies into humans in his *Food for Thought* article aptly titled: *Look Back in Anger – What Clinical Studies Tell Us About Preclinical Work* (91). It is this disparity in results between preclinical and clinical studies, and indeed between clinical trials and post-marketing surveillance, that is responsible for the billions of dollars 'wasted' in pharmaceutical research and development. With the deficiencies in *in vivo* models, researchers are aiming at reducing reliance on animal models, moving instead towards *in silico* screening and the use of bioinformatics tools (91,92).

1.5.1.1 In vitro methods

In vitro assays have long been established as efficient and cost effective alternatives to *in vivo* toxicological studies. Typically, the reaction of interest is studied under controlled conditions, and various factors are varied in a systematic manner to determine their influence on the reaction.

While *in vitro* methods, particularly high throughput assays, are commonly used to investigate iDILI, debates ensue over the suitability of different cell types for these kinds of studies (93). The three most commonly used cell lines are primary hepatocytes, immortalised cell lines and hepatocellular carcinoma cell lines. Primary hepatocytes are thought to be the gold standard, as they are the closest representation of the human liver out of the three options. However, primary hepatocytes are short lived, hard to culture and difficult to obtain since sacrificing the animal is required. Another disadvantage of human primary hepatocytes is a lack of reproducibility across various donors. Moreover, the health of the donors can affect results. HepG2 (liver hepatocellular carcinoma) is a commonly used hepatocellular cell line used in toxicological studies. While these cells are relatively inexpensive and easy to obtain, they have a low expression of phase I enzymes, and as such, may not accurately reflect the situation *in vivo*, especially if metabolic activation is required.

Not surprisingly, using different types of hepatocytes can give different results in toxicity testing (94).

To overcome some of the problems associated with using single cell lines, researchers have attempted co-culture models, where two or more cell lines are cultured simultaneously. Atienzar *et al.* developed a co-culture approach where dog primary hepatocytes were uniformly dispersed with stromal cells. Cell viability and glutathione concentrations were used to quantify the level of toxicity. The resultant co-culture system maintained metabolic capabilities for up to two weeks, which they suggest is sufficient for use in long term metabolism studies (95).

Liver cells have a particular architecture that facilitates their role in detoxification. The move towards 3D models of liver cells comes amid increasing recognition that simple toxicological assays using single cell lines or even a co-culture of cells are unable to replicate *in vivo* toxicity (96). Since iDILI is influenced by a multitude of risk factors, a working model must be able to capture and distil the complexity of the various pathways involved in iDILI.

As a step towards this, Ramaigari *et al.* developed a liver 3D model where HepG2 carcinoma cells were organised into multiple polarised spheroids. HepG2 cells in spheroid form regained some metabolic capability, as well as other functions such as storage of glycogen and transportation of bile salts. This increase in functionality appeared to translate into increased sensitivity in DILI screening (97). Similarly, Aritomi *et al.* found that although conventional cultures of HepG2 cells were unsuitable for modelling paracetamol DILI, 3D cultures of HepG2 cells in nano-culture plates were able to replicate key features of paracetamol DILI, including the creation of reactive metabolites (98).

Adding another level of complexity, newer 3D models allow cells to aggregate and develop structures and communication networks. Bhushan *et al.* created a 3D co-culture of cells that effectively mimics a functional unit of the human liver. This *liver-on-a-chip* technology comprises of 4 different cell types: hepatocytes, endothelial, stellate and Kupffer cells. Preliminary work to prepare the model for use in early DILI detection appears to be promising (99). Similarly, Larson *et al.* also reports the use of liver microtissues for long term toxicity studies (100).

The success of these approaches highlights the need to move beyond traditional assays which focus on a single reaction and towards big picture approaches which better reflect the complexity of *in vivo* systems.

1.5.1.2 In vivo methods

One frustrating aspect of iDILI is the inability to reproduce the human manifestations of toxicity in animal models. In part, this may be due to differences between the test animal and humans, but it is also likely that, just as in humans, iDILI is rare and idiosyncratic in animals - *i.e.* host related susceptibility factors are required to enhance the intrinsic toxicity of a drug that will otherwise pass unnoticed. Knowledge of the susceptibility factors, proteins and pathways involved in the toxicity will be critical to developing an animal model that can replicate iDILI in humans (13).

There are many difficulties with animal studies, including poor reproducibility and difficulties translating the results into humans or even between species (91). Traditionally, regulatory sciences have used high doses in animals to test for toxicity. This approach may be of limited benefit for toxicity which does not appear to be dose dependent.

One method by which researchers have attempted to improve translatability between animals and humans is to make use of chimeric rodents with humanized livers. These are created by transplanting human hepatocytes into immunocompromised mice. The metabolic capabilities of these models are similar to that in humans, and so have been utilised in a number of pharmacological studies, as well as in the study of liver infections (101). However, chimeric mice failed to reproduce the liver injury caused by troglitazone, which was withdrawn due to iDILI. This may be due to the lack of B- and T- lymphocytes in chimeric mice, and hence their inability to model immune-mediated DILI (102).

Given the limitations of animal models and with continual improvements in technology, the FDA is looking to replace animal studies with *in silico* and *in vitro* toxicity assays in the near future (92).

1.5.1.3 In silico methods

Rapid advancements in computing technology and capacity have seen many researchers turn to *in silico* modelling as a cost effective alternative to *in vitro* and *in vivo* studies. For DILI, computational modelling has proven to be very versatile, with applications ranging from developing structural alerts for identifying hepatotoxic drugs by using the formation of reactive metabolites (49) to Quantitative Structure Toxicity Studies and mathematical modelling of mechanistic interactions between compounds and the liver (103). In addition, *in silico* technologies are often used in conjunction with bioinformatics and systems approaches in order to make sense of the large volumes of data generated by these techniques.

One disadvantage with *in silico* methodologies is that when hypotheses are generated, there is still a need to test the hypothesis with *in vitro* or *in vivo* assays. Hence *in silico* technologies are most helpfully applied to preliminary screenings or in a setting where the technology has already been validated by another method.

1.5.2 Bioinformatics approaches

Bioinformatics or so-called '*omics*' approaches have recently become popular because of the large amount of data that can be generated using these approaches, and the increasing availability of the technology to analyse such data. Bioinformatics techniques attempt to capture a snapshot of the biological content in the sample at a moment in time. By comparing the data captured during periods of disease and the 'normal' state, it is possible to use these snapshots as biomarkers of various diseases.

Proteomics qualitatively and quantitatively measures the proteins that are present in a cell or in the extra cellular matrix. A sample of biological fluid is taken and then put through liquid chromatography-mass spectrometry (LC-MS). Identification of constituents is done by comparing the results to the spectra of known proteins. However, this is by no means an easy task since the level and range of proteins present in biological fluids can vary based on the timing and site of collection. Rodriguez-Suarez *et al.* analysed the proteomes of extracellular vesicles secreted by primary hepatocytes (104). By cataloguing the proteins secreted by hepatocytes that have been exposed to hepatotoxins, these researchers

discovered patterns in protein expression that differed between healthy and damaged hepatocytes which could be developed into novel non-invasive biomarkers of DILI (104).

The Centre for Omic Sciences defines transcriptomics as 'the study of transcriptomes – the complete set of RNA transcripts produced by the genome at any one time' (omicscentre.com). The contribution of transcriptomics in the study of ADRs has been summarised in a recent review by Fernandez *et al.* (105). In short, researchers have found patterns in gene expression which differ between samples obtained from intoxicated and healthy patients. Blood borne gene expression markers can then serve as biomarkers of ADRs, including DILI (105). Similarly, Benet *et al.* investigated transcription factor expression profiles for cells exposed to known steatotic drugs and were able to identify three transcription factors as predictive biomarkers of drug induced hepatic steatosis (106).

Although *omics* technologies are now commonly used in academia and industry, relative few research groups have utilised approaches combining multiple methods (107,108). In a recent review, Khan *et al.* argue that a holistic approach, combining proteomics, transcriptomics, metabolomics *etc*. is useful as a means of gathering comprehensive information, and that the use of bioinformatics tools may eventually revolutionise the drug discovery paradigm (88).

1.5.3 Epidemiological approaches

Due to the rare incidence of DILI, there is a need to identify cases by which to study the pathophysiology of the disease. Post-marketing data collected by pharmaceutical companies or regulatory authorities consists of adverse drug reaction (ADR) reports, and typically contain information on patient demographics, information on suspected drugs and details of the experienced ADR. Using case/non-case methodology, researchers can measure the strength of an association between particular ADRs (*e.g.* DILI) and drug exposure and hence identify DILI cases out of population data. Networks and registries have also been set up specifically to collect DILI cases for study.

Table 1.1 lists some examples of DILI associations that have been found by analysing pharmacovigilance databases around the world.

Table 1.1 Examples of DILI studies conducted using various data sources.

Data source	Study focus
Portuguese, French, Spanish, Italian pharmacovigilance system	Hepatotoxicity with agometaline and newer antidepressents (109)
Spanish DILI registry	Characteristics of DILI cases (10)
U.S. DILI network	Characteristics of statin DILI (110)
U.S. DILI network	DILI due to herbal products (111)

1.6 Struggles & Challenges

The lack of understanding of the biological targets and pathways behind IMDILI makes it difficult to develop models to study the disease. The various study methodologies have revealed glimpses of the diverse associations and risk factors influencing IMDILI. The challenge in moving forward will be to integrate the current knowledge of IMDILI into a unified picture. It is becoming increasing clear that IMDILI is a multidimensional problem, and that multidisciplinary experimental approaches are required to solve it.

1.7 Rationale for project and hypothesis

This thesis presents an approach to expose relationships between IMDILI and the three-dimensional structural features of toxic drug molecules and their metabolites. The analyses focus on immune mediated DILI (IMDILI) since these reactions have defined clinical characteristics, allowing for the identification of cases from population adverse drug event data.

The series of analyses in the following chapters test the hypothesis that drugs (or their metabolites) which produce similar patterns of toxicity interact with targets within common toxicological pathways and that activation of the underlying mechanisms depends on structural similarity among toxic molecules.

Firstly, a probe set of drugs for IMDILI must be identified. Any similarities within this set of drugs in terms of common biological pathways or structural features are then identified. These similarities can subsequently be used to reveal potential targets in the toxicity pathway of drugs implicated in IMDILI.

Chapter 2: Identification of probe IMDILI drugs

2.1 Introduction

2.1.1 Pharmacovigilance

There are many gaps in the current understanding of immune-mediated drug-induced liver injury (IMDILI). Inconsistencies in cross species translation necessitate *in vivo* human toxicological data to aid in the understanding of the mechanisms of toxicity (13). Such data is first made available when the drug progresses from preclinical animal studies into human clinical trials. However, clinical trials are typically conducted in a relatively small number of otherwise healthy individuals and as such are inadequately powered to detect rare adverse drug reactions (ADRs). Hence drug regulatory authorities such as the US Food and Drug Administration (FDA) and Australia's Therapeutic Goods Administration (TGA) usually require pharmaceutical companies to collect post-marketing information regarding the safety and efficacy of their drug once it is approved for marketing and made available to a significantly larger and diverse patient population.

Spontaneous ADR reports collected by drug regulatory authorities and by pharmaceutical companies as part of their monitoring responsibilities are collated and stored in pharmacovigilance databases. While valuable, the usability of information contained in these databases is highly dependent on the quality of the data, which in turn is dependent on the skill and clinical expertise of the reporter.

Reports typically consist of information regarding patient demographics (*e.g.* age, sex), a list of drugs suspected of causing the ADR, drug information (*e.g.* drug name, brand name, dosage, batch number), and a list of ADRs reported.

ADRs are described using sets of standardised terminology. An example is the Coding Symbols for a Thesaurus of Adverse Reaction Terms (COSTART) (112), which was subsequently superseded by the Medical Dictionary for Regulatory Authorities (MedDRA) (113).

MedDRA was developed by the International Conference on Harmonisation of Technical Requirements for Registration of Pharmaceuticals for Human Use (ICH) to facilitate the sharing of regulatory information internationally for medical products used by humans

(113). It lists each ADR in a hierarchy of terms and is available in multiple languages. Body systems are grouped into System Organ Classes (SOC), which are further subdivided into Higher Level Group Terms (HLGT), Higher Level Terms (HLT), Preferred Terms (PT) and Lower Level Terms (LLT), with each layer giving a more specific description of the ADR (Figure 2.1).

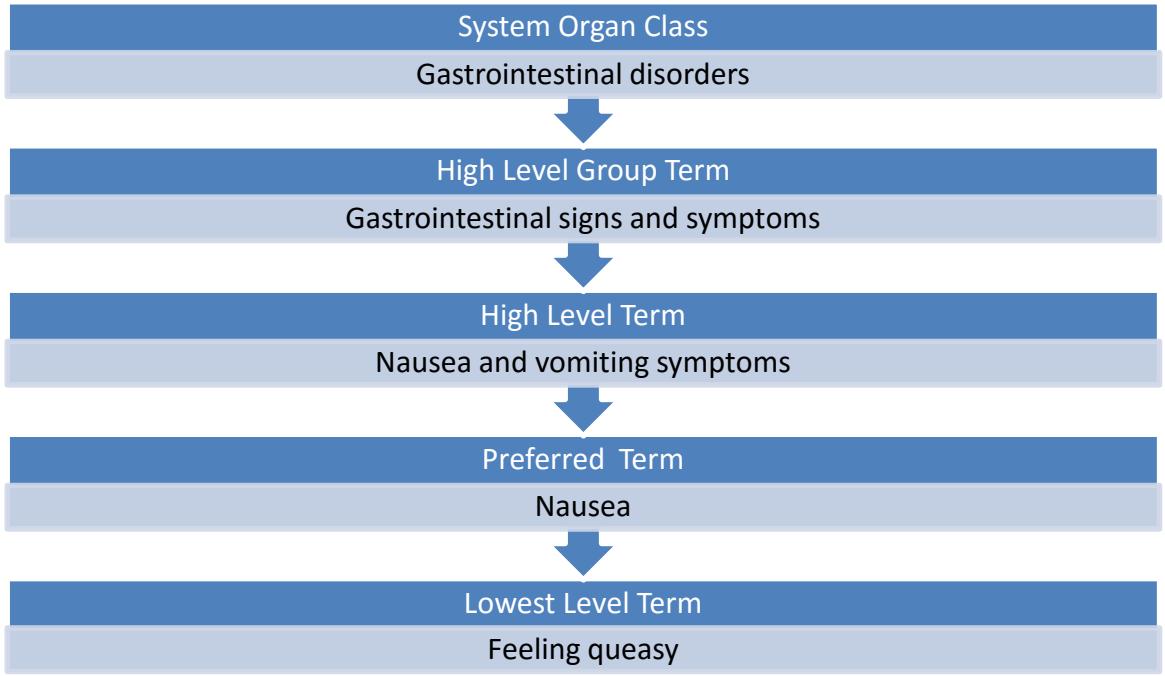

Figure 2.1 Example of Adverse Drug Reaction (ADR) terms classified under the MedDRA Hierarchy. (113)

2.1.1.1 Data sources

To facilitate the study of DILI, cases of DILI are required. Case information can be obtained from the post-marketing, pharmacovigilance databases described above. Alternatively, there are also large databases dedicated to collecting and storing DILI information, such as the Drug Induced Liver Injury Network (DILIN) (https://dilin.dcri.duke.edu/) and LiverTox (livertox.nih.gov/).

The Drug Induced Liver Injury Network (DILIN) was established in 2003 by the US National Institute of Diabetes and Digestive and Kidney Diseases (NIDDK). Its aim is 'to collect and analyze cases of severe liver injury caused by prescription drugs, over-the-counter drugs, and alternative medicines, such as herbal products and supplements'. Since 2008, the investigators have published close to 30 publications over a spectrum of topics ranging from causality assessment, (114) to characteristics of DILI, (4,45,115) to drugs, herbs and supplements implicated in DILI (110,111).

The LiverTox database is another initiative of the NIDDK, in conjunction with the DILIN and the U.S. National Library of Medicine. It provides "*up-to-date, accurate, and easily accessed information on the diagnosis, cause, frequency, patterns, and management of liver injury attributable to prescription and non-prescription medications, herbals and dietary supplements*" (116). It is a helpful resource summarising the known evidence from current scientific literature. Monographs typically contain sections on background regarding the drug; evidence for hepatotoxicity; mechanism of injury and outcome and management advice. Each of these drug monographs are reviewed by at least one external researcher, many of whom are investigators in the DILIN (51).

The U.S. Food and Drug Administration (FDA) stores ADR reports in its own database, the FDA Adverse Event Reporting System (FAERS). The database consists of adverse events and medication errors cases that are voluntarily reported by health care professionals or consumers. Although large and publicly available, the quality of the reports in the FAERS is poor. The lack of standardisation of drug names, misspellings and duplicated cases mean that extensive data cleaning is required before the database is analysable (117). The work undertaken to prepare the FDA database for analysis was published in the journal *Pharmacoepidemiology and drug safety* (117) (Appendix 1: Peer Reviewed Scientific Publications arising from this thesis).

Australia's drug regulatory authority, the Therapeutic Goods Administration (TGA), also collects reports of ADRs as part of its monitoring activity. The database collated by the TGA contains ADR reports from 1971 to the present. Each drug is entered as both the brand name and the generic name with standardised spelling. Cases are reviewed by a health care professional before inclusion into the database. Reports include information on patient demographics; drug exposure (generic name, dose, frequency, dose form) and adverse reaction terms coded as MedDRA preferred terms (PT) and lower level terms (LLT).

At the time of the analyses described below, two subsets of this TGA ADR data were available; one which contains 240,137 spontaneous ADR reports to the end of 2008 and the other 247,391 ADR reports to the end of 2011. The seemingly relatively modest increase in the numbers of reports between the two datasets is due to the inclusion of non-general market drugs (*e.g.* drugs undergoing clinical trial or medicines made available through the

TGA's Special Access Scheme) in the 2008 dataset. In the 2011 dataset, non-general market cases were removed by the TGA on the basis that the data was usually incomplete with regard to patient, reaction or reporter information, and/or not comparable to other data.

The following analyses focus on the TGA database since it is perceived to be of greater accuracy and reliability than the FAERS data. The subset of spontaneous ADR reports to 2008 was chosen in order to capture as much data as possible, including the reports from clinical trials.

2.1.1.2 Disproportionality analyses

Due to the immense number of spontaneous ADR reports, it would take much meticulous and time consuming work to manually examine each report for cases of ADR. Moreover, there is a need to quantify the strength of association between drug exposure and ADR outcomes to determine if such associations are statistically significant and to inform clinical practice guidelines which govern the use of the drugs under scrutiny.

Disproportionality analyses test the statistical *null* hypothesis that there is no difference in the incidence of reported exposure to a drug of interest between cases and non-cases. A number of statistical measures are available, including the Reporting Odds Ratio (ROR), Proportional Reporting Ratio (PRR), Yule's Q, the Poisson probability, Chi-square test and Bayesian measures such as the Information Component (IC) (118).

From a 2 x 2 contingency table (Table 2.1), disproportionality measures quantify the 'disproportionality' between based on the frequency that would be expected in each cell of the table if there was no association between the ADR and drug exposure and the actual frequency.

Table 2.1 Two by two contingency table of ADR reports. The table displays the frequency distribution of variables. 'a' is the number of reports containing the drug of interest and the ADR of interest. 'b' is the total number of reports for the drug of interest, excluding those with the ADR of interest. 'c' is the total number of reports for the ADR of interest, excluding those with the drug of interest. 'd' is the number of reports that do not contain the drug of interest nor the ADR of interest.

	Reports with ADR of interest	All other reports
Reports with drug exposure	a	b
All other reports	c	d

The PRR (Equation 1) compares the proportion of reports of a particular ADR *versus* reports for all other ADRs in cases with exposure to the drug of interest against cases without. If there is no association between the drug of interest and the ADR of interest, then one would expect a PRR of 1 (119).

The ROR (Equation 2) measures the strength of association between exposure and outcome in case control studies. Rather than testing to see if drug exposure increases the risk of an ADR, case-control studies determine if the outcome of ADR is significantly associated with exposure to a drug (120). Lewallen and Courtright defined the ROR as "the ratio of the odds of an exposure in the case group to the odds of an exposure in the control group" (120). A ROR of 1 would be expected if there was no association between exposure and outcome.

The properties of the different measures of disproportionality and the concordance between them have been compared by van Puijenbroek *et al.* (118). The level of concordance was high between all measures and particularly high when there were 4 or more reports containing the ADR and drug combination. The ROR offers the advantage that different adjustments are possible in logistic regression, such as the use of interaction terms (118).

The ROR was chosen as the measure of disproportionality for the following analyses since it is a transparent measure that is not influenced by non-selective underreporting of drugs or adverse drug reactions (118).

Proportional Reporting Ratio (PRR)

$$PRR = \frac{\frac{a}{a+b}}{\frac{c}{c+d}} \qquad (1)$$

Reporting Odds Ratio (ROR)

$$ROR = \frac{\frac{a}{c}}{\frac{b}{d}} = ad/bc$$

2.1.1.3 Logistic regression

Since the outcome variable of interest (IMDILI) is binary, logistic regression can be used to describe the relationship between IMDILI and other variables (*i.e.* drugs of interest and confounding factors). Logistic regression describes the probability that the outcome occurs (Y = 1) based on variables in the equation. If the probability that Y = 1 is written as p, then the probability that Y = 0 is (1 – p). Equation 3 gives the general logistic regression equation. The ROR for each variable (X_1, X_2,…) is given by the coefficients (B_1, B_2,…) respectively.

General logistic regression equation

$$\ln\left(\frac{p}{1-p}\right) = Bo + B_1X_1 + B_2X_2 + \cdots \quad (3)$$

Stepwise regression describes regression models that are built using an automated procedure to examine the impact of each of the covariates on the model. Forward stepwise regression begins with no variables in the equation. Each variable is then examined, and the variable that improves the model the most is added into the equation. The process is then repeated until the addition of variables no longer improves the model.

The overall 'fit' of the model can be measured by the likelihood ratio test which is based on the chi-square statistic (Equation 4). If the addition of a variable to the equation improves the model, the deviance (D) should decrease, indicating that the expected values from the model are closer to the observed values.

The likelihood ratio test (121)

$$\chi^2 = D\ (for\ the\ model\ without\ the\ variable) - D\ (for\ the\ model\ with\ the\ variable) \quad (4)$$

2.1.2 Correction for multiple testing

In the present study, the null hypothesis (H_o) is that there is no difference in the incidence of reported exposure to a drug of interest between cases and non-cases. Setting a statistical significance level aids in making a decision regarding whether or not to reject the null hypothesis by quantifying the probability that the observed results are due to chance. Typically, a significance level (α) of 5% is deemed to be reasonable. A 5% significance level

(or $p < 0.05$) means that if the null hypothesis is true, then there is < 5% chance that the observed results are due to chance.

There are two types of error that can be made when using significance levels. A type 1 error occurs when the null hypothesis is rejected, even though it is in fact true. This can happen when the significance level is set too high. Conversely, a type 2 error occurs when the null hypothesis is accepted, even though it is false. This can happen when the significance level is set too low. Therefore, care needs to be taken in choosing an appropriate significance level for the study.

The need for adjusting the significance level in multiple testing has been described by Bender and Lange (122):

> *"If one significance test at level α is performed, the probability of the type 1 error (i.e., rejecting the individual null hypothesis although it is in fact true) is the comparisonwise error rate (CER) α, also called individual level or individual error rate. Hence, the probability of not rejecting the true null hypothesis is (1-α). If k independent tests are performed, the probability of not rejecting all k null hypotheses when in fact all are true is $(1-\alpha)^k$. Hence, the probability of rejecting at least one of the k independent null hypotheses when in fact all are true is the experimentwise error rate (EER) under the complete null hypothesis $EER = 1 - (1 - \alpha)^k$, also called global level, or familywise error rate (considering the family of k tests as one experiment). If the number k of tests increases, the EER also increases. For α = 0.05 and k = 100 tests EER amounts to 0.994. Hence, in testing 100 independent true null hypotheses one can almost be sure to get at least one false significant result. The expected number of false significant tests in this case is 100 x 0.05 = 5."*

The aim of this chapter is to develop a probe set of IMDILI drugs for use in further analyses. Hence the interest is in controlling the maximum experimentwise error rate (MEER). This is defined as "the probability of rejecting falsely at least one true individual null hypothesis, irrespective of which and how many of the other individual null hypotheses are true"(122). In other words, the aim is to minimise the probability of finding an association between a drug and IMDILI when in fact there is no association.

The simplest procedure to adjust for multiple testing is the Bonferroni correction, where the experimental significance level is divided by the number of independent tests (122).

2.1.3 Rationale

Since the diagnosis of IMDILI is based upon the exclusion of all other conditions, as described in Chapter 1, there is a degree of uncertainty in evaluating a drug's potential to cause IMDILI. While drugs associated with IMDILI may be identified from the literature, sometimes these associations are drawn from case reports or there may be conflicting evidence as to a drug's IMDILI potential. To facilitate further study of the biological mechanisms behind IMDILI it is necessary to derive a set of probe drugs with definite IMDILI potential. This chapter aims to achieve this high degree of confidence by identifying drugs associated with IMDILI from a pharmacovigilance database and then confirming this association with the literature.

2.2 Methods

2.2.1 Pharmacovigilance data source

Pharmacovigilance data was obtained from Australia's Database of Adverse Event Notifications (DAEN) (http://www.tga.gov.au/safety/daen.htm#.UzAVgc4VXjs). The subset of data used from the DAEN contained 240,137 spontaneous ADR reports voluntarily reported to the TGA from 1972 to December 2008. Reports were excluded when data were absent for patient age, sex, drug name or adverse reaction term. This led to 37,293 reports being excluded, leaving 204,844 ADR records for analysis.

2.2.2 Case definition

Cases of IMDILI were defined as reports which included a combination of at least one MedDRA preferred term indicative of liver injury (*e.g.* hepatic failure) and at least one MedDRA preferred term which indicated an immunological reaction (*e.g.* drug allergy). The full list of MedDRA terms used in the case definition is presented in Table 2.2. Non-cases were defined as all reports which do not meet the case definition.

Table 2.2 List of MedDRA preferred terms (PT) used to define cases of immune medicated drug induced liver injury (IMDILI). Cases of IMDILI were defined as reports which included at least one MedDRA PT describing liver injury and at least one MedDRA PT which indicated an immunological reaction.

Liver injury preferred terms	Immunological reaction preferred terms
Cholestasis	Allergic hepatitis
Hepatitis cholestatic	Dermatitis allergic
Jaundice	Hypersensitivity
Jaundice acholuric	Skin reaction
Jaundice cholestatic	Stevens-Johnson syndrome
Jaundice hepatocellular	Type I hypersensitivity
Hepatobiliary disease	Type II hypersensitivity
Liver disorder	Type III immune complex mediated reaction
Mitochondrial hepatopathy	Type IV hypersensitivity reaction
Hepatic function abnormal	Allergy to chemicals
Hypertransaminasaemia	Drug eruption
Acute hepatic failure	Drug hypersensitivity
Chronic hepatic failure	Drug rash with eosinophilia and systemic symptoms
Hepatic failure	Toxic skin eruption
Allergic hepatitis	Idiopathic urticaria
Autoimmune hepatitis	Urticaria
Cholestatic liver injury	Autoimmune disorder
Chronic hepatitis	Immune system disorder
Hepatitis	Butterfly rash
Hepatitis acute	Fixed eruption
Hepatitis chronic active	Rash
Hepatitis chronic persistent	Rash generalised
Hepatitis fulminant	Rash macular
Hepatitis toxic	Rash maculo-papular
Hepatocellular injury	Rash morbilliform
Hepatotoxicity	Systemic lupus erythematosus rash
Mixed liver injury	Eosinophilia

Liver injury preferred terms	Immunological reaction preferred terms
Mitochondrial toxicity	Hepatic infiltration eosinophilic
Alanine aminotransferase	Hyperpyrexia
Alanine aminotransferase abnormal	
Alanine aminotransferase increased	
Aspartate aminotransferase	
Aspartate aminotransferase abnormal	
Aspartate aminotransferase increased	
Liver function test	
Liver function test abnormal	
Mitochondrial aspartate aminotransferase increased	
Transaminases	
Transaminases abnormal	
Transaminases increased	

2.2.3 Drug exposure

Where literature evidence of IMDILI exists for at least one member of the drug class, all drugs from a therapeutic class were selected for inclusion in disproportionality analyses. Therapeutic classes were defined according to the *Australian Medicines Handbook* (Adelaide, Australia, 2010). The full list of 328 drugs that were included is presented in Table 2.4.

Drug exposure was defined as case reports which contained at least 1 entry of the drug. Variations in dosage form and different salt forms were grouped.

2.2.4 Confounders

There are a number of variables which may confound potential toxicity signals from drugs. These were entered as covariates in the logistic regression. This allowed the identification of all the factors which are significantly associated with IMDILI. Table 2.3 lists the confounders included in the analysis.

Table 2.3 List of confounders included in the logistic regression analysis.

Confounder	Rationale
Age (as a continuous variable)	Increasing age is associated with polypharmacy and deteriorating liver function.
Sex	Females are at an increased risk of DILI
Antivirals indicated for viral hepatitis	These were used as surrogate markers of underlying liver disease

2.2.5 Statistical analysis

Statistical analyses were conducted using the SPSS 20.0.0 software (SPSS Inc. Chicago, IL, USA).

Univariate analyses were carried out to quantify the association between each drug with IMDILI. Those drugs that were significantly associated with IMDILI were then included in multivariate logistic regression analysis. This was carried out using the forward stepwise inclusion method based on the likelihood ratio. The ROR and 95% confidence interval (95% CI) were reported.

To minimise the risk of type-1 error associated with multiple tests, the overall alpha level was set at 0.00015 following the use of the Bonferroni Correction to account for the 328 drugs investigated simultaneously (122).

2.2.6 Antibiotic/Non-antibiotic Stratification

The results of the multiple logistical regression analysis were divided into two groups: non-antibiotic IMDILI drugs and antibiotic IMDILI drugs. The interaction between the non-antibiotic IMDILI drugs group and antibiotic use (excluding the antibiotic IMDILI drugs) was investigated using logistic regression analysis. Multivariate logistic regression analysis was carried out using the forward stepwise inclusion method based on the likelihood ratio statistic. The ROR and 95% confidence interval (95% CI) were reported.

2.2.7 Literature confirmation of toxicity classification

A literature investigation was performed for each of the drugs significantly associated with IMDILI as identified by the multivariate logistic regression. A Medline search was conducted

using the Subject Heading "Drug Induced Liver Injury". This was then combined with a search using the drug name. Hits were reviewed for evidence of hepatotoxicity presenting with immune features. The relevant drug monographs from the LiverTox database were also reviewed.

2.3 Results

2.3.1 Frequencies of reports

The total numbers of reports for each of the drugs of interest are listed in Table 2.4.

780 cases of IMDILI were identified.

Table 2.4 Full list of drugs included in the disproportionality analysis, showing the total number of reports of this drug in the database. Therapeutic classes are taken from the Australian Medicines Handbook (2010).

Therapeutic class	Drug	Frequency
Inhaled anaesthetics	Desflurane	10
Inhaled anaesthetics	Isoflurane	167
Inhaled anaesthetics	Methoxyflurane	6
Inhaled anaesthetics	Sevoflurane	105
Antifungals	Fluconazole	597
Antifungals	Itraconazole	127
Antifungals	Ketoconazole	254
Antifungals	Miconazole	152
Antifungals	Posaconazole	14
Antifungals	Voriconazole	108
Other antifungals	Amphotericin	533
Other antifungals	Caspofungin	27
Other antifungals	Flucytosine	39
Other antifungals	Griseofulvin	334
Other antifungals	Nystatin	595
Other antifungals	Pentamidine	69
Other antifungals	Terbinafine	724
Antiretrovirals	Abacavir	181
Antiretrovirals	Didanosine	239

Therapeutic class	Drug	Frequency
Antiretrovirals	Emtricitabine	8
Antiretrovirals	Lamivudine	706
Antiretrovirals	Stavudine	333
Antiretrovirals	Zidovudine	275
Antiretrovirals	Efavirenz	127
Antiretrovirals	Etravirine	1
Antiretrovirals	Nevirapine	235
Antiretrovirals	Atazanavir	44
Antiretrovirals	Darunavir	12
Antiretrovirals	Fosamprenavir	0
Antiretrovirals	Indinavir	307
Antiretrovirals	Lopinavir (includes combination with ritonavir)	53
Antiretrovirals	Ritonavir (includes combination with lopinavir)	185
Antiretrovirals	Saquinavir	80
Antiretrovirals	Tipranavir	5
Antiretrovirals	Enfuvirtide	16
Antiretrovirals	Maraviroc	0
Antiretrovirals	Raltegravir	9
Antiretrovirals	Tenofovir	108
Antivirals for viral hepatitis	Adefovir	23
Antivirals for viral hepatitis	Entecavir	7
Antivirals for viral hepatitis	Interferon alpha	774
Antivirals for viral hepatitis	Ribavirin	347
Antituberculous drugs	Ethambutol	290
Antituberculous drugs	Isoniazid	382
Antituberculous drugs	Pyrazinamide	180
Antituberculous drugs	Rifampicin	598
Cephalosporins	Cefaclor	1492

Therapeutic class	Drug	Frequency
Cephalosporins	Cefalotin	0
Cephalosporins	Cefepime	122
Cephalosporins	Cefotaxime	561
Cephalosporins	Cefoxitin	161
Cephalosporins	Ceftazidime	281
Cephalosporins	Ceftriaxone	1272
Cephalosporins	Cefuroxime	74
Cephalosporins	Cephalexin	1699
Cephalosporins	Cephazolin	727
Macrolides	Azithromycin	294
Macrolides	Clarithromycin	307
Macrolides	Erythromycin	2107
Macrolides	Roxithromycin	1282
Penicillins	Amoxicillin alone	2340
Penicillins	Clavulanic acid (in combination with amoxicillin or ticarcillin)	2654
Penicillins	Ampicillin	1678
Penicillins	Benzathine penicillin	32
Penicillins	Benzylpenicillin	731
Penicillins	Dicloxacillin	388
Penicillins	Flucloxacillin	2679
Penicillins	Phenoxymethylpenicillin	437
Penicillins	Piperacillin	227
Penicillins	Procaine penicillin	209
Penicillins	Ticarcillin alone	105
Quinolones	Ciprofloxacin	1164
Quinolones	Moxifloxacin	78
Quinolones	Norfloxacin	548
Tetracyclines	Doxycycline	1360
Tetracyclines	Minocycline	602

Therapeutic class	Drug	Frequency
Tetracyclines	Tetracycline	254
Other antibacterials	Aztreonam	39
Other antibacterials	Chloramphenicol	422
Other antibacterials	Colistin	34
Other antibacterials	Daptomycin	0
Other antibacterials	Hexamine hippurate	135
Other antibacterials	Linezolid	51
Other antibacterials	Nitrofurantoin	685
Other antibacterials	Sodium fusidate	221
Other antibacterials	Sulfadiazine	86
Other antibacterials	Tigecycline	5
Other antibacterials	Trimethoprim	964
Other antibacterials	Sulfamethoxazole (& trimethoprim)	4370
ACE inhibitors	Captopril	5639
ACE inhibitors	Enalapril	4622
ACE inhibitors	Fosinopril	732
ACE inhibitors	Lisinopril	1325
ACE inhibitors	Perindopril	2092
ACE inhibitors	Quinapril	449
ACE inhibitors	Ramipril	1668
ACE inhibitors	Trandolapril	428
Sartans	Candesartan	769
Sartans	Eprosartan	96
Sartans	Irbesartan	2643
Sartans	Losartan	312
Sartans	Olmesartan	21
Sartans	Telmisartan	586
Sartans	Valsartan	4
Endothelin antagonists	Ambrisentan	0

Therapeutic class	Drug	Frequency
Endothelin antagonists	Bosentan	82
Other antihypertensives	Clonidine	627
Other antihypertensives	Diazoxide	30
Other antihypertensives	Hydralazine	575
Other antihypertensives	Methyldopa	1973
Other antihypertensives	Minoxidil	85
Other antihypertensives	Moxonidine	20
Other antihypertensives	Nitroprusside (sodium)	9
Statins	Atorvastatin	3728
Statins	Fluvastatin	313
Statins	Pravastatin	1143
Statins	Rosuvastatin	262
Statins	Simvastatin	4978
Fibrates	Fenofibrate	126
Fibrates	Gemfibrozil	889
Antiarrhythmics	Adenosine	3
Antiarrhythmics	Amiodarone	1396
Antiarrhythmics	Atropine	602
Antiarrhythmics	Digoxin	5034
Antiarrhythmics	Disopyramide	188
Antiarrhythmics	Esmolol	4
Antiarrhythmics	Flecainide	211
Antiarrhythmics	Isoprenaline	11
Antiarrhythmics	Lignocaine	761
Antiarrhythmics	Sotalol	534
Other antianginal drugs	Ivabradine	0
Other antianginal drugs	Nicorandil	151
Other antianginal drugs	Perhexiline	249
Retinoids (oral)	Acitretin	85
Retinoids (oral)	Isotretinoin	498

Therapeutic class	Drug	Frequency
Antithyroid drugs	Carbimazole	405
Antithyroid drugs	Propylthiouracil	137
Other drugs for erectile dysfunction	Alprostadil	139
Other drugs for erectile dysfunction	Papaverine	12
Immunosuppressants (RA)	Azathioprine	801
Immunosuppressants (RA)	Cyclosporin	753
Immunosuppressants (RA)	Leflunomide	876
Immunosuppressants (RA)	Methotrexate	1612
Nonsteroidal Anti-androgens	Bicalutamide	37
Nonsteroidal Anti-androgens	Flutamide	132
Nonsteroidal Anti-androgens	Nilutamide	25
TNF-alpha antagonists	Adalimumab	139
TNF-alpha antagonists	Etanercept	187
TNF-alpha antagonists	Infliximab	220
Tyrosine kinase inhibitors	Dasatinib	27
Tyrosine kinase inhibitors	Erlotinib	10
Tyrosine kinase inhibitors	Gefitinib	25
Tyrosine kinase inhibitors	Imatinib	161
Tyrosine kinase inhibitors	Lapatinib	6
Tyrosine kinase inhibitors	Nilotinib	2
Tyrosine kinase inhibitors	Pazopanib	0
Tyrosine kinase inhibitors	Sorafenib	8
Tyrosine kinase inhibitors	Sunitinib	240
Barbiturates	Phenobarbitone	235
Barbiturates	Primidone	182
Other antiepileptics	Acetazolamide	2952
Other antiepileptics	Carbamazepine	229
Other antiepileptics	Ethosuximide	35
Other antiepileptics	Gabapentin	567
Other antiepileptics	Lacosamide	0

Therapeutic class	Drug	Frequency
Other antiepileptics	Lamotrigine	655
Other antiepileptics	Levetiracetam	124
Other antiepileptics	Oxcarbazepine	35
Other antiepileptics	Phenytoin	2491
Other antiepileptics	Pregabalin	247
Other antiepileptics	Sulthiame	42
Other antiepileptics	Tiagabine	37
Other antiepileptics	Topiramate	235
Other antiepileptics	Valproate	2204
Other antiepileptics	Vigabatrin	323
Other antiepileptics	Zonisamide	0
Other drugs for neurological conditions	Baclofen	302
Other drugs for neurological conditions	Botulinum toxin	55
Other drugs for neurological conditions	Dantrolene	26
Other drugs for neurological conditions	Modafinil	14
Other drugs for neurological conditions	Riluzole	47
Other drugs for neurological conditions	Ropinirole	13
Other drugs for neurological conditions	Tetrabenazine	28
ADHD drugs	Atomoxetine	71
ADHD drugs	Dexamphetamine	111
ADHD drugs	Methylphenidate	186
Antidepressants	Phenelzine	157
Antidepressants	Tranylcypromine	151

Therapeutic class	Drug	Frequency
Antidepressants	Citalopram	1081
Antidepressants	Escitalopram	360
Antidepressants	Fluoxetine	1540
Antidepressants	Fluvoxamine	405
Antidepressants	Paroxetine	2089
Antidepressants	Sertraline	4609
Antidepressants	Amitriptyline	1823
Antidepressants	Clomipramine	232
Antidepressants	Dothiepin	844
Antidepressants	Doxepin	947
Antidepressants	Imipramine	653
Antidepressants	Nortriptyline	224
Antidepressants	Trimipramine	167
Antidepressants	Agomelatine	0
Antidepressants	Desvenlafaxine	2
Antidepressants	Duloxetine	41
Antidepressants	Mianserin	584
Antidepressants	Mirtazapine	812
Antidepressants	Moclobemide	977
Antidepressants	Reboxetine	206
Antidepressants	Venlafaxine	1772
Antipsychotics	Amisulpride	305
Antipsychotics	Aripiprazole	206
Antipsychotics	Asenapine	0
Antipsychotics	Chlorpromazine	816
Antipsychotics	Clozapine	4657
Antipsychotics	Droperidol	307
Antipsychotics	Flupenthixol	170
Antipsychotics	Fluphenazine	364
Antipsychotics	Haloperidol	1088

Therapeutic class	Drug	Frequency
Antipsychotics	Olanzapine	1361
Antipsychotics	Paliperidone	4
Antipsychotics	Pericyazine	157
Antipsychotics	Quetiapine	594
Antipsychotics	Risperidone	1114
Antipsychotics	Sertindole	0
Antipsychotics	Trifluoperazine	427
Antipsychotics	Ziprasidone	90
Antipsychotics	Zuclopenthixol	164
Anxiolytics and hypnotics	Alprazolam	563
Anxiolytics and hypnotics	Bromazepam	80
Anxiolytics and hypnotics	Clobazam	124
Anxiolytics and hypnotics	Diazepam	3179
Anxiolytics and hypnotics	Flunitrazepam	248
Anxiolytics and hypnotics	Lorazepam	399
Anxiolytics and hypnotics	Nitrazepam	1582
Anxiolytics and hypnotics	Oxazepam	1740
Anxiolytics and hypnotics	Temazepam	2786
Anxiolytics and hypnotics	Triazolam	16
Anxiolytics and hypnotics	Buspirone	31
Anxiolytics and hypnotics	Melatonin	19
Anxiolytics and hypnotics	Zolpidem	1248
Anxiolytics and hypnotics	Zopiclone	125
Antigout	Allopurinol	3463
Antigout	Colchicine	540
Antigout	Probenecid	303
NSAIDs	Celecoxib	3882
NSAIDs	Diclofenac	2643
NSAIDs	Etoricoxib	1589
NSAIDs	Ibuprofen	1589

Therapeutic class	Drug	Frequency
NSAIDs	Indomethacin	1971
NSAIDs	Ketoprofen	3763
NSAIDs	Ketorolac	216
NSAIDs	Mefenamic	107
NSAIDs	Meloxicam	720
NSAIDs	Naproxen	2365
NSAIDs	Parecoxib	90
NSAIDs	Piroxicam	1468
NSAIDs	Sulindac	877
NSAIDs	Tiaprofenic	360
Other antirheumatics	Hydroxychloroquine	456
Other antirheumatics	Penicillamine	239
Other antirheumatics	Sulfasalazine	960

2.3.2 Multivariate Logistic Regression

Multivariate logistic regression identified 18 drugs (representing 12 drug classes) that were significantly associated with IMDILI ($P<0.00015$, Bonferroni-adjusted limit for significance) (Figure 2.2).

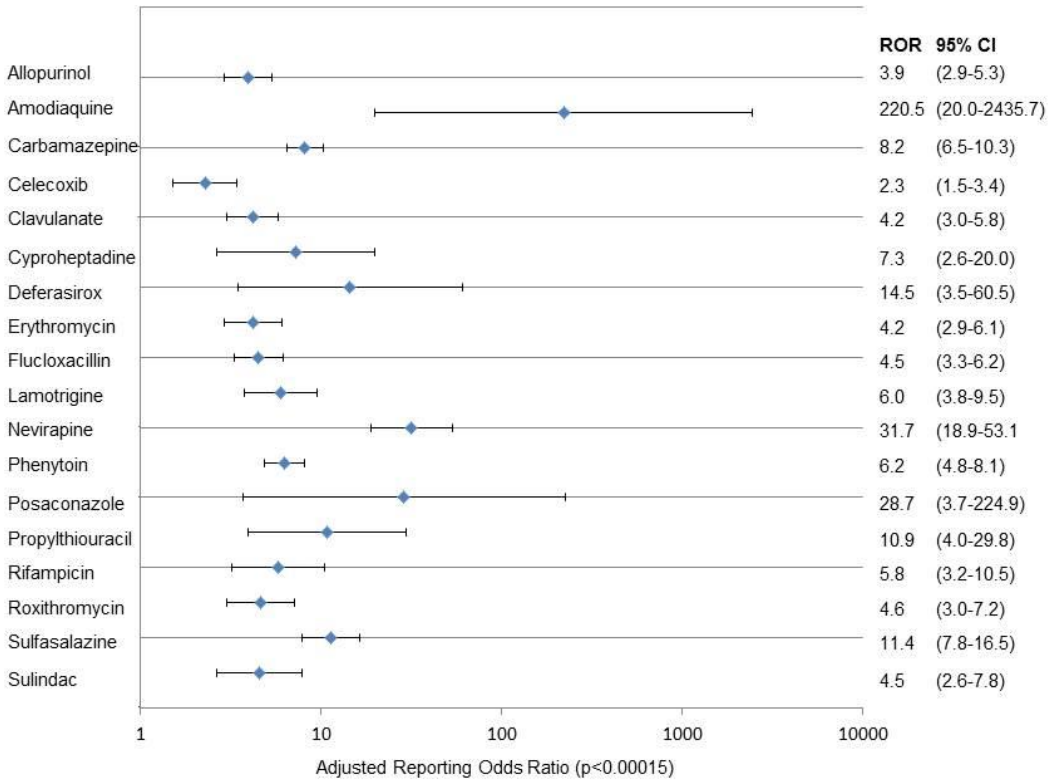

Figure 2.2 Adjusted Reporting Odds Ratio (with 95% CI) for drugs significantly associated with immune-mediated drug induced liver injury as identified from Australia's post-marketing adverse drug reaction surveillance system. (P<0.00015 – Bonferroni adjusted).

2.3.3 Antibiotics/non-antibiotic stratification

The results of the antibiotics stratification are shown in Table 2.5. The non-antibiotic IMDILI drugs group and the antibiotics group were positively correlated with IMDILI (ROR > 1), while there appears to be a negative association when antibiotics are taken concurrently with IMDILI drugs.

Table 2.5 Results of binary logistic regression for antibiotic stratification (p<0.05).

	Significance (p)	ROR
Non-antibiotic IMDILI drugs	<0.001	10.2 (8.7-12.0)
Antibiotics (excluding antibiotic IMDILI drugs)	<0.001	2.0 (1.6-2.5)
Antibiotics by IMDILI drugs	0.001	0.5 (0.3-0.8)

2.4 Discussion

As with all pharmacovigilance datasets, the present data is limited by the information contained in the spontaneous ADR case reports. The most important consideration for the present study is that one cannot be certain of the causal relationship between a drug and an ADR. This may result in the misclassification of a drug's IMDILI potential. For example, it is common for patients to be on multiple medications concurrently. In the event of an ADR, the case reporter would need to take a comprehensive medical history before attempting to identify the drug responsible for the ADR. Hence it is possible that the medication responsible for the ADR was not included in the ADR report due to either: 1) it was missed in the patient history gathering, or 2) the reporter falsely attributed the ADR to another drug and neglected to include the drug truly responsible.

Misclassification can also occur at the analytical level. Within each case report there are often multiple medications and multiple ADRs, and it can difficult to identify which drugs are responsible for particular ADRs. Since drug exposure was defined as any case report containing at least entry of the drug, it is possible that IMDILI due to a particular drug was falsely attributed to another medication within the same report.

Of the 18 drugs significantly associated with IMDILI in the analysis, 11 have been reported to cause IMDILI in the literature (Table 2.6).

Table 2.6 Evidence for IMDILI for each of the drugs identified as IMDILI through multivariate logistic regression analysis. Data is sourced from the livertox database (http://livertox.nih.gov/) which provides "up-to-date, accurate, and easily accessed information on the diagnosis, cause, frequency, patterns, and management of liver injury attributable to prescription and non-prescription medications, herbals and dietary supplements" (116).

Drug	Evidence for IMDILI from the livertox database (http://livertox.nih.gov/)
Allopurinol	Acute liver injury associated with fever, rash, eosinophilia and systemic symptoms.
Carbamazepine	Hypersensitivity reactions linked to *HLA-B*1502*. Liver involvement is common in the hypersensitivity syndrome.
Celecoxib	Hepatotoxicity may be linked to previous sulfonamide allergy. Immunoallergic features are not uncommon in presentations of liver injury.

Drug	Evidence for IMDILI from the livertox database (http://livertox.nih.gov/)
Clavulanic acid	Hepatotoxicity of amoxicillin/clavulanic acid is thought to be due to the clavulanic acid component, is linked with multiple HLA-haplotypes and associated with rash, fever, arthralgias and eosinophilia.
Flucloxacillin	Liver injury is increased in the presence of *HLA-B*5701* genotype.
Lamotrigine	Liver injury occurs as part of a systemic hypersensitivity syndrome, presenting with fever, rash, vomiting and nausea.
Nevirapine	Liver injury is more common in people with higher CD4 T cells and has been associated with HLA genotypes.
Phenytoin	Liver injury resembles immunoallergic hepatotoxicity, occurring the context of a systemic hypersensitivity syndrome.
Propylthiouracil	Liver injury has delayed onset and presentation with fever, rash and eosinophilia is not uncommon.
Sulfasalazine	Liver injury has features of hypersensitivity, including fever and rash.
Sulindac	Liver injury commonly presents with features of immunoallergic hepatitis.

Surprisingly, neither age nor sex was found to be significantly associated with IMDILI. Although increased age and female sex are known risk factors for DILI (123), it is possible that their signals were not strong enough to pass the statistical significance cut-off of 0.00015. Similarly, none of the drugs indicated for viral hepatitis were significantly associated. The final logistic regression equation did however contain 5 antibiotics. This raises the question regarding whether this is a true association of IMDILI with each antibiotic, or whether the risk of IMDILI is increased in the presence of an underlying bacterial infection, of which the antibiotics are acting as a surrogate marker.

From Table 2.5, it is noted that while patients who experienced IMDILI were more likely to have taken a non-antibiotic IMDILI drug or an antibiotic, they were less likely to have been on both a non-antibiotic IMDILI drug and an antibiotic concurrently. The high odds ratio for

the non-antibiotic IMDILI drugs is expected, since these were the drugs that were identified as significantly associated with IMDILI in the initial multivariate logistic regression. The odds ratio of 2.0 (1.6-2.5) for the antibiotics group is somewhat suprising, given that the 5 IMDILI antibiotics were excluded from this analysis. This may be evidence that the antibiotics are acting as a surrogate marker for an underlying bacterial infection which is increasing the risk of IMDILI. However, if this is the case, then one would expect a potentiation or synergistic effect between non-antibiotic IMDILI drugs and the antibiotic group, resulting in a ROR that is greater than 1 for the antibiotics by IMDILI drugs interaction term. Unexpectly, the ROR for the interaction term is 0.50 (0.33-0.76), indicating that somehow, antibiotics may have a protective effect against the hepatotoxicity induced by IMDILI drugs. Ironically, this may also be explained by the underly bacterial infection hypothesis where the antibiotic is decreasing the bacterial load in the body, thereby reducing the potentiation effect. Further investigation is required in order to clarify the role that antibiotics play in the mechanism of IMDILI.

2.5 Conclusion

The research described in this chapter has identified a set of probe drugs for IMDILI. The next steps involve searching for similarities between the biological pathways and molecular structures of these probe drugs. As such, there is a need to be certain of the IMDILI potential of each of the drugs in our probe set. For this reason, literature confirmation and refinement of toxicity classification was an important step in of the method and acted as a safety net to filter out potentially false signals generated from the pharmacovigilance data. Once their toxicity was confirmed, the drugs of interest became a powerful set of probe molecules by which to study IMDILI.

The following drugs were used as the probe set for IMDIL: allopurinol (a), carbamazepine (b), celecoxib (c), clavulanic acid (d), flucloxacillin (e), lamotrigine (f), nevirapine (g), phenytoin (h), propylthiouracil (i), sulfasalazine (j), sulindac (k).

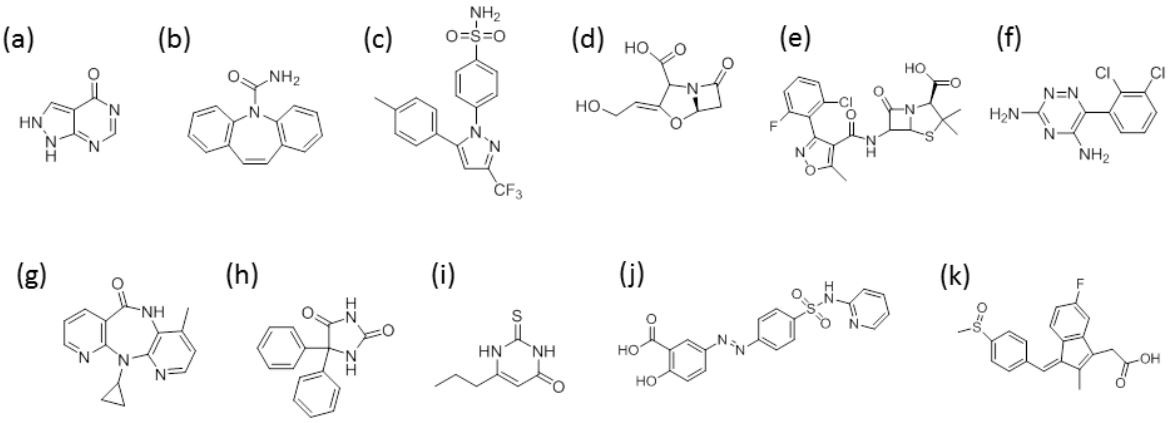

2.6 Publication

The work that was undertaken to clean the FDA database for use has been published in the journal *Pharmacoepidemiology and drug safety* (117). The full publication is presented in Appendix 1: Peer Reviewed Scientific Publications arising from this thesis.

Chapter 3: Searching for similarities: Network map tools

3.1 Introduction

There is an immense diversity in the research that is happening across the globe, ranging from the arts to the environmental sciences, computer sciences and life sciences. As the volume of data increases, the process of locating and accessing relevant information becomes exponentially more difficult. To reduce duplications and increase research efficacy, it is of vital importance not merely to be able to share information over the internet, but also to have systems in place which allow information to be searched and accessed quickly and easily.

3.1.1 The Semantic Web

The use of search engines such as Google or Yahoo is a common way by which to search for information on the internet. The results are presented as a list of links to HTML pages. Human interpretation is then required to determine which links are relevant and access the information.

The Semantic Web was envisaged by Berners-Lee as a network of data and information that is easily read and interpretable by computers (124). Rather than having human eyes sift through all the available data on the internet and using the human mind to identify relevant information, agents can be programed to extract and interpret information from various sources before presenting it in a human friendly form. An idealised application of the Semantic Web was illustrated with the example of a young couple who needed to make an appointment with a specialist doctor (124).

A software program (a semantic web 'agent') on the couple's mobile phone could go online and search for webpages of doctors with the required speciality within a certain radius of the specified postcode. From there, the agent would identify those doctors which had free appointment times which coincided with free times in the couple's calendar stored on the phone. A consolidated list of suitable doctors, the addresses of the surgeries and available appointment times would then be displayed. The aim of such an automated process would be to delegate to computers any task that does not require human judgement.

In the above example, most of the information required to make the appointment, such as doctors' addresses and available appointment times are readily available through the websites of doctors and medical centres. However, they are generally only interpretable by human readers. For example, on the doctor's webpage, a human would scroll down to find the doctor's qualifications and the hyperlink for the appointment times. Conversely, it would be very difficult for an automated process to identify which texts on the page pertained to a doctor's qualification and which links are related to appointment times.

One method to overcome this problem would be to enforce a standardised layout for all webpages, which would be impractical. Alternatively, data could be collected from various sources into a centralised repository. However, this is still restrictive and limits access to data not contained within the repository. Moreover, such a repository will quickly become unmanageable as it increases in size and scope.

The Semantic Web offers a solution by proposing a series of standards, such that computers can 'interpret' data in ways that previously required human intervention. These standards include the Resource Description Framework (RDF) format for documents and Web Ontology Language (OWL) for ontologies, which are lists defining the concepts and relationships used to describe and represent an area of concern (124,125).

RDF encodes meaning in triplets; a subject, predicate and object. For example:
<Sam> <is a> <person>.
<Sam> <is a friend of> <Dai>.
<Sam> <likes to play> <Souls>.
< Souls> <was recommended by> <Dai>.
<Souls> < is a prequel to> <Souls 2>.

The above relationships demonstrate that the same resource can be referenced multiple times. Sam is the subject three times and Souls appears as the subject of two and the object of another triple. These relationships can be also expressed as an RDF graph with the subjects and objects as nodes and the predicates as arcs (Figure 3.1).

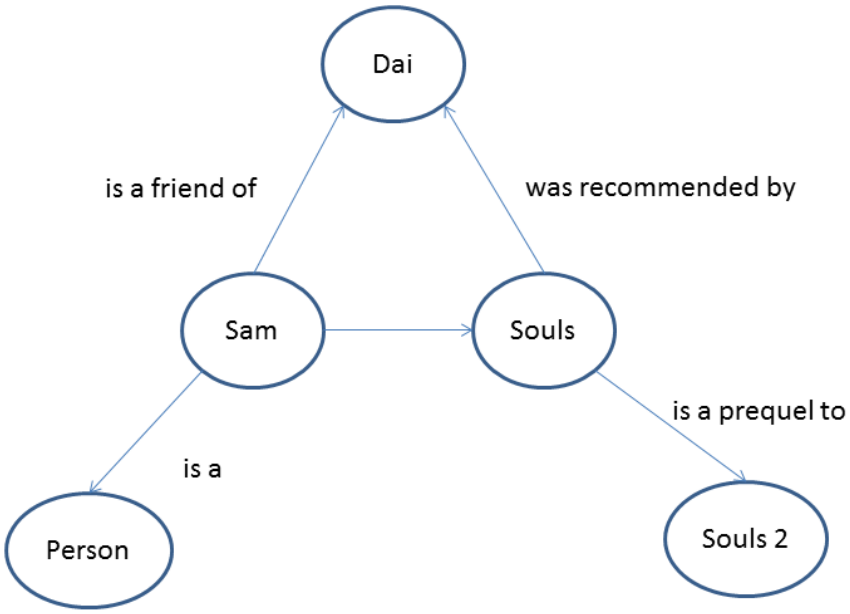

Figure 3.1 Informal graph of sample Resource Description Framework (RDF) triplets. The relationship is phrased directionally from the subject to the object.

One of the goals of implementing RDF is to allow the automatic merging of information from multiple sources (126). The use of RDF triples serves as the starting point for merging data. However, merely standardising the format is insufficient, since there are many terms which have different meanings depending on the context (*e.g.* the term 'virus' in biology compared with computing science refers to completely different things). To overcome this, RDF assigns International Resource Identifiers (IRI) to identify the specific resource to which the term refers. For example, DBpedia (127) uses IRIs of the form http://dbpedia.org/resource/Name to denote the thing described by the corresponding Wikipedia article (126). The use of IRIs to define terms grants flexibility, since new vocabularies or ontologies can be created to define new concepts.

The use of RDF has three underlying principles (126):

1. The IRIs used to name the subject, predicate and object are "global" in scope, naming the same thing each time they are used.
2. Each triple is "true" exactly when the predicate relation actually exists between the subject and the object.
3. An RDF graph is "true" exactly when all the triples in it are "true".

From these principles, systems can be designed to draw logical inferences; given a set of "true" input triples, a system can deduce that other triples must, logically, also be true.

3.1.2 Network Pharmacology

Network pharmacology challenges the traditional 'one-drug one target' drug discovery paradigm, where drugs are designed with high specificity with the aim of activating the single biological target that is responsible for the disease. In a *News and Views* article, Andrew Hopkins briefly summarises a number of studies indicating that many drugs (*e.g.* β-lactam and fluoroquinolone antibiotics, antipsychotic and cancer drugs) exhibit their pharmacological action by acting on multiple proteins (128). Moreover, studies on biological systems have revealed many built in redundancies, resulting in networks which are resilient to change. These realisations have led to the development of a paradigm shift imtowards 'systems' approaches to drug design and development (128). In this view, an understanding of the physiological network is key to identifying the nodes which must be targeted simultaneously in order to overcome the built-in redundancies.

The rise of 'systems thinking' approaches has encouraged researchers to look not only at single drug-protein interactions but to also consider the how the interaction fits into the big picture of the body's functioning. This has sparked a number of ambitious projects, including The Human Interactome Project, an initiative of the Center for Cancer Systems Biology, which seeks to characterise the protein-protein interactions between all proteins in the human body (129).

3.1.3 Data Repositories

With the rise of *omics* methodologies and technological advances, large amounts of information have become publically available on the internet. Accordingly, a number of repositories have been compiled to store and index this information (Table 3.1).

While each database summarises the relevant information for the topic of interest, the information may still be difficult to use for researchers seeking to, for example, draw links between a drug, its adverse drug reactions and biological pathways since the data is scattered across several different databases. To overcome this barrier, the information contained in various data repositories need to be linked together so that researchers can draw inferences from data spread across different sources.

The Bio2RDF project is a system that applies semantic web technology to bioinformatics databases, with one of its main goals to covert publically available databases into RDF format (130). Chem2bio2RDF (http://cheminfov.informatics.indiana.edu:8080/) is a semantic framework that builds upon the work of Bio2RDF by creating an RDF resource for integrated chemical and biological information (131). A network is created, with each node representing a data source. Nodes are linked if there is cross referencing between the data sources (131). As on May 2015, 24 databases have been linked (Table 3.1).

Table 3.1 List of databases included in Chem2bio2RDF.

Database	Type	Description
Binding Database (132)	Experimental	BindingDB is a public, web-accessible database of measured binding affinities, focusing chiefly on the interactions of proteins considered to be drug-targets with small, drug-like molecules
Binding MOAD (133)	Experimental	Binding MOAD's goal is to be the largest collection of well resolved protein crystal structures with clearly identified biologically relevant ligands, annotated with experimentally determined binding data extracted from literature.
BioGRID (134)	Organisation	An online interaction repository
Carcinogen (135)	Organisation	An international resource of the results of 6540 chronic, long-term animal cancer tests on 1547 chemicals.
ChEBI (136)	Experimental	A freely available dictionary of molecular entities focused on “small” chemical compounds
ChEMBL (137,138)	Literature	An open large-scale bioactivity database.
Comparative Toxicogenomics Database (CTD) (139)	Literature	Provides manually curated information about chemical–gene/protein interactions, chemical–disease and gene–disease relationships.

Database	Type	Description
Drug Combination Database (DCDB) (140,141)	Literature	A database devoted to the research and development of multi-component drugs.
Database of Interacting Proteins (DIP) (142)	Experimental	Catalogues experimentally determined interactions between proteins.
DrugBank (143)	Literature	A unique bioinformatics and cheminformatics resource that combines detailed drug data with comprehensive drug target information.
UNIPROT (144)		A catalogue of information on proteins.
HUGO Gene Nomenclature Committee (HGNC) (145)	Organisation	A committee responsible for approving unique symbols and names for human loci, including protein coding genes, ncRNA genes and pseudogenes.
Human Protein Reference Database (HPRD) (146,147)	Literature	Represents a centralised platform to visually depict and integrate information pertaining to domain architecture, post-translational modifications, interaction networks and disease association for each protein in the human proteome.
KEGG: Kyoto Encyclopaedia of Genes and Genomes (148)	Literature	A database resource for understanding high-level functions and utilities of the biological system.
PDSP (149)	Literature	A database of K_i values for receptors and targets.
Manually Annotated Targets and Drugs Online Resource (MATADOR) (150,151)	Literature	A resource for protein-chemical interactions.

Database	Type	Description
Online Mendelian Inheritance in Man (OMIM) (152)	Literature	An Online Catalogue of Human Genes and Genetic Disorders
Protein Data Bank in Europe (PDBe)	Literature	The European resource for the collection, organisation and dissemination of data on biological macromolecular structures
PharmGKB (153)	Literature	A comprehensive resource that curates knowledge about the impact of genetic variation on drug response for clinicians and researchers.
PubChem (154,155)	Experimental	A bioassay collection.
PubMed (156)	Literature	A collection of citations for biomedical literature from MEDLINE.
Reactome (157)	Literature	A free, open-source, curated and peer reviewed pathway database.
SIDER (158)	Literature	Contains information on marketed medicines and their recorded adverse drug reactions. The information is extracted from public documents and package inserts.
Therapeutic Target Database (TTD) (159)	Literature	Provides information about the known and explored therapeutic protein and nucleic acid targets, the targeted disease, pathway information and the corresponding drugs directed at each of these targets.

3.1.4 Semantic Link for Association Prediction (SLAP)

Semantic Link for Association Prediction (SLAP) is a Drug Target Prediction tool developed by the creators of Chem2Bio2RDF (1). Network pharmacology proponents have already stressed the importance profiling the effects of drugs on multiple protein targets (160). Large scale analyses of the effects of drugs on biological pathway systems are needed to

reveal the relationships between ADRs and protein targets (131). These analyses are facilitated by the use of semantic linked data, such as the Chem2Bio2RDF repository (1).

Using knowledge of existing links, 'missing' links between nodes can sometimes be predicted by comparing the topology of nodes, such as sharing a certain number of neighbouring nodes or similar shortest paths between nodes. These concepts are commonly utilised in social media and advertising contexts. For example, social media programs may suggest people as 'friends' based on the number of 'mutual friends' and supermarkets may conduct targeted advertising based on a consumer's purchasing history.

SLAP is a statistical model which queries a heterogeneous network of 290,000 nodes and 720,000 edges containing data on drug target interactions. Drug-target interaction information were extracted from datasets included in the Chem2Bio2RDF set (1). 'Missing links' in the network, *i.e.* drug-protein interactions for which there is as yet no experimental evidence, are predicted based on analysing the topology of neighbouring nodes. The strength of the predicted association is reported as an association score, which is calculated from the number of shortest paths and the properties of the links between the nodes (1).

The SLAP methodology was validated by comparing the association scores of 1000 known drug target pairs from DrugBank (143) with that of 1000 random pairs of drugs and targets sampled from DrugBank. For each drug target pair, their direct link was first removed, so that only the neighbourhood properties were used in the score calculation (1).

SLAP was able to correctly identify drug-target pairs in the data and was shown to outperform similar link prediction methods used in social networking (1). The method offers the advantage of considering pathway relationships from a systems level, rather than just known binding affinity data. In addition to direct drug target interactions, SLAP is also capable of identifying indirect interactions, such as changes in gene expression levels. Hence it is a useful tool with which to compare the biological functions of drugs.

SLAP is publically available online at http://cheminfov.informatics.indiana.edu:8080/slap/. Compounds can be queried by drug name, SMILES string or their PubChem ID. Proteins can be queried by their name, UniProt ID or Gene Symbol. Results are presented in tabular

format, listing known and predicted interactions along with an association score calculated by SLAP.

3.1.5 Search Tool for InTeracting CHemicals (STITCH)

The Search Tool for InTeracting CHemicals (STITCH) is another searchable, online database of known and predicted interactions between chemicals and proteins (161). A consolidated set of chemicals was derived from the PubChem database. Associations between chemicals were classified into 4 groups: reactions from pathway databases, literature associations, similar structures and similar activities (161). Chemical-protein interactions were imported from the PDSP K_i Database and the Protein Data Bank (PDB). Interactions between metabolites and proteins were extracted pathway databases such as KEGG, Reactome and the NCI-Nature Pathway Interaction Database. Drug target relations were imported from DrugBank and MATADOR. Literature associations were obtained by text-mining the MEDLINE and OMIM databases. The full list of databases included in STITCH is presented in Table 3.2.

Table 3.2 List of databases included in STITCH 4.0.

Database	Description
ChEMBL (137)	A freely available dictionary of molecular entities focused on "small" chemical compounds
PDSP (149)	A database of K_i values for receptors and targets.
Protein Data Bank (PDB) (162)	An information portal to biological macromolecular structures.
DrugBank (143)	A unique bioinformatics and cheminformatics resource that combines detailed drug data with comprehensive drug target information.
GLIDA (163)	A database for those who work in the field of GPCRs-related drug discover

Database	Description
	and need information on both GPCRs and their known ligands.
Manually Annotated Targets and Drugs Online Resource (MATADOR) (150,151)	A resource for protein-chemical interactions.
Therapeutic Target Database (TTD) (159)	Provides information about the known and explored therapeutic protein and nucleic acid targets, the targeted disease, pathway information and the corresponding drugs directed at each of these targets
Comparative Toxicogenomics Database (CTD) (139)	Provides manually curated information about chemical–gene/protein interactions, chemical–disease and gene–disease relationships.
KEGG: Kyoto Encyclopaedia of Genes and Genomes (148)	A database resource for understanding high-level functions and utilities of the biological system.
NCI/Nature Pathway Interaction Database (164)	Biomolecular interactions and cellular processes assembled into authoritative human signalling pathways
Reactome (157)	A free, open-source, curated and peer reviewed pathway database.
BioCyc (165)	A collection of 5711 Pathway/Genome Databases (PGDBs) plus software tools for understanding their data.

The STITCH database is publically available at the web portal http://stitch.embl.de/.Drugs can be entered by chemical name or generic name. STITCH returns the top predicted interacting partners in tabular format. The output from STITCH can be viewed in Confidence

View, where stronger associations are represented by thicker lines; Evidence View, where different coloured lines are used to represent the type of evidence for the interaction and Actions View, where modes of action are differentiated by colour. Associations between chemicals and proteins are predicted by text mining of the scientific literature, and the results are ranked by a confidence score.

Databases which contain manually annotated interactions receive high sores and interactions based on experimental information are scored by the confidence or relevance of the reported information (161).

STITCH is a well-known source of data and is queried more than 100 times each week (166), and has been used in published studies including those to identify targets of anti-tuberculosis compounds in *Mycobacterium tuberculosis* (167), study the conservation of protein-chemical interactions between yeast species (168) and as a benchmark for predicted drug-target interactions (169,170).

3.2 Rationale

From Chapter 2, a number of drugs that are implicated in IMDILI have been identified. Once ingested, each of these drugs will pass through the pharmacokinetic stages of absorption, disposition, metabolism and excretion. Through these processes the drug will interact with many biological proteins, in addition to the protein interactions that occur as part of the drug's pharmacological action. Logically, adverse drug reactions to the drug must be initiated by one or more of these interactions. By comparing the known and predicted interactions with each of the IMDILI probe drugs and examining the interactions that are common between the drugs, it should be possible to identify potential toxicity targets involved in the pathogenesis of IMDILI (Figure 3.2). In light of the current hypotheses regarding the mechanisms behind IMDILI, it is hypothesised that interactions with proteins involved in the activation of the immune system would be shared among a high proportion of the investigated drugs.

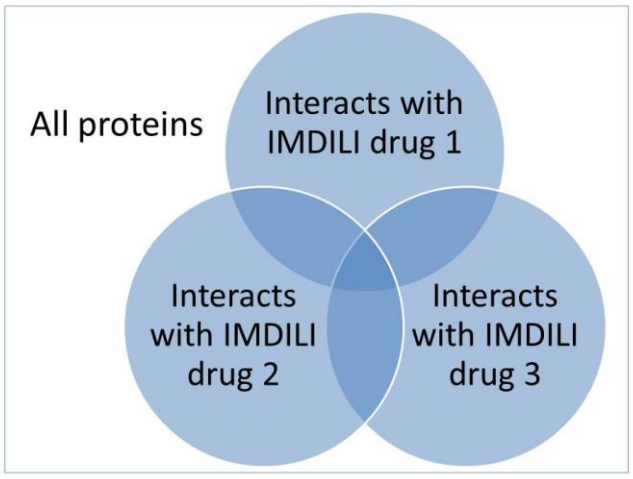

Figure 3.2 Schematic representation of the methodological approach. When ingested, each drug will interact with various body proteins. By comparing the known and predicted interactions with each of our IMDILI probe drugs, and examining the interactions that are common, it should be possible to identify potential toxicity targets involved in the pathogenesis of IMDILI.

3.3 Methods

3.3.1 SLAP for Drug Target Prediction

The Pubchem Compound Identifiers of the probe IMDILI set of drugs (allopurinol, carbamazepine, celecoxib, clavulanic acid, flucloxacillin, lamotrigine, nevirapine, phenytoin, propylthiouracil, sulfasalazine, sulindac) were obtained. These were then used to query the SLAP tool for Drug Target Prediction (http://cheminfov.informatics.indiana.edu:8080/slap/).

3.3.2 STITCH 4.0

Each of the IMDILI set of drugs was entered by name into the STITCH 4.0 web portal (http://stitch.embl.de/).

STITCH was asked to return at most 50 predicted functional partners in Homo sapiens. Interactions are only listed if they are of at least medium confidence (score > 0.400).

3.1 Results

SLAP and STITCH identified a total of 333 known and predicted protein interaction partners for the probe set of IMDILI drugs. 58 proteins were identified by both the SLAP and STITCH analyses. 110 proteins were identified by the SLAP analysis only. 165 proteins were identified by the STITCH analysis only. The full list of identified proteins and a brief description of their function is presented in Appendix 2: Consolidated list of proteins.

3.1.1 SLAP for Drug Target Prediction

The 284 incidences of interactions between dug set and the 165 proteins identified by SLAP to be known and predicted interacting partners with the IMDILI probe set of drugs are summarised in Table 3.3. The full list of known and predicted proteins, along with the SLAP association score, is presented in Appendix 3: Results of SLAP.

No protein interactions were predicted for clavulanic acid, flucloxacillin, nevirapine and sulindac. Celecoxib had the highest number of known and predicted interactions at 126, followed by carbamazepine with 63 predicted interactions; lamotrigine with 41 and phenytoin with 34.

The highest number of probe IMDILI drugs predicted to interact with a particular protein was 4. There were six proteins with 4 interactions; ABCB1, ABCC2 CYP3A4, HRH1, KCNH2 and SCN1A. The same 4 drugs were predicted to interact with each of these proteins: carbamazepine, celecoxib, lamotrigine and phenytoin.

Table 3.3 Summary of the SLAP results, showing the proteins which are known and predicted to interact with the IMDILI probe set of drugs.

	allopurinol	carbamazepine	celecoxib	clavulanic acid	flucloxacillin	lamotrigine	nevirapine	phenytoin	propylthiouracil	sulfasalazine	sulindac	Total
ABCB1		1	1			1		1				4
ABCB11		1										1
ABCC1		1				1		1				3
ABCC2		1	1			1		1				4
ABCC4			1									1
ABCG2		1				1		1				3
ADAM17			1									1
ADRA1A			1			1						2
ADRA1B			1									1
ADRA1D			1									1
ADRA2A		1	1									2

	allopurinol	carbamazepine	celecoxib	clavulanic acid	flucloxacillin	lamotrigine	nevirapine	phenytoin	propylthiouracil	sulfasalazine	sulindac	Total
ADRA2B			1									1
ADRA2C			1									1
ADRB1			1									1
ADRB2			1									1
AKT1			1									1
AKT2			1									1
ALOX5			1									1
AR		1	1									2
ASL			1									1
BCL2			1									1
BCL2L1			1									1
CA1			1							1		2
CA10			1									1
CA11			1							1		2
CA12			1							1		2
CA13			1							1		2
CA14			1							1		2
CA2			1							1		2
CA3			1							1		2
CA4			1							1		2
CA5A			1							1		2
CA5B			1							1		2
CA7			1							1		2
CA8			1									1
CA9			1							1		2
CACNA1C						1		1				2

	allopurinol	carbamazepine	celecoxib	clavulanic acid	flucloxacillin	lamotrigine	nevirapine	phenytoin	propylthiouracil	sulfasalazine	sulindac	Total
CACNA1D						1						1
CACNA1F						1						1
CACNA1G						1		1				2
CACNA1H						1		1				2
CACNA1I						1		1				2
CACNA1S						1						1
CALM1						1						1
CASP1			1									1
CASP3			1									1
CASP7			1									1
CCL2			1									1
CCND1			1									1
CCR5			1			1						2
CDK2			1									1
CDK4			1									1
CHRM1			1									1
CHRM2			1									1
CHRM3			1									1
CHRM4			1									1
CHRM5			1									1
CHRNA7		1	1									2
CNR1			1									1
CNR2			1									1
CYP11B1		1										1

	allopurinol	carbamazepine	celecoxib	clavulanic acid	flucloxacillin	lamotrigine	nevirapine	phenytoin	propylthiouracil	sulfasalazine	sulindac	Total
CYP17A1		1						1				2
CYP19A1		1	1					1				3
CYP1A2		1	1						1			3
CYP2A6		1						1				2
CYP2B6		1	1					1				3
CYP2C18		1										1
CYP2C8		1	1					1				3
CYP2C9		1	1					1				3
CYP3A4		1	1			1		1				4
CYP4A11								1				1
DDC			1									1
DHFR						1						1
DRD1		1	1			1						3
DRD2		1	1			1						3
DRD3		1	1									2
DRD4		1	1									2
DRD5		1	1									2
EPHX2		1						1				2
ESR1		1										1
FGF1			1									1
FGF2			1									1
FPR1		1				1		1				3
GRIN2B						1						1
GSTA1		1										1
GSTM1		1										1
GSTP1		1	1									2
HNMT			1									1

	allopurinol	carbamazepine	celecoxib	clavulanic acid	flucloxacillin	lamotrigine	nevirapine	phenytoin	propylthiouracil	sulfasalazine	sulindac	Total
HRH1		1	1			1		1				4
HRH2			1									1
HRH3			1									1
HRH3						1						1
HRH4			1									1
HTR1A		1	1									2
HTR1B		1	1									2
HTR1D		1	1									2
HTR1E		1	1									2
HTR1F		1	1									2
HTR2A		1										1
HTR2A			1			1						2
HTR2B		1	1									2
HTR2C		1	1			1						3
HTR3A		1	1									2
HTR4		1	1									2
HTR6		1	1									2
HTR7		1	1									2
IL1B	1		1							1		3
JUN		1								1		2
KCNH2		1	1			1		1				4
KCNMA1			1									1
KCNQ1						1						1
MAOA		1										1
MAPK1			1									1
MAPK12			1									1
MAPK14			1									1

	allopurinol	carbamazepine	celecoxib	clavulanic acid	flucloxacillin	lamotrigine	nevirapine	phenytoin	propylthiouracil	sulfasalazine	sulindac	Total
MMP1			1									1
MMP11			1									1
MMP13			1									1
MMP14			1									1
MMP2			1									1
MMP3			1									1
MMP7			1									1
MMP8			1									1
MMP8										1		1
MMP9			1									1
NFKB1		1	1							1		3
NFKB2		1	1							1		3
NISCH			1									1
NR1I2		1						1				2
NR1I3		1										1
NR3C1		1										1
NR3C2		1										1
OPRK1			1									1
OPRM1			1									1
PDPK1			1									1
PGR		1	1					1				3
PLA2G4A			1									1
PNMT			1									1
PPARA			1									1
PPARD			1									1
PPARG			1									1
PRKACA			1									1

	allopurinol	carbamazepine	celecoxib	clavulanic acid	flucloxacillin	lamotrigine	nevirapine	phenytoin	propylthiouracil	sulfasalazine	sulindac	Total
PTGER1			1									1
PTGER2			1									1
PTGER3			1									1
PTGER4			1									1
PTGS1		1										1
PTGS1			1									1
PTGS2		1	1									2
ROCK1			1									1
ROCK2			1									1
SCN10A		1				1		1				3
SCN11A						1		1				2
SCN1A		1	1			1		1				4
SCN1B						1		1				2
SCN2A		1				1		1				3
SCN2B						1		1				2
SCN3A		1				1		1				3
SCN3B						1		1				2
SCN4A		1				1		1				3
SCN4B						1		1				2
SCN5A		1				1		1				3
SCN9A		1				1		1				3
SLC12A1			1									1
SLC12A3			1									1
SLC22A6			1									1
SLC6A2						1						1
SLC6A3			1			1						2
SLC6A4		1	1			1						3

	allopurinol	carbamazepine	celecoxib	clavulanic acid	flucloxacillin	lamotrigine	nevirapine	phenytoin	propylthiouracil	sulfasalazine	sulindac	Total
TNF			1									1
TP53		1	1									2
TPH1			1							1		2
TOTAL:	1	63	126	0	0	41	0	34	1	18	0	284

3.1.2 STITCH 4.0

The 327 incidences of interactions with the 223 proteins identified by STITCH to be known and predicted interacting partners with the IMDILI probe set of drugs are summarised in Table 3.4. The full list of known and predicted proteins, along with the SLAP association score, is presented in Appendix 4: Results from STITCH 4.0. An example of the output is show in Figure 3.3.

Celecoxib and sulindac had the highest number of known and predicted interactions at 50 each, followed by phenytoin with 48 and carbamazepine with 42.

The highest number of probe IMDILI drugs predicted to interact with a particular protein was 7. This was attained by CYP3A4, which was predicted to interact with carbamazepine, celecoxib, flucloxacillin, lamotrigine, nevirapine, phenytoin and propylthiouracil.

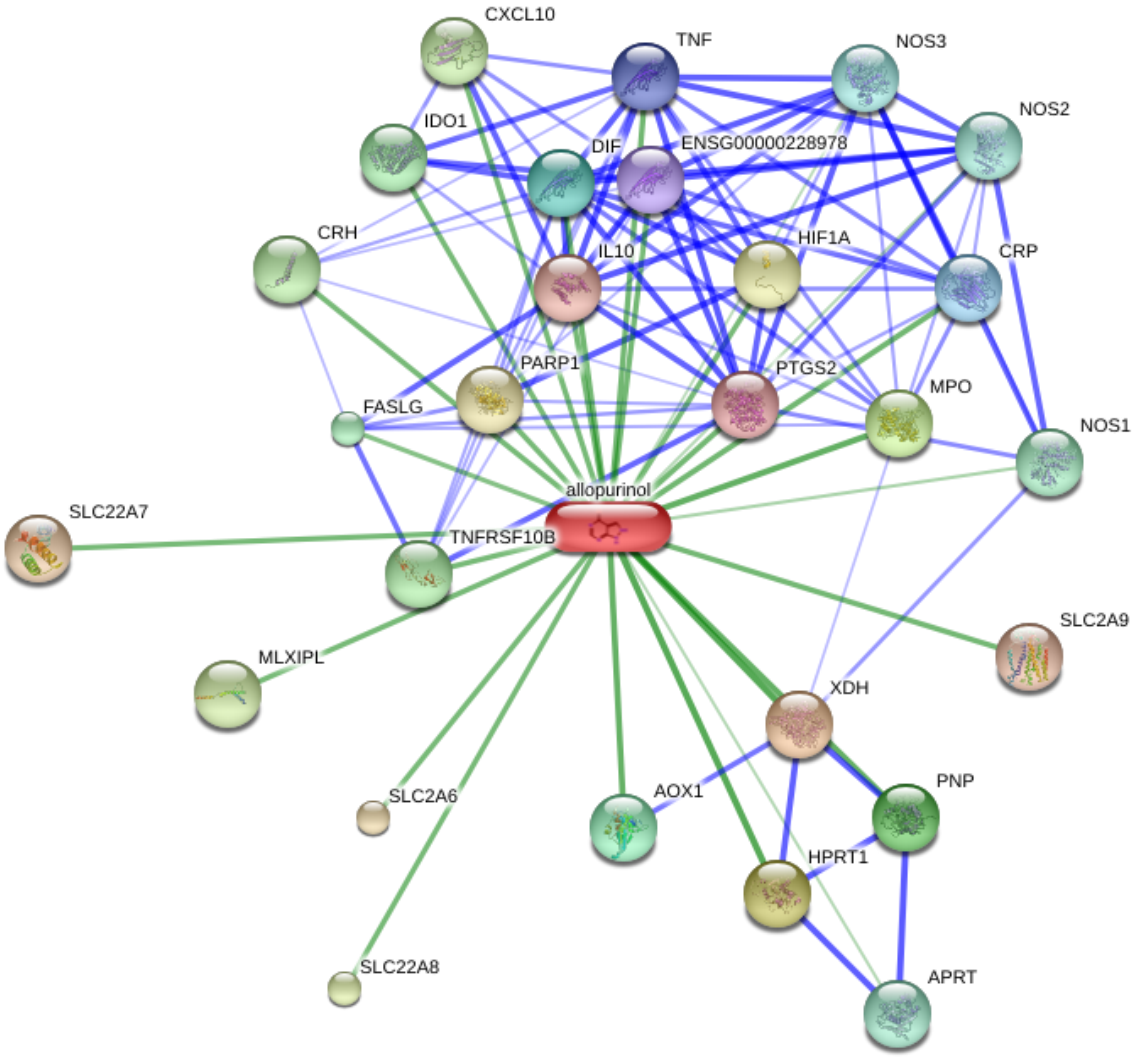

Figure 3.3 Predicted protein functional partners for allopurinol as determined by STITCH 4.0.

Table 3.4 Summary of the STITCH 4.0 results, showing the proteins which are known and predicted to interact with the IMDILI probe set of drugs.

	allopurinol	carbamazepine	celecoxib	clavulanic acid	flucloxacillin	lamotrigine	nevirapine	phenytoin	propylthiouracil	sulfasalazine	sulindac	Total
ABCB1		1				1		1				3
ABCC1			1									1
ABCC2		1						1		1		3
ABCC4			1									1

	allopurinol	carbamazepine	celecoxib	clavulanic acid	flucloxacillin	lamotrigine	nevirapine	phenytoin	propylthiouracil	sulfasalazine	sulindac	Total
ABCG2										1		1
ACAT1										1		1
AKR1C1											1	1
AKR1C2											1	1
AKR1C3											1	1
AKT1			1									1
ALB			1					1				2
ALOX15										1		1
ALOX15B										1		1
ALOX5			1							1		2
ALOX5AP										1		1
AOX1	1											1
APRT	1											1
AR			1									1
ATIC										1		1
BAX											1	1
BDNF		1										1
BIRC5											1	1
C8orf4											1	1
CA12			1									1
CA13			1									1
CA2			1									1
CA5B			1									1
CA6			1									1
CA9			1									1
CASP3			1							1	1	3
CASP8			1								1	2

	allopurinol	carbamazepine	celecoxib	clavulanic acid	flucloxacillin	lamotrigine	nevirapine	phenytoin	propylthiouracil	sulfasalazine	sulindac	Total
CASP9			1							1		2
CAV1			1									1
CCND1			1								1	2
CD248				1								1
CD4							1					1
CD59				1								1
CD79A									1			1
CDIPT				1								1
CDK2			1									1
CDKN1A			1								1	2
CFLAR			1									1
CHUK										1		1
CRH	1								1			2
CRP	1									1		2
CTNNB1											1	1
CTSB								1				1
CTSL1								1				1
CXCL10	1											1
CYP11B1								1				1
CYP17A1		1				1						2
CYP19A1			1			1		1				3
CYP1A1									1		1	2
CYP1A2		1					1				1	3
CYP2A13								1				1
CYP2A6						1	1					2
CYP2B6		1				1	1	1				4
CYP2C18		1						1				2

	allopurinol	carbamazepine	celecoxib	clavulanic acid	flucloxacillin	lamotrigine	nevirapine	phenytoin	propylthiouracil	sulfasalazine	sulindac	Total
CYP2C19		1						1				2
CYP2C8		1	1					1				3
CYP2C9		1	1				1	1				4
CYP2D6			1				1	1				3
CYP2D7P1								1				1
CYP2E1						1		1				2
CYP3A4		1	1		1	1	1	1	1			7
CYP3A43		1										1
CYP3A5		1					1	1		1		4
CYP3A7		1					1	1				3
DBH						1			1			2
DDIT3			1									1
DGCR2			1									1
DIABLO											1	1
DIF	1		1									2
DIO1									1			1
DIO2									1			1
DIO3									1			1
DPH2								1				1
DPH3								1				1
DRD2						1						1
EGFR			1								1	2
EGR1											1	1
ENSG00000167494										1		1
ENSG00000168937										1		1

	allopurinol	carbamazepine	celecoxib	clavulanic acid	flucloxacillin	lamotrigine	nevirapine	phenytoin	propylthiouracil	sulfasalazine	sulindac	Total
ENSG00000204490										1		1
ENSG00000228978	1											1
EPHX1		1										1
EPX									1			1
ERBB2		1									1	2
FASLG	1											1
FASN			1									1
FMO3											1	1
G6PD									1			1
GDF15			1								1	2
GNAT3									1			1
GNLY						1						1
GSTM1		1										1
HDAC3		1										1
HIF1A	1									1		2
HLA-C					1							1
HMBS		1										1
HPRT1	1											1
HSD3B2		1				1						2
HSPA5											1	1
ICAM1			1							1		2
IDO1	1											1
IGF1R			1									1
IKBKB										1	1	2
IL10	1											1

	allopurinol	carbamazepine	celecoxib	clavulanic acid	flucloxacillin	lamotrigine	nevirapine	phenytoin	propylthiouracil	sulfasalazine	sulindac	Total
IL1A			1					1				2
IL1B										1		1
IL6			1				1					2
ILK											1	1
IMPA1		1										1
INS			1				1	1				3
ITGA2								1				1
JUN			1									1
KCNA5									1			1
KCNH2						1		1				2
KCNK18						1						1
LEF1											1	1
MAPK1								1				1
MAPK14			1									1
MAPK3								1			1	2
MAPK8											1	1
MC2R						1						1
MDK											1	1
MGMT								1				1
MLXIPL	1											1
MMP7											1	1
MMP9			1							1		2
MPO	1								1	1		3
MTHFR										1		1
NAT2										1		1
NFKB1											1	1
NFKB2										1		1

	allopurinol	carbamazepine	celecoxib	clavulanic acid	flucloxacillin	lamotrigine	nevirapine	phenytoin	propylthiouracil	sulfasalazine	sulindac	Total
NFKBIA								1		1	1	3
NFKBIZ								1				1
NOS1	1							1				2
NOS2	1									1		2
NOS3	1											1
NR1I2		1						1				2
NR1I3								1				1
NR3C1						1						1
ODC1									1			1
ORM1		1										1
ORM2		1										1
PARP1	1										1	2
PCNA			1									1
PDPK1			1									1
PLAU			1									1
PNP	1											1
POMC		1										1
PPARD											1	1
PPARG			1							1		2
PPIG		1						1				2
PRB3									1			1
PTEN									1			1
PTGER4											1	1
PTGS1			1							1	1	3
PTGS2	1		1							1	1	4
PTH								1				1
RALBP1		1										1

	allopurinol	carbamazepine	celecoxib	clavulanic acid	flucloxacillin	lamotrigine	nevirapine	phenytoin	propylthiouracil	sulfasalazine	sulindac	Total
RELA										1	1	2
REN									1		1	2
S100A4											1	1
SAT1											1	1
SCN10A		1				1		1				3
SCN11A		1				1		1				3
SCN1A		1				1		1				3
SCN1B		1						1				2
SCN2A						1		1				2
SCN2B		1										1
SCN3A		1				1		1				3
SCN4A		1				1		1				3
SCN5A		1				1		1				3
SCN7A		1				1		1				3
SCN8A		1				1		1				3
SCN9A		1				1						2
SERPINA7									1			1
SHBG		1						1				2
SLC22A1											1	1
SLC22A11											1	1
SLC22A2											1	1
SLC22A6											1	1
SLC22A7	1										1	2
SLC22A8	1											1
SLC2A6	1											1
SLC2A9	1											1
SLC46A1										1		1

	allopurinol	carbamazepine	celecoxib	clavulanic acid	flucloxacillin	lamotrigine	nevirapine	phenytoin	propylthiouracil	sulfasalazine	sulindac	Total
SLC7A11										1		1
SLCO1C1								1				1
SP1			1								1	2
SRC											1	1
SST		1						1				2
ST6GAL1					1							1
STAR									1			1
STAT3											1	1
SULT1E1											1	1
TAS2R1									1			1
TAS2R10									1			1
TAS2R14									1			1
TAS2R30									1			1
TAS2R38									1			1
TAS2R4									1			1
TBXAS1										1		1
TFAP2A		1										1
TG									1			1
THRA										1		1
TMSB10									1			1
TNF	1		1									2
TNFRSF10B	1		1								1	3
TNFRSF1B										1		1
TNFSF10											1	1
TPO									1			1
TRH									1			1
TSHR									1			1

	allopurinol	carbamazepine	celecoxib	clavulanic acid	flucloxacillin	lamotrigine	nevirapine	phenytoin	propylthiouracil	sulfasalazine	sulindac	Total
UGT1A3						1						1
UGT1A4						1						1
UGT2B7		1										1
VEGFA			1									1
VEGFC			1									1
XDH	1											1
YWHAE											1	1
TOTAL:	27	42	50	3	3	27	11	48	30	36	50	327

3.2 Discussion

Although SLAP incorporates more databases than STITCH, overall STITCH predicted more protein interacting partners than SLAP. This is an unexpected result since most the databases included in STITCH are also included in the SLAP set.

Even more surprising is the small degree of overlap between the predicted proteins. Given the substantial number of data sources, one would expect similar proteins to be predicted as interacting partners for each drug. In contrast, substantial differences were apparent in the number of proteins reported for each drug and also the proteins that were returned, with only 17-20% concordance between the two search tools.

These discrepancies may be due to the differences in how predicted functional partners are calculated; SLAP bases calculations on the topology of the nodes in the network while STITCH extracts interaction data from the indexed data sources and full-text articles freely available from PubMed Central or publishers' websites (2).

Metabolic enzymes, such as the cytochrome P450 enzymes, and drug transporters had the highest number of interactions. This is not unexpected, given that these are enzymes known

to process large numbers of drugs. Even then the majority of identified proteins were only thought to interact with 3 or 4 of the 11 IMDILI drugs included in the analyses. Moreover, these 3-4 drugs tend to be of the same therapeutic class (*e.g.* carbamazepine, lamotrigine and phenytoin from the SLAP results). This suggests that these proteins are shared because of the drugs' common pharmacological action, rather than a toxicological pathway. No protein targets were found to be common to all the drugs in the probe set.

3.3 Conclusion

In this chapter, the known and predicted protein interactions for each of the IMDILI probe drugs were examined. However, due to the apparent lack of overlap between protein interactions, it is difficult to ascertain whether any of the known and predicted proteins associated with the IMDILI probe set of drugs are potential toxicity targets involved in the pathogenesis of IMDILI.

Nevertheless, large scale drug-target prediction tools such as SLAP and STITCH are important resources for the research community due to their ability to search and integrate well-known publically available databases. The results from the use of these search tools can be unexpectedly varied and hence further investigations, such as *in vitro* assays, are needed to confirm whether the predicted proteins for the input drugs are true drug-target pairs.

Chapter 4: Searching for similarities: Pharmacophore modelling

4.1 Computer Aided Drug Design

Technological advances in the past two decades have seen the rise of computer aided drug design where state-of-the art technologies are used to speed up the process of drug-design and development (171). While traditional approaches relied on trial and error to uncover pharmacologically active compounds, computer aided drug design utilises structure-based and/or ligand-based screening for specific targets. This allows for more efficient and cost effective drug discovery.

Powerful tools, such as X-ray crystallography and Nuclear Magnetic Resonance spectroscopy (NMR) have characterised the structure of many biological molecules. Knowledge of the structure of biological targets allows for the use of structure-based computer aided drug design techniques. The interaction between ligands and targets can be studied to aid in the identification of other molecules with activity on the target. Moreover, by establishing the mode of binding, new compounds can be designed with the required functional groups to agonise/antagonise the target site.

However, the structure of the receptor is not always available in these situations; hence the use of ligand-based computer aided drug design techniques is required to create models by comparing characteristics of known and active ligands.

While seemingly unusual, there has been growing interest in the use of *in silico* drug design technologies in toxicology. New computational technologies are transforming the field of regulatory science, with the FDA working towards replacing animal studies with a combination of *in silico* and *in vitro* approaches (92).

Ursem and colleagues, in work led by the US Food and Drug Administration (FDA), recently combined pharmacovigilance data with *in silico* QSAR modelling techniques (172–174) to generate predictive models for idiosyncratic hepatobiliary and urinary tract adverse reactions. Toxicity was classified by clustering adverse event terms under broad endpoints (*e.g.* liver disorder) and drug-event association signals were quantified using disproportionality analysis. This information was subsequently used to create QSAR models which predicted drug induced hepatobiliary and urinary tract toxicity in humans with low to

moderate sensitivity (172). The researchers propose that this approach has utility in directing or prioritising pharmacovigilance activities by regulators, sponsors and researchers. While this application of QSAR promises to be a useful decision-support tool in drug development, the toxicity signals used to develop QSAR models were derived from broad toxicity endpoints which may arise from interactions of different molecules with different targets and pathways. These models therefore do not necessarily shed light on the mechanisms underlying the toxicity.

4.1.1 Quantitative Structure Activity Relationships

Both a drug's pharmacodynamics (the drug's action on the body) and pharmacokinetic (the body's action on the drug) properties are based on the drug's physiochemical properties, which in turn are derived from the drug's molecular structure. Recognition of this led to the development of Quantitative Structure Activity Relationships (QSAR) (175).

In QSAR modelling, the physicochemical properties of compounds are quantified into a number of QSAR descriptors. These can be grouped into measures of steric, electrostatic and hydrophobicity (Table 4.1).

Regression analyses can then be used to estimate the relationship between the dependent variable, typically biological activity, with the independent variables, which are the QSAR descriptors (Equation 5). Techniques such as multiple linear regression and principle component analysis assign coefficients to the variables in the equation, quantifying the impact of each descriptor on biological activity.

Table 4.1 Examples of Quantitative Structure Activity Relationship (QSAR) descriptors (176).

Property grouping	Examples of QSAR descriptors
Steric	van der Waals radii; molecular volume, surface area; molecular weight; hashed fingerprints; structural keys; counts of specific atoms, rings or other features; molecular connectivity χ indices; atom pairs topological torsions; polar surface area
Electrostatic	Polarity, ionisation properties; calculated molar refractivity; κ shape indices; electrotopological indices; dipole moment
Hydrophobic	cLogP; octanol/water partition coefficient

General QSAR equation

$$Biological\ activity = f(physicochemical\ properties) \qquad (5)$$

Once a model has been built using a set of molecules (the training set), it needs to be validated on a test set of molecules. A leave-one-out or leave-some-out cross-validation can be used where a subset of the training set will be 'left out' during the model creation process and used as the test set. The process is then systematically repeated using a different subset until all molecules of the training set have been 'left out'. The cross-validation process provides some measure of the predictive ability and robustness of the model. The cross-validated correlation coefficient q^2 is calculated by Equation 6. A QSAR model with a high q^2, ($q^2 > 0.5$) is considered by some researchers to be highly predictive (177). Once statistical stability has been achieved, *i.e.* the model is a good predictor of training set data, the model can then be externally validated with a group of molecules not used in generating the model (177).

Cross-validated correlation coefficient (q^2). y_i, $\hat{y}_i$, $\bar{y}_i$, are the actual, estimated and average activities respectively.

$$q^2 = 1 - \frac{\Sigma(y_i - \hat{y}_i)^2}{\Sigma(y_i - \bar{y}_i)^2} \qquad (6)$$

Fragment based 2D QSAR methods are examples of advances in QSAR modelling which have built upon the traditional method described above. Hologram QSAR (HQSAR) splits compounds into molecular fragments. These fragments contain topological and compositional information regarding the molecule and hence can be used as structural descriptors as part of the QSAR equation (178).

The QSAR methods described so far are what have been termed 2D QSAR methods since all the descriptors can be calculated from the molecular formula alone. Unlike 2D QSAR methods, 3D QSAR approaches require knowledge of the bioactive conformations of molecules and can be broadly categorised into alignment-dependent methods and alignment-independent methods (179).

Comparative Molecular Field Analysis (CoMFA) is a popular alignment-dependent 3D QSAR approach. Bioactive conformers of the training set compounds are aligned on a grid. A probe atom is then used to quantify the steric and electrostatic energies at each grid point for each molecule using Lennard-Jones and Coulombic functions (180). Comparative

Molecular Similarity Indices (CoMSIA) uses a Gaussian distance function instead of the Lennard Jones and Coulombic functions in calculating the energies and also expands the molecular fields to include hydrophobic, hydrogen bond acceptor and hydrogen bond donor properties in addition to steric and electrostatic parameters (181,182). The major weakness of CoMFA, CoMSIA and indeed all alignment-dependent 3D QSAR methods is the need for ligands to be aligned with respect to all the other ligands in the set (179). An absolute orientation of a single conformation needs to be identified for each ligand, and this is assumed to be the aligned conformation that will bind to the receptor *in vivo*. This can be a difficult task, especially in the absence of a co-crystallised receptor-ligand complex, or dissimilar ligands.

Improvements on the CoMFA method include Topomer CoMFA , where automated alignment tools are used to generate both a conformation and orientation of a molecular fragment from the 2D structure (183). 3D QSAR methods which are completely alignment-independent are also available. Examples include comparative molecular moment analysis (CoMMA) (184), Weighted Holistic Invariant Molecular (WHIM) (185) and GRid-Independent descriptors (GRIND) (186).

The weakness of QSAR lies in the ability to identify only molecules that are similar to the training set. Since the equation considers the molecule as a whole, it is difficult to create meaningful QSAR models when there are large structural variations within the training set. Although molecules may belong to different structural classes of compounds, they may still share a 3D arrangement of molecular features which allow them to interact with a common receptor.

4.1.2 Pharmacophore perception

A pharmacophore is a set of features that is common to a group of molecules with activity on a target. The IUPAC defines a pharmacophore as "*an ensemble of steric and electronic features that is necessary to ensure the optimal supramolecular interactions with a specific biological target and to trigger (or block) its biological response*" (187). An example of a pharmacophore is presented in Figure 4.1. The quality of pharmacophore models is dependent upon the structural diversity as well as the size of the training set. Successful

pharmacophore models have been generated from a training set of around 15-20 compounds (188).

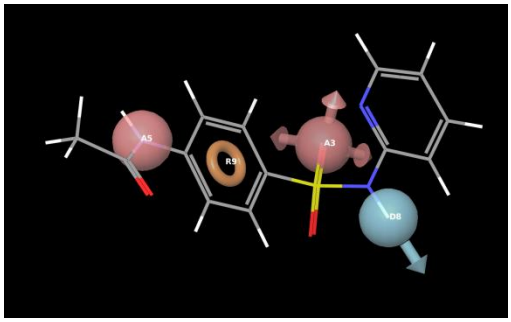

Figure 4.1 Example of a pharmacophore containing 2 hydrogen bond acceptors (red), 1 hydrogen bond donor (blue) and 1 ring moiety (orange).

The concept of feature groups is based on bioisosteres, which are chemical substituents or functional groups with similar chemical and biological properties. Features which are typically included in pharmacophore analyses include: hydrogen bond acceptors (HBA), hydrogen bond donors (HBD), hydrophobes (H), ring structures, positively and negatively charged groups. Examples of bioisoteric groups which have these properties are given in Table 4.2.

By studying the structure-activity relationship between the feature groups and biological activity, it is possible to extrapolate structural information about the biological receptor. Assuming the 3D arrangement of pharmacophore features is critical for receptor binding these features will reflect complementary sites at the receptor. For this assumption to be true, the conformation of the molecule aligned to the pharmacophore must also be the bioactive conformation. Hence a thorough sampling of low energy conformations is of vital importance to ensure that the molecule's bioactive conformation is among the set of conformations input into the pharmacophore perception program.

DISCO (DIStance COmparison) is one of the earliest programs able to automate the pharmacophore searching process (189). Each conformation from an inputted set is transformed into a set of interpoint distances between pharmacophore features. The Bron-Kerbosh clique-detection algorthim is used for distance comparisons to determine the maximum common substructure common to the training set compounds. A weakness with this approach is that a compound needs to be specified as the reference for the

conformational comparisons, which makes it difficult to find a common pharmacophore if all the compounds of the training set are highly flexible (189).

Table 4.2 Examples of pharmacophoric bioisotere groups.

Pharmacophore Group	Example Structures
Hydrogen Bond Donor	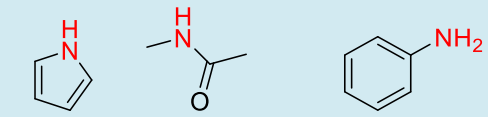
Hydrogen Bond Acceptor	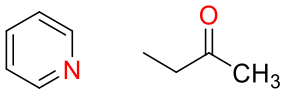
Hydrogen Bond Donor and Acceptor	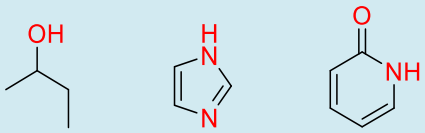
Acid (Negative Ionizable)	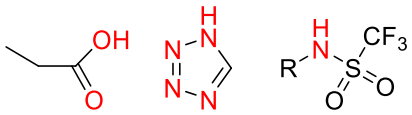
Base (Positive Ionizable)	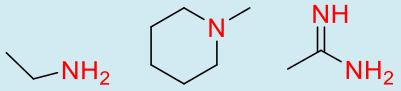
Hydrophobic / Aromatic	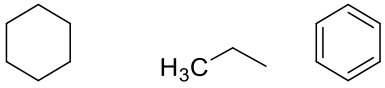
Atoms not considered pharmacophoric	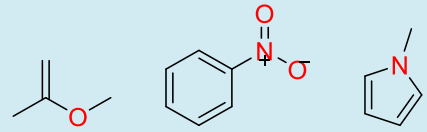

Newer pharmacophore perception software includes Catalyst (190,191), GASP (192) and Schrödinger's Phase (193). The work outlined here utilised the Phase program so discussion will focus on the methods of pharmacophore determination available with this software.

4.1.3 Schrödinger's Phase program

Schrödinger's Phase program (version 3.4, Schrödinger, LLC, New York, NY, 2012.) utilises state-of-the-art algorithms for pharmacophore perception, structure alignment activity prediction and 3D database searching (194). It has been widely utilised for pharmacophore perception and 3D QSAR modelling from the development of novel breast cancer

drugs(195,196) to virtual screening of potentially new anti-diabetic compounds (197) and identifying the critical functional groups for anti-tubercular activity (198).

The Phase workflow for building pharmacophore models from a set of known ligands has four steps (with a fifth optional step) (Figure 4.2). Each step is described in further detail below. Briefly, a set of molecules with affinity for a common receptor are inputted. These molecules are converted into 3D and energy minimized. Low energy conformations are generated and pharmacophore sites created. Pharmacophore hypotheses common to multiple ligands are then identified.

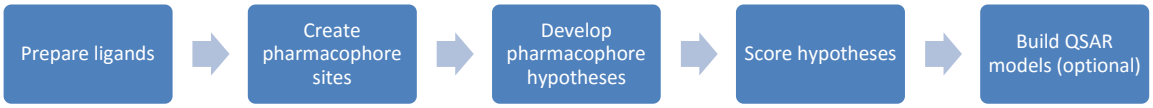

Figure 4.2 Overview of Phase workflow for building pharmacopohore models from a set of ligands.

4.1.3.1 Prepare ligands

4.1.3.1.1 2D to 3D conversion

Pharmacophore development requires all atom 3D representations of molecules. Hence any structures which are presented in 2D (*e.g. sdf* files downloaded from the DrugBank database) must first be converted into 3D. This can be done by minimisation or through the use of the LigPrep (Ligand Preparation) program (199). The use of LigPrep is recommended to prepare ligands for further analyses, since it is also able to ionise molecules at designated pH (typically 7.0 ± 2) and generate stereoisomers.

4.1.3.1.2 Energy Minimisation

Energy minimisation of the output molecules can be conducted with Macromodel (200). A number of methods are available for energy minimisation including Polak-Ribiere Conjugate Gradient (PRCG), Truncated Newton Conjugate Gradient (TNCG), Oren-Spedicato Variable Metric (OSVM) and Steepest Descent (SD). Of these, PRCG is thought to be best general method for minimization (200) and was therefore used in this study.

4.1.3.1.3 Conformer generation

Low energy conformations can be generated externally and imported or produced as part of the Phase workflow. The two methods for conformer generation offered by Phase are Mixed Monte-Carlo Multiple Minimum/Low Mode (MCMM/LMOD) and ConfGen. These are further explained below.

During the MCMM search, random changes are made in torsion angles. Hence this method is highly efficient in performing global searching, decreasing the risk of 'becoming stuck' on a local minima rather than the global minimum. However, if more than 10-15 flexible torsions are present, the complexity of the search will increase, leading to increased searching times (200).

In the ConfGen (201,202) methodology, molecules are divided into a core and a periphery. The Phase user manual defines peripheral groups as those that "have only one rotatable bond between terminal groups and the rest of the molecule. All the non-peripheral rotatable bonds are assigned to the core". All core configurations are generated during the search process before the peripheral configurations are varied. Although two sampling options are available (Rapid and Thorough), the Phase manual notes that a Thorough conformational search does not significantly improve the final pharmacophore model compared with a Rapid search (203).

4.1.3.1.4 Ligand groupings

Once all the molecules have been prepared, the "pharm set" for pharmacophore perception must be defined. This can be done by manually assigning molecules to the "active" or "inactive" set, or an activity threshold can be set to automatically assign the pharm set based on an imported activity value.

It is also possible to group multiple ligands such that they will be seen as "the same ligand" in the Develop pharmacophore hypotheses step – *i.e.* only one ligand in the group needs to match for the purpose of finding common pharmacophores.

4.1.3.2 Create pharmacophore sites

To find commonalities between active ligands, the areas within each ligand which are capable of interacting with a receptor are identified. Phase supports 6 types of pharmacophore feature by default:

- Hydrogen bond acceptor (A)
- Hydrogen bond donor (D)
- Hydrophobic group (H)
- Negatively charged group (N)
- Positively charged group (P)
- Aromatic ring (R)

Excluding hydrophobic groups and aromatic rings, each of these features is defined by a set of Smiles ARbitary Target Specification (SMARTS) patterns, a language for describing substructures within molecules developed by Daylight Chemical Information Systems (204). SMARTS uses rules that are straightforward extensions of SMILES. Tables outlining SMARTS primitives are presented in Appendix 5: SMARTS notation primitives.

Within each set, the pharmacophore features are further categorised by the physical characteristics of the site; namely point, vector and group. Vector characteristics are helpful for features which have direction. For example, oxygen atoms have lone pairs of electrons which point in specific directions.

If deemed inappropriate, default feature definitions can be ignored. Users can also define additional features using SMARTS patterns if required.

Once the feature set has been finalised, Phase creates and stores the site points for each conformer of each ligand (Figure 4.3).

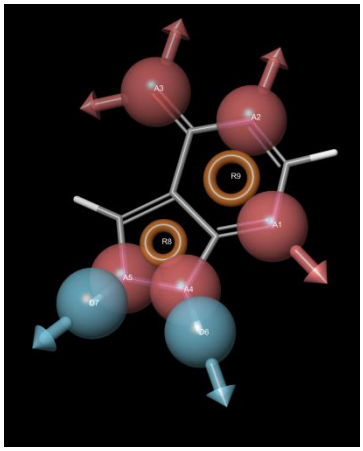

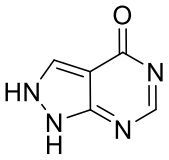

Figure 4.3 Total pharmacophore sites for allopurinol. Hydrogen bond acceptors (A) are shown in red; hydrogen bond donors (D) are shown in blue; hydrophobic sites (H) are shown in green; aromatic rings (R) are represented by an orange ring.

4.1.3.3 Develop common pharmacophore hypotheses

In this step, Phase uses a tree-based partitioning technique to group together similar pharmacophores by their intersite distances, *i.e.* the distance between two pharmacophore features. A *k*-point pharmacophore is represented by a vector of *n* distances, where $n = (k(k-1))/2$. Each of the *n* distances is filtered through a binary decision tree into categories of user defined length. The length of each category is termed the final box size. From the final box size and the user specified maximum tree depth, the size of the initial box size is calculated (Initial box size = Final box size ^ Maximum tree depth). The final box size and the tree depth need to be set such that the initial box is large enough to encompass the largest molecule under consideration. Figure 4.4 shows an example of a tree with final box size of 2Å and a tree depth of 3. This gives an initial box size of 2^3=8Å.

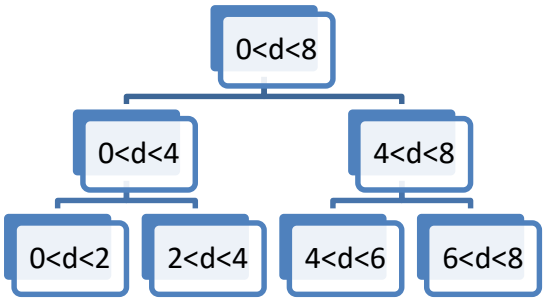

Figure 4.4 Sample Phase binary decision tree with final box size 2Å and tree depth 3. This gives an initial box size of 2^3=8Å.

Families of pharmacophores that have the same number of pharmacophore feature types are termed variants. For example pharmacophores belonging to the AADR variant will

contain 2 hydrogen bond acceptors, 1 hydrogen bond donor and 1 ring. Similarly, pharmacophores in the ADHR variant will contain 1 hydrogen bond acceptor, 1 hydrogen bond donor, 1 hydrophobe and 1 ring.

The number of pharmacophore sites in the hypotheses and the number of ligands that much match to form a valid hypothesis is set by the user. Partial matching is not possible. *i.e.* compounds are required to match all *k* sites of a *k*-point pharmacophore.

Users can also specify a minimum intersite distance. This is the minimum distance which must be present between any two pharmacophore features. Any pharmacophore hypotheses with features closer than this distance will be rejected in the selection process.

4.1.3.4 Score hypotheses

From the previous step, several sets of pharmacophores will be produced. Each set will contain pharmacophores which have similar intersite distances, with each pharmacophore based on a different reference ligand. For each pharmacophore in the set, all of the other ligands are aligned with the reference ligand using a standard least squares procedure. Alignments are scored on their root mean squared deviations (RMSD) from site positions, a vector score, and a volume score. The pharmacophore and its corresponding reference ligand in the set which produces the highest scoring ligand alignments is taken as the pharmacophore hypothesis for that set.

Following this step, a percentage cut-off to the overall alignment score can be used to eliminate low scoring hypotheses.

The remaining hypotheses are then ranked based on volume and selectivity scoring. The volume score is calculated as the proportion of overlap between the reference ligand and non-reference ligands for each hypothesis, based on van der Waals models of non-hydrogen atoms (Equation 7). The selectivity score is a rough estimate of the rarity of the hypothesis, or the proportion of all molecules that will match the hypothesis.

Volume score formula used to determine the quality of pharmacophore alignments. Taken from the Phase user manual.

$$S_{vol} = \frac{V_{common}(i)}{V_{total}(i)} \qquad (7)$$

Within the Score Actives dialogue box, there is an option to set the allowed Root Mean Square deviation of intersite distances. This is the RMSD of the pharmacophore site distance from any contributing ligand to those of the reference ligand. Lower RMSD reflects stricter criteria, requiring alignments to more closely reflect that of the reference ligand.

4.1.3.5 Advanced pharmacophore screening

Phase provides a functionality to screen compounds using pharmacophore hypotheses. A hypothesis can be used to search a prepared database of 3D structures. Conformations can be generated externally and included as part of a database, or Phase can generate conformers using ConfGen (202) during the search process.

Structures are searched for the required pharmacophore sites and intersite distances needed to match the input pharmacophore hypothesis. Conformers which fulfil these requirements are aligned to the hypothesis as a 'hit'. Hits are assigned fitness scores based on the quality of the alignment to the pharmacophore hypothesis.

There is an option to set the intersite distance matching tolerance (IDMT). This is the maximum allowed deviation from the pharmacophore site. Lower IDMT reflects stricter criteria, requiring alignments to more closely reflect that of the pharmacophore hypothesis.

4.2 Rationale

In this chapter, relationships between IMDILI and the three-dimensional structural features of toxic drug molecules and their metabolites are exposed. Pharmacophore perception tools are used to identify whether there are similarities in molecular structures between toxic drugs.

In the following analyses a molecule's biological activity is defined as its IMDILI potential - *i.e.* active drugs are drugs that have known IMDILI potential and inactive drugs are drugs that are not known to cause IMDILI.

4.3 Methods

High molecular weight drugs tend to have high numbers of functional groups due to the increased number of atoms especially in less accessible regions of the molecule (*e.g.* in the centre). As such, inclusion of these drugs will increase the rate of false positives in the

identification of relevant pharmacophore features. For this reason, drugs with molecular weight >500 Da were excluded from all *in silico* analyses.

Platform dependent differences have been noted from previous experiences so to ensure consistency of results, the pharmacophore perception process was repeated on four different computers across Linux (Ubuntu 12.04), MacOSX (Version 10.6.8) and Windows (Windows 7) platforms.

4.3.1 Literature confirmation of toxicity classification

The correct assignment of activity is essential for the development and validation of pharmacophore models. The IMDILI potential (or lack thereof) of the all drugs included in the pharmacophore analyses was confirmed by reviewing published literature. A drug was only included in the training set if there was published evidence of DILI with immune features (*e.g.* fever, rash or eosinophilia), or if genetic studies have identified associations with proteins known to activate the adaptive immune system (Table 2.6). This acted as a validation step to filter out potentially false signals generated from the pharmacovigilance data.

4.3.2 Identification of metabolites

Since drug metabolites are known to be involved in at least some DILI, all drugs were grouped with their known and proposed metabolites. Published literature was reviewed to identify known and proposed metabolites of all drugs in the training set. The full list of drugs and metabolites included in the training set for pharmacophore perception is presented in Table 4.3.

Table 4.3 List of drugs and metabolites included in the training set for pharmacophore perception. Metabolites have been assigned an arbitrary number and are named as M(x). *E.g.* Allopurinol M1 denotes allopurinol metabolite 1.

Drug/metabolite	Structure
Allopurinol	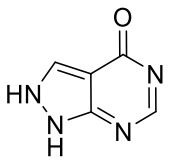
Allopurinol M1 (205)	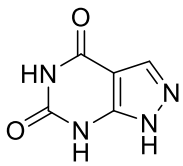

Drug/metabolite	Structure
Allopurinol M2 (205)	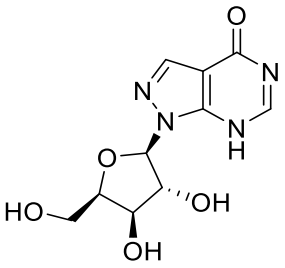
Allopurinol M3 (205)	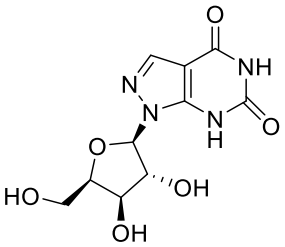
Allopurinol M4 (205)	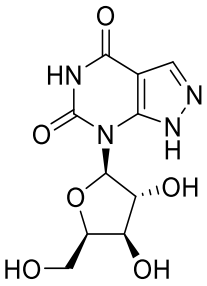
Carbamazepine	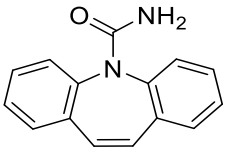
Carbamazepine M1 (206)	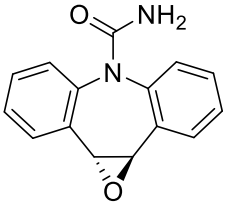
Carbamazepine M2 (206)	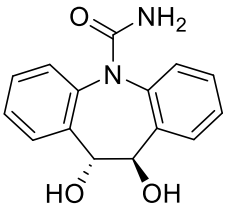
Carbamazepine M3 (206)	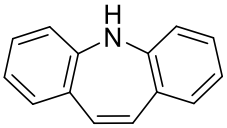
Carbamazepine M4 (206)	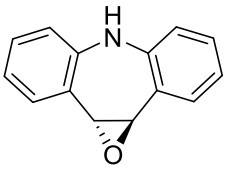

Drug/metabolite	Structure
Carbamazepine M5 (206)	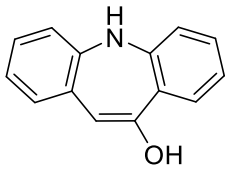
Carbamazepine M6 (206)	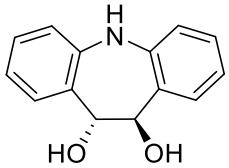
Celecoxib	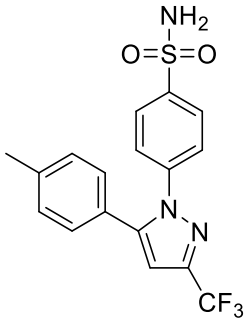
Celeboxicb M1 (207)	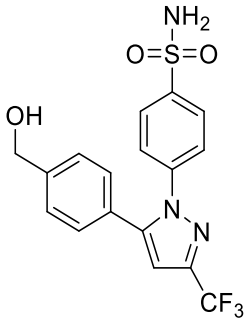
Celeboxib M2 (207)	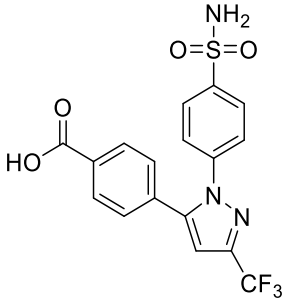
Clavulanic acid	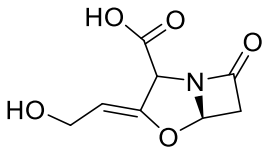
Clavulanic acid M1 (208)	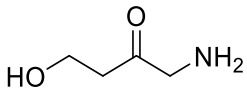
Clavulanic acid M2 (208)	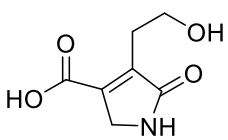

Drug/metabolite	Structure
Flucloxacillin	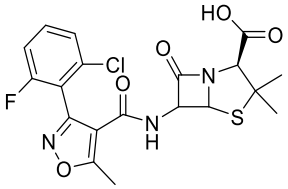
Flucloxacillin M1 (209)	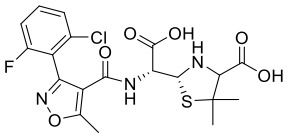
Flucloxacillin M2 (209)	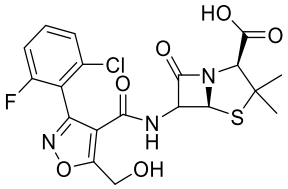
Flucloxacillin M3 (209)	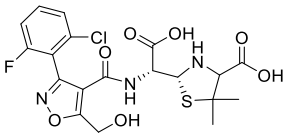
Lamotrigine	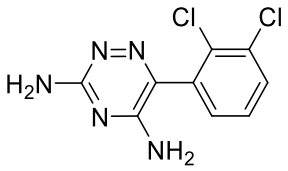
Lamotrigine M1 (210)	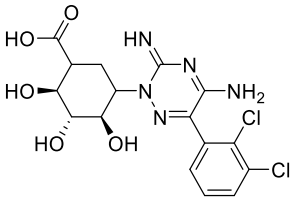
Lamotrigine M2 (210)	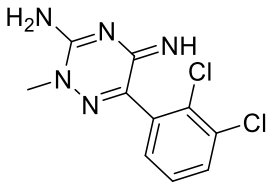
Nevirapine	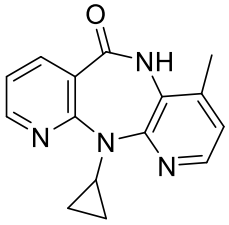
Nevirapine M1 (211)	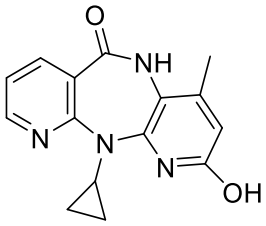

Drug/metabolite	Structure
Nevirapine M2 (211)	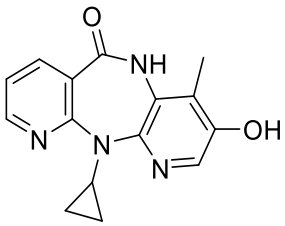
Nevirapine M3 (211)	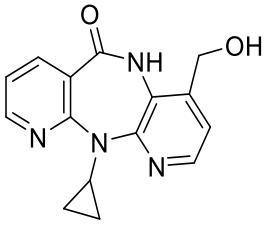
Nevirapine M4 (211)	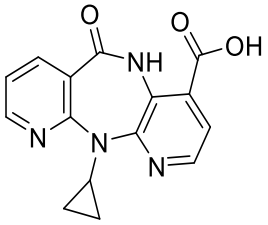
Nevirapine M5 (211)	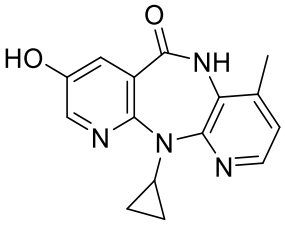
Phenytoin	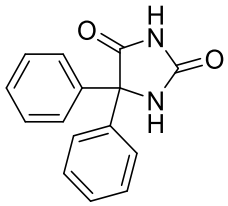
Phenytoin M1(212)	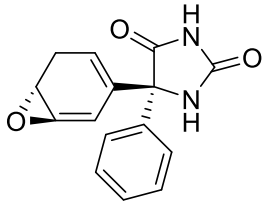
Phenytoin M2 (212)	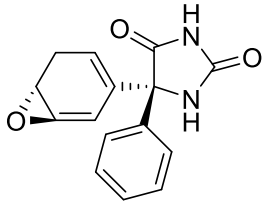

Drug/metabolite	Structure
Phenytoin M3 (212)	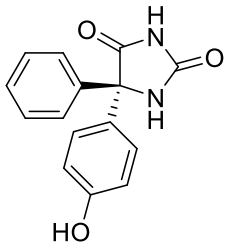
Phenytoin M4 (212)	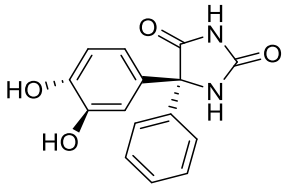
Phenytoin M6 (212)	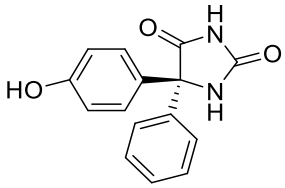
Propylthiouracil	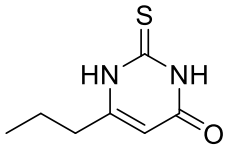
Propylthiouracil M2 (213)	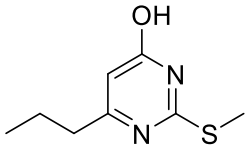
Propylthiouracil M6 (213)	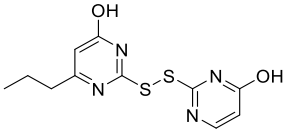
Propylthiouracil M7 (213)	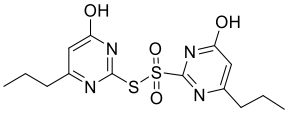
Propylthiouracil M8 (213)	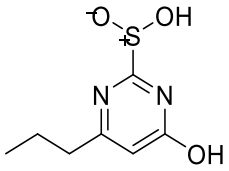
Propylthiouracil M9 (213)	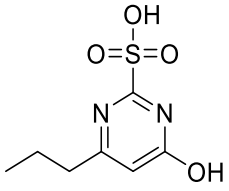
Sulfasalazine	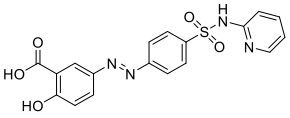

Drug/metabolite	Structure
Sulfasalazine M1 (214)	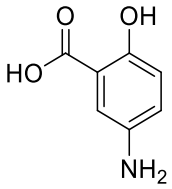
Sulfasalazine M2 (214)	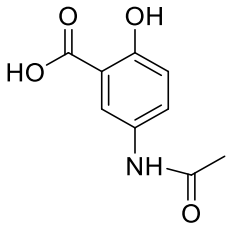
Sulfasalazine M3 (214)	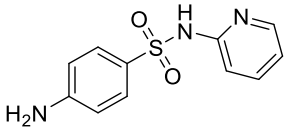
Sulfasalazine M4 (214)	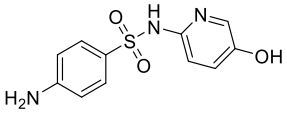
Sulfasalazine M5 (214)	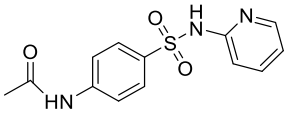
Sulfasalazine M6 (214)	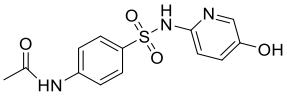
Sulindac	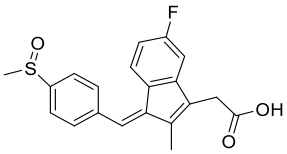
Sulindac M1 (215)	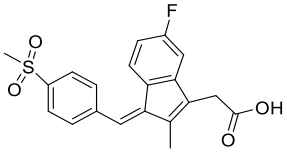
Sulindac M2 (215)	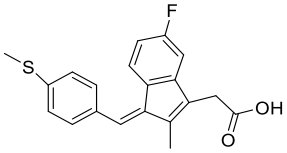

4.3.3 Prepare ligands

All molecules were built with the molecular modelling and graphical user interface package, Maestro (version 9.3, Schrödinger, LLC, New York, NY, 2012.). Parent drug structures were downloaded in Simple Data Format (sdf) from the DrugBank database (www.drugbank.ca). Metabolites were drawn in using Maestro's 2D sketcher tool.

The LigPrep program (version 2.8, Schrödinger, LLC, New York, NY, 2013) was used to convert the downloaded *sdf* files from 2D to 3D. Molecules were ionised at physiological pH 7 (± 2.0). LigPrep was asked to generate one low energy ring conformation for each ligand using the OPLS_2005 forcefield (216). Specified chiralities were retained and unspecified chiralities were varied up to a maximum of 32 stereoisomers per ligand.

The global minimal energy state of all molecules was determined with MacroModel (version 9.9, Schrödinger, LLC, New York, NY, 2012). Structures were minimised using the PRCG method. The convergence threshold was set to 0.05, based on gradient. Up to a maximum of 5000 iterations were allowed. The OPLS_2005 forcefield was used with a constant solvent dielectric of 1.0. Subsequently each molecule was visually inspected to confirm that minimisation had given chemically correct structures. These were then imported into a Phase run.

Conformers were generated within the Phase workflow, using the OPLS_2005 forcefield with a distance-dependent electrostatic treatment. The ConfGen search method was used with Rapid sampling of the conformational space. Redundant conformers were eliminated using a RMSD cutoff of 0.5Å.

Each drug of the training set was grouped with its known and proposed metabolites as an active ligand group.

4.3.4 Create pharmacophore sites

Pharmacophore sites were identified using both point and vector geometries. The feature definitions used in the pharmacophore perception are presented in Appendix 6: Definitions of the pharmacophore features included in the genernation of pharmacophore hypotheses.

4.3.5 Develop common pharmacophore hypothesis

Phase was asked to identify common pharmacophore hypotheses with a maximum of 7 and a minimum of 4 site points. Hypotheses were required to match at least 9 of 11 active groups (82%).

The initial box size was set to 32Å, with a final box size of 1Å and maximum tree depth of 5. The minimum intersite distance was set to 2Å.

4.3.6 Scoring actives

Hypotheses were scored using the survival formula. The maximum RMSD of the intersite distances of any contributing ligand from those of the reference ligand was set at 1.2Å.

4.3.7 External Validation

4.3.7.1 Compilation of active test set

Drugs withdrawn from the market because of DILI concerns as identified by Guengerich (217) were included in the active test set (Table 4.4).

4.3.7.2 Compilation of inactive test set

Australia's DAEN database was searched for drugs with >200 case reports, none of which contain ADR descriptors indicative of DILI. Six drugs met these criteria, and were included in the inactive test set. Since the number of inactive drugs was significantly smaller than the number of active drugs (in the training and test sets), a second set of inactives was identified from the literature. Chen *et al*. (43) lists two datasets of drugs and the DILI potential of each drug as identified by two different sources.

The 7 drugs identified in both data sources as without DILI potential were added into the inactive test set (Table 4.4).

4.3.7.3 Molecular preparation

The Test set molecules were prepared in the same manner as the Training Set. The IMDILI potential (or lack thereof) of each drug was confirmed by reviewing published literature. A drug was only included in the active test set if there was published evidence of DILI with immune features (*e.g.* fever, rash or eosinophilia), or if there were genetic associations with proteins known to activate the adaptive immune system. Drugs were excluded from the inactive test set if there was literature evidence of any hepatotoxicity (not necessarily immune mediated). Published literature was reviewed to identify known and proposed metabolites of all drugs in both test sets. The full list of drugs and metabolites included in both test sets is presented in Table 4.4.

Molecules were built and minimised in the same manner as the Training Set (see section 4.3.3 Prepare ligands). Conformations were generated as part of the Screening workflow.

Table 4.4 List of drugs and metabolites included in the active and inactive test sets.

Set	Drug/metabolite	Structure
Active test set	Bromfenac	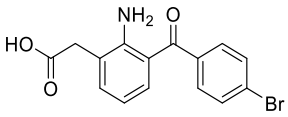
	Bromfenac M1 (218)	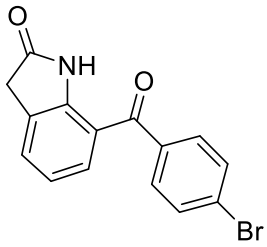
	Bromfenac M2a (218)	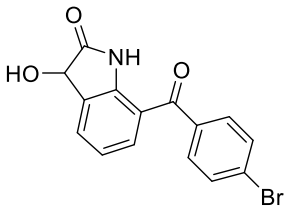
	Bromfenac M3 (218)	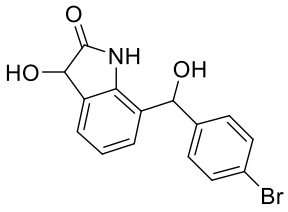
	Chlormezanone	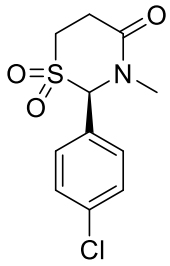
	Chlormezanone M1 (219,220)	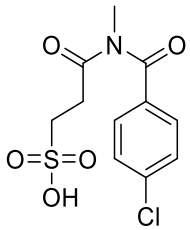
	Chlormezanone M2 (219,220)	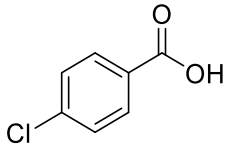
	Chlormezanone M3 (219,220)	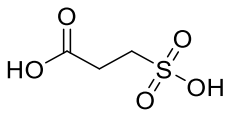
	Chlormezanone M4 (219,220)	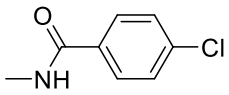

Set	Drug/metabolite	Structure
	Chlormezanone M5 (219,220)	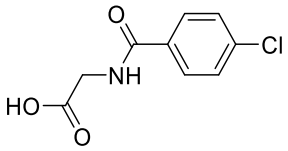
	Chlormezanone M6 (219,220)	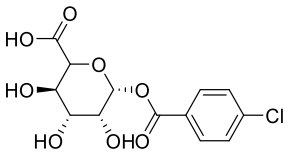
	Lumiracoxib	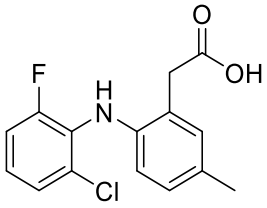
	Lumiracoxib M1 (221,222)	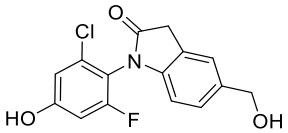
	Lumiracoxib M2 (221,222)	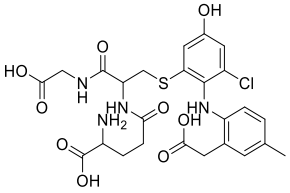
	Lumiracoxib M3 (221,222)	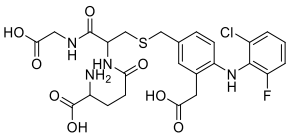
	Lumiracoxib M4 (221,222)	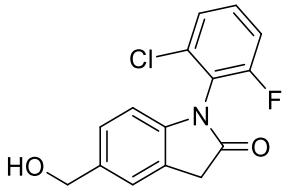
	Lumiracoxib M5 (221,222)	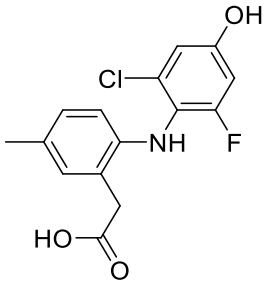
	Lumiracoxib M6 (221,222)	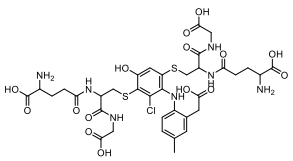
	Lumiracoxib M7 (221,222)	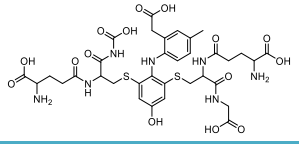

Set	Drug/metabolite	Structure
	Lumiracoxib M8 (221,222)	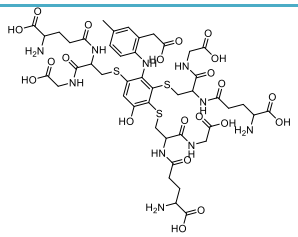
	Lumiracoxib M9 (221,222)	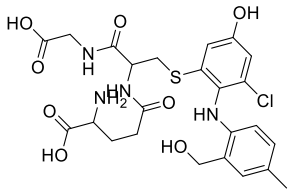
	Lumiracoxib M10 (221,222)	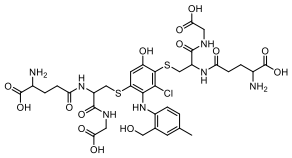
	Lumiracoxib M11 (221,222)	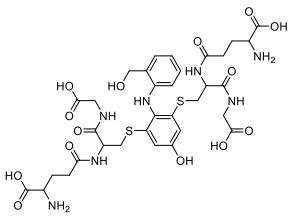
	Lumiracoxib M12 (221,222)	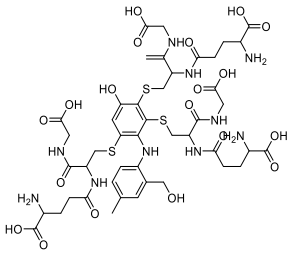
	Lumiracoxib M13 (221,222)	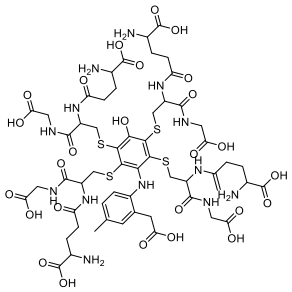
	Lumiracoxib M14 (221,222)	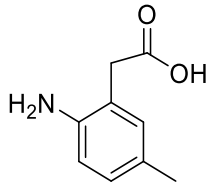

Set	Drug/metabolite	Structure
	Lumiracoxib M15 (221,222)	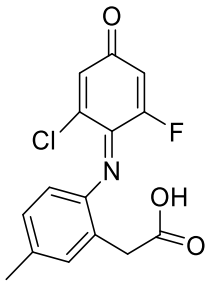
	Lumiracoxib M16(221,222)	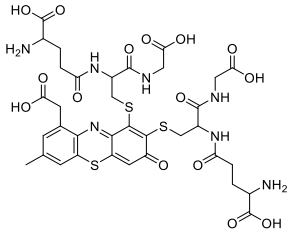
	Lumiracoxib M17 (221,222)	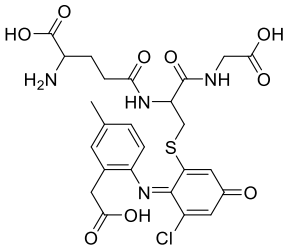
	Lumiracoxib M18 (221,222)	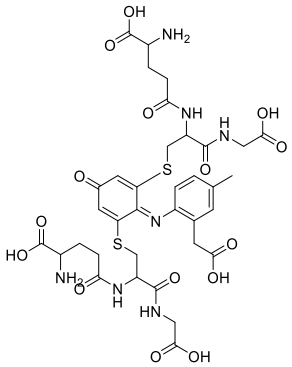
	Nomifensine	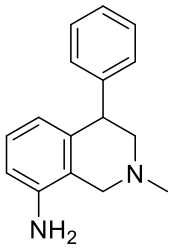
	Nomifensine M1 (223–225)	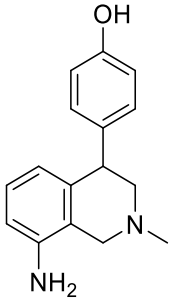

Set	Drug/metabolite	Structure
	Nomifensine M2 (223–225)	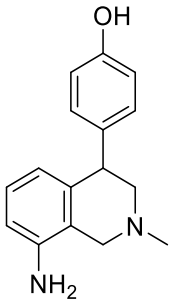
	Nomifensine M3 (223–225)	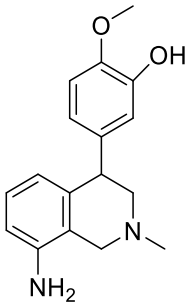
	Nomifensine M4a (223–225)	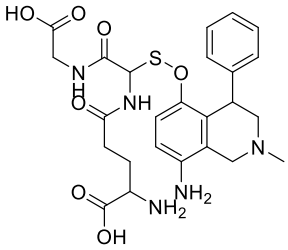
	Nomifensine M4ia (223–225)	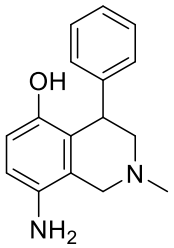
	Nomifensine M4ib (223–225)	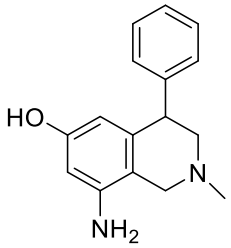
	Nomifensine M4ic (223–225)	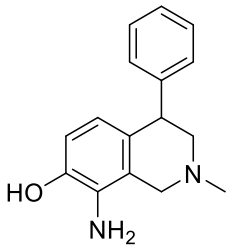

Set	Drug/metabolite	Structure
	Nomifensine M5 (223–225)	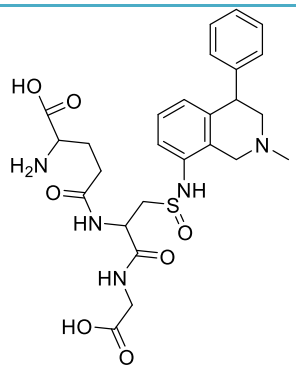
	Nomifensine M5i (223–225)	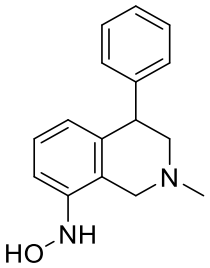
	Oxyphenisatin	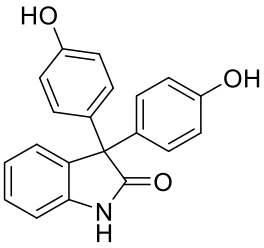
	Pemoline	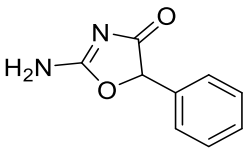
	Tienilic acid	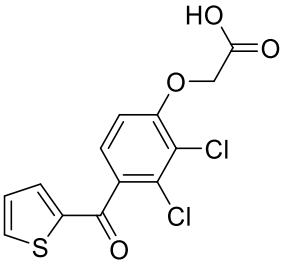
	Tienilic acid M1 (226–229)	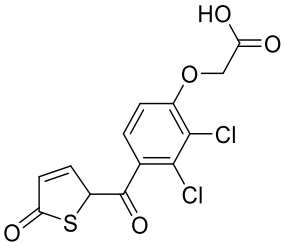
	Tienilic acid M1i (226–229)	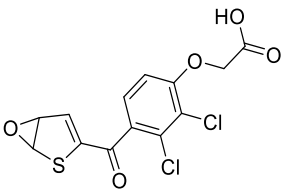

Set	Drug/metabolite	Structure
	Tienilic acid M2 (226–229)	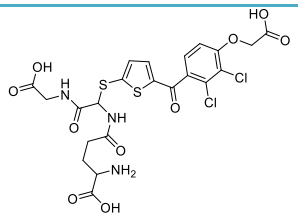
	Tienilic acid M2i (226–229)	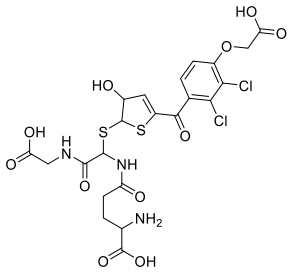
	Tienilic acid M3 (226–229)	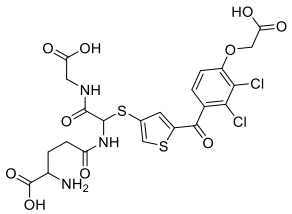
	Tienilic acid M3i (226–229)	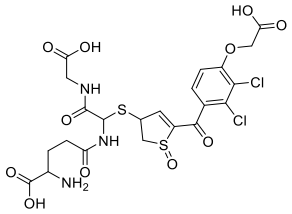
	Tienilic acid M4 (226–229)	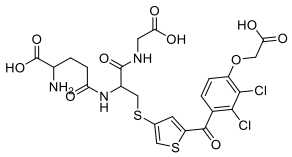
	Tienilic acid M4i (226–229)	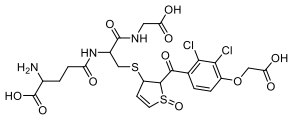
	Tienilic acid M5 (226–229)	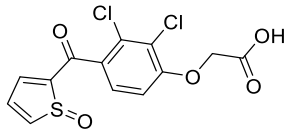
	Ximelagatran	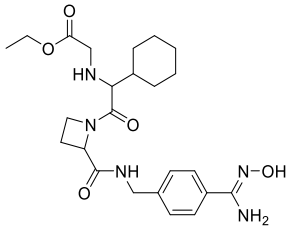

Set	Drug/metabolite	Structure
	Ximelagatran M1 (230–233)	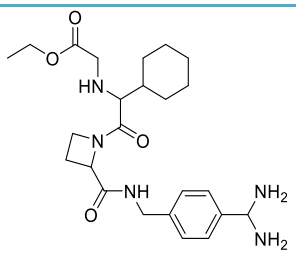
	Ximelagatran M2 (230–233)	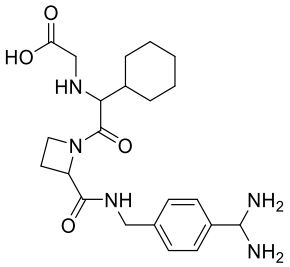
	Ximelagatran M3 (230–233)	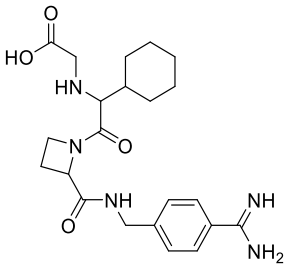
	Ximelagatran M4 (230–233)	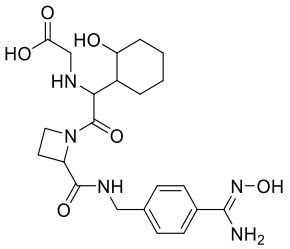
	Ximelagatran M5 (230–233)	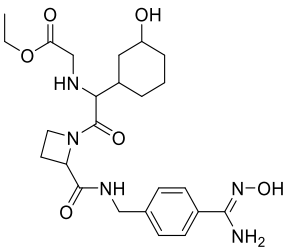
	Ximelagatran M6 (230–233)	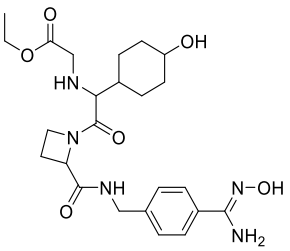
Inactive test set	Alprazolam	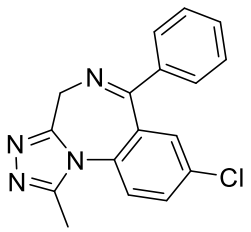

Set	Drug/metabolite	Structure
	Alprazolam M1 (234)	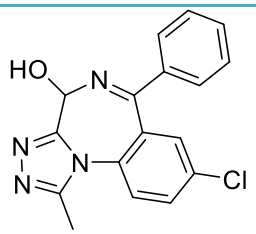
	Alprazolam M2 (234)	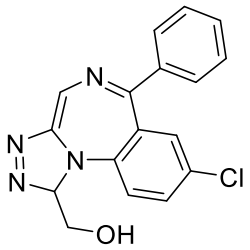
	Aripiprazole	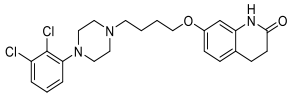
	Baclofen	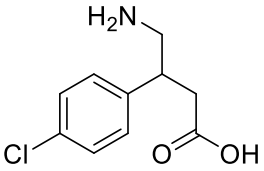
	Baclofen M1 (235)	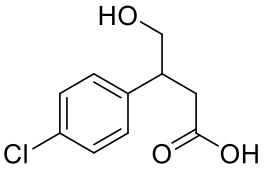
	Fluvoxamine	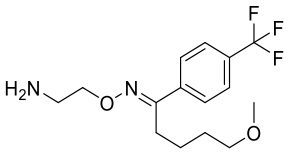
	Fluvoxamine M1 (236,237)	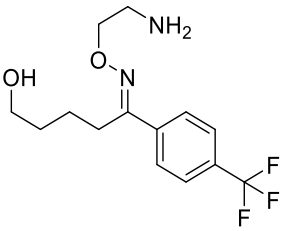
	Fluvoxamine M2 (236,237)	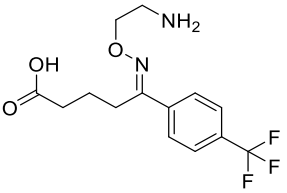

Set	Drug/metabolite	Structure
	Ketorolac	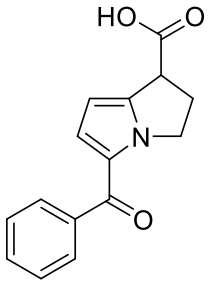
	Ketorolac M1 (238)	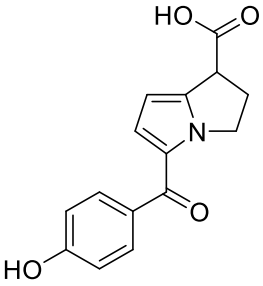
	Pregablin	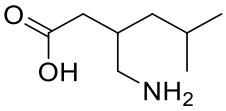
	Betaine	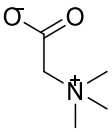
	Clemastine	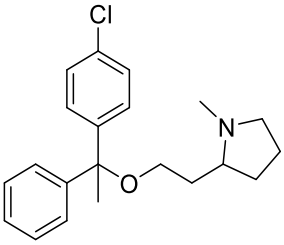
	Clemastine M1 (239–241)	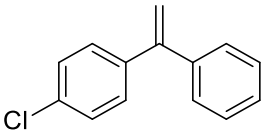
	Clemastine M2 (239–241)	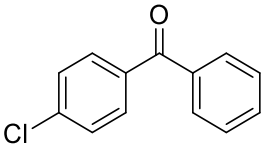
	Clemastine M3 (239–241)	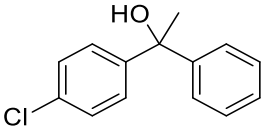
	Clemastine M4a (239–241)	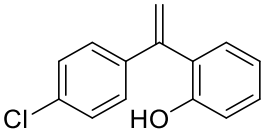
	Clemastine M4b (239–241)	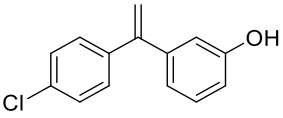

Set	Drug/metabolite	Structure
	Clemastine M4c (239–241)	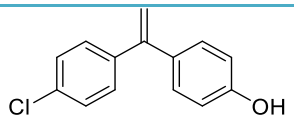
	Clemastine M6 (239–241)	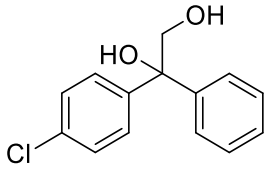
	Clemastine M7 (239–241)	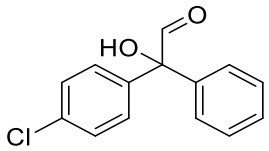
	Diphenhydramine	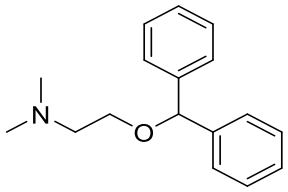
	Diphenhydramine M1 (242,243)	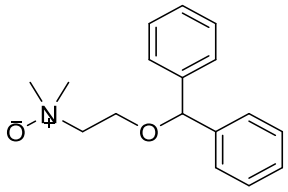
	Diphenhydramine M2 (242,243)	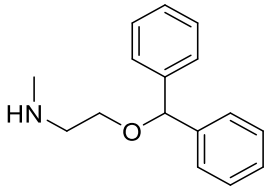
	Diphenhydramine M3 (242,243)	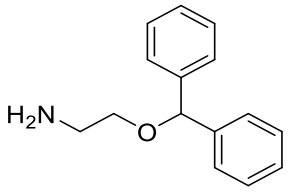
	Diphenhydramine M4 (242,243)	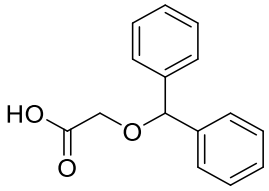
	Diphenhydramine M5 (242,243)	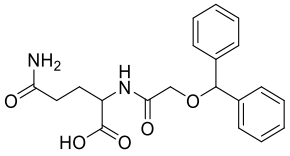
	Diphenhydramine M6 (242,243)	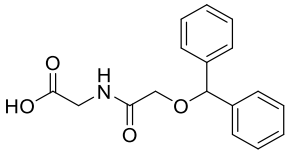

Set	Drug/metabolite	Structure
	Isoproterenol	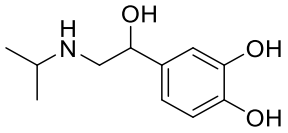
	Isoproterenol M1 (244)	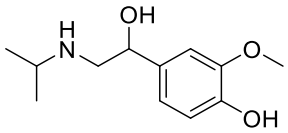
	Methysergide	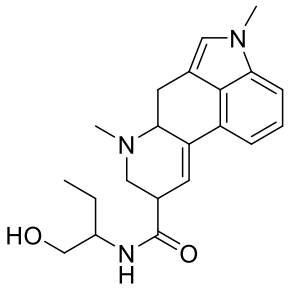
	Methysergide M1 (245,246)	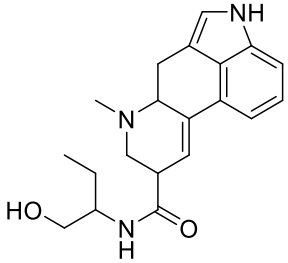
	Oxybutynin	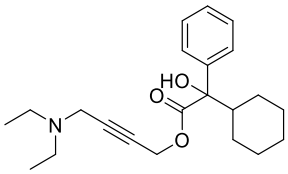
	Oxybutynin M1 (247–249)	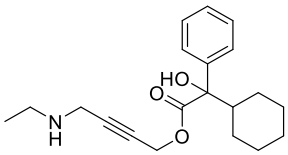
	Phenoxybenzamin	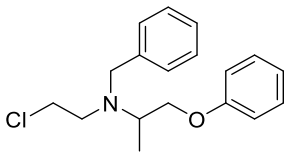

4.3.7.4 Advanced Pharmacophore Screening of Test set

The Phase (version 3.4, Schrödinger, LLC, New York, NY, 2012) Advanced Pharmacophore Screening tool was used to screen the active and inactive test sets for matches. The intersite distance matching tolerance was set to 2Å. The predictive performance measures sensitivity, specificity, accuracy, Matthews Correlation Coefficient, positive prediction value

and negative predictive value were calculated based on the number of drug/metabolite groups containing at least one molecule matching the pharmacophore hypothesis (250).

4.4 Results

The largest number of occurrences for each pharmacophore feature among the training set are listed in Table 4.5.

Table 4.5 The largest number of occurrences for each pharmacophore feature among the training set molecules.

Pharmacophore feature	Largest number of occurrences among molecules of training set
Hydrogen bond acceptor	8
Hydrogen bond donor	4
Hydrophobe	3
Negative ionisable	1
Positive ionisable	0
Ring	2

No 7, 6 or 5 point hypotheses were found to be common for the required number of active groups (9 out of 11).

Of the 4 point pharmacophore hypotheses that were returned, the AADR and AADD variants were identified as high performing, based on the Phase survival score and visual inspection. Each of the hypotheses within these two variants was used to screen the active and inactive Test sets. The screening results for the AADR and AADD variants are presented in Table 4.6 and Table 4.7 respectively.

It is interesting to note that typically, only 2 of the 9 training set drug/metabolite groups which match the pharmacophore include the parent drug. The majority of the molecules which match the pharmacophore hypotheses are metabolites rather than parent drugs. This trend is also observed in the Test tests.

Out of all the pharmacophore hypotheses investigated, the highest scoring was the

AADR.4989 hypothesis. This hypothesis had a Matthew's Correlation Coefficient of 0.69, which indicates a strong positive relationship. The model was able to differentiate between molecules in the Active and Inactive Test sets with sensitivity and specificity of 75% and 92% respectively. Hence, this hypothesis was taken to the be one that best captures the structural similarities between the molecules implicated in IMDILI and will henceforth be referred to as the toxicophore hypothesis. The site measurements for the toxicophore hypothesis are presented in Figure 4.5.

a)

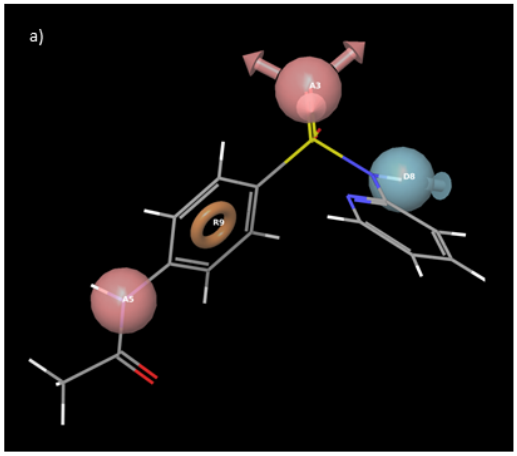

b)

Site 1	Site 2	Distance (Å)
A3	A5	6.4
A3	D8	3.5
A3	R9	4.0
A5	D8	7.1
A5	R9	2.7
D8	R9	4.9

Site 1	Site 2	Site 3	Angle (°)
A5	A3	D8	85.2
A5	A3	R9	12.3
D8	A3	R9	80.3
A3	A5	D8	29.6
A3	A5	R9	18.8
D8	A5	R9	27.3
A3	D8	A5	65.2
A3	D8	R9	54.5
A5	D8	R9	14.5
A3	R9	A5	148.9
A3	R9	D8	45.2
A5	R9	D8	138.2

c)

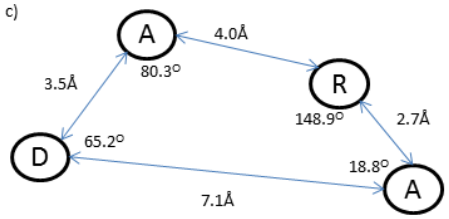

Figure 4.5 Primary toxicophore hypothesis common to drugs/metabolites implicated in IMDILI. The hypothesis consists of 2 hydrogen bond acceptors (A), 1 hydrogen bond donor (D) and 1 ring structure (R). a) The toxicophore superimposed on its model ligand N4-acetylsulfapyridine. b) Site measurements for the pharmacophore. c) Schematic of the pharmacophore site measurements.

Table 4.6 List of molecules that match AADR pharmacophore hypotheses. "P" = only the parent drug matches the pharmacophore. "P+M" = both parent and metabolite drug molecules match the pharmacophore. "M" = only metabolite molecules match the pharmacophore hypothesis.

		AADR.4989	AADR.3653	AADR.5301	AADR.3975	AADR.22
Training Set	Allopurinol	M	M	M	M	M
	Carbamazepine	M	M	M	M	P+M
	Celecoxib	P+M	P+M	P+M	P+M	P+M
	Clavulanic acid					
	Flucloxacillin	M	M	M	M	M
	Lamotrigine	M	M	M	M	M
	Nevirapine	M	M	M	M	P+M
	Phenytoin	M	M	M	M	P+M
	Propylthiouracil	M	M	M	M	M
	Sulfasalazine	P+M	P+M	P+M	P+M	P+M
	Sulindac					
	TOTAL (of 11)	**9**	**9**	**9**	**9**	**9**
Active Test Set	Bromfenac	P+M	P+M	P+M	P+M	P+M
	Chlormezanone		M			M
	Lumiracoxib	P+M	P+M	M	M	P+M
	Nomifensine	M	M	M	M	M
	Oxyphenisatin	P	P	P		P
	Pemoline					P
	Tienilic acid	M	P+M	P+M		P+M
	Ximelagatran	P+M	P+M	P+M	P+M	P+M
	TOTAL (of 8)	**6**	**7**	**6**	**4**	**8**
Inactive Test Set	Alprazolam					
	Aripiprazole					
	Baclofen					
	Betaine hydrochloride					
	Clemastine					M
	Diphenhydramine		M			M
	Fluvoxamine					
	Isoproterenol	P+M	P+M	P+M	P+M	P+M
	Ketorolac					
	Methysergide		M	M		
	Oxybutynin					P
	Phenoxybenzaine					
	Pregabalin					
	TOTAL (of 13)	**1**	**3**	**2**	**1**	**4**

		AADR.4989	AADR.3653	AADR.5301	AADR.3975	AADR.22
Model Statistics	Matthew's Correlation Coefficient	0.69	0.63	0.60	0.48	0.68
	Accuracy	0.86	0.81	0.81	0.76	0.81
	Sensitivity	0.75	0.88	0.75	0.50	1.00
	Specificity	0.92	0.77	0.85	0.92	0.69
	Positive predictive value	0.86	0.70	0.75	0.80	0.67
	Negative predictive value	0.86	0.91	0.85	0.75	1.00
	True positive	6	7	6	4	8
	False positive	1	3	2	1	4
	False negative	2	1	2	4	0
	True negative	12	10	11	12	9

Table 4.7 List of molecules that match AADD pharmacophore hypotheses. "P" = only the parent drug matches the pharmacophore. "P+M" = both parent and metabolite drug molecules match the pharmacophore. "M" = only metabolite molecules match the pharmacophore hypothesis.

		AADD.428	AADD.3709	AADD.2715	AADD.4634	AADD.2702	AADD.3220
Training Set	Allopurinol	M	M	M	M	M	M
	Carbamazepine	M	M	M	M	M	M
	Celecoxib						
	Clavulanic acid	P	P+M	P+M	P+M	P+M	P+M
	Flucloxacillin	P+M	P+M	P+M	P+M	P+M	P+M
	Lamotrigine	M	M	M	M	M	M
	Nevirapine	M	M	M	M	M	M
	Phenytoin	M	M	M	M	M	M
	Propylthiouracil	M	M	M	M	M	M
	Sulfasalazine	M	M	M	M	M	M
	Sulindac						
	TOTAL (of 11)	**9**	**9**	**9**	**9**	**9**	**9**
Active Test Set	Bromfenac	M	M	M	M	M	P+M
	Chlormezanone	M	M	M	M	M	M
	Lumiracoxib	M	M	M	M	M	P+M
	Nomifensine		M	M	M	M	M
	Oxyphenisatin						P
	Pemoline						
	Tienilic acid	M	P	M	M	M	M
	Ximelagatran	P+M	P+M	P+M	P+M	P+M	P+M
	TOTAL (of 8)	**5**	**6**	**6**	**6**	**6**	**7**
Inactive Test Set	Alprazolam						
	Aripiprazole						
	Baclofen						
	betaine hydrochloride						
	Clemastine						
	Diphenhydramine	M	M	M	M	M	M
	Fluvoxamine						
	Isoproterenol		P	P+M	P+M	P+M	P+M
	Ketorolac						
	Methysergide						
	Oxybutynin	M	M	M	M	M	M
	Phenoxybenzaine						
	Pregabalin						
	TOTAL (of 13)	**2**	**3**	**3**	**3**	**3**	**3**

		AADD.428	AADD.3709	AADD.2715	AADD.4634	AADD.2702	AADD.3220
Model Statistics	Matthew's Correlation Coefficient	0.49	0.51	0.51	0.51	0.51	0.63
	Accuracy	0.76	0.76	0.76	0.76	0.76	0.81
	Sensitivity	0.63	0.75	0.75	0.75	0.75	0.88
	Specificity	0.85	0.77	0.77	0.77	0.77	0.77
	Positive predictive value	0.71	0.67	0.67	0.67	0.67	0.70
	Negative predictive value	0.79	0.83	0.83	0.83	0.83	0.91
	True positive	5	6	6	6	6	7
	False positive	2	3	3	3	3	3
	False negative	3	2	2	2	2	1
	True negative	11	10	10	10	10	10

4.5 Discussion

The research outlined in this chapter has exposed relationships between the three-dimensional structural features of drugs and their metabolites and IMDILI. Parent or metabolite structures for many drugs implicated in IMDILI share common molecular features (in the form of a 4-point pharmacophore) that are largely not present in non-hepatotoxic drugs. This is consistent with the hypothesis that one of the prerequisites for IMDILI is possession of structural features that interact with common targets within common pathways to initiate or potentiate the toxicity reaction.

The prominence of metabolites among the matches to the pharmacophore is an interesting observation, since metabolites are not always taken into account in previous work of a similar nature (172). The literature has identified increased hepatic metabolism as a risk factor for IMDILI (see section 1.3.1 Characteristics of medications), and hence it is logical to infer that metabolites may have a role in the pathogenesis of toxicity. This highlights the importance of taking hepatic metabolism into account when developing models; both *in silico*, to ensure known and proposed metabolites are included in the analyses and *in vitro* and *in vivo*, to ensure the experimental system has metabolic capabilities.

Traditionally, QSAR and pharmacophore perception methodologies have focussed on a single drug class in order to refine and perfect one lead compound out of a pool of similar molecules. The drugs used in this analysis had considerably varied structures, with the

training set alone covering 7 different therapeutic drug classes. Given the varied pharmacological effects of these drugs it is unlikely that the common pharmacophore hypothesis is related to the drugs' mechanisms of action; rather the 3D arrangements of structural features may reflect as yet unidentified receptors in a shared toxicity pathway.

Similarly, traditional drug discovery attempts have generally focussed on designing drugs with specific agonist/antagonist activity on a single target. Network pharmacology acknowledges the inherent resistance and redundancies built into many biological systems and proposes that instead of targeting single receptors, drugs need to exhibit activity on multiple targets within a pathway to achieve the desired effect. In this view, the drug design process aims to optimise multiple structure-activity relationships at once (128).

Given the complexity and variety of risk factors influencing IMDILI (see section 1.3 Associations & Risk Factors for iDILI), it is likely that there is more than one receptor of importance within the toxicity pathway of IMDILI. One possibility is that the toxicophore hypothesis mirrors the active sites of multiple biological targets. Alternatively, there may be multiple pharmacophores which are important, with each corresponding to a different biological target within the toxicity pathway. For example, the toxicophore hypothesis may reflect the structural configuration needed to activate an adaptive immune system protein, and a second pharmacophore hypothesis, such as one of the high scoring AADD variants from Table 4.7, may reflect the structural configuration needed to active a protein of the innate immune system, with toxicity manifesting only when both proteins have been activated.

Such a so-called multiple toxicophore hypothesis would be difficult to test using *in vitro* and *in vivo* experimental systems since the system would have to replicate the complex interaction between the innate and adaptive immune systems. The first step towards testing such a hypothesis would be to identify possible biological targets using *in silico* screening. Secondly, the ability of implicated drugs to activate these targets separately can be tested *in vitro*. Finally, an *in vivo* experimental system can be developed to examine whether activating a combination of proteins will lead to IMDILI.

4.6 Conclusion

This chapter has identified a 4-point toxicophore hypothesis that captures the structural similarities between the molecules implicated in IMDILI. Presumably, this three-dimensional arrangement of molecular features is important in the activation of the toxicity pathway for IMDILI, and may reflect the features required to activate one or more biological proteins within this pathway.

Using the toxicophore as a starting point, the following chapters of the thesis will begin this process of identifying potential toxicity targets for IMDILI.

Chapter 5: The Search for Potential Toxicity Targets

5.1 Virtual Screening

Virtual screening describes the process by which compound libraries are searched for potential leads in the drug discovery process. This can take various forms depending on the search criteria. The previous chapters of this thesis have identified:

1. Literature evidence for the involvement of both adaptive and innate immunity in IMDILI.
2. A set of probe molecules for investigating IMDILI.
3. A 4-point pharmacophore hypothesis common to drugs implicated in IMDILI. This 4-point pharmacophore hypothesis will be referred to as the primary toxicophore hypothesis.

5.2 Pharmacophore based virtual screening of the DrugBank database

5.2.1 Introduction

Pharmacophore based virtual screening can be undertaken to search compound libraries for molecules which contain the 3D arrangement of molecular features, or pharmacophore, required for biological activity.

A number of tools, both commercial and open source are available for pharmacophore screening. There are typically two different types of scoring algorithms that are used during the screening process (251):

Root Mean Square Deviation (RMSD) based methods measure the distance of the feature group in the molecule to the centre of the pharmacophore feature. Molecules with chemical features which align to the pharmacophore within the specified distance tolerances are considered hits.

Overlay based methods take into consideration the radii of the feature and the atoms involved. Hits are identified when the radii of the pharmacophoric feature of the molecule overlap with the radii of the pharmacophore.

The work in this section was undertaken using two RMSD based pharmacophore screening programs: Schrödinger's Phase (193) and Pharmer (252).

5.2.1.1 Phase

Phase offers the option of generating conformations during the search process. Compounds are filtered based on their pharmacophore feature frequencies. For example if the input pharmacophore is AADR, hits must have at least 2 hydrogen bond acceptors, 1 hydrogen bond donor and 1 ring. Compounds which do not have the required features are eliminated from the search. Conformers are eliminated if the distances between pharmacophore sites are insufficiently close to those of the hypothesis. Conformations which survive this process are aligned to the pharmacophore hypothesis. Whether an alignment is identified as a hit to the pharmacophore is determined by the Intersite Distance Matching Tolerance (IDMT). This is the RMSD of the intersite distances between the molecule under investigation and the reference ligand used to generate the pharmacophore hypothesis (203); *i.e.* the distance between the molecule and the centre of the pharmacophoric feature. The default is 2.0Å.

Since all compounds in the database are investigated, the computational resource required for the search increases in proportion to the size of the database queried.

5.2.1.2 Pharmer

Pharmer is a computational approach to pharmacophore screening that scales more with the complexity of the pharmacophore search, rather than the size of the database. Pharmacophore features in compounds are identified using SMARTS patterns. The spatial relationships between each of the features within a compound are stored as a series of coordinate triangles. The pharmacophore search query is broken down into triplets of features. The compound database is then searched for all the feature triangles that are able to match each triplet. The triangles are then reassembled to produce the compound and the conformation that is able to align to the pharmacophore. Using this method millions of compounds in a library can be searched within a few seconds (252).

Matches to the pharmacophore are determined by the radii of the pharmacophoric features; *i.e.* the distance between the molecule and the center of the pharmacophoric feature, which is the same as the Phase software. The default is 0.5Å.

5.2.2 Datasource

DrugBank is an open data drug and drug target database (143). As of 2/06/2015 the database contains a total of 7759 drug entries, including small molecule approved drugs,

protein/peptide approved drugs, nutraceuticals and experimental drugs. The full database is available for download (www.drugbank.ca/downloads#structures).

5.2.3 Rationale

Previous chapters of this work have identified a toxicophore hypothesis that is able to differentiate between drugs implicated in IMDILI and drugs devoid of DILI. Therefore, drugs with structural elements which are able to match the toxicophore should be more likely to be associated with IMDILI than drugs which do not match the hypothesis.

Examining the number of matches to the toxicophore within the DrugBank database will give an indication of the specificity of the hypothesis and may aid in identifying drugs associated with IMDILI which were not identified in Chapter 2 of this thesis.

To examine the implications of differences in the default feature tolerances values between the two programs (Phase: 2.0Å; Pharmer 0.5Å), the screening was repeated using three different tolerance settings: 0.5Å, 1.0Å and 2.0Å.

5.2.4 Methods

5.2.4.1 Molecular preparation

Since Pharmer does not have molecular manipulation tools, all molecules were prepared with Schrödinger software and subsequently exported for use in Pharmer.

All drugs held in the DrugBank database as of 20/08/13 were downloaded as a single *sdf* file and imported into Maestro (253). Drugs with MW > 500 Daltons were excluded from further analyses.

The global minimal energy state of all molecules was determined with MacroModel (version 9.9, Schrödinger, LLC, New York, NY, 2012). Structures were minimised using the PRCG method (see section 4.1.3.1.2 Energy Minimisation). The convergence threshold was set to 0.05, based on gradient. Up to a maximum of 5000 iterations were allowed. The OPLS_2005 forcefield was used with a constant solvent dielectric of 1.0. Subsequently each molecule was visually inspected to confirm that minimisation had given chemically correct structures. The LigPrep (199) program was used to perform the 2D to 3D conversion for any structures not adequately minimised by the minimisation process using MacroModel (see examples in Figure 5.1 and Figure 5.2).

Conformations were generated with Confgen (202) using rapid sampling of the conformational space. Redundant conformers were eliminated using a RMSD cutoff of 0.5Å.

Structures were subsequently exported as a single *sdf* file.

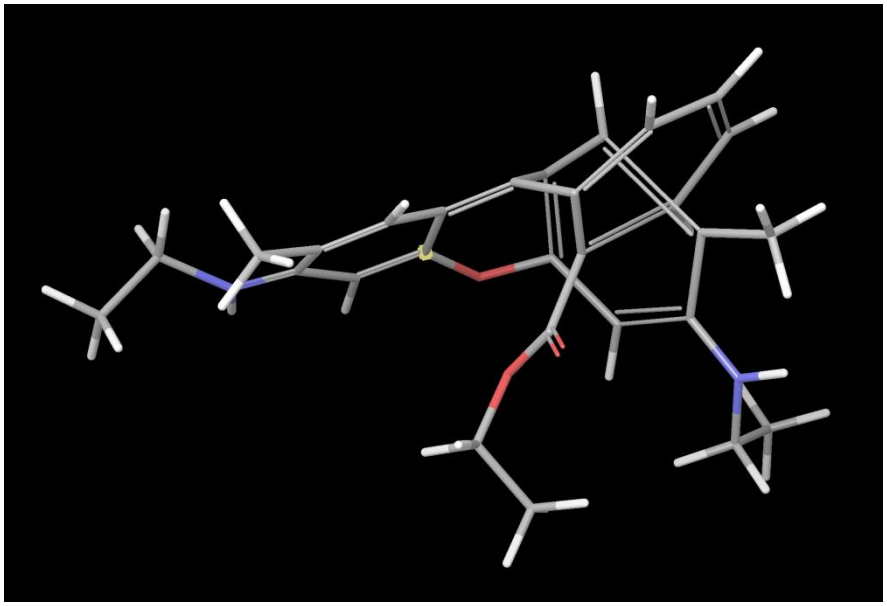

Figure 5.1 Output of multiple minimisation, showing distorted conformation of Rhodamine with intersecting rings. (Potential Energy: 12,857kcal).

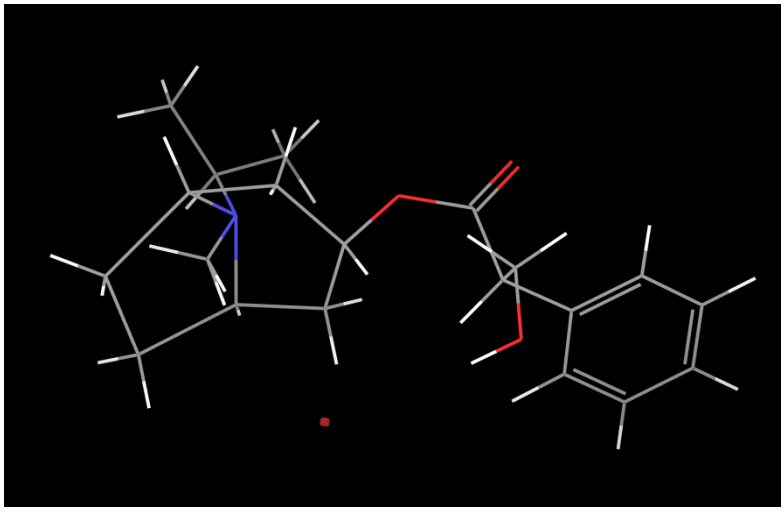

Figure 5.2 Output of multiple minimisation, showing distorted conformation of ipratropium with a methyl group inside a ring structure. (Potential Energy: 4154kcal).

5.2.4.2 Pharmacophore screening

The Phase Advanced Pharmacophore Screening tool and the Pharmer program were used to screen the DrugBank dataset for matches to the toxicophore hypothesis.

5.2.4.2.1 Phase

The site measurements of the toxicophore hypothesis (Figure 4.5) and the prepared DrugBank structures were imported into a Maestro project. The Phase Advanced Pharmacophore Screening tool was used to screen the DrugBank molecules for matches to the toxicophore.

Since conformations had already been generated during the Molecular Preparation step, the "Use existing conformers" option was selected during the pharmacophore screening.

Matches were required to align with all 4 site points of the toxicophore hypothesis.

The analysis was repeated with 3 different settings for the intersite distance matching tolerance: 0.5Å, 1.0Å or 2.0Å (default).

5.2.4.2.2 Pharmer

The site measurements of the toxicophore hypothesis were manually entered into the Pharmer software. The *sdf* file containing the DrugBank molecules was used to create a pharmer database. Matches were required to align with all 4 site points of the toxicophore hypothesis. The analysis was repeated with 3 different settings for the radii of the pharmacophore features: 0.5Å (default), 1.0Å or 2.0Å.

5.2.5 Results

The number of drugs returned as hits to the pharmacophore are presented in Table 5.1. For both Phase and Pharmer, decreasing the pharmacophore feature tolerance results in a lower number of matches to the pharmacophore. The Phase screen runs returned less matches than the Pharmer runs at the higher pharmacophore feature tolerance settings (all except 0.5Å). The full lists of drugs that match the toxicophore as determined by Phase and Pharmer at the smallest feature tolerance setting are presented in Appendix 7: List of DrugBank molecules which match the toxicophore hypothesis (Table 15.1 and Table 15.2 respectively).

Table 5.1 Results of DrugBank screen carried out using the Phase Advanced Pharmacophore Screening (193)and Pharmer (252) programs. The number of molecules within the DrugBank database which were returned as hits to the primary toxicophore hypothesis is shown for each run.

Run	*Phase:* Intersite Distance Matching Tolerance (Å) *Pharmer:* Radii of feature (Å)	# DrugBank Matches (out of 5757)
Phase 1	2.0 (default)	2040
Phase 2	1.0	705
Phase 3	0.5	333
Pharmer 1	2.0	2383
Pharmer 2	1.0	1014
Pharmer 3	0.5 (default)	61

5.2.6 Discussion

From Figure 5.1 and Figure 5.2, it is interesting to note that sometimes molecular manipulation software can return structures with high potential energies that are unlikely to exist *in vivo*. This highlights the need to visually inspect molecules with unusually high energies to confirm that structures have been reasonably energy minimised.

While the number of hits appear to be comparable between the two programs at IDMT/radii settings of 2.0Å and 1.0Å, it is important to take into account the differences between the two settings. Since the IDMT used by Phase relates to the deviation of the distance between the centres of two pharmacophoric sites, it is approximately equivalent to twice the radii of feature used by Pharmer, which relates to the distance deviation from 1 site point only. Hence, an IDMT of 2.0Å in Phase would approximately correspond with a 1.0Å setting in Pharmer. When this is taken into account, Pharmer is returning substantially fewer hits than Phase at the corresponding tolerance settings.

The Phase run with the default IDMT of 2.0Å returned 2040 hits, which is a substantial proportion (35%) of the DrugBank database. Since these molecules contain the toxicophore hypothesis, they share structural features with drugs which are implicated in IMDILI. Hence, they may also be capable of activating the required biological pathways which lead to IMDILI. The rare incidence of IMIDLI is related to patient exposure, rather than the number of drugs implicated – *i.e.* it is possible for a large number of drugs to be implicated in IMDILI, with IMDILI manifesting in only a small minority of people who are exposed to the drugs.

One of the aims of this section was to identify drugs which are associated with IMDILI. In the absence of an *in vitro* confirmation assay, it is difficult to determine whether the returned hits are drugs which have true hepatotoxic potential. Similarly, without the means to verify the results, it is difficult to determine the optimal tolerance setting for the pharmacophore screening process. Until a reliable screening assay is developed, the use of the toxicophore as a screening tool will remain limited.

5.3 Screening of Toll-Like Receptor 7 agonists

5.3.1 Introduction

TLRs have a role in liver injury, with recent research linking TLR9 and liver fibrosis (254) and TLR 2 with neutrophil recruitment in acute and chronic liver injury (255). Lipopolysachharides from Gram-negative bacterial cell walls, TLR4 ligands, have also been known to potentiate DILI of trovafloxacin in animal models (256). TLR7, a cytoplasmic endosomal TLR, the subtype investigated in this study, is similar to TLR9 and is one of the few TLRs for which there are known small molecule modulators. All TLRs, with the exception of TLR3, are known to activate the MyD88 pathway (257), the downstream effects of which include the production of inflammatory cytokines and the expression of costimulatory molecules required for the activation of the adaptive immune system (65).

5.3.2 Rationale

Loxoribine, a model TLR7 agonist, possesses an arrangement of structural features that is consistent with the primary toxicophore hypothesis identified in the previous chapter of this thesis. Moreover loxoribine, abacavir and allopurinol (from the training set used in the pharmacophore perception) all share an imidazopyridine-like ring structure which is also present in the purine derived nucleobases adenine and guanine (Figure 5.3). Since TLR7 has a role in the identification of ssRNA from viruses (64), TLR7 agonists can share structural similarities with the nucleobases (258). This suggests that TLR7 may be a potential IMDILI toxicity target. If this is the case, it is expected that the pharmacophore hypothesis would be more prevalent in a group of molecules with known TLR7 activity than in a group devoid of this activity.

In this section two related analyses were undertaken: 1) Screening of a set of TLR7 agonists using the toxicophore hypothesis, and 2) Development of a pharmacophore hypothesis from the set of TLR7 agonists.

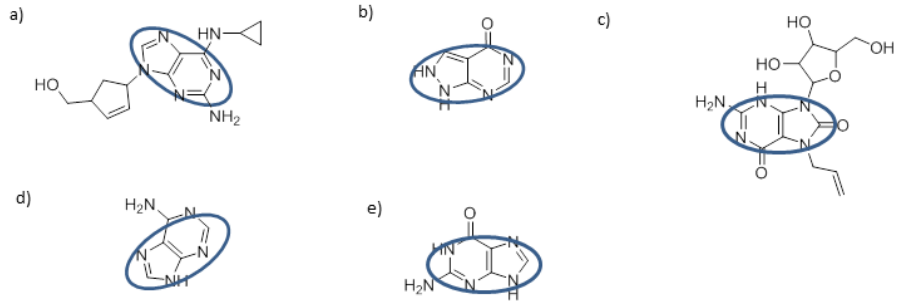

Figure 5.3 Chemical structures of a) abacavir, b) allopurinol, c) loxoribine, d) adenine and e) guanine with the imidazopyridine-like ring structure highlighted.

5.3.3 Methods

5.3.3.1 Molecular Preparation

Structures of 36 compounds, including 23 TLR7 agonists and 13 without activity on TLR7, were identified from Yoo *et al.*(258) and drawn into Masetro using the 2D sketcher tool (253). The structures used in the analyses are presented in Table 5.2.

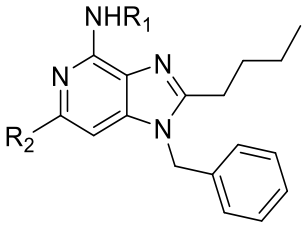

Table 5.2 Structures of Toll-like receptor 7 agonistic 1*H*-imidazo[4,5-*c*]pyridines as described by Yoo *et al.* (207)

Compound	R1	R2
5	H	H
6a	$COCH_3$	H
6b	COC_3H_7	H
11a	C_4H_9	H
11b	$CH_2C_6H_5$	H
17	H	Cl
19a	H	NH_2

Compound	R1	R2
19b	H	NHC_4H_9
19c	H	NHC_7H_{15}
19d	H	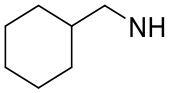
19e	H	NHC_6H_5
19f	H	$NHCH_2C_6H_5$
19g	H	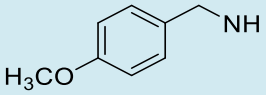
19h	H	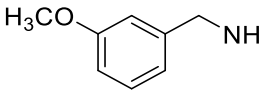
19i	H	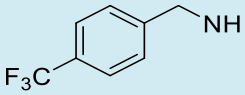
19j	H	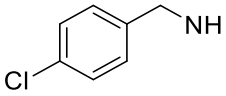
19k	H	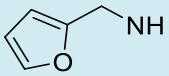
19l	H	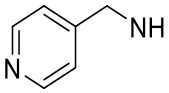
19m	H	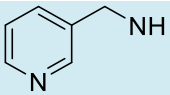
19n	H	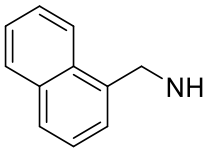
19o	H	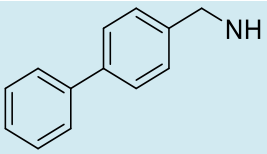
19p	H	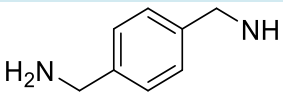
19q	H	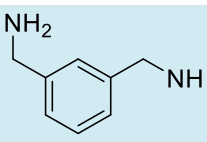

Compound	R1	R2
19r	H	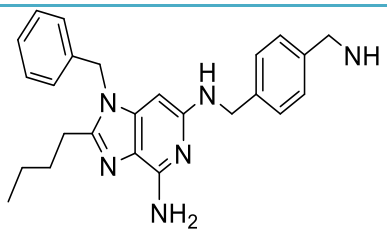
19s	H	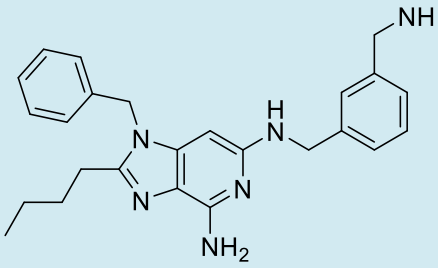
23a	H	C_4H_9
23b	H	C_6H_5
23c	H	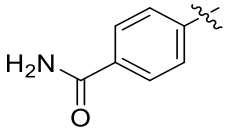
23d	H	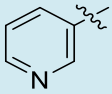
23e	H	
23f	H	
23g	H	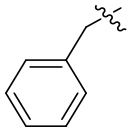
23h	H	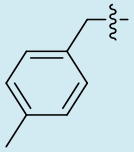
23i	H	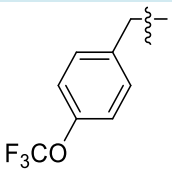

Compound	R1	R2
23j	H	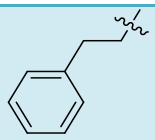
30	Full molecule:	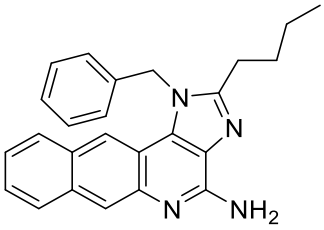

The global minimal energy state of all molecules was determined with MacroModel (200). Structures were minimised using the PRCG method (see section 4.1.3.1.2 Energy Minimisation). The convergence threshold was set to 0.05, based on gradient. Up to a maximum of 5000 iterations were allowed. The OPLS_2005 forcefield was used with a constant dielectric of 1.0. Subsequently each molecule was visually inspected to confirm that minimisation had given chemically correct structures.

5.3.3.2 Screening of TLR7 agonists using the toxicophore hypothesis

The Phase Advanced Pharmacophore Screening tool was used to screen the compounds for matches using the toxicophore hypothesis. The intersite distance matching tolerance was set to 2.0Å. Conformations were generated during the search using the Rapid Sampling method (see 4.1.3.1.3 Conformer generation). Matches were required to align with all 4 site points of the toxicophore hypothesis.

The predictive performance measures: sensitivity, specificity, accuracy, Matthews Correlation Coefficient, positive predictive value and negative predictive value, were calculated.

5.3.3.3 Development of a pharmacophore from TLR7 agonists

A pharmacophore hypothesis was generated from these molecules using the methodology described in Chapter 4 (4.3.4 Create pharmacophore sites; 4.3.5 Develop common pharmacophore hypothesis and 4.3.6 Scoring actives).

5.3.4 Results

5.3.4.1 Screening of a set of TLR7 agonists using the toxicophore hypothesis

The results of the toxicophore screening are presented in Table 5.3. The toxicophore hypothesis matched 17 of 23 (74%) of compounds with activity on TLR7 and 4 of 13 (31%) of the inactives. This corresponds to a sensitivity and specificity of 74% and 54% respectively. The 5 most potent agonists according to Yoo *et al.* (258) (19f,g,k,l,m) are among those that match the pharmacophore.

Table 5.3 List of compounds active and inactive on Toll-like Receptor 7 and whether or not the compounds match the primary toxicophore hypothesis.

Compound	Activity on TLR7	Matches Toxicophore
5	Yes	No
6a	No	No
6b	No	No
11a	No	No
11b	No	No
17	No	No
19a	Yes	Yes
19b	Yes	Yes
19c	Yes	Yes
19d	Yes	Yes
19e	Yes	Yes
19f	Yes	Yes
19g	Yes	Yes
19h	Yes	Yes
19i	Yes	Yes
19j	Yes	Yes
19k	Yes	Yes
19l	Yes	Yes
19m	Yes	Yes
19n	No	Yes
19o	Yes	Yes

Compound	Activity on TLR7	Matches Toxicophore
19p	Yes	Yes
19q	Yes	Yes
19r	Yes	Yes
19s	No	Yes
23a	Yes	No
23b	No	No
23c	No	Yes
23d	No	No
23e	No	No
23f	No	No
23g	Yes	No
23h	Yes	No
23i	No	Yes
23j	Yes	No
30	Yes	No

5.3.4.2 Develop a pharmacophore hypothesis from the set of TLR7 agonists

Phase identified 21 pharmacophore variants which matched 17 out of 23 TLR7 agonists: AAAA, AAAD, AAAH, AAAR, AADD, AADH, AADR, AAHR, AARR, ADDH, ADDR, ADHR, ADRR, AHRR, ARRR, DDHR, DDRR, DHRR, DRRR, HRRR, RRRR.

The survival scores for these hypotheses ranged from 2.24 to 3.87. Among the top scoring hypotheses with a survival score of 3.87 is an AADR pharmacophore which was able to differentiate between compounds with activity on TLR7 and compounds without activity with a sensitivity of 74% and a specificity of 69%. The statistical performance values are presented in Table 5.4. This pharmacophore has similar site measurements (Figure 5.4) to the toxicophore hypothesis. Figure 5.5 depicts the significant overlap between this pharmacophore and the toxicophore hypothesis.

Table 5.4 Performance measures for an AADR pharmacophore hypothesis which matched 17 out of 23 TLR7 agonists.

Performance measure	Score
True positive	17
False positive	4
False negative	6
True negative	9
MCC	0.42
Accuracy	0.72
Sensitivity	0.74
Specificity	0.69
Positive predictive value	0.81
Negative predictive value	0.60

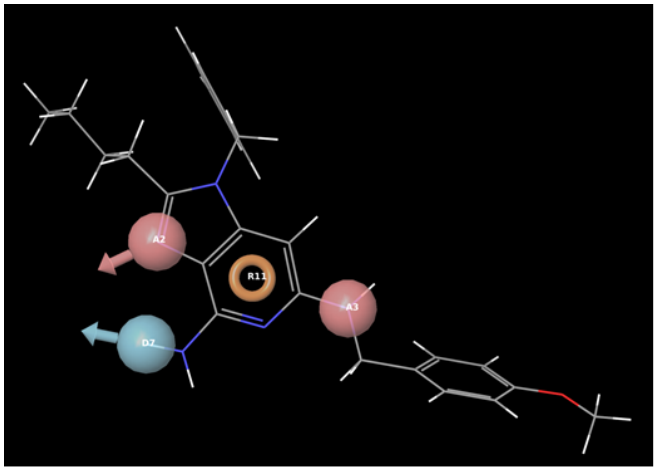

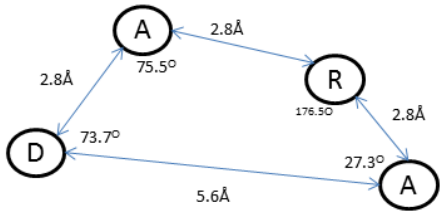

Site 1	Site 2	Distance (Å)
A2	A3	5.5
A2	D7	2.8
A2	R11	2.8
A3	D7	5.6
A3	R11	2.8
D7	R11	3.4

Site 1	Site 2	Site 3	Angle (°)
A3	A2	D7	77.3
A3	A2	R11	1.7
D7	A2	R11	75.5
A2	A3	D7	29.1
A2	A3	R11	1.7
D7	A3	R11	27.3
A2	D7	A3	73.7
A2	D7	R11	51.9
A3	D7	R11	21.8
A2	R11	A3	176.5
A2	R11	D7	52.6
A3	R11	D7	130.9

Figure 5.4 Pharmacophore generated from 1H-imidazo[4,5-c]pyridine Toll-Like Receptor 7 agonists, matching 17 out of 23 actives.

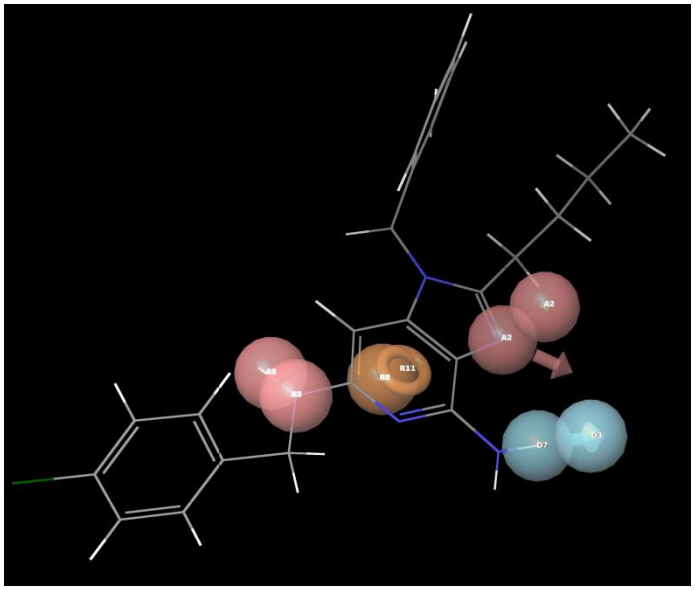

Figure 5.5 Superimposed images of the AADR pharmacophore generated from TLR7 agonists and the toxicophore hypothesis.

5.3.5 Discussion

Part 1 of this section revealed that the toxicophore was able to match 17 out of 23 TLR7 agonists. Hence it is not surprising that a pharmacophore with similar site measurements to the toxicophore would be able to be perceived from the same set of TLR7 agonists. It is interesting to note however that the toxicophore-like hypothesis ranked among the top scoring hypotheses perceived in Part 2 of this section – *i.e.* not only is the hypothesis an adequate model for the requirements for TLR7 activity, it is one of the better models available. This strongly suggests that the IMDILI probe set of drugs, which also contains these pharmacophoric elements, may be able to activate TLR7. As such, TLR7 is identified as a potential target that is common to the toxicity pathways of these drugs.

5.4 Structure based virtual screening (molecular docking)

5.4.1 Introduction

Molecular docking is a structure based drug design technique. If a protein structure is known, algorithms can be used to predict the interaction between ligands and the protein.

Prediction of the ligand-receptor complex is difficult for a number of reasons:

1. The binding site of the ligand may not be known. It has been shown that even compounds with similar mechanisms of action can have different binding modes.

2. Since both the ligand and the receptor site have flexibility, simulating the molecular dynamics of the *in* vivo ligand-receptor interaction is computationally demanding.
3. It difficult to determine the *in vivo* binding conformation. A highly efficient scoring algorithm must be in place to allow the screening of large numbers of molecules in a reasonable amount of time.

The strength of the interaction between the receptor and the ligand can be quantified by calculating the free energy of binding. This can be broken down in a number of ways, commonly in the form (259):

Contributions to the binding free energy (259).

$$\Delta G_{bind} = \Delta G_{solvent} + \Delta G_{conf} + \Delta G_{int} + \Delta G_{motion} \quad (8)$$

Most of the methods available for molecular docking assume that the receptor site is rigid; conformational flexibility is allowed only for the ligand.

Examples of molecular docking programs are DOCK (260), Flex-X (261,262), GOLD (263), SURFLEX (264), GLIDE (265). The work outlined here utilised the GLIDE program, so discussion will focus on the molecular docking methods available within this software.

5.4.1.1 Schrödinger's GLIDE program

Schrödinger's GLIDE (Grid-based Ligand Docking with Energetics) program simulates the interactions between one or more ligand molecules and a protein receptor (265). In GLIDE docking experiments, proteins are usually held rigidly – *i.e.* conformational changes in the protein are not considered.

5.4.1.1.1 Protein preparation

Before ligand-receptor interactions can be simulated, the receptor binding site must first be identified. If a co-crystal of a ligand-receptor complex is available, this can be examined to see if the binding site is likely to be shared among other ligands. If a number of co-crystallised structures are available, a single reference complex is chosen. All the other complexes are then superimposed onto it. The user can then examine the superimposed ligands to determine if they would be a reasonable fit for the reference binding site – *i.e.* there are no major steric clashes. If this is not the case, then the sites can be taken as independent, and separate docking experiments would have to be performed. Similarly, if a

number of binding sites are apparent from co-crystallised structures, separate docking experiments would have to be performed for each of these sites (266).

Protein structural information is generally sourced from the Research Collaboratory for Structural Bioinformatics (RCSB) Protein Data Bank (PDB) (www.rcsb.org). Structural data is derived from X-ray crystallographic studies, and generally only consists of heavy atoms, waters molecules, cofactors and metal ions. Structures may also be multimeric, containing one or more sub units. Bond orders and ionisation states are unassigned, and terminal amide groups can be misaligned. These missing elements of PDB files need to be filled in before forcefields can be used to calculate ligand binding energies.

Schrödinger provides a Protein Preparation Wizard to assist in identifying and resolving common problems in the PDB structure (267). PDB structures can be imported directly by the wizard. Waters not thought to be involved in ligand binding are deleted. Redundant subunits or protein chains not involved in ligand binding are also removed to increase computational efficiency. Missing information for residues near the active site and formal charges for metal ions and ligating groups can also be added in. Covalent bonds from the protein to any co-crystallised ligand cannot be handled by GLIDE and must be deleted (266).

A restrained minimisation of the input protein coordinates is then run to reorient side-chain hydroxyl groups and resolve potential steric clashes.

Following preparation, the protein structure should be checked for errors. This can be done by visually inspecting for steric clashes or by docking the native ligand.

5.4.1.1.2 Ligand preparation

Ligand structures used for docking must not be covalently bonded to the receptor and should be a form that is likely to exist in the *in vivo* environment. Typically this means all atom 3D structures which are ionised at physiological pH (7±2.0) and globally minimised to a low energy state.

Schrödinger's LigPrep program (199) is designed to prepare a large number of ligands for docking. In accordance with the Glide user manual, structures are refined through the following series of steps (266):

1. Convert structure format into 3D
2. Add hydrogen atoms
3. Neutralized charged groups
4. Generate ionization states
5. Generate tautomers
6. Filter structures
7. Generate alternative chiralities
8. Generate low-energy ring conformations
9. Remove problematic structures
10. Optimize the geometries
11. Convert output file to desired format

5.4.1.1.3 Receptor Grid generation

At the ligand binding site, the shape and properties of the receptor are represented by a series of grid points. Pre-calculating the values of these grid points decreases the time and computational resources required to process the docking of large numbers of molecules. If there is more than one receptor binding conformation, multiple grids may be required (266). The binding site can be identified either by selecting a co-crystallised ligand or by marking the relevant amino acid residues.

While Glide does not allow for flexibility in the receptor during the docking process, slight 'give' in the receptor and in the ligand can be modelled by modifying the van der Waals radii scaling of nonpolar atoms. Decreasing the van der Waals radii of nonpolar atoms lowers the penalties for close contacts and provides some leniency for receptor flexibility (266).

5.4.1.1.4 Ligand docking

Ligand docking is conducted using the OPLS_2005 forcefield. Three levels of docking precision are available:

- HTVS (high-throughput virtual screening) is designed for the rapid screening of a huge number of ligands. Conformational sampling is restricted in order to decrease computational resources.
- SP (standard precision) is used for screening large numbers of compounds of unknown quality.

- XP (extra precision) is intended for ligands that have been identified by Standard Precision docking as high scoring. XP mode utilises a custom scoring function combined with a powerful sampling method to identify false positives and improve the correlation between good poses and good scores. XP mode is considerably more computationally demanding than SP docking. XP descriptor information can be requested to allow for visualisation of the scoring terms at a later stage.

A number of ligand sampling options are also available:

- Score in place: with this option no docking or optimisation is conducted. The input coordinates for the ligand are used for scoring. Accurate initial placement of the ligand with respect to the receptor is required.
- Refined in place: with this option, no docking is performed. Rather, Glide identifies the best-scoring pose that is geometrically similar to the input pose by optimising the ligand structure in the field of the receptor.
- Rigid: in rigid docking, no conformations are generated; the input conformation of the ligand is only translated or rigidly rotated with respective to the binding site.
- Flexible: in flexible sampling, conformations are generated during the docking process. This option was used for the analysis.

5.4.1.1.5 Visualizing Docking results

Poses are orientations of molecules that are aligned with respect to the receptor. Poses created during a docking run are saved into a pose viewer file. Such files can be viewed using the Ligand Interaction Diagram facility in Maestro (253). In addition to displaying the poses, Maestro can also display hydrogen bonds, contacts and interactions with residues.

For XP runs, the results can be displayed and analysed with the Glide XP Visualizer (266). This displays a table of XP terms for each ligand and allows the selective evaluation of ligands. The terms included in the XP scoring function are listed in

Table 5.5. The GlideScore (GScore) is the sum of the XP terms and summarises the overall binding affinity of the ligand for the receptor (266).

Table 5.5 List of terms included in the Glide XP (extra precision) docking scoring function (266).

XP Term	Description
LipophilicEvdW	Lipophilic term derived from hydrophobic grid potential at the hydrophobic ligand atoms
PhobEn	Hydrophobic enclosure reward
PhobEnHB	Reward for hydrophobically packed H-bond
PhoEnPairHB	Reward for hydrophobically packed correlated H-bonds
HBond	ChemScore H-bond pair term
Electro	Electrostatic rewards; includes Coulomb and metal terms
SiteMap	SiteMap ligand-receptor non-H-bonding polar-hydrophobic terms
π Stack	Pi-pi stacking reward
π Cat	Reward for pi-cation interactions
ClBr	Reward for Cl or Br in a hydrophobic environment that pack against Asp or Glu
LowMW	Reward for ligands with low molecular weight
Penalties	Polar atom burial and desolvation penalties, and penalty for intro-ligand contacts
BPenal	Penalty for ligands with large hydrophobic contacts and low H-bond scores
ExposPenal	Penalty for solvent-exposed ligand groups; cancels van der Waals terms
RotPenal	Rotatable bond penalty

5.4.2 Methods

The crystal structure of *HLA-B*5701* complexed with peptide V and abacavir was obtained from the protein data bank (PDB: 3UPR Biological Assembly 1). All waters were removed and the protein was optimized and minimised using Maestro's Protein Preparation Wizard.

Flucloxacillin and its metabolites were drawn in using Maestro's 2D sketcher tool (Table 5.6).

Drug	Structure
Flucloxacillin	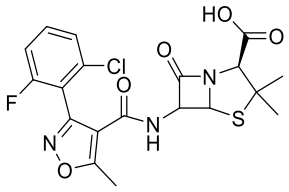
Flucloxacillin M1 (209)	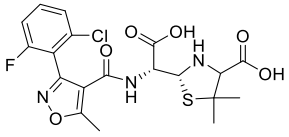
Flucloxacillin M2 (209)	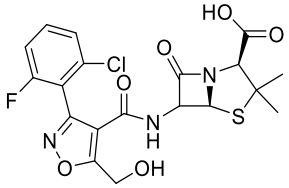
Flucloxacillin M3 (209)	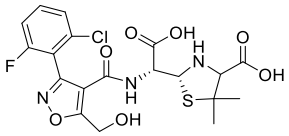

Table 5.6 Structures of flucloxacillin and its metabolites.

Ligprep (199) was used to ionise the molecules at physiological pH (7±2.0) and to energy minimise the structures.

Glide (version 5.8, Schrödinger, LLC, New York, NY, 2012.)(265) was used to generate a 14Å cubic receptor grid centred on the crystallised abacavir. Scaling of van der Waals radii was set to 0.8 with a partial charge cut off of 0.15.

Extra precision flexible docking of flucloxacillin and its metabolites was then conducted.

Ligand interaction diagrams were generated using Maestro's Ligand Interaction Diagram tool (253).

5.4.3 Results

XP docking showed that flucloxacillin and its metabolites were able to interact with *HLA-B*5701* in the same binding pocket as abacavir (Figure 5.6). The pharmacophoric features were positioned to interact with complementary amino acid residues within the HLA binding groove. Three examples are given in Figure 5.7, Figure 5.8 and Figure 5.9.

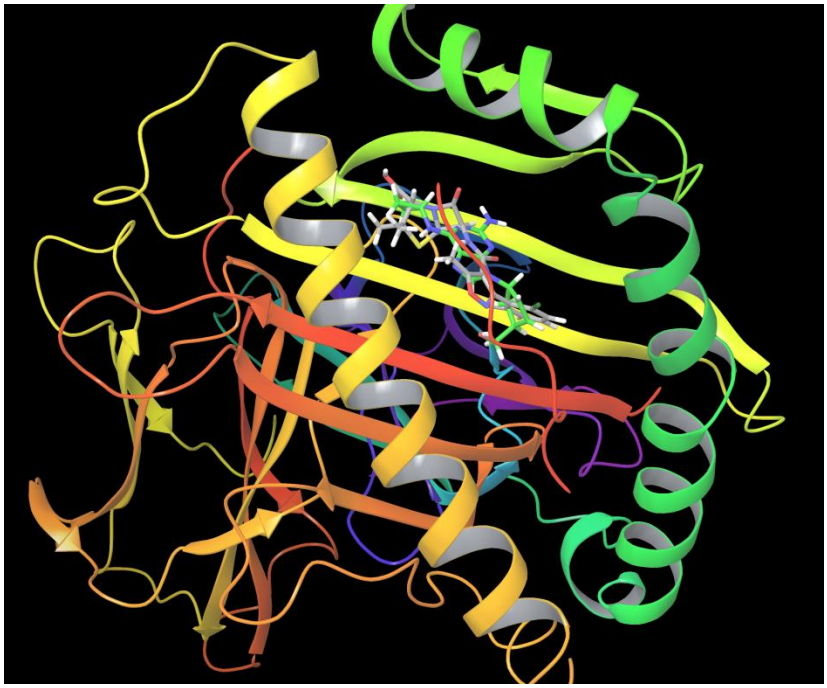

Figure 5.6 Abacavir (green) and flucloxacillin overlapped in the F-pocket of the HLA-B*5701 binding groove.

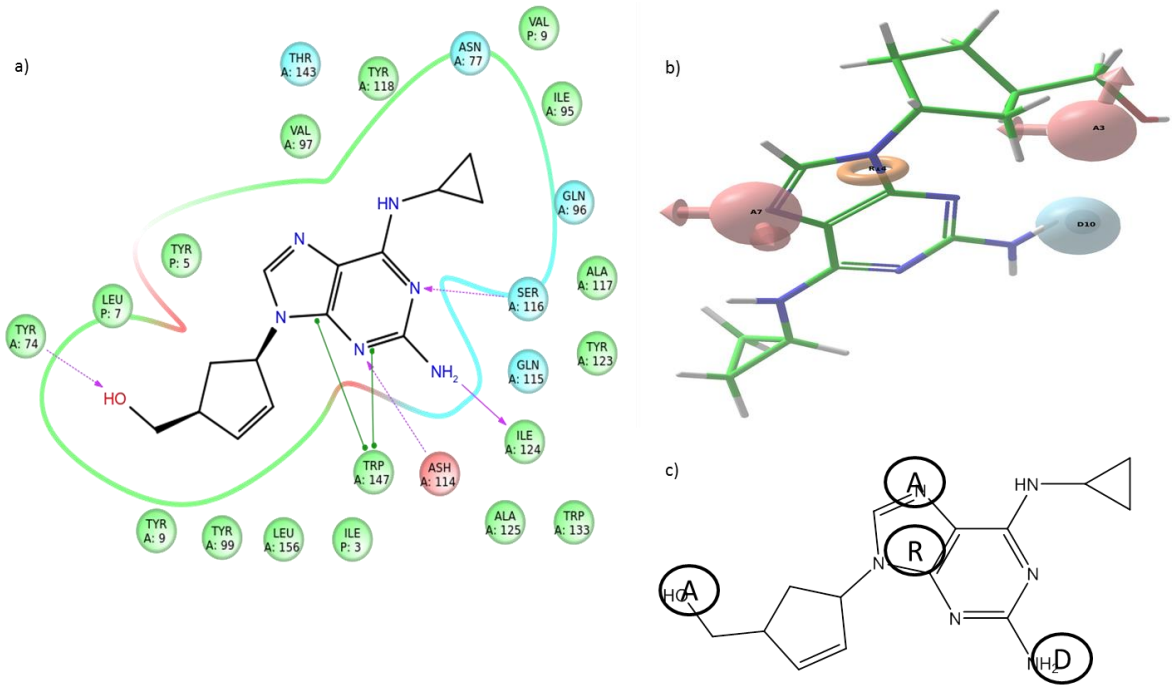

Figure 5.7 a) Ligand interaction diagrams showing the interactions between amino acids of *HLA-B*5701*, peptide V and abacavir. b) Abacavir superimposed on the AADR toxicophore hypothesis from Chapter 4. c) Schematic showing the chemical groups contributing to the pharmacophore.

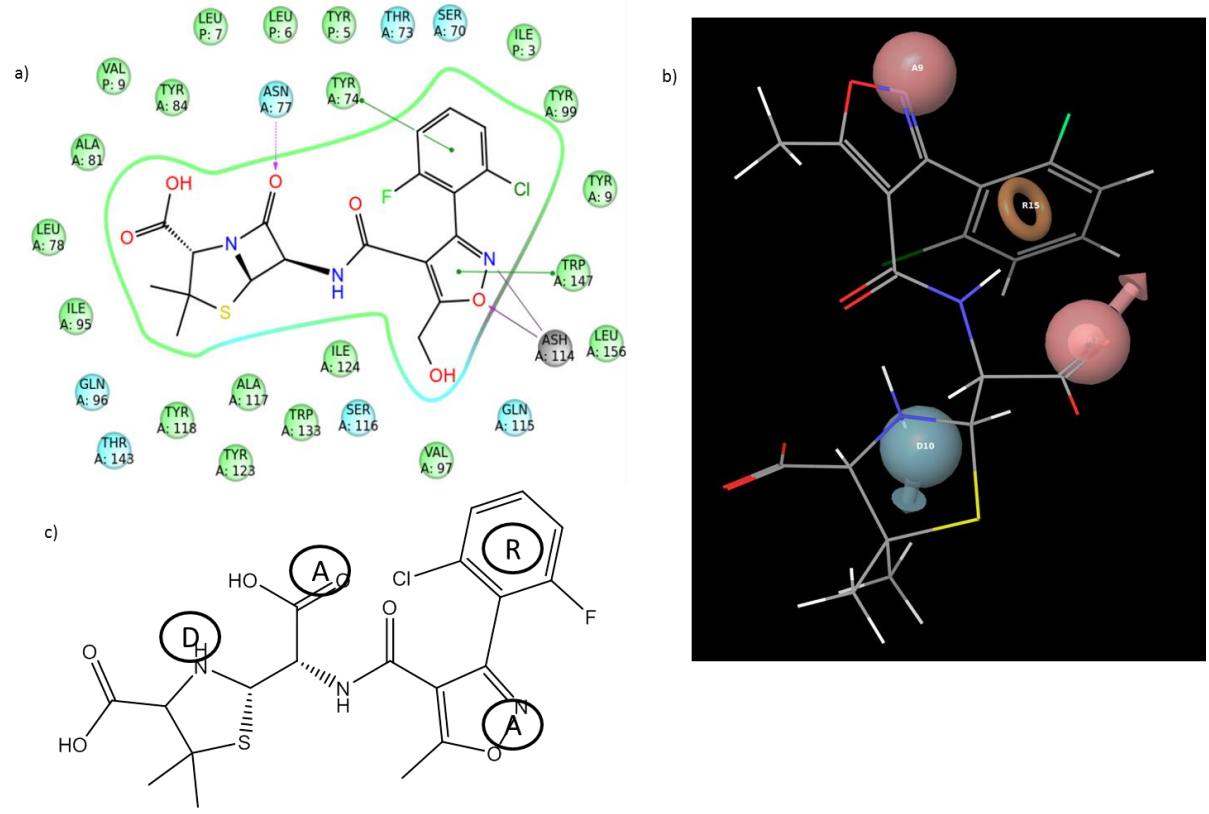

Figure 5.8 a) Ligand interaction diagrams showing the interactions between amino acids of HLA-B*5701, peptide V and flucloxacillin M1. b) Flucloxacillin M1 superimposed on the AADR pharmacophore hypothesis from Chapter. c) Schematic showing the chemical groups contributing to the pharmacophore.

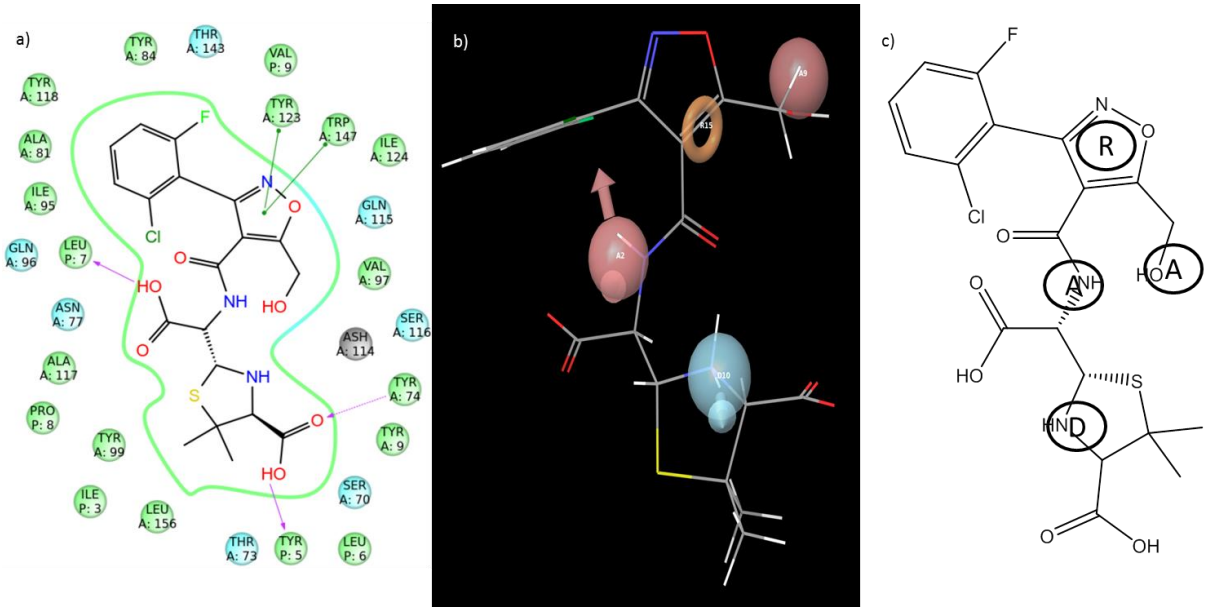

Figure 5.9 a) Ligand interaction diagrams showing the interactions between amino acids of *HLA-B*5701*, peptide V and flucloxacillin M3. b) Flucloxacillin M3 superimposed on the AADR pharmacophore hypothesis from Chapter. c) Schematic showing the chemical groups contributing to the pharmacophore.

5.4.4 Discussion

The results from this section show that flucloxacillin and its metabolites are able to bind to the same binding pocket as abacavir.

A recently published paper on abacavir hypersensitivity (53) provides evidence for a modified p-i hypothesis (see 1.4.4 Pharmacological interaction (p-i) hypothesis) which the authors termed the altered self-peptide repertoire model. In this model, abacavir binds in the F-pocket at the base of the *HLA-B*5701* groove. The presence of abacavir alters the set of endogenous peptides presented to T-cells by *HLA-B*5701*, and this is thought to be the mechanism behind abacavir's observed *HLA-B*5701* restricted hypersensitivity (53). The residues Tyr9, Tyr-74, Ile-95, Val97, Tyr99,Tyr123, Ile-124, Trp147, Ile3, Leu7, and Val9 were thought to be those important in abacavir binding (53).

Interestingly, these residues also appear to be important in the binding of the penicilloic acid metabolites of flucloxacillin and of its 5-hydroxymethyl derivative (Figure 5.7, Figure 5.8, Figure 5.9). This suggests that the metabolites of flucloxacillin are interacting with *HLA-B*5701* and the co-crystallised peptide in a similar manner to abacavir and hence T-cell activation *via HLA-B*5701* may be a common toxicity pathway for both abacavir and flucloxacillin. This is consistent with recent literature which has demonstrated the

importance of cytotoxic T-cells in mediating flucloxacillin induced DILI in *HLA-B*5701* positive patients (268).

Moreover, the residues that are associated with binding are positioned to interact with the structural elements in the abacavir and flucloxacillin metabolite molecules which contribute to the toxicophore hypothesis.

Although *HLA-B*5701* has not previously been associated with abacavir induced liver injury, patients exposed to abacavir have been known to develop DILI with immune features (51). Since *HLA-B*5701* positive patients are at increased risk of abacavir induced hypersensitivity reactions, it is possible that *HLA-B*5701* may also play a role in mediating abacavir induced liver injury.

Similarly, since the toxicophore is shared by molecules which are implicated in IMDILI, and the structural elements contributing to the toxicophore appear to be important in the binding interaction with *HLA-B*5701*, *HLA-B*5701* may be a potential toxicity target within the toxicity pathway.

5.5 Conclusions

Starting from a relationship between drug structure and hepatotoxicity in the form of a 4-point toxicophore hypothesis, this chapter has used virtual screening methods to identify more drugs associated with IMDILI as well as biological targets which may be involved in the toxicity pathway, namely the immune-system proteins *HLA-B*5701* and TLR7.

There is evidence for a role of the toxicophore within the toxicity pathway, which supports the hypothesis that drugs (or their metabolites) which produce similar patterns of toxicity interact with targets within common toxicological pathways and that activation of the underlying mechanisms depends on structural similarity among toxic molecules.

From the literature knowledge regarding the mechanisms of IMDIL, these are both plausible toxicity targets that warrant further investigation. This may take the form of *in vitro* assays to determine whether drugs of the training set are able to activate an immune response *via* *HLA-B*5701* and TLR7.

5.6 Publication

The work presented in this Chapter in conjunction with that of Chapters 2 and 4 has been published in the journal *CPT Pharmacometrics and Systems Pharmacology* (269). The full publication is presented in Appendix 1: Peer Reviewed Scientific Publications arising from this thesis.

Chapter 6: Experimental verification

6.1 Introduction

The previous chapters have identified TLR7 as a potential toxicity target for drugs implicated in IMDILI. This chapter an experiment to test whether or not the probe IMDILI set of drugs are able to activate TLR7 *in vitro*.

All TLRs, with the exception of TLR3 activate the MyD88 adaptor molecule and activation of NFκB and mitogen-activated protein kinases (MAP kinases) which leads to the induction of inflammatory cytokines (257). Within the signalling pathway, IκB has an inhibitory effect on NFκB. When IκB is phosphorlated, this inhibitory effect is removed and results in the production of inflammatory cytokines (3).

Cherfils-Vicini *et al.* used a Western Blotting procedure to demonstrate that loxoribine is able to promote the phosphorylation of IκB through the activation of TLR7 (3). Western Blotting is a technique used in cell and molecular biology to semi-quantitatively identify the presence of specific proteins within cells. This technique is described in further detail below.

6.1.1 Western Blotting

The Western Blotting technique has been recently described in detail by Mahmood and Yang (270) and Yang and Ma (271). Briefly, this technique consists of the following elements:

1. Sample preparation
2. Gel electrophoresis
3. Blotting
4. Antibody incubation
5. Detection

6.1.1.1 Sample Preparation

The proteins of interest need to be extracted from the cells. Samples taken from cell culture are cooled or frozen rapidly with protein inhibitors to prevent the proteins from denaturing. Tissue samples display a higher degree of structure and need to be homogenised using sonication or mechanical force before the proteins can be extracted.

Once extracted, the proteins are added into a buffer solution containing a dye and a detergent. The detergent, typically sodium dodecyl sulfate (SDS), surrounds the protein with a negative charge, which will become important at a later stage where an electric field is applied to move the proteins. The dye, typically bromophenol blue, is added to allow the researcher to visually gauge the progress of the separation. The samples are then boiled for 1 to 5 minutes to denature the protein higher order structure and loaded side-by-side into wells on a gel.

6.1.1.2 *Gel Electrophoresis*

Typically polyacrylamide gels are used for gel electrophoresis. The proteins loaded into the gel have a negative charge and will travel towards the positive electrode when voltage is applied. The speed of the protein through the gel is dependent upon the size of the pores in the gel and the size of the proteins, thus separating a mixture of proteins into bands based on their molecular weight. Two lanes on the gel are generally reserved for a positive and a negative control. The positive control, or a bench mark, can be a commercially available mixture of proteins of known molecular weights or a known source of the target protein. This serves as a marker to confirm the identity of the target protein. A negative control is a null cell line, and is used to confirm that the staining is not nonspecific. For example, actin can be included to ensure that there are a similar number of cells in each well for the western blot.

6.1.1.3 Blotting

Once the separation is complete, the proteins in the polyacrylamide gel need to be transferred to a membrane for further analyses. A membrane typically made of nitrocellulose or polyvinylidene fluoride (PVDF) is laid on the gel. A voltage is then applied perpendicularly to the surface of the gel to move the negatively charged proteins from the gel onto the membrane.

6.1.1.4 Antibody incubation

To allow for detection, a label-antibody is used to bind the proteins of interest. Before the antibody is applied, blocking is conducted, typically with 5% bovine serum albumin (BSA) or nonfat dried milk diluted in Tris Buffered Saline with Tween® (TBST), in order prevent antibodies from binding to the membrane non-specifically.

Following incubation with the antibody, the membrane must be washed thoroughly to remove unbound antibody and minimise background signals in the detection step.

6.1.1.5 Detection

The presence of proteins of interest can be determined by the strength of the colorimetric or photometric signal emitted by the label antibody. Western Blotting is considered a semi-quantitative technique since it provides a relative comparison of protein levels rather than specifically measuring the quantity of protein present in the initial sample.

6.2 Rationale

The experiment was conducted using airway smooth muscle cells (A549) which are known to express a number of TLRs, including TLR7. Since the activation of TLRs is asociated with the phosphoroylation of IκB, phosphorylated IκB (pIκB) can be used as a surrogate measure of TLR activity. If an effect on IκB is demonstrated, the experiment can be repeated using TLR7 knockout cells. A lack of response will confirm that the effect is due to TLR7 rather than another TLR subtype. The aim of this experiment ito compare the ability of probe IMDILI drugs to phosphoralate IκB with that of loxoribine in order to test whether the probe set of IMDILI drugs are active on TLR7.

6.3 Methods

Eight compounds were included in the analysis (Table 6.1). Loxoribine was chosen as the active control. For the actives, abacavir and allopurinol were included because of their structural similarity to loxoribine. Flucloxacillin was included due to the potential shared toxicity pathway with abacavir. The remaining active, nevirapine, and the 3 inactive controls, clemastine; oxybutynin and baclofen were randomly chosen. All chemicals were purchased from Sigma-Aldrich.

A549 airway smooth muscle cells were cultured as per Appendix 8: A549 Cell Culture.

The cells were then stimulated with the compounds listed in Table 6.1 at a concentration of 10µg/mL for 30 minutes.

Table 6.1 Compounds included in the *in vitro* analysis.

Compound	
Loxoribine	Active control
Abacavir sulfate	Active
Allopurinol	Active
Flucloxacillin	Active
Nevirapine	Active
Clemastine fumarate	Negative control
Oxybutynin chloride	Negative control
Baclofen	Negative control

Cells were prepared for Western Blotting as follows:

1. Remove supernatant from 6-well dishes.
2. Wash with 2 x 2 mL sterile phosphate-buffered saline (PBS).
3. Add 300 µL 1X sample buffer and dithiothreitol (DTT) to each well.
4. Scrape and collect in small tubes.
5. Boil for 5 minutes and store at -80°C.
6. Boil samples again for 5 minutes when ready to use for Western blotting.

The experiment was subsequently repeated with loxoribine only at a number of different concentrations: 10; 25 and 50 µg/mL. For this second experiment, two time points for cell treatment (30 and 60 minutes) were used.

A third run was conducted with the cells stimulated for 30 minutes at a concentration of 20µg/mL. This run was conducted using only a subset of the drugs (loxoribine, abacavir, nevirapine, oxybutynin and flucloxacillin).

6.4 Results

Figure 6.1 shows the expression of IκB following an incubation period of 30 minutes with each compound at a concentration of 10 µg/mL. IκB is present in all cells with the exception of those treated with TNFα. Correspondingly, Figure 6.2 shows the presence of phosphorolated IκB (pIκB) in these cells. pIκB was only present in cells treated with TNFα.

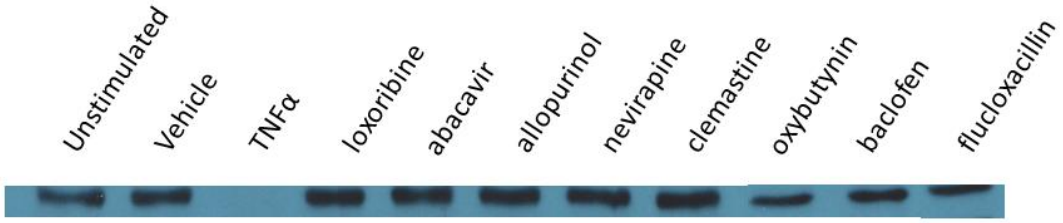

Figure 6.1 Expression of IκB in A549 cells. Cells were stimulated for 30 minutes with the respective compounds.

Figure 6.2 Expression of pIκB in A549 cells. Cells were stimulated for 30 minutes with the respective compounds.

Figure 6.3 shows the expression of IκB following an incubation period of either 30 or 60 minutes withTNFα or loxoribine at 10; 25 or 50 µg/mL. IκB is present in all cells with the exception of those treated with TNFα. Correspondingly, Figure 6.4 shows the presence of phosphorolated IκB (pIκB) in these cells. pIκB was only present in cells treated with TNFα.

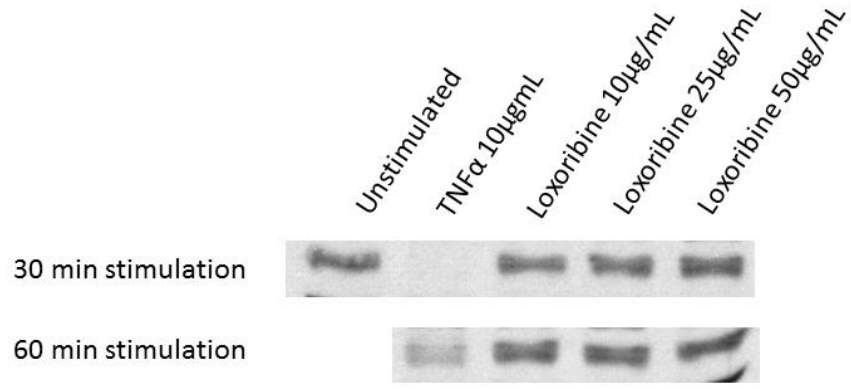

Figure 6.3 Expression of IκB in A549 cells. Cells were stimulated with loxoribine or TNFα for 30 minutes or 60 minutes at the respective concentrations.

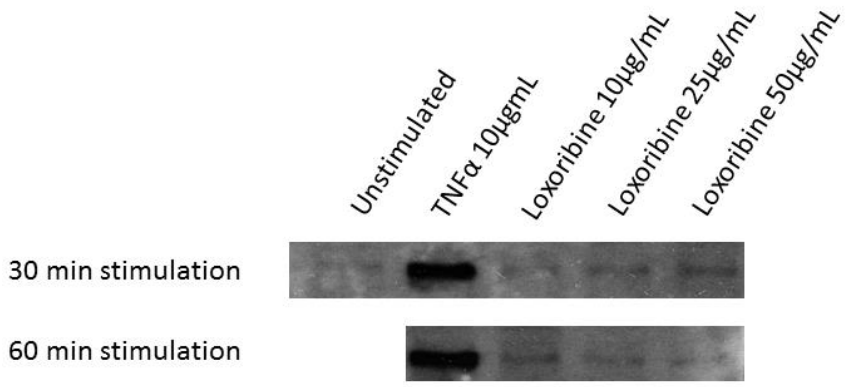

Figure 6.4 Expression of pIκB in A549 cells. Cells were stimulated with loxoribine or TNFα for 30 minutes or 60 minutes at the respective concentrations.

Figure 6.5 shows the expression of IκB following an incubation period of 30 minutes with each compound at a concentration of 10 µg/mL. IκB is present in all cells with the exception of those treated with TNFα. Correspondingly, Figure 6.6 shows the presence of phosphorolated IκB (pIκB) in these cells. pIκB was only present in cells treated with TNFα.

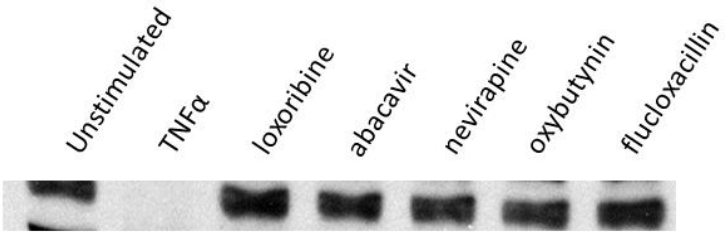

Figure 6.5 Expression of IκB in A549 cells. Cells were stimulated for 30 minutes with the respective compounds at 20µg/mL.

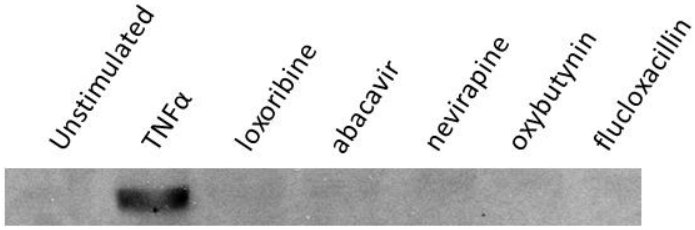

Figure 6.6 Expression of pIκB in A549 cells. Cells were stimulated for 30 minutes with the respective compounds at 20µg/mL.

6.5 Discussion

Although IκB was present in all the examined cells, none of the drugs were able to induce the phosphorylation of IκB. Neither varying the incubation time nor increasing the concentration of the drug increased the phosphorylation of IκB. The presence of pIκB in cells treated with TNFα was expected. TNFα is known to induce the phosphorylation of IκB and was used as the negative control in this experiment.

Surprisingly, loxoribine, a model TLR7 agonist and the positive control for this experiment was also unable to induce the phosphorylation of IκB. This implies that the negative results for the tested drugs are due to a fault in the experimental setup rather than a true result indicating a lack of activity on TLR7.

The inability to replicate the extent of loxoribine induced IκB phosphorylation that was reported by Cherfils-Vicini *et al.* (3) could be due to a number of experimental reasons. Likely suspects include differences in cell plating and/or experimental conditions, such as the room temperature. Further investigations are required to determine the exact differences responsible.

Alternative strategies may include the use of macrophages instead of A549 cells. Immortalised macrophage cell lines derived from bone marrow are available. Endogenous macrophages activate in response to foreign material in the body. Hence, they may provide an indicator of whether the tested compounds are able to activate the innate immune system.

6.6 Conclusion

This chapter described an experimental attempt to test whether or not the probe IMDILI set of drugs are able to activate TLR7 *in* vitro. Although the *in vitro* confirmation studies were not successful, the failure was due to an inability to develop a satisfactory experimental setup, rather than a negative result. Hence one avenue for future work would be to develop an experimental system by which to confirm the results of the *in silico* studies.

Conclusions and Future work

7.1 Overview

A major barrier to the study of rare and multifactorial diseases, such as IMDILI, is the lack of data. Researchers are faced with the conundrum of developing methods for screening or identifying drugs with the potential to cause idiosyncratic hepatotoxicity without knowledge of the underlying pathophysiology, while concomitantly confronting the challenge of revealing the mechanisms behind the toxicity in the absence of reliable *in vitro* or *in vivo* experimental methods.

The presented work has outlined a multidisciplinary stepwise approach for the study of IMDILI. This combination approach makes efficient use of existing data in order to generate new hypotheses regarding toxicological targets. The overall aim was to test the hypothesis that drugs which produce similar patterns of toxicity interact with targets within common toxicological pathways and that activation of the underlying mechanisms depends on structural similarity among toxic molecules.

The structure-toxicity relationship derived in this thesis adds to the growing use of toxicophores within the pharmaceutical industry. A recent review has highlighted the implementation of a step to identify chemical sub-structures within drug molecules as an essential step in the preliminary screening process for new chemical entities (272). Importantly, the results from Chapter 4 demonstrate the need to consider the chemical structures of any proposed metabolites in the screening process. Although increased hepatic metabolism is a known risk factor for DILI, there has been little direct evidence to link chemically reactive metabolites with DILI (273).

7.2 Summary of key findings

Chapter 2 described the use of pharmacovigilance data collected by the TGA to identify a set of 18 drugs, representing 12 drug classes, which were found to be significantly associated with IMDILI. The IMDILI potential of the drugs used in the probe set was confirmed by reviewing the literature in order to increase the confidence that these drugs are truly associated with IMDILI. This set of drugs served as a probe set of drugs to facilitate the study of IMDILI.

Chapter 3 used the network map tools SLAP and STITCH to compare the known and predicted protein interactions for drugs in the probe set in the hope of identifying commonalities in the biological pathways of these drugs. There were substantial differences in the results obtained from each search tool. Hence it was difficult to ascertain whether any of the known and predicted proteins associated with the IMDILI probe set of drugs are potential toxicity targets involved in the pathogenesis of IMDILI.

Chapter 4 described the use of drug design technologies to identify structural similarities between the IMDILI probe set of drugs and their metabolites. This relationship took the form of a four-point toxicophore hypothesis which consisted of 2 hydrogen-bond acceptors, 1 hydrogen-bond donor and 1 ring moiety. In external validation this model was able to differentiate between molecules in the Active and Inactive Test sets with sensitivity and specific of 75% and 92% respectively. Presumably, this three-dimensional arrangement of molecular features is important in the activation of the toxicity pathway for IMDILI, and may reflect the features required to activate one or more biological proteins within this pathway.

Chapter 5 made use of the toxicophore to explore biological proteins which may be involved in the toxicity pathway of IMDILI. Two putative targets within immune pathways that may interact to produce tissue injury in vulnerable individuals were identified; namely the major histocompatability complex (HLA) which is involved in activating T-cells as part of the adaptive immune response and TLR-7, a pattern-recognition receptor involved in the innate immune system, which may be involved in priming or augmenting the adaptive immune response. Both of these are plausible toxicity targets in light of what is already known regarding the involvement of both the adaptive and innate immune systems in the pathogenesis of DILI.

Chapter 6 described an experimental attempt to test whether or not the probe IMDILI set of drugs are able to activate TLR7 *in* vitro. Although the *in vitro* confirmation studies were not successful, the failure was due to an inability to develop a satisfactory experimental setup, rather than a negative result. One avenue for future work would be to develop an experimental system by which to confirm the results of the *in silico* studies.

7.3 Closing remarks

The series of studies that encompass this thesis highlights the potential for multidisciplinary approaches in the study of complex diseases. Importantly, linking information from clinical and chemical databases with knowledge from biological pathway and gene-association datasets can reveal potential mechanisms behind idiosyncratic drug reactions. Multidisciplinary approaches are particularly helpful for rare diseases where little knowledge is available, and may provide key insights into mechanisms of toxicity that cannot be gleaned from a single disciplinary study.

References

1. Chen B, Ding Y, Wild DJ. Assessing drug target association using semantic linked data. PLoS Comput Biol. 2012;8(7):e1002574.
2. Kuhn M, Szklarczyk D, Pletscher-Frankild S, Blicher TH, Von Mering C, Jensen LJ, et al. STITCH 4: Integration of protein-chemical interactions with user data. Nucleic Acids Res. 2014;42(D1):1–7.
3. Cherfils-vicini J, Platonova S, Gillard M, Laurans L, Validire P, Caliandro R, et al. Triggering of TLR7 and TLR8 expressed by human lung cancer cells induces cell survival and chemoresistance. 2010;120(4):1285–97.
4. Fontana RJ, Hayashi PH, Gu J, Reddy KR, Barnhart H, Watkins PB, et al. Idiosyncratic Drug Induced Liver Injury is associated with Substantial Morbidity and Mortality within 6 months From Onset. Gastroenterology [Internet]. Elsevier Ltd; 2014 Mar 26 [cited 2014 Apr 28];147(1):96–108. Available from: http://www.ncbi.nlm.nih.gov/pubmed/24681128
5. FDA U.S. Department of Health and Human Services. FDA Guidance for Industry. Drug-Induced Liver Injury: Premarketing Clinical Evaluation [Internet]. 2009. Available from: www.fda.gov/downloads/Drugs/GuidanceComplianceRegulatoryInformation/Guidances/UCM174090.pdf
6. Xie Y, McGill MR, Dorko K, Kumer SC, Schmitt TM, Forster J, et al. Mechanisms of acetaminophen-induced cell death in primary human hepatocytes. Toxicol Appl Pharmacol [Internet]. Elsevier B.V.; 2014 Jun 3 [cited 2014 Jul 12];279(3):266–74. Available from: http://www.ncbi.nlm.nih.gov/pubmed/24905542
7. Kaplowitz N. Drug-Induced Liver Injury. Clin Infect Dis. 2004;38(Suppl 2):S44–8.
8. Björnsson ES, Bergmann OM, Björnsson HK, Kvaran RB, Olafsson S. Incidence, presentation, and outcomes in patients with drug-induced liver injury in the general population of iceland. Gastroenterology [Internet]. AGA Institute American Gastroenterological Association; 2013 Jun [cited 2013 Jun 2];144(7):1419–25.e3. Available from: http://www.ncbi.nlm.nih.gov/pubmed/23419359
9. Kaniwa N, Saito Y. Pharmacogenomics of severe cutaneous adverse reactions and drug-induced liver injury. J Hum Genet [Internet]. Nature Publishing Group; 2013 Jun [cited 2013 Jul 17];58(6):317–26. Available from: http://www.ncbi.nlm.nih.gov/pubmed/23635947
10. Andrade RJ, Lucena MI, Fernández MC, Pelaez G, Pachkoria K, García-Ruiz E, et al. Drug-Induced Liver Injury: An Analysis of 461 Incidences Submitted to the Spanish Registry Over a 10-Year Period. Gastroenterology [Internet]. 2005 Aug [cited 2012 May 8];129(2):512–21. Available from: http://linkinghub.elsevier.com/retrieve/pii/S0016508505008760
11. Daly AK, Donaldson PT, Bhatnagar P, Shen Y, Pe'er I, Floratos A, et al. HLA-B*5701 genotype is a major determinant of drug-induced liver injury due to flucloxacillin. Nat Genet [Internet]. 2009;41(7):816–9. Available from: http://ezproxy.library.usyd.edu.au/login?url=http://ovidsp.ovid.com/ovidweb.cgi?T=JS&CSC=Y&NEWS=N&PAGE=fulltext&D=medl&AN=19483685
12. Paul WE. Bridging innate and adaptive immunity. Cell [Internet]. Elsevier Inc.; 2011 Dec 9 [cited 2012 Mar 2];147(6):1212–5. Available from: http://www.ncbi.nlm.nih.gov/pubmed/22153065
13. Shenton JM, Chen J, Uetrecht JP. Animal models of idiosyncratic drug reactions. Chem Biol Interact [Internet]. 2004;150(1):53–70. Available from: http://ezproxy.library.usyd.edu.au/login?url=http://ovidsp.ovid.com/ovidweb.cgi?T=JS&CSC=Y&NEWS=N&PAGE=fulltext&D=med4&AN=15522261

14. Uetrecht J. Immune-mediated adverse drug reactions. Chem Res Toxicol [Internet]. 2009 Jan;22(1):24–34. Available from: http://www.ncbi.nlm.nih.gov/pubmed/19149477

15. Andersson U, Lindberg J, Wang S, Balasubramanian R, Marcusson-Stahl M, Hannula M, et al. A systems biology approach to understanding elevated serum alanine transaminase levels in a clinical trial with ximelagatran. Biomarkers [Internet]. 2009;14(8):572–86. Available from: http://ezproxy.library.usyd.edu.au/login?url=http://ovidsp.ovid.com/ovidweb.cgi?T=JS&CSC=Y&NEWS=N&PAGE=fulltext&D=medl&AN=19780643

16. Kindmark A, Jawaid A, Harbron CG, Barratt BJ, Bengtsson OF, Andersson TB, et al. Genome-wide pharmacogenetic investigation of a hepatic adverse event without clinical signs of immunopathology suggests an underlying immune pathogenesis. Pharmacogenomics J [Internet]. 2008 Jun [cited 2012 Mar 30];8(3):186–95. Available from: http://www.ncbi.nlm.nih.gov/pubmed/17505501

17. Metushi IG, Sanders C, Lee WM, Uetrecht J. Detection of anti-isoniazid and anti-cytochrome P450 antibodies in patients with isoniazid-induced liver failure. Hepatology [Internet]. 2014 Mar [cited 2014 Mar 26];59(3):1084–93. Available from: http://www.ncbi.nlm.nih.gov/pubmed/23775837

18. James L, Roberts D. Isoniazid hepatotoxicity: progress in understanding the immunologic component. Hepatology [Internet]. 2014 Mar [cited 2014 Sep 25];59(3):746–8. Available from: http://www.ncbi.nlm.nih.gov/pubmed/24037911

19. Bath RK, Brar NK, Forouhar FA, Wu GY. A Review of Methotrexate-associated Hepatotoxicity. J Dig Dis [Internet]. 2014 Aug 20 [cited 2014 Sep 25];15(10):517–24. Available from: http://www.ncbi.nlm.nih.gov/pubmed/25139707

20. Maddrey WC. Clinical Manifestations and Management of Drug-Induced Liver Diseases [Internet]. Third Edit. Drug-Induced Liver Disease. Elsevier Inc.; 2013. 229-240 p. Available from: http://dx.doi.org/10.1016/B978-0-12-387817-5.00014-5

21. Hussaini SH, Farrington EA. Idiosyncratic drug-induced liver injury : an update on the 2007 overview. Expert Opin Drug Saf. 2014;13(1):67–81.

22. Verma S, Kaplowitz N. Diagnosis, management and prevention of drug-induced liver injury. Gut [Internet]. 2009 Nov [cited 2013 Jun 9];58(11):1555–64. Available from: http://www.ncbi.nlm.nih.gov/pubmed/19834119

23. Yoke J, Chan M, Fung C, Ping C. Early onset hepatotoxicity associated with low dose fluconazole therapy in a critically ill patient : A case report. East J Med. 2014;19:61–5.

24. Barrett P, Vuppalanchi R, Masuoka H, Chalasani N. Severe Drug-Induced Skin and Liver Injury from Rivaroxaban. Dig Dis Sci [Internet]. 2015;60(6):1856–8. Available from: http://link.springer.com/10.1007/s10620-014-3504-9

25. Watkins PB. Insight into hepatotoxicity: The troglitazone experience. Hepatology. 2005;41:229–30.

26. Uetrecht J. Idiosyncratic drug reactions: current understanding. Annu Rev Pharmacol Toxicol [Internet]. 2007;47:513–39. Available from: http://ezproxy.library.usyd.edu.au/login?url=http://ovidsp.ovid.com/ovidweb.cgi?T=JS&CSC=Y&NEWS=N&PAGE=fulltext&D=med4&AN=16879083

27. Antoine DJ, Harrill AH, Watkins PB, Park BK. Safety biomarkers for drug-induced liver injury - current status and future perspectives. Toxicol Res (Camb). 2014;3:75–85.

28. Borlak J, Chougule A, Singh PK. How useful are clinical liver function tests in in vitro human hepatotoxicity assays? Toxicol In Vitro [Internet]. 2014 Mar 28 [cited 2014 Apr 28];28(5):784–95. Available from: http://www.ncbi.nlm.nih.gov/pubmed/24685772

29. Corsini A, Ganey P, Ju C, Kaplowitz N, Pessayre D, Roth R, et al. Current challenges and controversies in drug-induced liver injury. Drug Saf [Internet]. 2012 Dec 1;35(12):1099–117. Available from: http://www.ncbi.nlm.nih.gov/pubmed/23137150

30. Shi Q, Hong H, Senior J, Tong W. Biomarkers for drug-induced liver injury. Expert Rev Gastroenterol Hepatol [Internet]. 2010;4(2):225–34. Available from: http://ezproxy.library.usyd.edu.au/login?url=http://ovidsp.ovid.com/ovidweb.cgi?T=JS&CSC=Y&NEWS=N&PAGE=fulltext&D=medl&AN=20350268

31. Wang Y, Chen T, Tong W. miRNAs and their application in drug-induced liver injury. Biomark Med [Internet]. 2014 Feb;8(2):161–72. Available from: http://www.ncbi.nlm.nih.gov/pubmed/24521012

32. Gooderham NJ, Koufaris C. Using microRNA profiles to predict and evaluate hepatic carcinogenic potential. Toxicol Lett [Internet]. Elsevier Ireland Ltd; 2014 Jul 15 [cited 2014 Sep 25];228(2):127–32. Available from: http://www.ncbi.nlm.nih.gov/pubmed/24793013

33. Amacher DE. Female gender as a susceptibility factor for drug-induced liver injury. Hum Exp Toxicol [Internet]. 2013 Dec 3 [cited 2013 Dec 20];33(9):928–39. Available from: http://www.ncbi.nlm.nih.gov/pubmed/24299907

34. Santos-Alves E, Marques-Aleixo I, Coxito P, Balça MM, Rizo-Roca D, Rocha-Rodrigues S, et al. Exercise mitigates diclofenac-induced liver mitochondrial dysfunction. Eur J Clin Invest [Internet]. 2014 Jul [cited 2014 Aug 10];44(7):668–77. Available from: http://www.ncbi.nlm.nih.gov/pubmed/24889192

35. Andrade RJ, Robles M, Ulzurrun E, Lucena MI. Drug-induced liver injury: insights from genetic studies. Pharmacogenomics [Internet]. 2009;10(9):1467–87. Available from: http://ezproxy.library.usyd.edu.au/login?url=http://ovidsp.ovid.com/ovidweb.cgi?T=JS&CSC=Y&NEWS=N&PAGE=fulltext&D=medl&AN=19761370

36. Saab L, Peluso J, Muller CD, Ubeaud-Sequier G. Implication of hepatic transporters (MDR1 and MRP2) in inflammation-associated idiosyncratic drug-induced hepatotoxicity investigated by microvolume cytometry. Cytometry A [Internet]. 2013 Apr [cited 2013 Jul 17];83(4):403–8. Available from: http://www.ncbi.nlm.nih.gov/pubmed/23401306

37. Schuetz JD, Swaan PW, Tweedie DJ. The Role of Transporters in Toxicity and Disease. Drug Metab Dispos. 2014;42(4):541–5.

38. Lee JK, Paine MF, Brouwer KLR. Sulindac and its metabolites inhibit multiple transport proteins in rat and human hepatocytes. J Pharmacol Exp Ther [Internet]. 2010;334(2):410–8. Available from: http://www.embase.com/search/results?subaction=viewrecord&from=export&id=L359241566

39. Yang K, Woodhead JL, Watkins PB, Howell B a, Brouwer KL. Systems Pharmacology Modeling Predicts Delayed Presentation and Species Differences in Bile Acid-Mediated Troglitazone Hepatotoxicity. Clin Pharmacol Ther [Internet]. 2014 Jul 28 [cited 2014 Aug 10];96(5):589–98. Available from: http://www.ncbi.nlm.nih.gov/pubmed/25068506

40. Shon J, Abernethy DR. Application of Systems Pharmacology to Explore Mechanisms of Hepatotoxicity. Clin Pharmacol Ther [Internet]. 2014 Nov [cited 2014 Dec 23];96(5):536–7. Available from: http://doi.wiley.com/10.1038/clpt.2014.167

41. Björnsson ES. Incidence and outcomes of DILI in Western patients. Clin Liver Dis [Internet]. 2014 Jul 25 [cited 2014 Aug 10];4(1):9–11. Available from: http://doi.wiley.com/10.1002/cld.368

42. Lammert C, Einarsson S, Saha C, Niklasson A, Bjornsson E, Chalasani N. Relationship between daily dose of oral medications and idiosyncratic drug-induced liver injury: search for signals.

Hepatology [Internet]. 2008 Jun [cited 2012 Mar 24];47(6):2003–9. Available from: http://www.ncbi.nlm.nih.gov/pubmed/18454504

43. Chen M, Borlak J, Tong W. High Lipophilicity and High Daily Dose of Oral Medications are Associated with Significant Risk for Drug-Induced Liver Injury. Hepatology [Internet]. 2013 Dec 19 [cited 2012 Dec 24];58(1):388–96. Available from: http://www.ncbi.nlm.nih.gov/pubmed/23258593

44. Yu K, Geng X, Chen M, Zhang J, Wang B, Ilic K, et al. High Daily Dose and Being a Substrate of Cytochrome P450 Enzymes are Two Important Predictors of Drug-induced Liver Injury. Drug Metab Dispos [Internet]. 2014 Jan 24 [cited 2014 Jan 31];42(4):744–50. Available from: http://www.ncbi.nlm.nih.gov/pubmed/24464804

45. Vuppalanchi R, Gotur R, Reddy KR, Fontana RJ, Ghabril M, Kosinski AS, et al. Relationship Between Characteristics of Medications and Drug-Induced Liver Disease Phenotype and Outcome. Clin Gastroenterol Hepatol [Internet]. Elsevier Ltd; 2014 Dec 19 [cited 2014 Jan 31];12(9):1550–5. Available from: http://www.ncbi.nlm.nih.gov/pubmed/24362054

46. Matthews EJ, Ursem CJ, Kruhlak NL, Daniel Benz R, Sabaté DA, Yang C, et al. Identification of structure-activity relationships for adverse effects of pharmaceuticals in humans: Part B. Use of (Q)SAR systems for early detection of drug-induced hepatobiliary and urinary tract toxicities. Regul Toxicol Pharmacol [Internet]. Elsevier Inc.; 2009 Jan 29 [cited 2012 Apr 13];54(1):23–42. Available from: http://www.ncbi.nlm.nih.gov/pubmed/19545506

47. Hewitt M, Enoch SJ, Madden JC, Przybylak KR, Cronin MTD. Hepatotoxicity: A scheme for generating chemical categories for read-across, structural alerts and insights into mechanism(s) of action. Crit Rev Toxicol [Internet]. 2013 Aug [cited 2013 Jul 30];43(7):537–58. Available from: http://www.ncbi.nlm.nih.gov/pubmed/23875763

48. Liu R, Yu X, Wallqvist A. Data-driven identification of structural alerts for mitigating the risk of drug-induced human liver injuries. J Cheminform. 2015;7(4).

49. Stepan AF, Walker DP, Bauman J, Price D a., Baillie T a., Kalgutkar AS, et al. Structural Alert/Reactive Metabolite Concept as Applied in Medicinal Chemistry to Mitigate the Risk of Idiosyncratic Drug Toxicity: A Perspective Based on the Critical Examination of Trends in the Top 200 Drugs Marketed in the United States. Chem Res Toxicol [Internet]. 2011 Jul 11;24(9):1345–410. Available from: http://pubs.acs.org/doi/abs/10.1021/tx200168d

50. Takai S, Higuchi S, Yano A, Tsuneyama K, Fukami T, Nakajima M, et al. Involvement of immune- and inflammatory-related factors in flucloxacillin-induced liver injury in mice. J Appl Toxicol [Internet]. 2015 Mar 20 [cited 2014 Apr 28];35(2):142–51. Available from: http://www.ncbi.nlm.nih.gov/pubmed/24652713

51. U.S. National Library of Medicine. Abacavir (monograph on the internet) [Internet]. 2015 [cited 2015 Mar 27]. Available from: http://livertox.nlm.nih.gov/Abacavir.htm

52. Lin I, Yang H, Strong C, Yang C. Liver injury in patients with DRESS : A clinical study of 72 cases. J Am Acad Dermatology [Internet]. Elsevier Inc; 2015;72(6):984–91. Available from: http://dx.doi.org/10.1016/j.jaad.2015.02.1130

53. Ostrov DA, Grant BJ, Pompeu YA, Sidney J, Harndahl M, Southwood S, et al. Drug hypersensitivity caused by alteration of the MHC-presented self-peptide repertoire. PNAS [Internet]. 2012 Jun 19 [cited 2012 Nov 7];109(25):9959–64. Available from: http://www.pubmedcentral.nih.gov/articlerender.fcgi?artid=3382472&tool=pmcentrez&rendertype=abstract

54. Wuillemin N, Adam J, Fontana S, Krähenbühl S, Pichler WJ, Yerly D. HLA Haplotype Determines Hapten or p-i T cell Reactivity to Flucloxacillin. J Immunol [Internet]. 2013 May 15 [cited 2013 Jul 17];190(10):4956–64. Available from:

http://www.ncbi.nlm.nih.gov/pubmed/23596311

55. Metushi IG, Sanders C, Lee WM, Uetrecht J. Detection of anti-isoniazid and anti-cyp antibodies in patients with isoniazid-induced liver failure. Hepatology [Internet]. 2014 Jun 14 [cited 2013 Jul 17];59(3):1084–93. Available from: http://www.ncbi.nlm.nih.gov/pubmed/23775837

56. Yun J, Adam J, Yerly D, Pichler WJ. Human leukocyte antigens (HLA) associated drug hypersensitivity: consequences of drug binding to HLA. Allergy [Internet]. 2012 Sep 3 [cited 2012 Sep 11];67(11):1338–46. Available from: http://www.ncbi.nlm.nih.gov/pubmed/22943588

57. Daly AK. Using genome-wide association studies to identify genes important in serious adverse drug reactions. Annu Rev Pharmacol Toxicol [Internet]. 2012 Feb 10 [cited 2012 Mar 25];52:21–35. Available from: http://www.ncbi.nlm.nih.gov/pubmed/21819236

58. Venkatesan P. Carbamazepine oxcarbazepine and eslicarbazepine- serious skin reactions associated with the HLA-A3101 allele. Drug Saf Updat. 2012;6(5).

59. Hautekeete ML, Horsmans Y, Waeyenberge CVAN, Demanet C, Henrion J, Verbist L, et al. HLA Association of Amoxicillin-Clavulanate – Induced Hepatitis. Gastroenterology. 1999;117:1181–6.

60. Norcross M a, Luo S, Lu L, Boyne MT, Gomarteli M, Rennels AD, et al. Abacavir induces loading of novel self-peptides into HLA-B*57: 01: an autoimmune model for HLA-associated drug hypersensitivity. AIDS [Internet]. 2012 Jul 17 [cited 2012 Sep 13];26(11):F21–9. Available from: http://www.ncbi.nlm.nih.gov/pubmed/22617051

61. Frei R, Steinle J, Birchler T, Loeliger S, Roduit C, Steinhoff D, et al. MHC class II molecules enhance Toll-like receptor mediated innate immune responses. PLoS One [Internet]. 2010 Jan [cited 2013 Nov 7];5(1):e8808. Available from: http://www.pubmedcentral.nih.gov/articlerender.fcgi?artid=2808354&tool=pmcentrez&rendertype=abstract

62. Uetrecht JP. New concepts in immunology relevant to idiosyncratic drug reactions: the “danger hypothesis” and innate immune system. Chem Res Toxicol [Internet]. 1999 May;12(5):387–95. Available from: http://www.ncbi.nlm.nih.gov/pubmed/10328748

63. Broering R, Lu M, Schlaak JF. Role of Toll-like receptors in liver health and disease. Clin Sci (Lond) [Internet]. 2011 Nov [cited 2012 Apr 3];121(10):415–26. Available from: http://www.ncbi.nlm.nih.gov/pubmed/21797822

64. Petrasek J, Csak T, Szabo G. Toll-Like Receptors in Liver Disease. Adv Clin Chem [Internet]. 1st ed. Elsevier Inc.; 2013;59:155–201. Available from: http://dx.doi.org/10.1016/B978-0-12-405211-6.00006-1

65. Takeda K, Akira S. Toll-like receptors in innate immunity. Int Immunol [Internet]. 2005 Jan [cited 2014 Jul 15];17(1):1–14. Available from: http://www.ncbi.nlm.nih.gov/pubmed/15585605

66. Su GL. Lipopolysaccharides in liver injury: molecular mechanisms of Kupffer cell activation. Am J Physiol Gastrointest Liver Physiol [Internet]. 2002 Aug [cited 2013 Jun 26];283(2):G256–65. Available from: http://www.ncbi.nlm.nih.gov/pubmed/12121871

67. Cohen J. The immunopathogenesis of sepsis. Nature. 2002;420(6917):885–91.

68. Shaw PJ, Ditewig AC, Waring JF, Liguori MJ, Blomme E a., Ganey PE, et al. Coexposure of mice to trovafloxacin and lipopolysaccharide, a model of idiosyncratic hepatotoxicity, results in a unique gene expression profile and interferon gamma-dependent liver injury. Toxicol Sci. 2009;107(1):270–80.

69. Su Y, Zhang Y, Chen M, Jiang Z, Sun L, Wang T, et al. Lipopolysaccharide exposure augments isoniazide-induced liver injury. J Appl Toxicol [Internet]. 2014 Feb 6 [cited 2014 Mar 26];34(12):1436–42. Available from: http://doi.wiley.com/10.1002/jat.2979

70. Zou W, Roth RA, Younis HS, Burgoon LD, Ganey PE. Oxidative stress is important in the pathogenesis of liver injury induced by sulindac and lipopolysaccharide cotreatment. Toxicology [Internet]. 2010;272(1-3):32–8. Available from: http://www.embase.com/search/results?subaction=viewrecord&from=export&id=L50888926

71. Liu J, Sendelbach LE, Parkinson A, Klaassen CD. Endotoxin pretreatment protects against the hepatotoxicity of acetaminophen and carbon tetrachloride: Role of cytochrome P450 suppression. Toxicology. 2000;147(3):167–76.

72. Yu Z, Otsuka H, Yamaguchi K, Kuroishi T, Sasano T, Sugawara S, et al. Roles of platelets and macrophages in the protective effects of lipopolysaccharide against concanavalin A-induced murine hepatitis. Biochim Biophys Acta - Mol Basis Dis [Internet]. Elsevier B.V.; 2011;1812(9):1069–79. Available from: http://dx.doi.org/10.1016/j.bbadis.2011.06.005

73. Imaeda AB, Watanabe A, Sohail M a., Mahmood S, Mohamadnejad M, Sutterwala FS, et al. Acetaminophen-induced hepatotoxicity in mice is dependent on Tlr9 and the Nalp3 inflammasome. J Clin Invest. 2009;119(2):305–14.

74. Crespo MI, Zacca ER, Núñez NG, Ranocchia RP, Maccioni M, Maletto B a, et al. TLR7 triggering with polyuridylic acid promotes cross-presentation in CD8α+ conventional dendritic cells by enhancing antigen preservation and MHC class I antigen permanence on the dendritic cell surface. J Immunol [Internet]. 2013 Feb 1 [cited 2013 Nov 7];190(3):948–60. Available from: http://www.ncbi.nlm.nih.gov/pubmed/23284054

75. Ueta M, Tokunaga K, Sotozono C, Sawai H, Tamiya G, Inatomi T, et al. HLA-A*0206 with TLR3 polymorphisms exerts more than additive effects in Stevens-Johnson syndrome with severe ocular surface complications. PLoS One [Internet]. 2012 Jan [cited 2013 Nov 7];7(8):e43650. Available from: http://www.pubmedcentral.nih.gov/articlerender.fcgi?artid=3422242&tool=pmcentrez&rendertype=abstract

76. Lemasters JJ. V. Necrapoptosis and the mitochondrial permeability transition: shared pathways to necrosis and apoptosis. Gastrointest Liver Physiiology. 1999;276(1):G1–6.

77. Pessayre D, Fromenty B, Berson A, Robin MA, Letteron P, Moreau R, et al. Central role of mitochondria in drug-induced liver injury. Drug Metab Rev [Internet]. 2012;44(1):34–87. Available from: http://www.embase.com/search/results?subaction=viewrecord&from=export&id=L364098320

78. Rachek LI, Yuzefovych L V., LeDoux SP, Julie NL, Wilson GL. Troglitazone, but not rosiglitazone, damages mitochondrial DNA and induces mitochondrial dysfunction and cell death in human hepatocytes. Toxicol Appl Pharmacol [Internet]. Elsevier Inc.; 2009 Nov [cited 2012 May 8];240(3):348–54. Available from: http://linkinghub.elsevier.com/retrieve/pii/S0041008X09002944

79. Hang XZ, Iu FL, Hen XC, Hu XZ, Etrecht JU. Involvement of the Immune System in Idiosyncratic Drug Reactions. Drug Metab Pharmacokinet. 2011;26(1):47–59.

80. Matzinger P. Tolerance, Danger, and the Extended Family. Annu Rev Immunol. 1994;12:991–1045.

81. Seong S, Matzinger P. Hydrophobicity: an ancient damage-associated molecular pattern that initiates innate immune responses. Nat Rev Immunol. 2004;4(June):469–78.

82. Pichler WJ. The p-i Concept: Pharmacological Interaction of Drugs With Immune Receptors. World Allergy Organ J [Internet]. 2008 Jun;1(6):96–102. Available from: http://www.pubmedcentral.nih.gov/articlerender.fcgi?artid=3651037&tool=pmcentrez&rendertype=abstract

83. Uetrecht J. Role of the Adaptive Immune System in Idiosyncratic Drug-Induced Liver Injury [Internet]. Third Edit. Drug-Induced Liver Disease. Elsevier Inc.; 2013. 175-193 p. Available from: http://dx.doi.org/10.1016/B978-0-12-387817-5.00011-X

84. Wuillemin N, Adam J, Fontana S, Krähenbühl S, Pichler WJ, Yerly D. HLA Haplotype Determines Hapten or p-i T cell Reactivity to Flucloxacillin. J Immunol [Internet]. 2013 May 15 [cited 2013 Jul 17];190(10):4956–64. Available from: http://www.ncbi.nlm.nih.gov/pubmed/23596311

85. Legendre A, Jacques S, Dumont F, Cotton J, Paullier P, Fleury MJ, et al. Investigation of the hepatotoxicity of flutamide: pro-survival/apoptotic and necrotic switch in primary rat hepatocytes characterized by metabolic and transcriptomic profiles in microfluidic liver biochips. Toxicol In Vitro [Internet]. Elsevier Ltd; 2014 Aug [cited 2014 Sep 25];28(5):1075–87. Available from: http://www.ncbi.nlm.nih.gov/pubmed/24793618

86. Vliegenthart a DB, Tucker CS, Del Pozo J, Dear JW. Zebrafish as model organisms for studying drug induced liver injury. Br J Clin Pharmacol [Internet]. 2014 Apr 29 [cited 2014 Sep 25];78(6):1217–27. Available from: http://www.ncbi.nlm.nih.gov/pubmed/24773296

87. Sarich TC, Adams SP, Petricca G, Wright JM. Inhibition of isoniazid-induced hepatotoxicity in rabbits by pretreatment with an amidase inhibitor. J Pharmacol Exp Ther [Internet]. 1999;289(2):695–702. Available from: http://ezproxy.library.usyd.edu.au/login?url=http://ovidsp.ovid.com/ovidweb.cgi?T=JS&CSC=Y&NEWS=N&PAGE=fulltext&D=med4&AN=10215642

88. Khan SR, Baghdasarian A, Fahlman RP, Michail K, Siraki AG. Current status and future prospects of toxicogenomics in drug discovery. Drug Discov Today [Internet]. Elsevier Ltd; 2014 Nov [cited 2013 Nov 12];19(5):562–78. Available from: http://linkinghub.elsevier.com/retrieve/pii/S1359644613003954

89. Chalasani N, Bonkovsky HL, Fontana R, Lee W, Stolz A, Talwalkar J, et al. Features and Outcomes of 889 Patients with Drug-induced Liver Injury: The DILIN Prospective Study. Gastroenterology [Internet]. 2015;148(7):1340–52. Available from: http://linkinghub.elsevier.com/retrieve/pii/S001650851500311X

90. Chen M, Bisgin H, Tong L, Hong H, Fang H, Borlak J, et al. Toward predictive models for drug-induced liver injury in humans: are we there yet? Biomark Med [Internet]. 2014 Feb;8(2):201–13. Available from: http://www.ncbi.nlm.nih.gov/pubmed/24521015

91. Hartung T. Look Back in Anger – What Clinical Studies Tell Us About Preclinical Work. ALTEX. 2013;30(3):275–91.

92. Hamburg M a. Advancing regulatory science. Science [Internet]. 2011 Feb 25;331(6020):987. Available from: http://www.ncbi.nlm.nih.gov/pubmed/22342950

93. Wodzig WKWH, Delft JHM Van, Kleinjans JCS. Classification of Hepatotoxicants Using HepG2 Cells: A Proof of Principle Study. Chem Res Toxicol. 2014;

94. Sjogren A-KM, Liljevald M, Glinghammar B, Sagemark J, Li X-Q, Jonebring A, et al. Critical differences in toxicity mechanisms in induced pluripotent stem cell-derived hepatocytes, hepatic cell lines and primary hepatocytes. Arch Toxicol [Internet]. 2014 Jul [cited 2014 Aug 5];88(7):1427–37. Available from: http://www.ncbi.nlm.nih.gov/pubmed/24912781

95. Atienzar F a, Novik EI, Gerets HH, Parekh A, Delatour C, Cardenas A, et al. Predictivity of dog co-culture model, primary human hepatocytes and HepG2 cells for the detection of

hepatotoxic drugs in humans. Toxicol Appl Pharmacol [Internet]. Elsevier Inc.; 2014 Feb 15 [cited 2014 Mar 26];275(1):44–61. Available from: http://www.ncbi.nlm.nih.gov/pubmed/24333257

96. Roth A, Singer T. The application of 3D cell models to support drug safety assessment: Opportunities & challenges. Adv Drug Deliv Rev [Internet]. Elsevier B.V.; 2014 Dec 27 [cited 2014 Jan 28];2014(69-70):179–89. Available from: http://www.ncbi.nlm.nih.gov/pubmed/24378580

97. Ramaiahgari SC, den Braver MW, Herpers B, Terpstra V, Commandeur JNM, van de Water B, et al. A 3D in vitro model of differentiated HepG2 cell spheroids with improved liver-like properties for repeated dose high-throughput toxicity studies. Arch Toxicol [Internet]. 2014 Mar 6 [cited 2014 Mar 26];88(5):1083–95. Available from: http://www.ncbi.nlm.nih.gov/pubmed/24599296

98. Aritomi K, Ishitsuka Y, Tomishima Y, Shimizu D, Abe N, Shuto T, et al. Evaluation of Three-Dimensional Cultured HepG2 Cells in a Nano Culture Plate System: an In Vitro Human Model of Acetaminophen Hepatotoxicity. J Pharmacol Sci [Internet]. 2014 [cited 2014 Apr 28];124(2):218–29. Available from: http://jlc.jst.go.jp/DN/JST.JSTAGE/jphs/13135FP?lang=en&from=CrossRef&type=abstract

99. Bhushan A, Senutovitch N, Bale SS, Mccarty WJ, Hegde M, Jindal R, et al. Towards a three-dimensional microfl uidic liver platform for predicting drug effi cacy and toxicity in humans. 2013;4(Suppl 1):2–7.

100. Larson B, Banks P, Instruments B, Moeller T. The Impact of a 3-Dimensional Human Liver Microtissue Model on Long-term Hepatotoxicity Studies. BioTek. 2014.

101. Kitamura S, Sugihara K. Current status of prediction of drug disposition and toxicity in humans using chimeric mice with humanized liver. Xenobiotica [Internet]. 2014 Jan [cited 2014 Jan 31];44(2):123–34. Available from: http://www.ncbi.nlm.nih.gov/pubmed/24329499

102. Foster JR, Lund G, Sapelnikova S, Tyrrell DL, Kneteman NM. Chimeric rodents with humanized liver: bridging the preclinical/clinical trial gap in ADME/toxicity studies. Xenobiotica [Internet]. 2013 Dec 10 [cited 2013 Dec 20];8254:1–14. Available from: http://www.ncbi.nlm.nih.gov/pubmed/24320885

103. Shoda LKM, Woodhead JL, Siler SQ, Watkins PB, Howell B a. Linking physiology to toxicity using DILIsym®, a mechanistic mathematical model of drug-induced liver injury. Biopharm Drug Dispos [Internet]. 2014 Nov 10 [cited 2013 Nov 25];35(1):33–49. Available from: http://www.ncbi.nlm.nih.gov/pubmed/24214486

104. Rodríguez-Suárez E, Gonzalez E, Hughes C, Conde-Vancells J, Rudella A, Royo F, et al. Quantitative proteomic analysis of hepatocyte-secreted extracellular vesicles reveals candidate markers for liver toxicity. J Proteomics [Internet]. Elsevier B.V.; 2014 Apr 16 [cited 2014 Apr 28];103(30):227–40. Available from: http://www.ncbi.nlm.nih.gov/pubmed/24747303

105. Fernandez TD, Mayorga C, Gueant JL, Blanca M, Cornejo-Garcia JA. Contributions of pharmacogenetics and transcriptomics to the understanding of the hypersensitivity drug reactions. Allergy. 2014;

106. Benet M, Moya M, Donato MT, Lahoz A, Hervás D, Guzmán C, et al. A simple transcriptomic signature able to predict drug-induced hepatic steatosis. Arch Toxicol [Internet]. 2014 Jan 28 [cited 2014 Jan 29];88(4):967–82. Available from: http://www.ncbi.nlm.nih.gov/pubmed/24469900

107. Eun JW, Bae HJ, Shen Q, Park SJ, Kim HS, Shin WC, et al. Characteristic molecular and proteomic signatures of drug-induced liver injury in a rat model. J Appl Toxicol [Internet].

2014 Sep 18 [cited 2014 Sep 24];35(2):152–64. Available from: http://www.ncbi.nlm.nih.gov/pubmed/25231249

108. Cho Y, Moon P, Baek M. An integrated proteomic and transcriptomic approach to understanding azathioprine-induced hepatotoxicity in rat primary hepatocytes. Electrophoresis. 2014;35(6):911–22.

109. Montastruc F, Scotto S, Vaz IR, Guerra LN, Escudero A, Sáinz M, et al. Hepatotoxicity Related to Agomelatine and Other New Antidepressants: A Case/Noncase Approach With Information From the Portuguese, French, Spanish, and Italian Pharmacovigilance Systems. J Clin Psychopharmacol [Internet]. 2014 Feb 20 [cited 2014 Mar 26];34(3):327–30. Available from: http://www.ncbi.nlm.nih.gov/pubmed/24561328

110. Russo MW, Hoofnagle JH, Gu J, Fontana RJ, Barnhart H, Kleiner DE, et al. Spectrum of statin hepatotoxicity: Experience of the drug-induced liver injury network. Hepatology [Internet]. 2014 Apr 2 [cited 2014 Jul 24];60(2):679–86. Available from: http://www.ncbi.nlm.nih.gov/pubmed/24700436

111. Barnhart H, Davern T. Liver injury from Herbals and Dietary Supplements in the US Drug Induced Liver Injury Network. Hepatology. 2014;60(4):1399–408.

112. U.S. National Library of Medicine. Coding Symbols for Thesaurus of Adverse Reaction Terms (COSTART) Source Information [Internet]. 2010 [cited 2015 Jun 30]. Available from: www.nlm.nih.gov/research/umls/sourcereleasedocs/current/CST/

113. Medical Dictionary for Regulatory Activites (MedDRA) [Internet]. 2015 [cited 2015 Jun 30]. Available from: www.meddra.org

114. Hayashi PH, Barnhart HX, Fontana RJ, Chalasani N, Davern TJ, Talwalkar J a, et al. Reliability of causality assessment for drug, herbal and dietary supplement hepatotoxicity in the Drug-Induced Liver Injury Network (DILIN). Liver Int [Internet]. 2014 Mar 24 [cited 2014 Dec 23];1–10. Available from: http://www.ncbi.nlm.nih.gov/pubmed/24661785

115. Kleiner DE, Chalasani NP, Lee WM, Fontana RJ, Bonkovsky HL, Watkins PB, et al. Hepatic histological findings in suspected drug-induced liver injury: systematic evaluation and clinical associations. Hepatology [Internet]. 2014 Feb [cited 2014 Dec 23];59(2):661–70. Available from: http://www.pubmedcentral.nih.gov/articlerender.fcgi?artid=3946736&tool=pmcentrez&rendertype=abstract

116. Serrano J. LiverTox: An online information resource and a site for case report submission on drug-induced liver injury. Clin Liver Dis [Internet]. 2014 Jul 25 [cited 2014 Aug 10];4(1):22–5. Available from: http://doi.wiley.com/10.1002/cld.388

117. Wong CK, Ho SS, Saini B, Hibbs DE, Fois RA. Standardisation of the FEARS database: a systematic approach to manually recoding drug name variants. Pharmacoepidemiol Drug Saf. 2015;24:731–7.

118. van Puijenbroek EP, Bate A, Leufkens HGM, Lindquist M, Orre R, Egberts ACG. A comparison of measures of disproportionality for signal detection in spontaneous reporting systems for adverse drug reactions. Pharmacoepidemiol Drug Saf [Internet]. 2002;11(1):3–10. Available from: http://www.ncbi.nlm.nih.gov/pubmed/11998548

119. Evans SJW, Waller PC, Davis S. Use of proportional reporting ratios (PRRs) for signal generation from spontaneous adverse drug reaction reports. Pharmacoepidemiol Drug Saf. 2001;10(6):483–6.

120. Lewallen S, Courtright P. Epidemiology in practice: Case-control studies. Community Eye Heal J. 1998;11(28):57–8.

121. Newsom. Logistic Regression [Internet]. Data Analysis II. 2014. Available from: www.upa.pdx.edu/IOA/newsom/da2/ho_logistic.pdf

122. Bender R, Lange S. Adjusting for multiple testing--when and how? J Clin Epidemiol [Internet]. 2001 May;54(4):343–9. Available from: http://www.ncbi.nlm.nih.gov/pubmed/17530590

123. Chalasani N, Björnsson E. Risk Factors for Idiosyncratic Drug-Induced Liver Injury. Gastroenterology [Internet]. Elsevier Inc.; 2010 Jun [cited 2012 May 8];138(7):2246–59. Available from: http://linkinghub.elsevier.com/retrieve/pii/S0016508510005421

124. Berners-lee T, Hendler J, Lassila O. The Semantic Web. Sci Am. 2001;21:34–43.

125. Shadbolt N, Hall W, Berners-Lee T. The semantic web revisited. IEEE Intell Syst. 2006;21(3):96–101.

126. Schreiber G, Raimond Y. RDF 1.1 Primer [Internet]. W3C Working Group Note 25 February 2014. 2014 [cited 2015 Jul 31]. Available from: www.w3.org/TR/NOTE-rdf11-primer-20140225

127. DBpedia [Internet]. 2015 [cited 2015 Jul 31]. Available from: wiki.dbpedia.org

128. Hopkins AL. Network pharmacology: the next paradigm in drug discovery. Nat Chem Biol [Internet]. 2008 Nov [cited 2012 Oct 30];4(11):682–90. Available from: http://www.ncbi.nlm.nih.gov/pubmed/18936753

129. Venkatesan K, Rual J-F, Vazquez A, Stelzl U, Lemmens I, Hirozane-Kishikawa T, et al. An empirical framework for binary interactome mapping. Nat Methods [Internet]. 2009;6(1):83–90. Available from: http://ezproxy.library.usyd.edu.au/login?url=http://ovidsp.ovid.com/ovidweb.cgi?T=JS&CSC=Y&NEWS=N&PAGE=fulltext&D=medl&AN=19060904

130. Belleau F, Nolin MA, Tourigny N, Rigault P, Morissette J. Bio2RDF: Towards a mashup to build bioinformatics knowledge systems. J Biomed Inform. 2008;41(5):706–16.

131. Chen B, Dong X, Jiao D, Wang H, Zhu Q, Ding Y, et al. Chem2Bio2RDF: a semantic framework for linking and data mining chemogenomic and systems chemical biology data. BMC Bioinformatics [Internet]. 2010;11(1):255. Available from: http://www.biomedcentral.com/1471-2105/11/255

132. Binding Database [Internet]. Available from: www.bindingdb.org

133. Binding MOAD [Internet]. Available from: www.bindingmoad.org

134. BioGRID.

135. Carcinogen [Internet]. Available from: http://toxnet.nlm.nih.gov/cpdb/

136. ChEBI.

137. ChEMBL.

138. Bento a. P, Gaulton A, Hersey A, Bellis LJ, Chambers J, Davies M, et al. The ChEMBL bioactivity database: An update. Nucleic Acids Res. 2014;42(D1):1083–90.

139. Comparative Toxicogenomics Database (CTD).

140. Drug Combination Database (DCDB).

141. Liu Y, Wei Q, Yu G, Gai W, Li Y, Chen X. DCDB 2.0: a major update of the drug combination database. Database [Internet]. 2014;2014(0):bau124–bau124. Available from: http://database.oxfordjournals.org/cgi/doi/10.1093/database/bau124

142. Database of Interacting Proteins (DIP) [Internet]. Available from: http://databib.org/repository/472

143. DrugBank [Internet]. Available from: www.drugbank.ca

144. UNIPROCT [Internet]. Available from: http://www.uniprot.org/

145. HGNC.

146. Human Protein Reference Database (HPRD).

147. Keshava Prasad TS, Goel R, Kandasamy K, Keerthikumar S, Kumar S, Mathivanan S, et al. Human Protein Reference Database - 2009 update. Nucleic Acids Res. 2009;37(SUPPL. 1):767–72.

148. KEGG.

149. PDSP.

150. Manually Annotated Targets and Drugs Online (MATADOR).

151. Günther S, Kuhn M, Dunkel M, Campillos M, Senger C, Petsalaki E, et al. SuperTarget and Matador: Resources for exploring drug-target relationships. Nucleic Acids Res. 2008;36(SUPPL. 1):919–22.

152. Online Mendelian Inheritance in Man (OMIM).

153. PharmGKB.

154. PubChem.

155. Chen B, Wild D, Guha R. PubChem as a source of polypharmacology. J Chem Inf Model [Internet]. 2009 Sep;49(9):2044–55. Available from: http://www.ncbi.nlm.nih.gov/pubmed/19708682

156. PubMed.

157. Reactome.

158. SIDER.

159. Therapeutic Target Database (TTD) [Internet]. Available from: http://bidd.nus.edu.sg/group/cjttd/

160. Hopkins AL. Network pharmacology: the next paradigm in drug discovery. Nat Chem Biol [Internet]. 2008;4(11):682–90. Available from: http://ezproxy.library.usyd.edu.au/login?url=http://ovidsp.ovid.com/ovidweb.cgi?T=JS&CSC=Y&NEWS=N&PAGE=fulltext&D=medl&AN=18936753

161. Kuhn M, von Mering C, Campillos M, Jensen LJ, Bork P. STITCH: interaction networks of chemicals and proteins. Nucleic Acids Res [Internet]. 2008 Jan [cited 2013 Nov 15];36(Database issue):D684–8. Available from: http://www.pubmedcentral.nih.gov/articlerender.fcgi?artid=2238848&tool=pmcentrez&rendertype=abstract

162. RCSB Protein Data Bank [Internet]. Available from: http://www.rcsb.org/pdb/home/home.do

163. GLIDA: GPCR-Ligand Database.

164. NCI Nature Pathway Interaction Database.

165. BioCyc.

166. Kuhn M, Szklarczyk D, Franceschini A, Campillos M, von Mering C, Jensen LJ, et al. STITCH 2: an interaction network database for small molecules and proteins. Nucleic Acids Res [Internet]. 2010;38(Database issue):D552–6. Available from: http://ezproxy.library.usyd.edu.au/login?url=http://ovidsp.ovid.com/ovidweb.cgi?T=JS&CSC=Y&NEWS=N&PAGE=fulltext&D=medl&AN=19897548

167. Prathipati P, Ngai LM, Manjunatha UH, Bender A. Fishing the target of antitubercular

compounds: In silico target deconvolution model development and validation. J Proteome Res. 2009;8(6):2788–98.

168. Kapitzky L, Beltrao P, Berens TJ, Gassner N, Zhou C, Wüster A, et al. Cross-species chemogenomic profiling reveals evolutionarily conserved drug mode of action. Mol Syst Biol. 2010;6(451):451.

169. Kalinina O V., Wichmann O, Apic G, Russell RB. Combinations of protein-chemical complex structures reveal new targets for established drugs. PLoS Comput Biol. 2011;7(5):1–8.

170. Meslamani J, Rognan D. Enhancing the accuracy of chemogenomic models with a three-dimensional binding site kernel. J Chem Inf Model. 2011;51(7):1593–603.

171. Marshall, Garland R. Introduction to Chemoinformatics in Drug Discovery. In: Opera TI, editor. Chemoinformatics in Drug Discovery. KGaA Weinheim: WILEY-VCH Verlag GmbH & Co.; 2006.

172. Matthews EJ, Ursem CJ, Kruhlak NL, Daniel Benz R, Sabaté DA, Yang C, et al. Identification of structure-activity relationships for adverse effects of pharmaceuticals in humans: Part B. Use of (Q)SAR systems for early detection of drug-induced hepatobiliary and urinary tract toxicities. Regul Toxicol Pharmacol [Internet]. Elsevier Inc.; 2009 Jan 29 [cited 2012 Apr 13];54(1):23–42. Available from: http://www.ncbi.nlm.nih.gov/pubmed/19545506

173. Ursem CJ, Kruhlak NL, Contrera JF, Maclaughlin PM, Benz RD, Matthews EJ. Identification of structure-activity relationships for adverse effects of pharmaceuticals in humans. Part A: Use of FDA post-market reports to create a database of hepatobiliary and urinary tract toxicities. Regul Toxicol Pharmacol [Internet]. Elsevier Inc.; 2009 Jan 23 [cited 2012 Apr 11];54(1):1–22. Available from: http://www.ncbi.nlm.nih.gov/pubmed/19545508

174. Matthews EJ, Kruhlak NL, Benz RD, Sabaté DA, Marchant CA, Contrera JF. Identification of structure-activity relationships for adverse effects of pharmaceuticals in humans: Part C: Use of QSAR and an expert system for the estimation of the mechanism of action of drug-induced hepatobiliary and urinary tract toxicities. Regul Toxicol Pharmacol [Internet]. Elsevier Inc.; 2009 Jan 23 [cited 2012 Apr 13];54(1):43–65. Available from: http://www.ncbi.nlm.nih.gov/pubmed/19545512

175. Martin YC. Quantitative Drug Design: A Critical Introduction. 2nd ed. CRC Press; 2010.

176. Leach AR. The Use of Molecular Modelling and Cheminformatics. In: Molecular Modelling: Principles and Applications. 2nd ed. Essex: Pearson Education Limited; 2001. p. 669.

177. Golbraikh A, Tropsha A. Beware of q^2! J Mol Graph Model [Internet]. 2002;20(4):269–76. Available from: http://www.ncbi.nlm.nih.gov/pubmed/11858635

178. Salum LB, Andricopulo AD. Fragment-based QSAR: Perspectives in drug design. Mol Divers. 2009;13(3):277–85.

179. Myint KZ, Xie X-Q. Recent advances in fragment-based QSAR and multi-dimensional QSAR methods. Int J Mol Sci [Internet]. 2010 Jan [cited 2013 Nov 25];11(10):3846–66. Available from: http://www.pubmedcentral.nih.gov/articlerender.fcgi?artid=2996787&tool=pmcentrez&rendertype=abstract

180. Cramer RD, Patterson DE, Bunce JD. Comparative molecular field analysis (CoMFA). 1. Effect of shape on binding of steroids to carrier proteins. J Am Chem Soc [Internet]. 1988;110(18):5959–67. Available from: http://www.ncbi.nlm.nih.gov/pubmed/22148765

181. Klebe G, Abraham U, Mietzner T. Molecular similarity indices in a comparative analysis (CoMSIA) of drug molecules to correlate and predict their biological activity. J Med Chem. 1994;37(24):4130–46.

182. Dudek AZ, Arodz T, Galvez J. Computational Methods in Developing Quantitative Structure-

Activity Relationships (QSAR): A Review. Comb Chem High Throughput Screen. 2006;9(3):213–28.

183. Cramer RD. Topomer CoMFA: A design methodology for rapid lead optimization. J Med Chem. 2003;46(3):374–88.

184. Silverman BD, Platt DE. Comparative molecular moment analysis (coMMA): 3D-QSAR without molecular superposition. J Med Chem. 1996;39(11):2129–40.

185. Todeschini R, Lasagni M, Marengo E. New Molecular Descriptors for 2D- and 3D-structures. Theory JChemometrics. 1994;8(March 1993):263–73.

186. Pastor M, Cruciani G, McLay I, Pickett S, Clementi S. GRid-INdependent descriptors (GRIND): A novel class of alignment-independent three-dimensional molecular descriptors. J Med Chem. 2000;43(17):3233–43.

187. Wermuth CG, Ganellin CR, LindBerg P, Mitscher A. Glossary of Terms Used in Medicinal Chemistry. Pure Appl Chem. 1998;70(5):1129–43.

188. Michaux C, de Leval X, Julémont F, Dogné J-M, Pirotte B, Durant F. Structure-based pharmacophore of COX-2 selective inhibitors and identification of original lead compounds from 3D database searching method. Eur J Med Chem [Internet]. 2006 Dec [cited 2012 Sep 17];41(12):1446–55. Available from: http://www.ncbi.nlm.nih.gov/pubmed/17030482

189. Martin YC. DISCO: What We Did Right and What We Missed. In: Pharmacophore Perception, Development, and Use in Drug Design. La Jolla: International University Line; 2000. p. 47–68.

190. Langgård M, Bjørnholm B, Gundertofte K. Pharmacophore Modeling by Automated Methods: Possibilities and Limitations. In: Güner OF, editor. Pharmacophore Perception, Development, and Use in Drug Design. La Jolla: International University Line; 2000. p. 239–50.

191. Simulations M. Catalyst. San Diego;

192. Jones G, Willett P, Glen RC. A genetic algorithm for flexible molecular overlay and pharmacophore elucidation. J Comput Aided Mol Des. 1995;9(6):532–49.

193. Dixon SL, Smondyrev AM, Rao SN. PHASE: a novel approach to pharmacophore modeling and 3D database searching. Chem Biol Drug Des [Internet]. 2006 May [cited 2012 Nov 13];67(5):370–2. Available from: http://www.ncbi.nlm.nih.gov/pubmed/16784462

194. Dixon SL, Smondyrev AM, Knoll EH, Rao SN, Shaw DE, Friesner RA. PHASE: a new engine for pharmacophore perception, 3D QSAR model development, and 3D database screening: 1. Methodology and preliminary results. J Comput Aided Mol Des [Internet]. 2006 [cited 2013 Aug 7];20(10-11):647–71. Available from: http://www.ncbi.nlm.nih.gov/pubmed/17124629

195. Foudah AI, Sallam A a., Akl MR, El Sayed K a. Optimization, pharmacophore modeling and 3D-QSAR studies of sipholanes as breast cancer migration and proliferation inhibitors. Eur J Med Chem [Internet]. Elsevier Masson SAS; 2014;73:310–24. Available from: http://dx.doi.org/10.1016/j.ejmech.2013.11.039

196. Brogi S, Papazafiri P, Roussis V, Tafi A. 3D-QSAR using pharmacophore-based alignment and virtual screening for discovery of novel MCF-7 cell line inhibitors. Eur J Med Chem [Internet]. 2013 Sep [cited 2013 Nov 7];67:344–51. Available from: http://www.ncbi.nlm.nih.gov/pubmed/23880359

197. Guasch L, Ojeda MJ, González-Abuín N, Sala E, Cereto-Massagué A, Mulero M, et al. Identification of novel human dipeptidyl peptidase-IV inhibitors of natural origin (part I): virtual screening and activity assays. PLoS One [Internet]. 2012 Jan [cited 2013 Nov 7];7(9):e44971. Available from: http://www.pubmedcentral.nih.gov/articlerender.fcgi?artid=3440348&tool=pmcentrez&rendertype=abstract

198. Tawari NR, Degani MS. Pharmacophore Mapping and Electronic Feature Analysis for a Series of Nitroaromatic Compounds with Antitubercular Activity. J Comput Chem. 2010;31(4):739–51.

199. Schrödinger. LigPrep. New York, NY: LLC; 2013.

200. Schrödinger. MacroModel user manual. New York, NY: LLC; 2013.

201. Watts KS, Dalal P, Murphy RB, Sherman W, Friesner RA, Shelley JC. ConfGen: A Conformational Search Method for Efficient Generation of Bioactive Conformers. J Chem Inf Model [Internet]. 2010 Apr 26;50(4):534–46. Available from: http://www.ncbi.nlm.nih.gov/pubmed/20373803

202. Schrödinger. ConfGen. New York, NY: LLC; 2012.

203. Schrödinger. Phase user manual. New York, NY: LLC; 2013.

204. Daylight Chemical Information Systems. SMARTS Theory Manual [Internet]. [cited 2015 May 25]. Available from: http://www.daylight.com/dayhtml/doc/theory/theory.smarts.html

205. Day RO, Graham GG, Hicks M, McLachlan AJ, Stocker SL, Williams KM. Clinical pharmacokinetics and pharmacodynamics of allopurinol and oxypurinol. Clin Pharmacokinet [Internet]. 2007 Jan;46(8):623–44. Available from: http://www.ncbi.nlm.nih.gov/pubmed/17655371

206. Morselli PL, Frigerio A. Metabolism and Pharmacokinetics of Carbamazepine. Drug Metab Rev [Internet]. 1975 Jan;4(1):97–113. Available from: http://www.ncbi.nlm.nih.gov/pubmed/812689

207. Takashima-Hirano M, Takashima T, Katayama Y, Wada Y, Sugiyama Y, Watanabe Y, et al. Efficient sequential synthesis of PET Probes of the COX-2 inhibitor [11C]celecoxib and its major metabolite [11C]SC-62807 and in vivo PET evaluation. Bioorg Med Chem [Internet]. Elsevier Ltd; 2011 May 1 [cited 2012 Sep 17];19(9):2997–3004. Available from: http://www.ncbi.nlm.nih.gov/pubmed/21482120

208. Bolton GC, Allen GD, Davies BE, Filer CW, Jeffery DJ. The disposition of clavulanic acid in man. Xenobiotica [Internet]. 1986 Sep;16(9):853–63. Available from: http://www.ncbi.nlm.nih.gov/pubmed/3765664

209. Murai Y, Nakagawa T, Yamaoka K, Uno T. High-performance liquid chromatographic determination and moment analysis of urinary excretion of flucloxacillin and its metabolites in man. Int J Pharm [Internet]. 1983 Jul;15(3):309–20. Available from: http://linkinghub.elsevier.com/retrieve/pii/0378517383901643

210. Saracino MA, Bugamelli F, Conti M, Amore M, Raggi MA. Rapid HPLC analysis of the antiepileptic lamotrigine and its metabolites in human plasma. J Sep Sci [Internet]. 2007 Sep [cited 2012 Sep 17];30(14):2249–55. Available from: http://www.ncbi.nlm.nih.gov/pubmed/17683041

211. Grozinger KG, Byrne DP, Nummy LJ, Ridges MD, Salvagno A. Synthesis of Five Nevirapine Metabolites. J Heterocycl Chem. 2000;37:229–39.

212. McClanahan JS, Maguire JH. High-performance liquid chromatographic determination of the enantiomeric composition of urinary phenolic metabolites of phenytoin. J Chromatogr. 1986;381:438–46.

213. Sitar DS. Metabolism of thioamide antithyroid drugs. Drug Metab Rev [Internet]. 1990 Jan;22(5):477–502. Available from: http://www.ncbi.nlm.nih.gov/pubmed/1706656

214. Chungi VS, Dittert LW, Shargel L. Pharmacokinetics of Sulfasalazine Metabolities in Rats Following Concomitant Oral Administration of Riboflavin. Pharm Res. 1989;6(12):1067–72.

215. Sitar DS, Owen JA, MacDougall B, Hunter T, Mitenko PA. Effects of age and disease on the pharmacokinetics and pharmacodynamics of sulindac. Clin Pharmacol Ther [Internet]. 1985 Aug;38(2):228–34. Available from: http://www.ncbi.nlm.nih.gov/pubmed/4017423

216. Banks JL, Beard HS, Cao Y, Cho AE, Damm W, Farid R, et al. Integrated Modeling Program, Applied Chemical Theory (IMPACT). J Comput Chem. 2005;26(16):1752–80.

217. Guengerich FP. Mechanisms of Drug Toxicity and Relevance to Pharmaceutical Development. Drug Metab Pharmacokinet. 2011;26(1):3–14.

218. Osman M, Chandrasekaran A, Chan K, Scatina J, Ermer J, Cevallos W, et al. Metabolic Disposition of 14C-Bromfenac in Healthy Male Volunteers. J Clin Pharmacol. 1998;38(8):744–52.

219. McChesney EW, Banks WF, Portmann G a, Crain a V. Metabolism of chlormezanone in man and laboratory animals. Biochem Pharmacol [Internet]. 1967 May;16(5):813–26. Available from: http://www.ncbi.nlm.nih.gov/pubmed/6036732

220. Hakusui H, Tachizawa H, Sano M. Biotransformation of Chlomezanone, 2-(4-Chloro-phenyl)-3-methyl-4-metathiazanone-1,1-dioxide, a Muscle-Relaxing and Tranquillizing Agent: the Effect of combination with Aspirin on its Metabolitc Fate in Rats and Mice. Xenobiotica. 1978;8(4):229–38.

221. Kang P, Dalvie D, Smith E, Renner M. Bioactivation of Lumiracoxib by Peroxidases and Human Liver Microsomes: Identification of Multiple Quinone Imine Intermediates and GSH Adducts. Chem Res Toxicol [Internet]. 2009 Jan;22(1):106–17. Available from: http://www.ncbi.nlm.nih.gov/pubmed/19063590

222. Li Y, Slatter JG, Zhang Z, Li Y, Doss GA, Braun MP, et al. In Vitro Metabolic Activation of Lumiracoxib in Rat and Human Liver Preparations. Drug Metab Dispos. 2008;36(2):469–73.

223. Yu J, Brown DG, Burdette D. In Vitro Metabolism Studies of Nomifensine Monooxygenation Pathways: Metabolite Identification, Reaction Phenotyping, and Bioactivation Mechanism. Drug Metab Dispos. 2010;38(10):1767–78.

224. Yu J, Mathisen DE, Burdette D, Brown DG, Becker C, Aharony D. Identification of Multiple Glutathione Conjugates of 8-Amino- (Nomifensine) in Liver Microsomes and Hepatocyte Preparations: Evidence of the Bioactivation of Nomifensine. Drug Metab Dispos. 2010;38(1):46–60.

225. Obach RS, Dalvie DK. Metabolism of nomifensine to a dihydroisoquinolinium ion metabolite by human myeloperoxidase, hemoglobin, monoamine oxidase A, and cytochrome P450 enzymes. Drug Metab Dispos. 2006;34(8):1310–6.

226. Rademacher PM, Woods CM, Huang Q, Szklarz GD, Nelson SD. Differential Oxidation of Two Thiophene-Containing Regioisomers to Reactive Metabolites by Cytochrome P450 2C9. Chem Res Toxicol [Internet]. 2012 Apr 16;25(4):895–903. Available from: http://www.ncbi.nlm.nih.gov/pubmed/22329513

227. Nishiya T, Kato M, Suzuki T, Maru C, Kataoka H, Hattori C, et al. Involvement of cytochrome P450-mediated metabolism in tienilic acid hepatotoxicity in rats. Toxicol Lett [Internet]. 2008 Dec 15 [cited 2012 Aug 31];183(1-3):81–9. Available from: http://www.ncbi.nlm.nih.gov/pubmed/18992796

228. Valadon P, Dansette PM, Girault JP, Amar C, Mansuy D. Thiophene sulfoxides as reactive metabolites: formation upon microsomal oxidation of a 3-aroylthiophene and fate in the presence of nucleophiles in vitro and in vivo. Chem Res Toxicol [Internet]. 1996 Dec;9(8):1403–13. Available from: http://www.ncbi.nlm.nih.gov/pubmed/8951246

229. Mansuy D, Dansette PM, Foures C, Jaouen M, Moinet G, Bayer N. Metabolic Hydroxylation of

the Thiophene Ring: Isolation of the 5-Hydroxy-Tienilic acid as the Major Urinary Metabolite of Tienilic Acid in Man and Rat. Biochem Pharmacol. 1984;33(9):1429–35.

230. Matsson EM, Eriksson UG, Knutson L, Hoffmann K-J, Logren U, Fridblom P, et al. Biliary Excretion of Ximelagatran and Its Metabolites and the Influence of Erythromycin Following Intraintestinal Administration to Healthy Volunteers. J Clin Pharmacol [Internet]. 2011 May [cited 2012 Sep 27];51(5):770–83. Available from: http://www.ncbi.nlm.nih.gov/pubmed/20663994

231. Darnell M, Karlsson JE, Owen A, Hidalgo IJ, Li J, Zhang W, et al. Investigation of the Involvement of P-Glycoprotein and Multidrug Resistance-Associated Protein 2 in the Efflux of Ximelagatran and Its Metabolites by Using Short Hairpin RNA Knockdown in Caco-2 Cells ABSTRACT : Drug Metab Dispos. 2010;38(3):491–7.

232. Dunér K, Bäckström J, Magnell N, Svennberg H, Ahnoff M, Logren U. Determination of ximelagatran, melagatran and two intermediary metabolites in plasma by mixed-mode solid phase extraction and LC-MS/MS. J Chromatogr B Analyt Technol Biomed Life Sci [Internet]. 2007 Jun 1 [cited 2012 Sep 15];852(1-2):317–24. Available from: http://www.ncbi.nlm.nih.gov/pubmed/17296338

233. Clement B, Lopian K. Characterization of in vitro biotransformation of new, orally active, direct thrombin inhibitor ximelagatran, an amidoxime and ester prodrug. Drug Metab Dispos. 2003;31(5):645–51.

234. Kalma Product Information.

235. Sanchez-Ponce R, Wang L-Q, Lu W, von Hehn J, Cherubini M, Rush R. Metabolic and Pharmacokinetic Differentiation of STX209 and Racemic Baclofen in Humans. Metabolites [Internet]. 2012 Sep 11 [cited 2012 Oct 4];2(3):596–613. Available from: http://www.mdpi.com/2218-1989/2/3/596/

236. Miura M, Ohkubo T. Simultaneous Determination of Fluvoxamine and Its Metabolites in Human Liver Microsomes by High-Performance Liquid Chromatography with Solid-Phase Extraction. Anal Lett [Internet]. 2006 Sep [cited 2012 Oct 4];39(12):2405–15. Available from: http://www.tandfonline.com/doi/abs/10.1080/00032710600822825

237. Claassen V. Review of the animal pharmacology and pharmacokinetics of fluvoxamine. Br J Clin Pharmacol. 1983;15(Suppl 3):349S – 355S.

238. Ketorolac monograph [Internet]. Available from: www.drugbank.ca

239. Aberg AT, Lofgren H, Bondesson U, Hedeland M. Structural elucidation of N-oxidized clemastine metabolites by liquid chromatography / tandem mass spectrometry and the use of Cunninghamella elegans to facilitate drug metabolite identification. Rapid Commun Mass Spectrom. 2010;24:1447–56.

240. Tevell A, Bondesson U, Törneke K, Hedeland M. Identification of some new clemastine metabolites in dog, horse, and human urine with liquid chromatography/tandem mass spectrometry. Rapid Commun Mass Spectrom [Internet]. 2004 Jan [cited 2013 Jul 17];18(19):2267–72. Available from: http://www.ncbi.nlm.nih.gov/pubmed/15384147

241. Choi MH, Jung BH, Chung BC. Identification of Urinary Metabolites of Clemastine after Oral Administration to Man. J Pharm Pharmacol. 1999;51:53–9.

242. Baldacci A, Prost F, Thormann W. Identification of diphenhydramine metabolites in human urine by capillary electrophoresis-ion trap-mass spectrometry. Electrophoresis [Internet]. 2004 Jun [cited 2013 Jul 17];25(10-11):1607–14. Available from: http://www.ncbi.nlm.nih.gov/pubmed/15188248

243. Selinger K, Prevost J, Hill H. High-performance liquid chromatography method for the

determination of diphenhydramine in human plasma. J Chromatogr. 1990;526:597–602.

244. Conway WD, Minatoya H, Lands AM, Shekosky JM. Absorption and Elimination Profile of Isoproterenol III. J Pharm Sci. 1968;57(7):1135–41.

245. Bredberg U, Eyjolfsdottir GS, Paalzow L, Tfelt-Hansen P, Tfelt-Hansen V. Pharmacokinetics of methysergide and its metabolite methylergometrine in man. Eur J Clin Pharmacol [Internet]. 1986 Jan;30(1):75–7. Available from: http://www.ncbi.nlm.nih.gov/pubmed/3709634

246. Bianchine JR, Friedman a P. Metabolism of methysergide and retroperitoneal fibrosis. Arch Intern Med [Internet]. 1970 Aug;126(2):252–4. Available from: http://www.ncbi.nlm.nih.gov/pubmed/5433064

247. Mizushima H, Kinoshita K, Abe K, Ishizuka H, Yamada Y. Pharmacokinetics/pharmacodynamics analysis of the relationship between the in vivo micturition pressure and receptor occupancy of (R)-oxybutynin and its metabolite in rats. Biol Pharm Bull [Internet]. 2007 May;30(5):955–62. Available from: http://www.ncbi.nlm.nih.gov/pubmed/17473442

248. Mizushima H, Takanaka K, Abe K, Fukazawa I, Ishizuka H. Stereoselective pharmacokinetics of oxybutynin and N-desethyloxybutynin in vitro and in vivo. Xenobiotica [Internet]. 2007 Jan [cited 2013 Jul 17];37(1):59–73. Available from: http://www.ncbi.nlm.nih.gov/pubmed/17178634

249. Michel MC, Hegde SS. Treatment of the overactive bladder syndrome with muscarinic receptor antagonists: a matter of metabolites? Naunyn Schmiedebergs Arch Pharmacol [Internet]. 2006 Nov [cited 2013 Jul 17];374(2):79–85. Available from: http://www.ncbi.nlm.nih.gov/pubmed/17021853

250. Vihinen M. How to evaluate performance of prediction methods? Measures and their interpretation in variation effect analysis. BMC Genomics [Internet]. BioMed Central Ltd; 2012 Jan [cited 2012 Jul 31];13(Suppl 4):S2. Available from: http://www.pubmedcentral.nih.gov/articlerender.fcgi?artid=3303716&tool=pmcentrez&rendertype=abstract

251. Sanders MP a, Barbosa AJM, Zarzycka B, Nicolaes G a F, Klomp JPG, de Vlieg J, et al. Comparative analysis of pharmacophore screening tools. J Chem Inf Model [Internet]. 2012 Jun 25;52(6):1607–20. Available from: http://www.ncbi.nlm.nih.gov/pubmed/22646988

252. Koes DR, Camacho CJ. Pharmer : Efficient and Exact Pharmacophore Search. 2011;1307–14.

253. Schrödinger. Maestro. New York, NY: LLC; 2013.

254. Abu-Tair L, Axelrod JH, Doron S, Ovadya Y, Krizhanovsky V, Galun E, et al. Natural Killer Cell-Dependent Anti-Fibrotic Pathway in Liver Injury via Toll-Like Receptor-9. PLoS One [Internet]. 2013 Jan [cited 2013 Dec 20];8(12):e82571. Available from: http://www.ncbi.nlm.nih.gov/pubmed/24340043

255. Moles A, Murphy L, Wilson CL, Chakraborty JB, Fox C, Park EJ, et al. A TLR2/S100A9/CXCL-2 Signaling Network is Necessary for Neutrophil Recruitment in Acute and Chronic Liver Injury in the Mouse. J Hepatol [Internet]. European Association for the Study of the Liver; 2013 Dec 10 [cited 2013 Dec 20]; Available from: http://www.ncbi.nlm.nih.gov/pubmed/24333183

256. Shaw PJ, Ganey PE, Roth R a. Idiosyncratic drug-induced liver injury and the role of inflammatory stress with an emphasis on an animal model of trovafloxacin hepatotoxicity. Toxicol Sci [Internet]. 2010 Nov [cited 2014 Apr 28];118(1):7–18. Available from: http://www.pubmedcentral.nih.gov/articlerender.fcgi?artid=2955207&tool=pmcentrez&rendertype=abstract

257. Trinchieri G, Sher A. Cooperation of Toll-like receptor signals in innate immune defence. Nat Rev Immunol. 2007;7(3):179–90.

258. Yoo E, Crall BM, Balakrishna R, Malladi SS, Fox LM, Hermanson AR, et al. Structure-activity relationships in Toll-like receptor 7 agonistic 1H-imidazo[4,5-c]pyridines. Org Biomol Chem [Internet]. 2013 Oct 14 [cited 2013 Nov 7];11(38):6526–45. Available from: http://www.ncbi.nlm.nih.gov/pubmed/23974333

259. Ajay, Murcko MA. Computational Methods to Predict Binding Free Energy in Ligand-Receptor Complexes. J Med Chem. 1995;38(26):4953–67.

260. Sun Y, Ewing TJ, Skillman a G, Kuntz ID. CombiDOCK: structure-based combinatorial docking and library design. J Comput Aided Mol Des. 1998;12(6):597–604.

261. Kramer B, Rarey M, Lengauer T. Evaluation of the F LEX X Incremental Construction Algorithm for Protein – Ligand Docking. 1999;241(June):228–41.

262. Rarey M, Kramer B, Lengauer T, Klebe G. A fast flexible docking method using an incremental construction algorithm. J Mol Biol [Internet]. 1996;261(3):470–89. Available from: http://citeseerx.ist.psu.edu/viewdoc/download?doi=10.1.1.132.7748&rep=rep1&type=pdf\nhttp://www.ncbi.nlm.nih.gov/pubmed/8780787

263. Cambridge Crystallographic Data Centre. GOLD [Internet]. [cited 2015 Jul 2]. Available from: www.ccdc.cam.ac.uk/Solutions/GoldSuite/Pages/GOLD.aspx

264. Jain AN. Surflex-Dock 2.1: Robust performance from ligand energetic modeling, ring flexibility, and knowledge-based search. J Comput Aided Mol Des. 2007;21(5):281–306.

265. Friesner RA, Banks JL, Murphy RB, Halgren TA, Klicic JJ, Mainz DT, et al. Glide: a new approach for rapid, accurate docking and scoring. 1. Method and assessment of docking accuracy. J Med Chem [Internet]. 2004 Mar 25;47(7):1739–49. Available from: http://www.ncbi.nlm.nih.gov/pubmed/15027865

266. Schrödinger. Glide user manual. New York, NY: LLC; 2013.

267. Schrödinger. Protein Preparation Wizard user manual. New York, NY: LLC; 2009.

268. Wuillemin N, Terracciano L, Beltraminelli H, Schlapbach C, Fontana S, Krähenbühl S, et al. T Cells Infiltrate the Liver and Kill Hepatocytes in HLA-B(∗)57:01-Associated Floxacillin-Induced Liver Injury. Am J Pathol [Internet]. American Society for Investigative Pathology; 2014 Apr 9 [cited 2014 Apr 28];(April):1–6. Available from: http://www.ncbi.nlm.nih.gov/pubmed/24731753

269. Ho S, McLachlan A, Chen T, Hibbs D, Fois R. Relationships Between Pharmacovigilance, Molecular, Structural, and Pathway Data: Revealing Mechanisms for Immune-Mediated Drug-Induced Liver Injury. CPT Pharmacometrics Syst Pharmacol [Internet]. 2015;4(7):426–41. Available from: http://doi.wiley.com/10.1002/psp4.56

270. Mahmood T, Yang PC. Western blot: Technique, theory, and trouble shooting. N Am J Med Sci. 2012;4(9):429–34.

271. Yang Y, Ma H. Western Blotting and ELISA Techniques. Researcher. 2009;1(2):67–86.

272. Singh PK, Negi A, Gupta PK, Chauhan M, Kumar R. Toxicophore exploration as a screening technology for drug design and discovery: techniques, scope and limitations. Arch Toxicol [Internet]. Springer Berlin Heidelberg; 2015; Available from: "http://dx.doi.org/10.1007/s00204-015-1587-5

273. Williams DP, Naisbitt DJ. Toxicophores: groups and metabolic routes associated with increased safety risk. Curr Opin Drug Discov Dev [Internet]. 2002;5(1):104–15. Available from: http://www.ncbi.nlm.nih.gov/entrez/query.fcgi?cmd=Retrieve&db=PubMed&dopt=Citation&list_uids=11865664

Appendix 1: Peer Reviewed Scientific Publications arising from this thesis

Appendix 2: Consolidated list of proteins

	Gene	UniProct entry	Category	Protein	Function
Both	ABCB1	p08183	Transport	Multidrug resistance protein 1	Energy-dependent efflux pump responsible for decreased drug accumulation in multidrug-resistant cells.
SLAP	ABCB11	o95342	Transport	Bile salt export pump	Involved in the ATP-dependent secretion of bile salts into the canaliculus of hepatocytes.
Both	ABCC1	p33527	Transport	Multidrug resistance-associated protein 1	Mediates export of organic anions and drugs from the cytoplasm. Mediates ATP-dependent transport of glutathione and glutathione conjugates, leukotriene C4, estradiol-17-beta-o-glucuronide, methotrexate, antiviral drugs and other xenobiotics. Confers resistance to anticancer drugs. Hydrolyzes ATP with low efficiency.
Both	ABCC2	q92887	Transport	Canalicular multispecific organic anion transporter 1	Mediates hepatobiliary excretion of numerous organic anions. May function as a cellular cisplatin transporter.

Both	ABCC4	o15439	Transport	Multidrug resistance-associated protein 4	May be an organic anion pump relevant to cellular detoxification.
Both	ABCG2	q9unq0	Transport	ATP-binding cassette sub-family G member 2	High-capacity urate exporter functioning in both renal and extrarenal urate excretion. Plays a role in porphyrin homeostasis as it is able to mediates the export of protoporhyrin IX (PPIX) both from mitochondria to cytosol and from cytosol to extracellular space, and cellular export of hemin, and heme. Xenobiotic transporter that may play an important role in the exclusion of xenobiotics from the brain. Appears to play a major role in the multidrug resistance phenotype of several cancer cell lines. Implicated in the efflux of numerous drugs and xenobiotics: mitoxantrone, the photosensitizer pheophorbide, camptothecin, methotrexate, azidothymidine (AZT), and the anthracyclines daunorubicin and doxorubicin.
STITCH	ACAT1	p24752	Metabolism	Acetyl-CoA acetyltransferase, mitochondrial	Plays a major role in ketone body metabolism.

SLAP	ADAM17	p78536	Enzyme	Disintegrin and metalloproteinase domain-containing protein 17	Cleaves the membrane-bound precursor of TNF-alpha to its mature soluble form. Responsible for the proteolytical release of soluble JAM3 from endothelial cells surface. Responsible for the proteolytic release of several other cell-surface proteins, including p75 TNF-receptor, interleukin 1 receptor type II, p55 TNF-receptor, transforming growth factor-alpha, L-selectin, growth hormone receptor, MUC1 and the amyloid precursor protein. Acts as an activator of Notch pathway by mediating cleavage of Notch, generating the membrane-associated intermediate fragment called Notch extracellular truncation (NEXT). Plays a role in the proteolytic processing of ACE2.
SLAP	ADRA1A	p35348	Receptor	Alpha-1A adrenergic receptor	This alpha-adrenergic receptor mediates its action by association with G proteins that activate a phosphatidylinositol-calcium second messenger system. Its effect is mediated by G(q) and G(11) proteins. Nuclear ADRA1A-ADRA1B heterooligomers regulate phenylephrine(PE)-stimulated ERK signaling in cardiac myocytes.

SLAP	ADRA1B	p35368	Receptor	Alpha-1B adrenergic receptor	This alpha-adrenergic receptor mediates its action by association with G proteins that activate a phosphatidylinositol-calcium second messenger system. Its effect is mediated by G(q) and G(11) proteins. Nuclear ADRA1A-ADRA1B heterooligomers regulate phenylephrine (PE)-stimulated ERK signaling in cardiac myocytes
SLAP	ADRA1D	p25100	Receptor	Alpha-1D adrenergic receptor	This alpha-adrenergic receptor mediates its effect through the influx of extracellular calcium.
SLAP	ADRA2A	p08913	Receptor	Alpha-2A adrenergic receptor	Alpha-2 adrenergic receptors mediate the catecholamine-induced inhibition of adenylate cyclase through the action of G proteins. The rank order of potency for agonists of this receptor is oxymetazoline > clonidine > epinephrine > norepinephrine > phenylephrine > dopamine > p-synephrine > p-tyramine > serotonin = p-octopamine. For antagonists, the rank order is yohimbine > phentolamine = mianserine > chlorpromazine = spiperone = prazosin > propanolol > alprenolol = pindolol

SLAP	ADRA2B	p18089	Receptor	Alpha-2B adrenergic receptor	Alpha-2 adrenergic receptors mediate the catecholamine-induced inhibition of adenylate cyclase through the action of G proteins. The rank order of potency for agonists of this receptor is clonidine > norepinephrine > epinephrine = oxymetazoline > dopamine > p-tyramine = phenylephrine > serotonin > p-synephrine / p-octopamine. For antagonists, the rank order is yohimbine > chlorpromazine > phentolamine > mianserine > spiperone > prazosin > alprenolol > propanolol > pindolol.
SLAP	ADRA2C	p11118825	Receptor	Alpha-2C adrenergic receptor	Alpha-2 adrenergic receptors mediate the catecholamine-induced inhibition of adenylate cyclase through the action of G proteins.
SLAP	ADRB1	p08588	Receptor	Beta-1 adrenergic receptor	Beta-adrenergic receptors mediate the catecholamine-induced activation of adenylate cyclase through the action of G proteins. This receptor binds epinephrine and norepinephrine with approximately equal affinity. Mediates Ras activation through G(s)-alpha- and cAMP-mediated signaling.

SLAP	ADRB2	p07550	Receptor	Beta-2 adrenergic receptor	Beta-adrenergic receptors mediate the catecholamine-induced activation of adenylate cyclase through the action of G proteins. The beta-2-adrenergic receptor binds epinephrine with an approximately 30-fold greater affinity than it does norepinephrine.
STITCH	AKR1C1	q04828	Enzyme	Aldo-keto reductase family 1 member C1	Converts progesterone to its inactive form, 20-alpha-dihydroxyprogesterone (20-alpha-OHP). In the liver and intestine, may have a role in the transport of bile. May have a role in monitoring the intrahepatic bile acid concentration. Has a low bile-binding ability. May play a role in myelin formation.
STITCH	AKR1C2	p52895	Enzyme	Aldo-keto reductase family 1 member C2	Works in concert with the 5-alpha/5-beta-steroid reductases to convert steroid hormones into the 3-alpha/5-alpha and 3-alpha/5-beta-tetrahydrosteroids. Catalyzes the inactivation of the most potent androgen 5-alpha-dihydrotestosterone (5-alpha-DHT) to 5-alpha-androstane-3-alpha,17-beta-diol (3-alpha-diol). Has a high bile-binding ability.

STITCH	AKR1C3	p42330	Enzyme	Aldo-keto reductase family 1 member C3	Catalyzes the conversion of aldehydes and ketones to alcohols. Catalyzes the reduction of prostaglandin (PG) D2, PGH2 and phenanthrenequinone (PQ) and the oxidation of 9-alpha,11-beta-PGF2 to PGD2. Functions as a bi-directional 3-alpha-, 17-beta- and 20-alpha HSD. Can interconvert active androgens, estrogens and progestins with their cognate inactive metabolites. Preferentially transforms androstenedione (4-dione) to testosterone.
Both	AKT1	p31749	Kinase	RAC-alpha serine/threonine-protein kinase	AKT1 is one of 3 closely related serine/threonine-protein kinases (AKT1, AKT2 and AKT3) called the AKT kinase, and which regulate many processes including metabolism, proliferation, cell survival, growth and angiogenesis. This is mediated through serine and/or threonine phosphorylation of a range of downstream substrates. Over 100 substrate candidates have been reported so far, but for most of them, no isoform specificity has been reported. AKT is responsible of the regulation of glucose uptake by mediating insulin-induced translocation of the SLC2A4/GLUT4 glucose

transporter to the cell surface. Phosphorylation of PTPN1 at 'Ser-50' negatively modulates its phosphatase activity preventing dephosphorylation of the insulin receptor and the attenuation of insulin signaling. Phosphorylation of TBC1D4 triggers the binding of this effector to inhibitory 14-3-3 proteins, which is required for insulin-stimulated glucose transport. AKT regulates also the storage of glucose in the form of glycogen by phosphorylating GSK3A at 'Ser-21' and GSK3B at 'Ser-9', resulting in inhibition of its kinase activity. Phosphorylation of GSK3 isoforms by AKT is also thought to be one mechanism by which cell proliferation is driven. AKT regulates also cell survival via the phosphorylation of MAP3K5 (apoptosis signal-related kinase). Phosphorylation of 'Ser-83' decreases MAP3K5 kinase activity stimulated by oxidative stress and thereby prevents apoptosis. AKT mediates insulin-stimulated protein synthesis by phosphorylating TSC2 at 'Ser-939' and 'Thr-1462', thereby activating mTORC1 signaling and leading to

	both phosphorylation of 4E-BP1 and in activation of RPS6KB1. AKT is involved in the phosphorylation of members of the FOXO factors (Forkhead family of transcription factors), leading to binding of 14-3-3 proteins and cytoplasmic localization. In particular, FOXO1 is phosphorylated at 'Thr-24', 'Ser-256' and 'Ser-319'. FOXO3 and FOXO4 are phosphorylated on equivalent sites. AKT has an important role in the regulation of NF-kappa-B-dependent gene transcription and positively regulates the activity of CREB1 (cyclic AMP (cAMP)-response element binding protein). The phosphorylation of CREB1 induces the binding of accessory proteins that are necessary for the transcription of pro-survival genes such as BCL2 and MCL1. AKT phosphorylates 'Ser-454' on ATP citrate lyase (ACLY), thereby potentially regulating ACLY activity and fatty acid synthesis. Activates the 3B isoform of cyclic nucleotide phosphodiesterase (PDE3B) via phosphorylation of 'Ser-273', resulting in reduced cyclic AMP levels and inhibition of lipolysis.

	Phosphorylates PIKFYVE on 'Ser-318', which results in increased PI_3P-5 activity. The Rho GTPase-activating protein DLC1 is another substrate and its phosphorylation is implicated in the regulation cell proliferation and cell growth. AKT plays a role as key modulator of the AKT-mTOR signaling pathway controlling the tempo of the process of newborn neurons integration during adult neurogenesis, including correct neuron positioning, dendritic development and synapse formation. Signals downstream of phosphatidylinositol 3-kinase (PI_3K) to mediate the effects of various growth factors such as platelet-derived growth factor (PDGF), epidermal growth factor (EGF), insulin and insulin-like growth factor I (IGF-I). AKT mediates the antiapoptotic effects of IGF-I. Essential for the SPATA13-mediated regulation of cell migration and adhesion assembly and disassembly. May be involved in the regulation of the placental development. Phosphorylates STK4/MST1 at 'Thr-120' and 'Thr-387' leading to

	inhibition of its: kinase activity, nuclear translocation, autophosphorylation and ability to phosphorylate FOXO3. Phosphorylates STK3/MST2 at 'Thr-117' and 'Thr-384' leading to inhibition of its: cleavage, kinase activity, autophosphorylation at Thr-180, binding to RASSF1 and nuclear translocation. Phosphorylates SRPK2 and enhances its kinase activity towards SRSF2 and ACIN1 and promotes its nuclear translocation. Phosphorylates RAF1 at 'Ser-259' and negatively regulates its activity. Phosphorylation of BAD stimulates its pro-apoptotic activity. Phosphorylates KAT6A at 'Thr-369' and this phosphorylation inhibits the interaction of KAT6A with PML and negatively regulates its acetylation activity towards p53/TP53. AKT1-specific substrates have been recently identified, including palladin (PALLD), which phosphorylation modulates cytoskeletal organization and cell motility; prohibitin (PHB), playing an important role in cell metabolism and proliferation; and CDKN1A, for which phosphorylation at 'Thr-145'

					induces its release from CDK2 and cytoplasmic relocalization. These recent findings indicate that the AKT1 isoform has a more specific role in cell motility and proliferation. Phosphorylates CLK2 thereby controlling cell survival to ionizing radiation.
SLAP	AKT2	p31751	Kinase	RAC-beta serine/threonine-protein kinase	AKT2 is one of 3 closely related serine/threonine-protein kinases (AKT1, AKT2 and AKT3) called the AKT kinase, and which regulate many processes including metabolism, proliferation, cell survival, growth and angiogenesis. This is mediated through serine and/or threonine phosphorylation of a range of downstream substrates. Over 100 substrate candidates have been reported so far, but for most of them, no isoform specificity has been reported. AKT is responsible of the regulation of glucose uptake by mediating insulin-induced translocation of the SLC2A4/GLUT4 glucose transporter to the cell surface. Phosphorylation of PTPN1 at 'Ser-50' negatively modulates its phosphatase activity preventing dephosphorylation of the insulin receptor and the attenuation of insulin

signaling. Phosphorylation of TBC1D4 triggers the binding of this effector to inhibitory 14-3-3 proteins, which is required for insulin-stimulated glucose transport. AKT regulates also the storage of glucose in the form of glycogen by phosphorylating GSK3A at 'Ser-21' and GSK3B at 'Ser-9', resulting in inhibition of its kinase activity. Phosphorylation of GSK3 isoforms by AKT is also thought to be one mechanism by which cell proliferation is driven. AKT regulates also cell survival via the phosphorylation of MAP3K5 (apoptosis signal-related kinase). Phosphorylation of 'Ser-83' decreases MAP3K5 kinase activity stimulated by oxidative stress and thereby prevents apoptosis. AKT mediates insulin-stimulated protein synthesis by phosphorylating TSC2 at 'Ser-939' and 'Thr-1462', thereby activating mTORC1 signaling and leading to both phosphorylation of 4E-BP1 and in activation of RPS6KB1. AKT is involved in the phosphorylation of members of the FOXO factors (Forkhead family of transcription factors), leading to binding of 14-3-3

proteins and cytoplasmic localization. In particular, FOXO1 is phosphorylated at 'Thr-24', 'Ser-256' and 'Ser-319'. FOXO3 and FOXO4 are phosphorylated on equivalent sites. AKT has an important role in the regulation of NF-kappa-B-dependent gene transcription and positively regulates the activity of CREB1 (cyclic AMP (cAMP)-response element binding protein). The phosphorylation of CREB1 induces the binding of accessory proteins that are necessary for the transcription of pro-survival genes such as BCL2 and MCL1. AKT phosphorylates 'Ser-454' on ATP citrate lyase (ACLY), thereby potentially regulating ACLY activity and fatty acid synthesis. Activates the 3B isoform of cyclic nucleotide phosphodiesterase (PDE3B) via phosphorylation of 'Ser-273', resulting in reduced cyclic AMP levels and inhibition of lipolysis. Phosphorylates PIKFYVE on 'Ser-318', which results in increased PI3P-5 activity. The Rho GTPase-activating protein DLC1 is another substrate and its phosphorylation is implicated in the regulation cell

	proliferation and cell growth. AKT plays a role as key modulator of the AKT-mTOR signaling pathway controlling the tempo of the process of newborn neurons integration during adult neurogenesis, including correct neuron positioning, dendritic development and synapse formation. Signals downstream of phosphatidylinositol 3-kinase (PI3K) to mediate the effects of various growth factors such as platelet-derived growth factor (PDGF), epidermal growth factor (EGF), insulin and insulin-like growth factor I (IGF-I). AKT mediates the antiapoptotic effects of IGF-I. Essential for the SPATA13-mediated regulation of cell migration and adhesion assembly and disassembly. May be involved in the regulation of the placental development.One of the few specific substrates of AKT2 identified recently is PITX2. Phosphorylation of PITX2 impairs its association with the CCND1 mRNA-stabilizing complex thus shortening the half-life of CCND1. AKT2 seems also to be the principal isoform responsible of the regulation of

					glucose uptake. Phosphorylates C2CD5 on 'Ser-197' during insulin-stimulated adipocytes. AKT2 is also specifically involved in skeletal muscle differentiation, one of its substrates in this process being ANKRD2. Down-regulation by RNA interference reduces the expression of the phosphorylated form of BAD, resulting in the induction of caspase-dependent apoptosis. Phosphorylates CLK2 on 'Thr-343'.
STITCH	ALB	p02768	Binding	Serum albumin	Serum albumin, the main protein of plasma, has a good binding capacity for water, Ca^{2+}, Na^{+}, K^{+}, fatty acids, hormones, bilirubin and drugs. Its main function is the regulation of the colloidal osmotic pressure of blood. Major zinc transporter in plasma, typically binds about 80% of all plasma zinc.
STITCH	ALOX15	p16050	Enzyme	Arachidonate 15-lipoxygenase	Non-heme iron-containing dioxygenase that catalyzes the stereo-specific peroxidation of free and esterified polyunsaturated fatty acids generating a spectrum of bioactive lipid mediators. Converts arachidonic acid into 12-hydroperoxyeicosatetraenoic acid/12-HPETE and 15-hydroperoxyeicosatetraenoic acid/15-HPETE.

	Also converts linoleic acid to 13-hydroperoxyoctadecadienoic acid. May also act on (12S)-hydroperoxyeicosatetraenoic acid/(12S)-HPETE to produce hepoxilin A3. Probably plays an important role in the immune and inflammatory responses. Through the oxygenation of membrane-bound phosphatidylethanolamine in macrophages may favor clearance of apoptotic cells during inflammation by resident macrophages and prevent an autoimmune response associated with the clearance of apoptotic cells by inflammatory monocytes. In parallel, may regulate actin polymerization which is crucial for several biological processes, including macrophage function. May also regulate macrophage function through regulation of the peroxisome proliferator activated receptor signaling pathway. Finally, it is also involved in the cellular response to IL13/interleukin-13. In addition to its role in the immune and inflammatory responses, may play a role in epithelial wound healing in the cornea maybe through

					production of lipoxin A4. May also play a role in endoplasmic reticulum stress response and the regulation of bone mass.
STITCH	ALOX15B	o15296	Enzyme	Arachidonate 15-lipoxygenase B	Non-heme iron-containing dioxygenase that catalyzes the stereo-specific peroxidation of free and esterified polyunsaturated fatty acids generating a spectrum of bioactive lipid mediators. Converts arachidonic acid to 15S-hydroperoxyeicosatetraenoic acid/(15S)-HPETE. Also acts on linoleic acid to produce 13-hydroxyoctadecadienoic acid/13-HPODE. Has no detectable 8S-lipoxygenase activity but reacts with (8S)-HPETE to produce (8S,15S)-diHPETE. May regulate progression through the cell cycle and cell proliferation. May also regulate cytokine secretion by macrophages and therefore play a role in the immune response. May also regulate macrophage differentiation into proatherogenic foam cells.
Both	ALOX5	p09917	Enzyme	Arachidonate 5-lipoxygenase	Catalyzes the first step in leukotriene biosynthesis, and thereby plays a role in inflammatory processes.

STITCH	ALOX5AP	p20292	Binding	Arachidonate 5-lipoxygenase-activating protein	Required for leukotriene biosynthesis by ALOX5 (5-lipoxygenase). Anchors ALOX5 to the membrane. Binds arachidonic acid, and could play an essential role in the transfer of arachidonic acid to ALOX5. Binds to MK-886, a compound that blocks the biosynthesis of leukotrienes.
STITCH	AOX1	q06278	Metabolism	Aldehyde oxidase	Oxidase with broad substrate specificity, oxidizing aromatic azaheterocycles, such as N1-methylnicotinamide and N-methylphthalazinium, as well as aldehydes, such as benzaldehyde, retinal, pyridoxal, and vanillin. Plays a key role in the metabolism of xenobiotics and drugs containing aromatic azaheterocyclic substituents. Participates in the bioactivation of prodrugs such as famciclovir, catalyzing the oxidation step from 6-deoxypenciclovir to penciclovir, which is a potent antiviral agent. Is probably involved in the regulation of reactive oxygen species homeostasis. May be a prominent source of superoxide generation via the one-electron reduction of molecular oxygen. Also may catalyze nitric oxide

					(NO) production via the reduction of nitrite to NO with NADH or aldehyde as electron donor. May play a role in adipogenesis.
STITCH	APRT	p07741	Enzyme	Adenine phosphoribosyltransferase	Catalyzes a salvage reaction resulting in the formation of AMP, that is energically less costly than de novo synthesis.
Both	AR	p10275	Receptor	Androgen receptor	Steroid hormone receptors are ligand-activated transcription factors that regulate eukaryotic gene expression and affect cellular proliferation and differentiation in target tissues. Transcription factor activity is modulated by bound coactivator and corepressor proteins. Transcription activation is down-regulated by NR0B2. Activated, but not phosphorylated, by HIPK3 and ZIPK/DAPK3.
SLAP	ASL	p04424	Enzyme	Argininosuccinate lyase	argininosuccinate lyase activity
STITCH	ATIC	p31939	Enzyme	Bifunctional purine biosynthesis protein PURH	Bifunctional enzyme that catalyzes 2 steps in purine biosynthesis
STITCH	BAX	q07812	Regulator	Apoptosis regulator BAX	Accelerates programmed cell death by binding to, and antagonizing the apoptosis repressor BCL2 or its

					adenovirus homolog E1B 19k protein. Under stress conditions, undergoes a conformation change that causes translocation to the mitochondrion membrane, leading to the release of cytochrome c that then triggers apoptosis. Promotes activation of CASP3, and thereby apoptosis.
SLAP	BCL2	p10415	Regulator	Apoptosis regulator Bcl-2	Suppresses apoptosis in a variety of cell systems including factor-dependent lymphohematopoietic and neural cells. Regulates cell death by controlling the mitochondrial membrane permeability. Appears to function in a feedback loop system with caspases. Inhibits caspase activity either by preventing the release of cytochrome c from the mitochondria and/or by binding to the apoptosis-activating factor (APAF-1)
SLAP	BCL2L1	q07817	Regulator	Bcl-2-like protein 1	Potent inhibitor of cell death. Inhibits activation of caspases. Appears to regulate cell death by blocking the voltage-dependent anion channel (VDAC) by binding to it and preventing the release of the caspase activator, CYC1, from the mitochondrial membrane.

					Also acts as a regulator of G2 checkpoint and progression to cytokinesis during mitosis.Isoform Bcl-X(L) also regulates presynaptic plasticity, including neurotransmitter release and recovery, number of axonal mitochondria as well as size and number of synaptic vesicle clusters. During synaptic stimulation, increases ATP availability from mitochondria through regulation of mitochondrial membrane ATP synthase F1F0 activity and regulates endocytic vesicle retrieval in hippocampal neurons through association with DMN1L and stimulation of its GTPase activity in synaptic vesicles.Isoform Bcl-X(S) promotes apoptosis.
STITCH	BDNF	p23560	Regulator	Brain-derived neurotrophic factor	During development, promotes the survival and differentiation of selected neuronal populations of the peripheral and central nervous systems. Participates in axonal growth, pathfinding and in the modulation of dendritic growth and morphology. Major regulator of synaptic transmission and plasticity at adult synapses in many regions of the CNS. The versatility of BDNF is emphasized by its contribution

					to a range of adaptive neuronal responses including long-term potentiation (LTP), long-term depression (LTD), certain forms of short-term synaptic plasticity, as well as homeostatic regulation of intrinsic neuronal excitability.
STITCH	BIRC5	o15392	Regulator	Baculoviral IAP repeat-containing protein 5	Multitasking protein that has dual roles in promoting cell proliferation and preventing apoptosis. Component of a chromosome passage protein complex (CPC) which is essential for chromosome alignment and segregation during mitosis and cytokinesis. Acts as an important regulator of the localization of this complex; directs CPC movement to different locations from the inner centromere during prometaphase to midbody during cytokinesis and participates in the organization of the center spindle by associating with polymerized microtubules. The complex with RAN plays a role in mitotic spindle formation by serving as a physical scaffold to help deliver the RAN effector molecule TPX2 to microtubules. May counteract a default induction of

					apoptosis in G2/M phase. The acetylated form represses STAT3 transactivation of target gene promoters. May play a role in neoplasia. Inhibitor of CASP3 and CASP7. Isoform 2 and isoform 3 do not appear to play vital roles in mitosis. Isoform 3 shows a marked reduction in its anti-apoptotic effects when compared with the displayed wild-type isoform.
STITCH	C8orf4	q9nr00	Regulator	Uncharacterized protein C8orf4	May decrease apoptosis.
SLAP	CA1	p00915	Enzyme	Carbonic anhydrase 1	Reversible hydration of carbon dioxide. Can hydrates cyanamide to urea.
SLAP	CA10	q9ns85	*Uncertain*	Carbonic anhydrase-related protein 10	Does not have a catalytic activity.
SLAP	CA11	o75493	*Uncertain*	Carbonic anhydrase-related protein 11	Does not have a catalytic activity.
Both	CA12	o43570		Carbonic anhydrase 12	Reversible hydration of carbon dioxide.
Both	CA13	q8n1q1	Enzyme	Carbonic anhydrase 13	Reversible hydration of carbon dioxide.

SLAP	CA14	q9ulx7	Enzyme	Carbonic anhydrase 14	Reversible hydration of carbon dioxide.
Both	CA2	p00918	Enzyme	Carbonic anhydrase 2	Essential for bone resorption and osteoclast differentiation (By similarity). Reversible hydration of carbon dioxide. Can hydrate cyanamide to urea. Involved in the regulation of fluid secretion into the anterior chamber of the eye. Contributes to intracellular pH regulation in the duodenal upper villous epithelium during proton-coupled peptide absorption. Stimulates the chloride-bicarbonate exchange activity of SLC26A6.
SLAP	CA3	p07451	Enzyme	Carbonic anhydrase 3	Reversible hydration of carbon dioxide.
SLAP	CA4	p22748	Enzyme	Carbonic anhydrase 4	Reversible hydration of carbon dioxide. May stimulate the sodium/bicarbonate transporter activity of SLC4A4 that acts in pH homeostasis. It is essential for acid overload removal from the retina and retina epithelium, and acid release in the choriocapillaris in the choroid

SLAP	CA5A	p35218	Enzyme	Carbonic anhydrase 5A, mitochondrial	Reversible hydration of carbon dioxide. Low activity.
Both	CA5B	q9y2d0	Enzyme	Carbonic anhydrase 5B, mitochondrial	Reversible hydration of carbon dioxide.
STITCH	CA6	p23280	Enzyme	Carbonic anhydrase 6	Reversible hydration of carbon dioxide. Its role in saliva is unknown.
SLAP	CA7	p43166	Enzyme	Carbonic anhydrase 7	Reversible hydration of carbon dioxide.
SLAP	CA8	p35219	*Uncertain*	Carbonic anhydrase-related protein	Does not have a carbonic anhydrase catalytic activity.
Both	CA9	q16790	Enzyme	Carbonic anhydrase 9	Reversible hydration of carbon dioxide. Participates in pH regulation. May be involved in the control of cell proliferation and transformation. Appears to be a novel specific biomarker for a cervical neoplasia
SLAP	CACNA1C	q13936	Ion channel	Voltage-dependent L-type calcium channel subunit alpha-1C	Voltage-sensitive calcium channels (VSCC) mediate the entry of calcium ions into excitable cells and are also involved in a variety of calcium-dependent processes, including muscle contraction, hormone or neurotransmitter release, gene expression, cell

					motility, cell division and cell death. The isoform alpha-1C gives rise to L-type calcium currents. Long-lasting (L-type) calcium channels belong to the 'high-voltage activated' (HVA) group. They are blocked by dihydropyridines (DHP), phenylalkylamines, benzothiazepines, and by omega-agatoxin-IIIA (omega-Aga-IIIA). They are however insensitive to omega-conotoxin-GVIA (omega-CTx-GVIA) and omega-agatoxin-IVA (omega-Aga-IVA). Calcium channels containing the alpha-1C subunit play an important role in excitation-contraction coupling in the heart. The various isoforms display marked differences in the sensitivity to DHP compounds. Binding of calmodulin or CABP1 at the same regulatory sites results in an opposit effects on the channel function.
SLAP	CACNA1D	q01668	Ion channel	Voltage-dependent L-type calcium channel subunit alpha-1D	Voltage-sensitive calcium channels (VSCC) mediate the entry of calcium ions into excitable cells and are also involved in a variety of calcium-dependent processes, including muscle contraction, hormone or

					neurotransmitter release, gene expression, cell motility, cell division and cell death. The isoform alpha-1D gives rise to L-type calcium currents. Long-lasting (L-type) calcium channels belong to the 'high-voltage activated' (HVA) group. They are blocked by dihydropyridines (DHP), phenylalkylamines, benzothiazepines, and by omega-agatoxin-IIIA (omega-Aga-IIIA). They are however insensitive to omega-conotoxin-GVIA (omega-CTx-GVIA) and omega-agatoxin-IVA (omega-Aga-IVA).
SLAP	CACNA1F	o60840	Ion channel	Voltage-dependent L-type calcium channel subunit alpha-1F	Voltage-sensitive calcium channels (VSCC) mediate the entry of calcium ions into excitable cells and are also involved in a variety of calcium-dependent processes, including muscle contraction, hormone or neurotransmitter release, gene expression, cell motility, cell division and cell death. The isoform alpha-1F gives rise to L-type calcium currents. Long-lasting (L-type) calcium channels belong to the 'high-voltage activated' (HVA) group. They are blocked by dihydropyridines (DHP), phenylalkylamines,

					benzothiazepines, and by omega-agatoxin-IIIA (omega-Aga-IIIA). They are however insensitive to omega-conotoxin-GVIA (omega-CTx-GVIA) and omega-agatoxin-IVA (omega-Aga-IVA).
SLAP	CACNA1G	o43497	Ion channel	Voltage-dependent T-type calcium channel subunit alpha-1G	Voltage-sensitive calcium channels (VSCC) mediate the entry of calcium ions into excitable cells and are also involved in a variety of calcium-dependent processes, including muscle contraction, hormone or neurotransmitter release, gene expression, cell motility, cell division and cell death. The isoform alpha-1G gives rise to T-type calcium currents. T-type calcium channels belong to the "low-voltage activated (LVA)" group and are strongly blocked by mibefradil. A particularity of this type of channel is an opening at quite negative potentials and a voltage-dependent inactivation. T-type channels serve pacemaking functions in both central neurons and cardiac nodal cells and support calcium signaling in secretory cells and vascular smooth muscle. They may also be involved in the modulation of firing patterns of

					neurons which is important for information processing as well as in cell growth processes.
SLAP	CACNA1H	o95180	Ion channel	Voltage-dependent T-type calcium channel subunit alpha-1H	Voltage-sensitive calcium channels (VSCC) mediate the entry of calcium ions into excitable cells and are also involved in a variety of calcium-dependent processes, including muscle contraction, hormone or neurotransmitter release, gene expression, cell motility, cell division and cell death. The isoform alpha-1H gives rise to T-type calcium currents. T-type calcium channels belong to the "low-voltage activated (LVA)" group and are strongly blocked by nickel and mibefradil. A particularity of this type of channels is an opening at quite negative potentials, and a voltage-dependent inactivation. T-type channels serve pacemaking functions in both central neurons and cardiac nodal cells and support calcium signaling in secretory cells and vascular smooth muscle. They may also be involved in the modulation of firing patterns of neurons which is important for information processing as well as in cell growth processes.

SLAP	CACNA1I	q9p0x4	Ion channel	Voltage-dependent T-type calcium channel subunit alpha-1I	Voltage-sensitive calcium channels (VSCC) mediate the entry of calcium ions into excitable cells and are also involved in a variety of calcium-dependent processes, including muscle contraction, hormone or neurotransmitter release, gene expression, cell motility, cell division and cell death. Isoform alpha-1I gives rise to T-type calcium currents. T-type calcium channels belong to the "low-voltage activated (LVA)" group and are strongly blocked by nickel and mibefradil. A particularity of this type of channels is an opening at quite negative potentials, and a voltage-dependent inactivation. T-type channels serve pacemaking functions in both central neurons and cardiac nodal cells and support calcium signaling in secretory cells and vascular smooth muscle. They may also be involved in the modulation of firing patterns of neurons which is important for information processing as well as in cell growth processes. Gates in voltage ranges similar to, but higher than alpha 1G or alpha 1H (By similarity).

SLAP	CACNA1S	q13698	Ion channel	Voltage-dependent L-type calcium channel subunit alpha-1S	Voltage-sensitive calcium channels (VSCC) mediate the entry of calcium ions into excitable cells and are also involved in a variety of calcium-dependent processes, including muscle contraction, hormone or neurotransmitter release, gene expression, cell motility, cell division and cell death. The isoform alpha-1S gives rise to L-type calcium currents. Long-lasting (L-type) calcium channels belong to the 'high-voltage activated' (HVA) group. They are blocked by dihydropyridines (DHP), phenylalkylamines, benzothiazepines, and by omega-agatoxin-IIIA (omega-Aga-IIIA). They are however insensitive to omega-conotoxin-GVIA (omega-CTx-GVIA) and omega-agatoxin-IVA (omega-Aga-IVA). Calcium channels containing the alpha-1S subunit play an important role in excitation-contraction coupling in skeletal muscle.
SLAP	CALM1	p62158	Regulator	Calmodulin	Calmodulin mediates the control of a large number of enzymes, ion channels, aquaporins and other proteins by Ca^{2+}. Among the enzymes to be stimulated by the

					calmodulin-Ca^{2+} complex are a number of protein kinases and phosphatases. Together with CCP110 and centrin, is involved in a genetic pathway that regulates the centrosome cycle and progression through cytokinesis.
SLAP	CASP1	p29466	Enzyme	Caspase-1	Thiol protease that cleaves IL-1 beta between an Asp and an Ala, releasing the mature cytokine which is involved in a variety of inflammatory processes. Important for defense against pathogens. Cleaves and activates sterol regulatory element binding proteins (SREBPs). Can also promote apoptosis.
Both	CASP3	p42574	Enzyme	Caspase-3	Involved in the activation cascade of caspases responsible for apoptosis execution. At the onset of apoptosis it proteolytically cleaves poly(ADP-ribose) polymerase (PARP) at a '216-Asp-|-Gly-217' bond. Cleaves and activates sterol regulatory element binding proteins (SREBPs) between the basic helix-loop-helix leucine zipper domain and the membrane attachment domain. Cleaves and activates caspase-6, -7 and -9. Involved in the cleavage of huntingtin.

					Triggers cell adhesion in sympathetic neurons through RET cleavage.
SLAP	CASP7	p55210	Enzyme	Caspase-7	Involved in the activation cascade of caspases responsible for apoptosis execution. Cleaves and activates sterol regulatory element binding proteins (SREBPs). Proteolytically cleaves poly(ADP-ribose) polymerase (PARP) at a '216-Asp-|-Gly-217' bond. Overexpression promotes programmed cell death.
STITCH	CASP8	q14790	Enzyme	Caspase-8	Most upstream protease of the activation cascade of caspases responsible for the TNFRSF6/FAS mediated and TNFRSF1A induced cell death. Binding to the adapter molecule FADD recruits it to either receptor. The resulting aggregate called death-inducing signaling complex (DISC) performs CASP8 proteolytic activation. The active dimeric enzyme is then liberated from the DISC and free to activate downstream apoptotic proteases. Proteolytic fragments of the N-terminal propeptide (termed CAP3, CAP5 and CAP6) are likely retained in the DISC. Cleaves and activates CASP3, CASP4, CASP6, CASP7,

					CASP9 and CASP10. May participate in the GZMB apoptotic pathways. Cleaves ADPRT. Hydrolyzes the small-molecule substrate, Ac-Asp-Glu-Val-Asp-|-AMC. Likely target for the cowpox virus CRMA death inhibitory protein. Isoform 5, isoform 6, isoform 7 and isoform 8 lack the catalytic site and may interfere with the pro-apoptotic activity of the complex.
STITCH	CASP9	p55211	Enzyme	Caspase-9	Involved in the activation cascade of caspases responsible for apoptosis execution. Binding of caspase-9 to Apaf-1 leads to activation of the protease which then cleaves and activates caspase-3. Promotes DNA damage-induced apoptosis in a ABL1/c-Abl-dependent manner. Proteolytically cleaves poly(ADP-ribose) polymerase (PARP). Isoform 2 lacks activity is an dominant-negative inhibitor of caspase-9.
STITCH	CAV1	q03135	Immune activation	Caveolin-1	May act as a scaffolding protein within caveolar membranes. Interacts directly with G-protein alpha subunits and can functionally regulate their activity (By similarity). Involved in the costimulatory signal

					essential for T-cell receptor (TCR)-mediated T-cell activation. Its binding to DPP4 induces T-cell proliferation and NF-kappa-B activation in a T-cell receptor/CD3-dependent manner. Recruits CTNNB1 to caveolar membranes and may regulate CTNNB1-mediated signaling through the Wnt pathway.
SLAP	CCL2	p13500	Chemotatic	C-C motif chemokine 2	Chemotactic factor that attracts monocytes and basophils but not neutrophils or eosinophils. Augments monocyte anti-tumor activity. Has been implicated in the pathogenesis of diseases characterized by monocytic infiltrates, like psoriasis, rheumatoid arthritis or atherosclerosis. May be involved in the recruitment of monocytes into the arterial wall during the disease process of atherosclerosis.
Both	CCND1	p24385	Regulator	G1/S-specific cyclin-D1	Regulatory component of the cyclin D1-CDK4 (DC) complex that phosphorylates and inhibits members of the retinoblastoma (RB) protein family including RB1 and regulates the cell-cycle during G_1/S transition. Phosphorylation of RB1 allows dissociation of the

					transcription factor E2F from the RB/E2F complex and the subsequent transcription of E2F target genes which are responsible for the progression through the G_1 phase. Hypophosphorylates RB1 in early G_1 phase. Cyclin D-CDK4 complexes are major integrators of various mitogenenic and antimitogenic signals. Also substrate for SMAD3, phosphorylating SMAD3 in a cell-cycle-dependent manner and repressing its transcriptional activity. Component of the ternary complex, cyclin D1/CDK4/CDKN1B, required for nuclear translocation and activity of the cyclin D-CDK4 complex. Exhibits transcriptional corepressor activity with INSM1 on the NEUROD1 and INS promoters in a cell cycle-independent manner.
SLAP	CCR5	p51681	Receptor	C-C chemokine receptor type 5	Receptor for a number of inflammatory CC-chemokines including MIP-1-alpha, MIP-1-beta and RANTES and subsequently transduces a signal by increasing the intracellular calcium ion level. May play a role in the control of granulocytic lineage proliferation or differentiation. Acts as a coreceptor

					(CD4 being the primary receptor) for HIV-1 R5 isolates.
STITCH	CD248	q9hcu0		Endosialin	May play a role in tumor angiogenesis
STITCH	CD4	p01730	Immune activation	T-cell surface glycoprotein CD4	Accessory protein for MHC class-II antigen/T-cell receptor interaction. May regulate T-cell activation. Induces the aggregation of lipid rafts.
STITCH	CD59	p13987	Immune activation	CD59 glycoprotein	Potent inhibitor of the complement membrane attack complex (MAC) action. Acts by binding to the C8 and/or C9 complements of the assembling MAC, thereby preventing incorporation of the multiple copies of C9 required for complete formation of the osmolytic pore. This inhibitor appears to be species-specific. Involved in signal transduction for T-cell activation complexed to a protein tyrosine kinase. The soluble form from urine retains its specific complement binding activity, but exhibits greatly reduced ability to inhibit MAC assembly on cell membranes.

STITCH	CD79A	p11912	Immune activation	B-cell antigen receptor complex-associated protein alpha chain	Required in cooperation with CD79B for initiation of the signal transduction cascade activated by binding of antigen to the B-cell antigen receptor complex (BCR) which leads to internalization of the complex, trafficking to late endosomes and antigen presentation. Also required for BCR surface expression and for efficient differentiation of pro- and pre-B-cells. Stimulates SYK autophosphorylation and activation. Binds to BLNK, bringing BLNK into proximity with SYK and allowing SYK to phosphorylate BLNK. Also interacts with and increases activity of some Src-family tyrosine kinases. Represses BCR signaling during development of immature B-cells.
STITCH	CDIPT	o14735	Enzyme	CDP-diacylglycerol--inositol 3-phosphatidyltransferase	Catalyzes the biosynthesis of phosphatidylinositol (PtdIns) as well as PtdIns:inositol exchange reaction. May thus act to reduce an excessive cellular PtdIns content. The exchange activity is due to the reverse reaction of PtdIns synthase and is dependent on CMP, which is tightly bound to the enzyme.

Both	CDK2	p24941	Kinase	Cyclin-dependent kinase 2	Serine/threonine-protein kinase involved in the control of the cell cycle; essential for meiosis, but dispensable for mitosis. Phosphorylates CTNNB1, USP37, p53/TP53, NPM1, CDK7, RB1, BRCA2, MYC, NPAT, EZH2. Interacts with cyclins A, B1, B3, D, or E. Triggers duplication of centrosomes and DNA. Acts at the G1-S transition to promote the E2F transcriptional program and the initiation of DNA synthesis, and modulates G2 progression; controls the timing of entry into mitosis/meiosis by controlling the subsequent activation of cyclin B/CDK1 by phosphorylation, and coordinates the activation of cyclin B/CDK1 at the centrosome and in the nucleus. Crucial role in orchestrating a fine balance between cellular proliferation, cell death, and DNA repair in human embryonic stem cells (hESCs). Activity of CDK2 is maximal during S phase and G2; activated by interaction with cyclin E during the early stages of DNA synthesis to permit G1-S transition, and subsequently activated by cyclin A2 (cyclin A1 in germ

cells) during the late stages of DNA replication to drive the transition from S phase to mitosis, the G2 phase. EZH2 phosphorylation promotes H3K27me3 maintenance and epigenetic gene silencing. Phosphorylates CABLES1 (By similarity). Cyclin E/CDK2 prevents oxidative stress-mediated Ras-induced senescence by phosphorylating MYC. Involved in G1-S phase DNA damage checkpoint that prevents cells with damaged DNA from initiating mitosis; regulates homologous recombination-dependent repair by phosphorylating BRCA2, this phosphorylation is low in S phase when recombination is active, but increases as cells progress towards mitosis. In response to DNA damage, double-strand break repair by homologous recombination a reduction of CDK2-mediated BRCA2 phosphorylation. Phosphorylation of RB1 disturbs its interaction with E2F1. NPM1 phosphorylation by cyclin E/CDK2 promotes its dissociates from unduplicated centrosomes, thus initiating centrosome duplication. Cyclin E/CDK2-mediated phosphorylation

					of NPAT at G1-S transition and until prophase stimulates the NPAT-mediated activation of histone gene transcription during S phase. Required for vitamin D-mediated growth inhibition by being itself inactivated. Involved in the nitric oxide- (NO) mediated signaling in a nitrosylation/activation-dependent manner. USP37 is activated by phosphorylation and thus triggers G1-S transition. CTNNB1 phosphorylation regulates insulin internalization. Phosphorylates FOXP3 and negatively regulates its transcriptional activity and protein stability (By similarity).
SLAP	CDK4	p11802	Kinase	Cyclin-dependent kinase 4	Ser/Thr-kinase component of cyclin D-CDK4 (DC) complexes that phosphorylate and inhibit members of the retinoblastoma (RB) protein family including RB1 and regulate the cell-cycle during G_1/S transition. Phosphorylation of RB1 allows dissociation of the transcription factor E2F from the RB/E2F complexes and the subsequent transcription of E2F target genes which are responsible for the progression through the

					G_1 phase. Hypophosphorylates RB1 in early G_1 phase. Cyclin D-CDK4 complexes are major integrators of various mitogenenic and antimitogenic signals. Also phosphorylates SMAD3 in a cell-cycle-dependent manner and represses its transcriptional activity. Component of the ternary complex, cyclin D/CDK4/CDKN1B, required for nuclear translocation and activity of the cyclin D-CDK4 complex.
STITCH	CDKN1A	p38936	Regulator	Cyclin-dependent kinase inhibitor 1	May be the important intermediate by which p53/TP53 mediates its role as an inhibitor of cellular proliferation in response to DNA damage. Binds to and inhibits cyclin-dependent kinase activity, preventing phosphorylation of critical cyclin-dependent kinase substrates and blocking cell cycle progression. Functions in the nuclear localization and assembly of cyclin D-CDK4 complex and promotes its kinase activity towards RB1. At higher stoichiometric ratios, inhibits the kinase activity of the cyclin D-CDK4 complex.

STITCH	CFLAR	o15519	Regulator	CASP8 and FADD-like apoptosis regulator	Apoptosis regulator protein which may function as a crucial link between cell survival and cell death pathways in mammalian cells. Acts as an inhibitor of TNFRSF6 mediated apoptosis. A proteolytic fragment (p43) is likely retained in the death-inducing signaling complex (DISC) thereby blocking further recruitment and processing of caspase-8 at the complex. Full length and shorter isoforms have been shown either to induce apoptosis or to reduce TNFRSF-triggered apoptosis. Lacks enzymatic (caspase) activity.
SLAP	CHRM1	p11229	Receptor	Muscarinic acetylcholine receptor M1	The muscarinic acetylcholine receptor mediates various cellular responses, including inhibition of adenylate cyclase, breakdown of phosphoinositides and modulation of potassium channels through the action of G proteins. Primary transducing effect is Pi turnover.
SLAP	CHRM2	p08172	Receptor	Muscarinic acetylcholine receptor M2	The muscarinic acetylcholine receptor mediates various cellular responses, including inhibition of adenylate cyclase, breakdown of phosphoinositides and modulation of potassium channels through the

					action of G proteins. Primary transducing effect is adenylate cyclase inhibition. Signaling promotes phospholipase C activity, leading to the release of inositol trisphosphate (IP3); this then triggers calcium ion release into the cytosol.
SLAP	CHRM3	p20309	Receptor	Muscarinic acetylcholine receptor M3	The muscarinic acetylcholine receptor mediates various cellular responses, including inhibition of adenylate cyclase, breakdown of phosphoinositides and modulation of potassium channels through the action of G proteins. Primary transducing effect is Pi turnover.
SLAP	CHRM4	p08173	Receptor	Muscarinic acetylcholine receptor M4	The muscarinic acetylcholine receptor mediates various cellular responses, including inhibition of adenylate cyclase, breakdown of phosphoinositides and modulation of potassium channels through the action of G proteins. Primary transducing effect is inhibition of adenylate cyclase.
SLAP	CHRM5	p08912	Receptor	Muscarinic acetylcholine receptor M5	The muscarinic acetylcholine receptor mediates various cellular responses, including inhibition of adenylate cyclase, breakdown of phosphoinositides

					and modulation of potassium channels through the action of G proteins. Primary transducing effect is Pi turnover.
SLAP	CHRNA7	q494w8	Ion channel	CHRNA7-FAM7A fusion protein	extracellular ligand-gated ion channel activity
STITCH	CHUK	o15111	Kinase	Inhibitor of nuclear factor kappa-B kinase subunit alpha	Serine kinase that plays an essential role in the NF-kappa-B signaling pathway which is activated by multiple stimuli such as inflammatory cytokines, bacterial or viral products, DNA damages or other cellular stresses. Acts as part of the canonical IKK complex in the conventional pathway of NF-kappa-B activation and phosphorylates inhibitors of NF-kappa-B on serine residues. These modifications allow polyubiquitination of the inhibitors and subsequent degradation by the proteasome. In turn, free NF-kappa-B is translocated into the nucleus and activates the transcription of hundreds of genes involved in immune response, growth control, or protection against apoptosis. Negatively regulates the pathway by phosphorylating the scaffold protein TAXBP1 and

thus promoting the assembly of the A20/TNFAIP3 ubiquitin-editing complex (composed of A20/TNFAIP3, TAX1BP1, and the E3 ligases ITCH and RNF11). Therefore, CHUK plays a key role in the negative feedback of NF-kappa-B canonical signaling to limit inflammatory gene activation. As part of the non-canonical pathway of NF-kappa-B activation, the MAP3K14-activated CHUK/IKKA homodimer phosphorylates NFKB2/p100 associated with RelB, inducing its proteolytic processing to NFKB2/p52 and the formation of NF-kappa-B RelB-p52 complexes. In turn, these complexes regulate genes encoding molecules involved in B-cell survival and lymphoid organogenesis. Participates also in the negative feedback of the non-canonical NF-kappa-B signaling pathway by phosphorylating and destabilizing MAP3K14/NIK. Within the nucleus, phosphorylates CREBBP and consequently increases both its transcriptional and histone acetyltransferase activities. Modulates chromatin accessibility at NF-

					kappa-B-responsive promoters by phosphorylating histones H3 at 'Ser-10' that are subsequently acetylated at 'Lys-14' by CREBBP. Additionally, phosphorylates the CREBBP-interacting protein NCOA3.
SLAP	CNR1	p21554	Receptor	Cannabinoid receptor 1	Involved in cannabinoid-induced CNS effects. Acts by inhibiting adenylate cyclase. Could be a receptor for anandamide. Inhibits L-type Ca^{2+} channel current. Isoform 2 and isoform 3 have altered ligand binding.
SLAP	CNR2	p34972	Receptor	Cannabinoid receptor 2	Heterotrimeric G protein-coupled receptor for endocannabinoid 2-arachidonoylglycerol mediating inhibition of adenylate cyclase. May function in inflammatory response, nociceptive transmission and bone homeostasis.
STITCH	CRH	p06850	Hormone	Corticoliberin	This hormone from hypothalamus regulates the release of corticotropin from pituitary gland.
STITCH	CRP	p02741	Immune functions	C-reactive protein	Displays several functions associated with host defense: it promotes agglutination, bacterial capsular swelling, phagocytosis and complement fixation through its calcium-dependent binding to

					phosphorylcholine. Can interact with DNA and histones and may scavenge nuclear material released from damaged circulating cells.
STITCH	CTNNB1	p35222	Regulator	Catenin beta-1	Key downstream component of the canonical Wnt signaling pathway. In the absence of Wnt, forms a complex with AXIN1, AXIN2, APC, CSNK1A1 and GSK3B that promotes phosphorylation on N-terminal Ser and Thr residues and ubiquitination of CTNNB1 via BTRC and its subsequent degradation by the proteasome. In the presence of Wnt ligand, CTNNB1 is not ubiquitinated and accumulates in the nucleus, where it acts as a coactivator for transcription factors of the TCF/LEF family, leading to activate Wnt responsive genes. Involved in the regulation of cell adhesion. Acts as a negative regulator of centrosome cohesion. Involved in the CDK2/PTPN6/CTNNB1/CEACAM1 pathway of insulin internalization. Blocks anoikis of malignant kidney and intestinal epithelial cells and promotes their anchorage-independent growth by down-regulating

					DAPK2. Disrupts PML function and PML-NB formation by inhibiting RANBP2-mediated sumoylation of PML (PubMed:17524503, PubMed:18077326, PubMed:18086858, PubMed:18957423, PubMed:21262353, PubMed:22647378, PubMed:22699938, PubMed:22155184). Promotes neurogenesis by maintaining sympathetic neuroblasts within the cell cycle (By similarity).
STITCH	CTSB	p07858	Enzyme	Cathepsin B	Thiol protease which is believed to participate in intracellular degradation and turnover of proteins. Has also been implicated in tumor invasion and metastasis.
STITCH	CTSL1	p07711	Enzyme	Cathepsin L1	Important for the overall degradation of proteins in lysosomes.
STITCH	CXCL10	p02778	Chemotatic	C-X-C motif chemokine 10	Chemotactic for monocytes and T-lymphocytes. Binds to CXCR3.
Both	CYP11B1	p15538	Metabolic enzmye	Cytochrome P450 11B1, mitochondrial	Has steroid 11-beta-hydroxylase activity. In addition to this activity, the 18 or 19-hydroxylation of steroids and the aromatization of androstendione to estrone have also been ascribed to cytochrome P450 XIB.

Both	CYP17A1	p05093	Metabolic enzmye	Steroid 17-alpha-hydroxylase/17,20 lyase	Conversion of pregnenolone and progesterone to their 17-alpha-hydroxylated products and subsequently to dehydroepiandrosterone (DHEA) and androstenedione. Catalyzes both the 17-alpha-hydroxylation and the 17,20-lyase reaction. Involved in sexual development during fetal life and at puberty
Both	CYP19A1	p11511	Metabolic enzmye	Aromatase	Catalyzes the formation of aromatic C18 estrogens from C19 androgens.
STITCH	CYP1A1	p04798	Metabolic enzmye	Cytochrome P450 1A1	Cytochromes P450 are a group of heme-thiolate monooxygenases. In liver microsomes, this enzyme is involved in an NADPH-dependent electron transport pathway. It oxidizes a variety of structurally unrelated compounds, including steroids, fatty acids, and xenobiotics.
Both	CYP1A2	p05177	Metabolic enzmye	Cytochrome P450 1A2	Cytochromes P450 are a group of heme-thiolate monooxygenases. In liver microsomes, this enzyme is involved in an NADPH-dependent electron transport pathway. It oxidizes a variety of structurally unrelated compounds, including steroids, fatty acids, and xenobiotics. Most active in catalyzing 2-hydroxylation.

					Caffeine is metabolized primarily by cytochrome CYP1A2 in the liver through an initial N3-demethylation. Also acts in the metabolism of aflatoxin B1 and acetaminophen. Participates in the bioactivation of carcinogenic aromatic and heterocyclic amines. Catalizes the N-hydroxylation of heterocyclic amines and the O-deethylation of phenacetin.
STITCH	CYP2A13	q16696	Metabolic enzmye	Cytochrome P450 2A13	Exhibits a coumarin 7-hydroxylase activity. Active in the metabolic activation of hexamethylphosphoramide, N,N-dimethylaniline, 2'-methoxyacetophenone, N-nitrosomethylphenylamine, and the tobacco-specific carcinogen, 4-(methylnitrosamino)-1-(3-pyridyl)-1-butanone. Possesses phenacetin O-deethylation activity.
Both	CYP2A6	p11509	Metabolic enzmye	Cytochrome P450 2A6	Exhibits a high coumarin 7-hydroxylase activity. Can act in the hydroxylation of the anti-cancer drugs cyclophosphamide and ifosphamide. Competent in the metabolic activation of aflatoxin B1. Constitutes

					the major nicotine C-oxidase. Acts as a 1,4-cineole 2-exo-monooxygenase. Possesses low phenacetin O-deethylation activity.
Both	CYP2B6	p20813	Metabolic enzmye	Cytochrome P450 2B6	Cytochromes P450 are a group of heme-thiolate monooxygenases. In liver microsomes, this enzyme is involved in an NADPH-dependent electron transport pathway. It oxidizes a variety of structurally unrelated compounds, including steroids, fatty acids, and xenobiotics. Acts as a 1,4-cineole 2-exo-monooxygenase.
Both	CYP2C18	p33260	Metabolic enzmye	Cytochrome P450 2C18	Cytochromes P450 are a group of heme-thiolate monooxygenases. In liver microsomes, this enzyme is involved in an NADPH-dependent electron transport pathway. It oxidizes a variety of structurally unrelated compounds, including steroids, fatty acids, and xenobiotics.
STITCH	CYP2C19	p33261	Metabolic enzmye	Cytochrome P450 2C19	Responsible for the metabolism of a number of therapeutic agents such as the anticonvulsant drug S-mephenytoin, omeprazole, proguanil, certain

					barbiturates, diazepam, propranolol, citalopram and imipramine.
Both	CYP2C8	p10632	Metabolic enzmye	Cytochrome P450 2C8	Cytochromes P450 are a group of heme-thiolate monooxygenases. In liver microsomes, this enzyme is involved in an NADPH-dependent electron transport pathway. It oxidizes a variety of structurally unrelated compounds, including steroids, fatty acids, and xenobiotics. In the epoxidation of arachidonic acid it generates only 14,15- and 11,12-cis-epoxyeicosatrienoic acids. It is the principal enzyme responsible for the metabolism the anti-cancer drug paclitaxel (taxol)
Both	CYP2C9	p11712	Metabolic enzmye	Cytochrome P450 2C9	Cytochromes P450 are a group of heme-thiolate monooxygenases. In liver microsomes, this enzyme is involved in an NADPH-dependent electron transport pathway. It oxidizes a variety of structurally unrelated compounds, including steroids, fatty acids, and xenobiotics. This enzyme contributes to the wide pharmacokinetics variability of the metabolism of

					drugs such as S-warfarin, diclofenac, phenytoin, tolbutamide and losartan.
STITCH	CYP2D6	p10635	Metabolic enzmye	Cytochrome P450 2D6	Responsible for the metabolism of many drugs and environmental chemicals that it oxidizes. It is involved in the metabolism of drugs such as antiarrhythmics, adrenoceptor antagonists, and tricyclic antidepressants.
STITCH	CYP2D7P1	*no entry*			
STITCH	CYP2E1	p05181	Metabolic enzmye	Cytochrome P450 2E1	Metabolizes several precarcinogens, drugs, and solvents to reactive metabolites. Inactivates a number of drugs and xenobiotics and also bioactivates many xenobiotic substrates to their hepatotoxic or carcinogenic forms.
Both	CYP3A4	p08684	Metabolic enzmye	Cytochrome P450 3A4	Cytochromes P450 are a group of heme-thiolate monooxygenases. In liver microsomes, this enzyme is involved in an NADPH-dependent electron transport pathway. It performs a variety of oxidation reactions (e.g. caffeine 8-oxidation, omeprazole sulphoxidation, midazolam 1'-hydroxylation and midazolam 4-

					hydroxylation) of structurally unrelated compounds, including steroids, fatty acids, and xenobiotics. Acts as a 1,8-cineole 2-exo-monooxygenase. The enzyme also hydroxylates etoposide
STITCH	CYP3A43	q9hb55	Metabolic enzmye	Cytochrome P450 3A43	Exhibits low testosterone 6-beta-hydroxylase activity.
STITCH	CYP3A5	p20815	Metabolic enzmye	Cytochrome P450 3A5	Cytochrome P450 3A5
STITCH	CYP3A7	p24462	Metabolic enzmye	Cytochrome P450 3A7	Cytochromes P450 are a group of heme-thiolate monooxygenases. In liver microsomes, this enzyme is involved in an NADPH-dependent electron transport pathway. It oxidizes a variety of structurally unrelated compounds, including steroids, fatty acids, and xenobiotics.
SLAP	CYP4A11	q02928	Metabolic enzmye	Cytochrome P450 4A11	Catalyzes the omega- and (omega-1)-hydroxylation of various fatty acids such as laurate, myristate and palmitate. Has little activity toward prostaglandins A1 and E1. Oxidizes arachidonic acid to 20-hydroxyeicosatetraenoic acid (20-HETE).

STITCH	DBH	p09172	Enzyme	Dopamine beta-hydroxylase	Conversion of dopamine to noradrenaline.
SLAP	DDC	p20711	Enzyme	Aromatic-L-amino-acid decarboxylase	Catalyzes the decarboxylation of L-3,4-dihydroxyphenylalanine (DOPA) to dopamine, L-5-hydroxytryptophan to serotonin and L-tryptophan to tryptamine.
STITCH	DDIT3	p35638	Regulator	DNA damage-inducible transcript 3 protein	Multifunctional transcription factor in ER stress response. Plays an essential role in the response to a wide variety of cell stresses and induces cell cycle arrest and apoptosis in response to ER stress. Plays a dual role both as an inhibitor of CCAAT/enhancer-binding protein (C/EBP) function and as an activator of other genes. Acts as a dominant-negative regulator of C/EBP-induced transcription: dimerizes with members of the C/EBP family, impairs their association with C/EBP binding sites in the promoter regions, and inhibits the expression of C/EBP regulated genes. Positively regulates the transcription of TRIB3, IL6, IL8, IL23, TNFRSF10B/DR5, PPP1R15A/GADD34, BBC3/PUMA, BCL2L11/BIM and

					ERO1L. Negatively regulates; expression of BCL2 and MYOD1, ATF4-dependent transcriptional activation of asparagine synthetase (ASNS), CEBPA-dependent transcriptional activation of hepcidin (HAMP) and CEBPB-mediated expression of peroxisome proliferator-activated receptor gamma (PPARG). Inhibits the canonical Wnt signaling pathway by binding to TCF7L2/TCF4, impairing its DNA-binding properties and repressing its transcriptional activity. Plays a regulatory role in the inflammatory response through the induction of caspase-11 (CASP4/CASP11) which induces the activation of caspase-1 (CASP1) and both these caspases increase the activation of pro-IL1B to mature IL1B which is involved in the inflammatory response.
STITCH	DGCR2	p98153	Receptor	Integral membrane protein DGCR2/IDD	Putative adhesion receptor, that could be involved in cell-cell or cell-matrix interactions required for normal cell differentiation and migration.
SLAP	DHFR	p00374	Enzyme	Dihydrofolate reductase	Key enzyme in folate metabolism. Contributes to the de novo mitochondrial thymidylate biosynthesis

					pathway. Catalyzes an essential reaction for de novo glycine and purine synthesis, and for DNA precursor synthesis. Binds its own mRNA and that of DHFRL1.
STITCH	DIABLO	q9nr28	Regulator	Diablo homolog, mitochondrial	Promotes apoptosis by activating caspases in the cytochrome c/Apaf-1/caspase-9 pathway. Acts by opposing the inhibitory activity of inhibitor of apoptosis proteins (IAP). Inhibits the activity of BIRC6/bruce by inhibiting its binding to caspases. Isoform 3 attenuates the stability and apoptosis-inhibiting activity of XIAP/BIRC4 by promoting XIAP/BIRC4 ubiquitination and degradation through the ubiquitin-proteasome pathway. Isoform 3 also disrupts XIAP/BIRC4 interacting with processed caspase-9 and promotes caspase-3 activation. Isoform 1 is defective in the capacity to down-regulate the XIAP/BIRC4 abundance.
STITCH	DIF	*uncertain*			
STITCH	DIO1	p49895	Enzyme	Type I iodothyronine deiodinase	Responsible for the deiodination of T4 (3,5,3',5'-tetraiodothyronine) into T3 (3,5,3'-triiodothyronine)

					and of T3 into T2 (3,3'-diiodothyronine). Plays a role in providing a source of plasma T3 by deiodination of T4 in peripheral tissues such as liver and kidney.
STITCH	DIO2	q92813	Enzyme	Type II iodothyronine deiodinase	Responsible for the deiodination of T4 (3,5,3',5'-tetraiodothyronine) into T3 (3,5,3'-triiodothyronine). Essential for providing the brain with appropriate levels of T3 during the critical period of development.
STITCH	DIO3	p55073	Enzyme	Type III iodothyronine deiodinase	Responsible for the deiodination of T4 (3,5,3',5'-tetraiodothyronine) into RT3 (3,3',5'-triiodothyronine) and of T3 (3,5,3'-triiodothyronine) into T2 (3,3'-diiodothyronine). RT3 and T2 are inactive metabolites. May play a role in preventing premature exposure of developing fetal tissues to adult levels of thyroid hormones. Can regulate circulating fetal thyroid hormone concentrations throughout gestation. Essential role for regulation of thyroid hormone inactivation during embryological development.
STITCH	DPH2	q9bqc3		Diphthamide biosynthesis protein 2	Required for the first step in the synthesis of diphthamide, a post-translational modification of

					histidine which occurs in translation elongation factor 2 (EEF2).
STITCH	DPH3	q96fx2		DPH3 homolog	Essential for the first step in the synthesis of diphthamide, a post-translational modification of histidine which occurs in elongation factor 2 (EEF2) and which can be ADP-ribosylated by diphtheria toxin and by Pseudomonas exotoxin A (Eta).
SLAP	DRD1	p21728	Receptor	D(1A) dopamine receptor	Dopamine receptor whose activity is mediated by G proteins which activate adenylyl cyclase.
Both	DRD2	p14416	Receptor	D(2) dopamine receptor	Dopamine receptor whose activity is mediated by G proteins which inhibit adenylyl cyclase.
SLAP	DRD3	p35462	Receptor	D(3) dopamine receptor	Dopamine receptor whose activity is mediated by G proteins which inhibit adenylyl cyclase. Promotes cell proliferation.
SLAP	DRD4	p21917	Receptor	D(4) dopamine receptor	Dopamine receptor responsible for neuronal signaling in the mesolimbic system of the brain, an area of the brain that regulates emotion and complex behavior. Its activity is mediated by G proteins which inhibit adenylyl cyclase. Modulates the circadian rhythm of contrast sensitivity by regulating the rhythmic

					expression of NPAS2 in the retinal ganglion cells (By similarity).
SLAP	DRD5	p21918	Receptor	D(1B) dopamine receptor	Dopamine receptor whose activity is mediated by G proteins which activate adenylyl cyclase.
STITCH	EGFR	p00533	Kinase	Epidermal growth factor receptor	Receptor tyrosine kinase binding ligands of the EGF family and activating several signaling cascades to convert extracellular cues into appropriate cellular responses. Known ligands include EGF, TGFA/TGF-alpha, amphiregulin, epigen/EPGN, BTC/betacellulin, epiregulin/EREG and HBEGF/heparin-binding EGF. Ligand binding triggers receptor homo- and/or heterodimerization and autophosphorylation on key cytoplasmic residues. The phosphorylated receptor recruits adapter proteins like GRB2 which in turn activates complex downstream signaling cascades. Activates at least 4 major downstream signaling cascades including the RAS-RAF-MEK-ERK, PI3 kinase-AKT, PLCgamma-PKC and STATs modules. May also activate the NF-kappa-B signaling cascade. Also directly phosphorylates other proteins like RGS16,

					activating its GTPase activity and probably coupling the EGF receptor signaling to the G protein-coupled receptor signaling. Also phosphorylates MUC1 and increases its interaction with SRC and CTNNB1/beta-catenin. Isoform 2 may act as an antagonist of EGF action.
STITCH	EGR1	p18146	Regulator	Early growth response protein 1	Transcriptional regulator. Recognizes and binds to the DNA sequence 5'-CGCCCCCGC-3'(EGR-site). Activates the transcription of target genes whose products are required for mitogenesis and differentiation.
STITCH	ENSG00000167494	*no entry*			
STITCH	ENSG00000168937	*no entry*			
STITCH	ENSG00000204490	*no entry*			
STITCH	ENSG00000228978	*no entry*			

STITCH	EPHX1	p07099	Enzyme	Epoxide hydrolase 1	Biotransformation enzyme that catalyzes the hydrolysis of arene and aliphatic epoxides to less reactive and more water soluble dihydrodiols by the trans addition of water.
SLAP	EPHX2	p34913	Enzyme	Bifunctional epoxide hydrolase 2	Bifunctional enzyme. The C-terminal domain has epoxide hydrolase activity and acts on epoxides (alkene oxides, oxiranes) and arene oxides. Plays a role in xenobiotic metabolism by degrading potentially toxic epoxides. Also determines steady-state levels of physiological mediators. The N-terminal domain has lipid phosphatase activity, with the highest activity towards threo-9,10-phosphonooxy-hydroxy-octadecanoic acid, followed by erythro-9,10-phosphonooxy-hydroxy-octadecanoic acid, 12-phosphonooxy-octadec-9Z-enoic acid, 12-phosphonooxy-octadec-9E-enoic acid, and p-nitrophenyl phospate.
STITCH	EPX	p11678	Immune functions	Eosinophil peroxidase	Mediates tyrosine nitration of secondary granule proteins in mature resting eosinophils. Shows significant inhibitory activity towards Mycobacterium

					tuberculosis H37Rv by inducing bacterial fragmentation and lysis.
STITCH	ERBB2	p04626	Kinase	Receptor tyrosine-protein kinase erbB-2	Protein tyrosine kinase that is part of several cell surface receptor complexes, but that apparently needs a coreceptor for ligand binding. Essential component of a neuregulin-receptor complex, although neuregulins do not interact with it alone. GP30 is a potential ligand for this receptor. Regulates outgrowth and stabilization of peripheral microtubules (MTs). Upon ERBB2 activation, the MEMO1-RHOA-DIAPH1 signaling pathway elicits the phosphorylation and thus the inhibition of GSK3B at cell membrane. This prevents the phosphorylation of APC and CLASP2, allowing its association with the cell membrane. In turn, membrane-bound APC allows the localization of MACF1 to the cell membrane, which is required for microtubule capture and stabilization. In the nucleus is involved in transcriptional regulation. Associates with the 5'-TCAAATTC-3' sequence in the PTGS2/COX-2 promoter and activates its

					transcription. Implicated in transcriptional activation of CDKN1A; the function involves STAT3 and SRC. Involved in the transcription of rRNA genes by RNA Pol I and enhances protein synthesis and cell growth.
SLAP	ESR1	p03372	Receptor	Estrogen receptor	Nuclear hormone receptor. The steroid hormones and their receptors are involved in the regulation of eukaryotic gene expression and affect cellular proliferation and differentiation in target tissues. Ligand-dependent nuclear transactivation involves either direct homodimer binding to a palindromic estrogen response element (ERE) sequence or association with other DNA-binding transcription factors, such as AP-1/c-Jun, c-Fos, ATF-2, Sp1 and Sp3, to mediate ERE-independent signaling. Ligand binding induces a conformational change allowing subsequent or combinatorial association with multiprotein coactivator complexes through LXXLL motifs of their respective components. Mutual transrepression occurs between the estrogen receptor (ER) and NF-kappa-B in a cell-type specific manner. Decreases NF-

	kappa-B DNA-binding activity and inhibits NF-kappa-B-mediated transcription from the IL6 promoter and displace RELA/p65 and associated coregulators from the promoter. Recruited to the NF-kappa-B response element of the CCL2 and IL8 promoters and can displace CREBBP. Present with NF-kappa-B components RELA/p65 and NFKB1/p50 on ERE sequences. Can also act synergistically with NF-kappa-B to activate transcription involving respective recruitment adjacent response elements; the function involves CREBBP. Can activate the transcriptional activity of TFF1. Also mediates membrane-initiated estrogen signaling involving various kinase cascades. Isoform 3 is involved in activation of NOS3 and endothelial nitric oxide production. Isoforms lacking one or several functional domains are thought to modulate transcriptional activity by competitive ligand or DNA binding and/or heterodimerization with the full length receptor. Essential for MTA1-mediated

					transcriptional regulation of BRCA1 and BCAS3. Isoform 3 can bind to ERE and inhibit isoform 1.
STITCH	FASLG	p48023	Immune functions	Tumor necrosis factor ligand superfamily member 6	Cytokine that binds to TNFRSF6/FAS, a receptor that transduces the apoptotic signal into cells. May be involved in cytotoxic T-cell mediated apoptosis and in T-cell development. TNFRSF6/FAS-mediated apoptosis may have a role in the induction of peripheral tolerance, in the antigen-stimulated suicide of mature T-cells, or both. Binding to the decoy receptor TNFRSF6B/DcR3 modulates its effects. The FasL intracellular domain (FasL ICD) cytoplasmic form induces gene transcription inhibition.
STITCH	FASN	p49327	Enzyme	Fatty acid synthase	Fatty acid synthetase catalyzes the formation of long-chain fatty acids from acetyl-CoA, malonyl-CoA and NADPH. This multifunctional protein has 7 catalytic activities and an acyl carrier protein.
SLAP	FGF1	p05230	Regulator	Fibroblast growth factor 1	Plays an important role in the regulation of cell survival, cell division, angiogenesis, cell differentiation and cell migration. Functions as potent mitogen in vitro.

SLAP	FGF2	p09038	Regulator	Fibroblast growth factor 2	Plays an important role in the regulation of cell survival, cell division, angiogenesis, cell differentiation and cell migration. Functions as potent mitogen in vitro.
STITCH	FMO3	p31513	Metabolism	Dimethylaniline monooxygenase [N-oxide-forming] 3	Involved in the oxidative metabolism of a variety of xenobiotics such as drugs and pesticides. It N-oxygenates primary aliphatic alkylamines as well as secondary and tertiary amines. Plays an important role in the metabolism of trimethylamine (TMA), via the production of TMA N-oxide (TMAO). Is also able to perform S-oxidation when acting on sulfide compounds.
SLAP	FPR1	p21462	Receptor	fMet-Leu-Phe receptor	High affinity receptor for N-formyl-methionyl peptides (fMLP), which are powerful neutrophil chemotactic factors (PubMed:2161213, PubMed:2176894, PubMed:10514456, PubMed:15153520). Binding of fMLP to the receptor stimulates intracellular calcium mobilization and superoxide anion release (PubMed:2161213, PubMed:1712023, PubMed:15153520). This response is mediated via a

					G-protein that activates a phosphatidylinositol-calcium second messenger system (PubMed:1712023, PubMed:10514456).
STITCH	G6PD	p11413	Enzyme	Glucose-6-phosphate 1-dehydrogenase	Catalyzes the rate-limiting step of the oxidative pentose-phosphate pathway, which represents a route for the dissimilation of carbohydrates besides glycolysis. The main function of this enzyme is to provide reducing power (NADPH) and pentose phosphates for fatty acid and nucleic acid synthesis.
STITCH	GDF15	q99988	Cytokine	Growth/differentiation factor 15	cytokine activity, transforming growth factor beta receptor binding
STITCH	GNAT3	a8mtj3		Guanine nucleotide-binding protein G(t) subunit alpha-3	Guanine nucleotide-binding protein (G protein) alpha subunit playing a prominent role in bitter and sweet taste transduction as well as in umami (monosodium glutamate, monopotassium glutamate, and inosine monophosphate) taste transduction. Transduction by this alpha subunit involves coupling of specific cell-surface receptors with a cGMP-phosphodiesterase; Activation of phosphodiesterase lowers intracellular levels of cAMP and cGMP which may open a cyclic

	nucleotide-suppressible cation channel leading to influx of calcium, ultimately leading to release of neurotransmitter. Indeed, denatonium and strychnine induce transient reduction in cAMP and cGMP in taste tissue, whereas this decrease is inhibited by GNAT3 antibody. Gustducin heterotrimer transduces response to bitter and sweet compounds via regulation of phosphodiesterase for alpha subunit, as well as via activation of phospholipase C for beta and gamma subunits, with ultimate increase inositol trisphosphate and increase of intracellular Calcium. GNAT3 can functionally couple to taste receptors to transmit intracellular signal: receptor heterodimer TAS1R2/TAS1R3 senses sweetness and TAS1R1/TAS1R3 transduces umami taste, whereas the T2R family GPCRs act as bitter sensors. Functions also as lumenal sugar sensors in the gut to control the expression of the Na+-glucose transporter SGLT1 in response to dietaty sugar, as well as the secretion of Glucagon-like peptide-1, GLP-1 and glucose-

					dependent insulinotropic polypeptide, GIP. Thus, may modulate the gut capacity to absorb sugars, with implications in malabsorption syndromes and diet-related disorders including diabetes and obesity.
STITCH	GNLY	p27749	Immune functions	Granulysin	Antimicrobial protein that kills intracellular pathogens. Active against a broad range of microbes, including Gram-positive and Gram-negative bacteria, fungi, and parasites. Kills Mycobacterium tuberculosis.
SLAP	GRIN2B	q13224	Receptor	Glutamate receptor ionotropic, NMDA 2B	NMDA receptor subtype of glutamate-gated ion channels with high calcium permeability and voltage-dependent sensitivity to magnesium. Mediated by glycine. In concert with DAPK1 at extrasynaptic sites, acts as a central mediator for stroke damage. Its phosphorylation at Ser-1303 by DAPK1 enhances synaptic NMDA receptor channel activity inducing injurious Ca2+ influx through them, resulting in an irreversible neuronal death (By similarity).
SLAP	GSTA1	p08263	Metabolism	Glutathione S-transferase A1	Conjugation of reduced glutathione to a wide number of exogenous and endogenous hydrophobic electrophiles.

Both	GSTM1	p09488	Metabolism	Glutathione S-transferase Mu 1	Conjugation of reduced glutathione to a wide number of exogenous and endogenous hydrophobic electrophiles.
SLAP	GSTP1	p09211	Metabolism	Glutathione S-transferase P	Conjugation of reduced glutathione to a wide number of exogenous and endogenous hydrophobic electrophiles. Regulates negatively CDK5 activity via p25/p35 translocation to prevent neurodegeneration.
STITCH	HDAC3	o15379	Enzyme	Histone deacetylase 3	Responsible for the deacetylation of lysine residues on the N-terminal part of the core histones (H2A, H2B, H3 and H4), and some other non-histone substrates. Histone deacetylation gives a tag for epigenetic repression and plays an important role in transcriptional regulation, cell cycle progression and developmental events. Histone deacetylases act via the formation of large multiprotein complexes. Participates in the BCL6 transcriptional repressor activity by deacetylating the H3 'Lys-27' (H3K27) on enhancer elements, antagonizing EP300 acetyltransferase activity and repressing proximal gene expression. Probably participates in the

					regulation of transcription through its binding to the zinc-finger transcription factor YY1; increases YY1 repression activity. Required to repress transcription of the POU1F1 transcription factor. Acts as a molecular chaperone for shuttling phosphorylated NR2C1 to PML bodies for sumoylation (PubMed:21444723, PubMed:23911289). Contributes, together with XBP1 isoform 1, to the activation of NFE2L2-mediated HMOX1 transcription factor gene expression in a PI_3K/mTORC2/Akt-dependent signaling pathway leading to endothelial cell (EC) survival under disturbed flow/oxidative stress
STITCH	HIF1A	q16665	Regulator	Hypoxia-inducible factor 1-alpha	Functions as a master transcriptional regulator of the adaptive response to hypoxia. Under hypoxic conditions, activates the transcription of over 40 genes, including erythropoietin, glucose transporters, glycolytic enzymes, vascular endothelial growth factor, HILPDA, and other genes whose protein products increase oxygen delivery or facilitate metabolic adaptation to hypoxia. Plays an essential

					role in embryonic vascularization, tumor angiogenesis and pathophysiology of ischemic disease. Binds to core DNA sequence 5'-[AG]CGTG-3' within the hypoxia response element (HRE) of target gene promoters. Activation requires recruitment of transcriptional coactivators such as CREBPB and EP300. Activity is enhanced by interaction with both, NCOA1 or NCOA2. Interaction with redox regulatory protein APEX seems to activate CTAD and potentiates activation by NCOA1 and CREBBP. Involved in the axonal distribution and transport of mitochondria in neurons during hypoxia.
STITCH	HLA-C	q29963	Immune functions	HLA class I histocompatibility antigen, Cw-6 alpha chain	Involved in the presentation of foreign antigens to the immune system.
STITCH	HMBS	p08397	Enzmye	Porphobilinogen deaminase	Tetrapolymerization of the monopyrrole PBG into the hydroxymethylbilane pre-uroporphyrinogen in several discrete steps.

SLAP	HNMT	p50135	Metabolism	Histamine N-methyltransferase	Inactivates histamine by N-methylation. Plays an important role in degrading histamine and in regulating the airway response to histamine.
STITCH	HPRT1	p00492	Enzmye	Hypoxanthine-guanine phosphoribosyltransferase	Converts guanine to guanosine monophosphate, and hypoxanthine to inosine monophosphate. Transfers the 5-phosphoribosyl group from 5-phosphoribosylpyrophosphate onto the purine. Plays a central role in the generation of purine nucleotides through the purine salvage pathway
SLAP	HRH1	p35367	Receptor	Histamine H1 receptor	In peripheral tissues, the H1 subclass of histamine receptors mediates the contraction of smooth muscles, increase in capillary permeability due to contraction of terminal venules, and catecholamine release from adrenal medulla, as well as mediating neurotransmission in the central nervous system.
SLAP	HRH2	p25021	Receptor	Histamine H2 receptor	The H2 subclass of histamine receptors mediates gastric acid secretion. Also appears to regulate gastrointestinal motility and intestinal secretion. Possible role in regulating cell growth and differentiation. The activity of this receptor is

					mediated by G proteins which activate adenylyl cyclase and, through a separate G protein-dependent mechanism, the phosphoinositide/protein kinase (PKC) signaling pathway (By similarity).
SLAP	HRH3	q9y5n1	Receptor	Histamine H3 receptor	The H3 subclass of histamine receptors could mediate the histamine signals in CNS and peripheral nervous system. Signals through the inhibition of adenylate cyclase and displays high constitutive activity (spontaneous activity in the absence of agonist). Agonist stimulation of isoform 3 neither modified adenylate cyclase activity nor induced intracellular calcium mobilization.
SLAP	HRH4	q9h3n8	Receptor	Histamine H4 receptor	The H4 subclass of histamine receptors could mediate the histamine signals in peripheral tissues. Displays a significant level of constitutive activity (spontaneous activity in the absence of agonist).
STITCH	HSD3B2	p26439	Enzmye	3 beta-hydroxysteroid dehydrogenase/Delta 5-->4-isomerase type 2	3-beta-HSD is a bifunctional enzyme, that catalyzes the oxidative conversion of Delta(5)-ene-3-beta-hydroxy steroid, and the oxidative conversion of ketosteroids. The 3-beta-HSD enzymatic system plays

					a crucial role in the biosynthesis of all classes of hormonal steroids.
STITCH	HSPA5	p11021	Structural	78 kDa glucose-regulated protein	Probably plays a role in facilitating the assembly of multimeric protein complexes inside the endoplasmic reticulum. Involved in the correct folding of proteins and degradation of misfolded proteins via its interaction with DNAJC10, probably to facilitate the release of DNAJC10 from its substrate.
SLAP	HTR1A	p08908	Receptor	5-hydroxytryptamine receptor 1A	G-protein coupled receptor for 5-hydroxytryptamine (serotonin). Also functions as a receptor for various drugs and psychoactive substances. Ligand binding causes a conformation change that triggers signaling via guanine nucleotide-binding proteins (G proteins) and modulates the activity of down-stream effectors, such as adenylate cyclase. Beta-arrestin family members inhibit signaling via G proteins and mediate activation of alternative signaling pathways. Signaling inhibits adenylate cyclase activity and activates a phosphatidylinositol-calcium second messenger system that regulates the release of Ca^{2+} ions from

					intracellular stores. Plays a role in the regulation of 5-hydroxytryptamine release and in the regulation of dopamine and 5-hydroxytryptamine metabolism. Plays a role in the regulation of dopamine and 5-hydroxytryptamine levels in the brain, and thereby affects neural activity, mood and behavior. Plays a role in the response to anxiogenic stimuli.
SLAP	HTR1B	p28222	Receptor	5-hydroxytryptamine receptor 1B	G-protein coupled receptor for 5-hydroxytryptamine (serotonin). Also functions as a receptor for ergot alkaloid derivatives, various anxiolytic and antidepressant drugs and other psychoactive substances, such as lysergic acid diethylamide (LSD). Ligand binding causes a conformation change that triggers signaling via guanine nucleotide-binding proteins (G proteins) and modulates the activity of down-stream effectors, such as adenylate cyclase. Signaling inhibits adenylate cyclase activity. Arrestin family members inhibit signaling via G proteins and mediate activation of alternative signaling pathways. Regulates the release of 5-hydroxytryptamine,

					dopamine and acetylcholine in the brain, and thereby affects neural activity, nociceptive processing, pain perception, mood and behavior. Besides, plays a role in vasoconstriction of cerebral arteries.
SLAP	HTR1D	p28221	Receptor	5-hydroxytryptamine receptor 1D	G-protein coupled receptor for 5-hydroxytryptamine (serotonin). Also functions as a receptor for ergot alkaloid derivatives, various anxiolytic and antidepressant drugs and other psychoactive substances. Ligand binding causes a conformation change that triggers signaling via guanine nucleotide-binding proteins (G proteins) and modulates the activity of down-stream effectors, such as adenylate cyclase. Signaling inhibits adenylate cyclase activity. Regulates the release of 5-hydroxytryptamine in the brain, and thereby affects neural activity. May also play a role in regulating the release of other neurotransmitters. May play a role in vasoconstriction.
SLAP	HTR1E	p28566	Receptor	5-hydroxytryptamine receptor 1E	G-protein coupled receptor for 5-hydroxytryptamine (serotonin). Also functions as a receptor for various

					alkaloids and psychoactive substances. Ligand binding causes a conformation change that triggers signaling via guanine nucleotide-binding proteins (G proteins) and modulates the activity of down-stream effectors, such as adenylate cyclase. Signaling inhibits adenylate cyclase activity.
SLAP	HTR1F	p30939	Receptor	5-hydroxytryptamine receptor 1F	G-protein coupled receptor for 5-hydroxytryptamine (serotonin). Also functions as a receptor for various alkaloids and psychoactive substances. Ligand binding causes a conformation change that triggers signaling via guanine nucleotide-binding proteins (G proteins) and modulates the activity of down-stream effectors, such as adenylate cyclase. Signaling inhibits adenylate cyclase activity.
SLAP	HTR2A	p28223	Receptor	5-hydroxytryptamine receptor 2A	G-protein coupled receptor for 5-hydroxytryptamine (serotonin). Also functions as a receptor for various drugs and psychoactive substances, including mescaline, psilocybin, 1-(2,5-dimethoxy-4-iodophenyl)-2-aminopropane (DOI) and lysergic acid diethylamide (LSD). Ligand binding causes a

					conformation change that triggers signaling via guanine nucleotide-binding proteins (G proteins) and modulates the activity of down-stream effectors. Beta-arrestin family members inhibit signaling via G proteins and mediate activation of alternative signaling pathways. Signaling activates phospholipase C and a phosphatidylinositol-calcium second messenger system that modulates the activity of phosphatidylinositol 3-kinase and promotes the release of Ca^{2+} ions from intracellular stores. Affects neural activity, perception, cognition and mood. Plays a role in the regulation of behavior, including responses to anxiogenic situations and psychoactive substances. Plays a role in intestinal smooth muscle contraction, and may play a role in arterial vasoconstriction.
SLAP	HTR2B	p41595	Receptor	5-hydroxytryptamine receptor 2B	G-protein coupled receptor for 5-hydroxytryptamine (serotonin). Also functions as a receptor for various ergot alkaloid derivatives and psychoactive substances. Ligand binding causes a conformation

change that triggers signaling via guanine nucleotide-binding proteins (G proteins) and modulates the activity of down-stream effectors. Beta-arrestin family members inhibit signaling via G proteins and mediate activation of alternative signaling pathways. Signaling activates a phosphatidylinositol-calcium second messenger system that modulates the activity of phosphatidylinositol 3-kinase and down-stream signaling cascades and promotes the release of Ca^{2+} ions from intracellular stores. Plays a role in the regulation of dopamine and 5-hydroxytryptamine release, 5-hydroxytryptamine uptake and in the regulation of extracellular dopamine and 5-hydroxytryptamine levels, and thereby affects neural activity. May play a role in the perception of pain. Plays a role in the regulation of behavior, including impulsive behavior. Required for normal proliferation of embryonic cardiac myocytes and normal heart development. Protects cardiomyocytes against apoptosis. Plays a role in the adaptation of pulmonary

					arteries to chronic hypoxia. Plays a role in vasoconstriction. Required for normal osteoblast function and proliferation, and for maintaining normal bone density. Required for normal proliferation of the interstitial cells of Cajal in the intestine.
SLAP	HTR2C	p28335	Receptor	5-hydroxytryptamine receptor 2C	G-protein coupled receptor for 5-hydroxytryptamine (serotonin). Also functions as a receptor for various drugs and psychoactive substances, including ergot alkaloid derivatives, 1-2,5,-dimethoxy-4-iodophenyl-2-aminopropane (DOI) and lysergic acid diethylamide (LSD). Ligand binding causes a conformation change that triggers signaling via guanine nucleotide-binding proteins (G proteins) and modulates the activity of down-stream effectors. Beta-arrestin family members inhibit signaling via G proteins and mediate activation of alternative signaling pathways. Signaling activates a phosphatidylinositol-calcium second messenger system that modulates the activity of phosphatidylinositol 3-kinase and down-stream signaling cascades and promotes the release of Ca^{2+}

					ions from intracellular stores. Regulates neuronal activity via the activation of short transient receptor potential calcium channels in the brain, and thereby modulates the activation of pro-opiomelacortin neurons and the release of CRH that then regulates the release of corticosterone. Plays a role in the regulation of appetite and eating behavior, responses to anxiogenic stimuli and stress. Plays a role in insulin sensitivity and glucose homeostasis.
SLAP	HTR3A	p46098	Receptor	5-hydroxytryptamine receptor 3A	This is one of the several different receptors for 5-hydroxytryptamine (serotonin), a biogenic hormone that functions as a neurotransmitter, a hormone, and a mitogen. This receptor is a ligand-gated ion channel, which when activated causes fast, depolarizing responses in neurons. It is a cation-specific, but otherwise relatively nonselective, ion channel.
SLAP	HTR4	q13639	Receptor	5-hydroxytryptamine receptor 4	This is one of the several different receptors for 5-hydroxytryptamine (serotonin), a biogenic hormone that functions as a neurotransmitter, a hormone, and

					a mitogen. The activity of this receptor is mediated by G proteins that stimulate adenylate cyclase.
SLAP	HTR6	p50406	Receptor	5-hydroxytryptamine receptor 6	This is one of the several different receptors for 5-hydroxytryptamine (serotonin), a biogenic hormone that functions as a neurotransmitter, a hormone, and a mitogen. The activity of this receptor is mediated by G proteins that stimulate adenylate cyclase. It has a high affinity for tricyclic psychotropic drugs (By similarity). Controls pyramidal neurons migration during corticogenesis, through the regulation of CDK5 activity (By similarity). Is an activator of TOR signaling
SLAP	HTR7	p34969	Receptor	5-hydroxytryptamine receptor 7	This is one of the several different receptors for 5-hydroxytryptamine (serotonin), a biogenic hormone that functions as a neurotransmitter, a hormone, and a mitogen. The activity of this receptor is mediated by G proteins that stimulate adenylate cyclase.
STITCH	ICAM1	p05362	Structural	Intercellular adhesion molecule 1	ICAM proteins are ligands for the leukocyte adhesion protein LFA-1 (integrin alpha-L/beta-2). During leukocyte trans-endothelial migration, ICAM1 engagement promotes the assembly of endothelial

					apical cups through ARHGEF26/SGEF and RHOG activation. In case of rhinovirus infection acts as a cellular receptor for the virus.
STITCH	IDO1	p14902	Enzyme	Indoleamine 2,3-dioxygenase 1	Catalyzes the cleavage of the pyrrol ring of tryptophan and incorporates both atoms of a molecule of oxygen.
STITCH	IGF1R	p08069	Kinase	Insulin-like growth factor 1 receptor	Receptor tyrosine kinase which mediates actions of insulin-like growth factor 1 (IGF1). Binds IGF1 with high affinity and IGF2 and insulin (INS) with a lower affinity. The activated IGF1R is involved in cell growth and survival control. IGF1R is crucial for tumor transformation and survival of malignant cell. Ligand binding activates the receptor kinase, leading to receptor autophosphorylation, and tyrosines phosphorylation of multiple substrates, that function as signaling adapter proteins including, the insulin-receptor substrates (IRS1/2), Shc and 14-3-3 proteins. Phosphorylation of IRSs proteins lead to the activation of two main signaling pathways: the PI3K-AKT/PKB pathway and the Ras-MAPK pathway. The result of activating the MAPK pathway is increased cellular

proliferation, whereas activating the PI3K pathway inhibits apoptosis and stimulates protein synthesis. Phosphorylated IRS1 can activate the 85 kDa regulatory subunit of PI3K (PIK3R1), leading to activation of several downstream substrates, including protein AKT/PKB. AKT phosphorylation, in turn, enhances protein synthesis through mTOR activation and triggers the antiapoptotic effects of IGFIR through phosphorylation and inactivation of BAD. In parallel to PI3K-driven signaling, recruitment of Grb2/SOS by phosphorylated IRS1 or Shc leads to recruitment of Ras and activation of the ras-MAPK pathway. In addition to these two main signaling pathways IGF1R signals also through the Janus kinase/signal transducer and activator of transcription pathway (JAK/STAT). Phosphorylation of JAK proteins can lead to phosphorylation/activation of signal transducers and activators of transcription (STAT) proteins. In particular activation of STAT3, may be essential for the transforming activity of IGF1R. The

	JAK/STAT pathway activates gene transcription and may be responsible for the transforming activity. JNK kinases can also be activated by the IGF1R. IGF1 exerts inhibiting activities on JNK activation via phosphorylation and inhibition of MAP3K5/ASK1, which is able to directly associate with the IGF1R. When present in a hybrid receptor with INSR, binds IGF1. PubMed:12138094 shows that hybrid receptors composed of IGF1R and INSR isoform Long are activated with a high affinity by IGF1, with low affinity by IGF2 and not significantly activated by insulin, and that hybrid receptors composed of IGF1R and INSR isoform Short are activated by IGF1, IGF2 and insulin. In contrast, PubMed:16831875 shows that hybrid receptors composed of IGF1R and INSR isoform Long and hybrid receptors composed of IGF1R and INSR isoform Short have similar binding characteristics, both bind IGF1 and have a low affinity for insulin.

STITCH	IKBKB	o14920	Kinase	Inhibitor of nuclear factor kappa-B kinase subunit beta	Serine kinase that plays an essential role in the NF-kappa-B signaling pathway which is activated by multiple stimuli such as inflammatory cytokines, bacterial or viral products, DNA damages or other cellular stresses. Acts as part of the canonical IKK complex in the conventional pathway of NF-kappa-B activation and phosphorylates inhibitors of NF-kappa-B on 2 critical serine residues. These modifications allow polyubiquitination of the inhibitors and subsequent degradation by the proteasome. In turn, free NF-kappa-B is translocated into the nucleus and activates the transcription of hundreds of genes involved in immune response, growth control, or protection against apoptosis. In addition to the NF-kappa-B inhibitors, phosphorylates several other components of the signaling pathway including NEMO/IKBKG, NF-kappa-B subunits RELA and NFKB1, as well as IKK-related kinases TBK1 and IKBKE. IKK-related kinase phosphorylations may prevent the overproduction of inflammatory mediators since they

					exert a negative regulation on canonical IKKs. Also phosphorylates other substrates including NCOA3, BCL10 and IRS1. Within the nucleus, acts as an adapter protein for NFKBIA degradation in UV-induced NF-kappa-B activation.
STITCH	IL10	p22301	Immune functions	Interleukin-10	Inhibits the synthesis of a number of cytokines, including IFN-gamma, IL-2, IL-3, TNF and GM-CSF produced by activated macrophages and by helper T-cells.
STITCH	IL1A	p01583	Immune functions	Interleukin-1 alpha	Produced by activated macrophages, IL-1 stimulates thymocyte proliferation by inducing IL-2 release, B-cell maturation and proliferation, and fibroblast growth factor activity. IL-1 proteins are involved in the inflammatory response, being identified as endogenous pyrogens, and are reported to stimulate the release of prostaglandin and collagenase from synovial cells.
Both	IL1B	p01584	Immune functions	Interleukin-1 beta	Produced by activated macrophages, IL-1 stimulates thymocyte proliferation by inducing IL-2 release, B-cell maturation and proliferation, and fibroblast

					growth factor activity. IL-1 proteins are involved in the inflammatory response, being identified as endogenous pyrogens, and are reported to stimulate the release of prostaglandin and collagenase from synovial cells.
STITCH	IL6	p05231	Immune functions	Interleukin-6	Cytokine with a wide variety of biological functions. It is a potent inducer of the acute phase response. Plays an essential role in the final differentiation of B-cells into Ig-secreting cells Involved in lymphocyte and monocyte differentiation. Acts on B-cells, T-cells, hepatocytes, hematopoietic progenitor cells and cells of the CNS. Required for the generation of T(H)17 cells. Also acts as a myokine. It is discharged into the bloodstream after muscle contraction and acts to increase the breakdown of fats and to improve insulin resistance. It induces myeloma and plasmacytoma growth and induces nerve cells differentiation.
STITCH	ILK	q13418	Kinase	Integrin-linked protein kinase	Receptor-proximal protein kinase regulating integrin-mediated signal transduction. May act as a mediator of inside-out integrin signaling. Focal adhesion protein

					part of the complex ILK-PINCH. This complex is considered to be one of the convergence points of integrin- and growth factor-signaling pathway. Could be implicated in mediating cell architecture, adhesion to integrin substrates and anchorage-dependent growth in epithelial cells. Phosphorylates beta-1 and beta-3 integrin subunit on serine and threonine residues, but also AKT1 and GSK3B.
STITCH	IMPA1	p29218	Enzyme	Inositol monophosphatase 1	Responsible for the provision of inositol required for synthesis of phosphatidylinositol and polyphosphoinositides and has been implicated as the pharmacological target for lithium action in brain. Has broad substrate specificity and can use myo-inositol monophosphates, myo-inositol 1,3-diphosphate, myo-inositol 1,4-diphosphate, scyllo-inositol-phosphate, D-galactose 1-phosphate, glucose-1-phosphate, glucose-6-phosphate, fructose-1-phosphate, beta-glycerophosphate, and 2'-AMP as substrates.
STITCH	INS	p01308	Hormone	Insulin	Insulin decreases blood glucose concentration. It increases cell permeability to monosaccharides,

					amino acids and fatty acids. It accelerates glycolysis, the pentose phosphate cycle, and glycogen synthesis in liver.
STITCH	ITGA2	p17301	Receptor	Integrin alpha-2	Integrin alpha-2/beta-1 is a receptor for laminin, collagen, collagen C-propeptides, fibronectin and E-cadherin. It recognizes the proline-hydroxylated sequence G-F-P-G-E-R in collagen. It is responsible for adhesion of platelets and other cells to collagens, modulation of collagen and collagenase gene expression, force generation and organization of newly synthesized extracellular matrix.
Both	JUN	p05412	Regulator	Transcription factor AP-1	Transcription factor that recognizes and binds to the enhancer heptamer motif 5'-TGA[CG]TCA-3'. Promotes activity of NR5A1 when phosphorylated by HIPK3 leading to increased steroidogenic gene expression upon cAMP signaling pathway stimulation.
STITCH	KCNA5	p22460	Ion channel	Potassium voltage-gated channel subfamily A member 5	Voltage-gated potassium channel that mediates transmembrane potassium transport in excitable membranes. Forms tetrameric potassium-selective channels through which potassium ions pass in

	accordance with their electrochemical gradient. The channel alternates between opened and closed conformations in response to the voltage difference across the membrane. Can form functional homotetrameric channels and heterotetrameric channels that contain variable proportions of KCNA1, KCNA2, KCNA4, KCNA5, and possibly other family members as well; channel properties depend on the type of alpha subunits that are part of the channel (PubMed:12130714). Channel properties are modulated by cytoplasmic beta subunits that regulate the subcellular location of the alpha subunits and promote rapid inactivation (PubMed:12130714). Homotetrameric channels display rapid activation and slow inactivation (PubMed:8505626, PubMed:12130714). May play a role in regulating the secretion of insulin in normal pancreatic islets. Isoform 2 exhibits a voltage-dependent recovery from inactivation and an excessive cumulative inactivation (PubMed:11524461).

Both	KCNH2	q12809	Ion channel	Potassium voltage-gated channel subfamily H member 2	Pore-forming (alpha) subunit of voltage-gated inwardly rectifying potassium channel. Channel properties are modulated by cAMP and subunit assembly. Mediates the rapidly activating component of the delayed rectifying potassium current in heart (IKr). Isoforms USO have no channel activity by themself, but modulates channel characteristics by forming heterotetramers with other isoforms which are retained intracellularly and undergo ubiquitin-dependent degradation.
STITCH	KCNK18	q7z418	Ion channel	Potassium channel subfamily K member 18	Outward rectifying potassium channel. Produces rapidly activating outward rectifier K^+ currents. May function as background potassium channel that sets the resting membrane potential. Channel activity is directly activated by calcium signal. Activated by the G(q)-protein coupled receptor pathway. The calcium signal robustly activates the channel via calcineurin, whereas the anchoring of 14-3-3/YWHAH interferes with the return of the current to the resting state after activation. Inhibited also by arachidonic acid and

					other naturally occurring unsaturated free fatty acids. Channel activity is also enhanced by volatile anesthetics, such as isoflurane. Appears to be the primary target of hydroxy-alpha-sanshool, an ingredient of Schezuan pepper. May be involved in the somatosensory function with special respect to pain sensation (By similarity)
SLAP	KCNMA1	q12791	Ion channel	Calcium-activated potassium channel subunit alpha-1	Potassium channel activated by both membrane depolarization or increase in cytosolic Ca^{2+} that mediates export of K^{+}. It is also activated by the concentration of cytosolic Mg^{2+}. Its activation dampens the excitatory events that elevate the cytosolic Ca^{2+} concentration and/or depolarize the cell membrane. It therefore contributes to repolarization of the membrane potential. Plays a key role in controlling excitability in a number of systems, such as regulation of the contraction of smooth muscle, the tuning of hair cells in the cochlea, regulation of transmitter release, and innate immunity. In smooth muscles, its activation by high level of Ca^{2+}, caused by

					ryanodine receptors in the sarcoplasmic reticulum, regulates the membrane potential. In cochlea cells, its number and kinetic properties partly determine the characteristic frequency of each hair cell and thereby helps to establish a tonotopic map. Kinetics of KCNMA1 channels are determined by alternative splicing, phosphorylation status and its combination with modulating beta subunits. Highly sensitive to both iberiotoxin (IbTx) and charybdotoxin (CTX).
SLAP	KCNQ1	p51787	Ion channel	Potassium voltage-gated channel subfamily KQT member 1	Probably important in cardiac repolarization. Associates with KCNE1 (MinK) to form the I(Ks) cardiac potassium current. Elicits a rapidly activating, potassium-selective outward current. Muscarinic agonist oxotremorine-M strongly suppresses KCNQ1/KCNE1 current in CHO cells in which cloned KCNQ1/KCNE1 channels were coexpressed with M1 muscarinic receptors. May associate also with KCNE3 (MiRP2) to form the potassium channel that is important for cyclic AMP-stimulated intestinal secretion of chloride ions, which is reduced in cystic

					fibrosis and pathologically stimulated in cholera and other forms of secretory diarrhea.
STITCH	LEF1	q9uju2	Regulator	Lymphoid enhancer-binding factor 1	Participates in the Wnt signaling pathway. Activates transcription of target genes in the presence of CTNNB1 and EP300. May play a role in hair cell differentiation and follicle morphogenesis. TLE1, TLE2, TLE3 and TLE4 repress transactivation mediated by LEF1 and CTNNB1. Regulates T-cell receptor alpha enhancer function. Binds DNA in a sequence-specific manner. PIAG antagonizes both Wnt-dependent and Wnt-independent activation by LEF1 (By similarity). Isoform 3 lacks the CTNNB1 interaction domain and may be an antagonist for Wnt signaling. Isoform 5 transcriptionally activates the fibronectin promoter, binds to and represses transcription from the E-cadherin promoter in a CTNNB1-independent manner, and is involved in reducing cellular aggregation and increasing cell migration of pancreatic cancer cells. Isoform 1 transcriptionally

					activates MYC and CCND1 expression and enhances proliferation of pancreatic tumor cells.
SLAP	MAOA	p21397	Enzyme	Amine oxidase [flavin-containing] A	Catalyzes the oxidative deamination of biogenic and xenobiotic amines and has important functions in the metabolism of neuroactive and vasoactive amines in the central nervous system and peripheral tissues. MAOA preferentially oxidizes biogenic amines such as 5-hydroxytryptamine (5-HT), norepinephrine and epinephrine.
Both	MAPK1	p28482	Kinase	Mitogen-activated protein kinase 1	Serine/threonine kinase which acts as an essential component of the MAP kinase signal transduction pathway. MAPK1/ERK2 and MAPK3/ERK1 are the 2 MAPKs which play an important role in the MAPK/ERK cascade. They participate also in a signaling cascade initiated by activated KIT and KITLG/SCF. Depending on the cellular context, the MAPK/ERK cascade mediates diverse biological functions such as cell growth, adhesion, survival and differentiation through the regulation of transcription, translation, cytoskeletal rearrangements. The MAPK/ERK cascade

	plays also a role in initiation and regulation of meiosis, mitosis, and postmitotic functions in differentiated cells by phosphorylating a number of transcription factors. About 160 substrates have already been discovered for ERKs. Many of these substrates are localized in the nucleus, and seem to participate in the regulation of transcription upon stimulation. However, other substrates are found in the cytosol as well as in other cellular organelles, and those are responsible for processes such as translation, mitosis and apoptosis. Moreover, the MAPK/ERK cascade is also involved in the regulation of the endosomal dynamics, including lysosome processing and endosome cycling through the perinuclear recycling compartment (PNRC); as well as in the fragmentation of the Golgi apparatus during mitosis. The substrates include transcription factors (such as ATF2, BCL6, ELK1, ERF, FOS, HSF4 or SPZ1), cytoskeletal elements (such as CANX, CTTN, GJA1, MAP2, MAPT, PXN, SORBS3 or STMN1), regulators of apoptosis (such as

	BAD, BTG2, CASP9, DAPK1, IER3, MCL1 or PPARG), regulators of translation (such as EIF4EBP1) and a variety of other signaling-related molecules (like ARHGEF2, DCC, FRS2 or GRB10). Protein kinases (such as RAF1, RPS6KA1/RSK1, RPS6KA3/RSK2, RPS6KA2/RSK3, RPS6KA6/RSK4, SYK, MKNK1/MNK1, MKNK2/MNK2, RPS6KA5/MSK1, RPS6KA4/MSK2, MAPKAPK3 or MAPKAPK5) and phosphatases (such as DUSP1, DUSP4, DUSP6 or DUSP16) are other substrates which enable the propagation the MAPK/ERK signal to additional cytosolic and nuclear targets, thereby extending the specificity of the cascade. Mediates phosphorylation of TPR in respons to EGF stimulation. May play a role in the spindle assembly checkpoint. Phosphorylates PML and promotes its interaction with PIN1, leading to PML degradation. Acts as a transcriptional repressor. Binds to a [GC]AAA[GC] consensus sequence. Repress the expression of interferon gamma-induced genes.

					Seems to bind to the promoter of CCL5, DMP1, IFIH1, IFITM1, IRF7, IRF9, LAMP3, OAS1, OAS2, OAS3 and STAT1. Transcriptional activity is independent of kinase activity.
SLAP	MAPK12	p53778	Kinase	Mitogen-activated protein kinase 12	Serine/threonine kinase which acts as an essential component of the MAP kinase signal transduction pathway. MAPK12 is one of the four p38 MAPKs which play an important role in the cascades of cellular responses evoked by extracellular stimuli such as proinflammatory cytokines or physical stress leading to direct activation of transcription factors such as ELK1 and ATF2. Accordingly, p38 MAPKs phosphorylate a broad range of proteins and it has been estimated that they may have approximately 200 to 300 substrates each. Some of the targets are downstream kinases such as MAPKAPK2, which are activated through phosphorylation and further phosphorylate additional targets. Plays a role in myoblast differentiation and also in the down-regulation of cyclin D1 in response to hypoxia in

	adrenal cells suggesting MAPK12 may inhibit cell proliferation while promoting differentiation. Phosphorylates DLG1. Following osmotic shock, MAPK12 in the cell nucleus increases its association with nuclear DLG1, thereby causing dissociation of DLG1-SFPQ complexes. This function is independent of its catalytic activity and could affect mRNA processing and/or gene transcription to aid cell adaptation to osmolarity changes in the environment. Regulates UV-induced checkpoint signaling and repair of UV-induced DNA damage and G2 arrest after gamma-radiation exposure. MAPK12 is involved in the regulation of SLC2A1 expression and basal glucose uptake in L6 myotubes; and negatively regulates SLC2A4 expression and contraction-mediated glucose uptake in adult skeletal muscle. C-Jun (JUN) phosphorylation is stimulated by MAPK14 and inhibited by MAPK12, leading to a distinct AP-1 regulation. MAPK12 is required for the normal kinetochore localization of PLK1, prevents

					chromosomal instability and supports mitotic cell viability. MAPK12-signaling is also positively regulating the expansion of transient amplifying myogenic precursor cells during muscle growth and regeneration.
Both	MAPK14	q16539	Kinase	Mitogen-activated protein kinase 14	Serine/threonine kinase which acts as an essential component of the MAP kinase signal transduction pathway. MAPK14 is one of the four p38 MAPKs which play an important role in the cascades of cellular responses evoked by extracellular stimuli such as proinflammatory cytokines or physical stress leading to direct activation of transcription factors. Accordingly, p38 MAPKs phosphorylate a broad range of proteins and it has been estimated that they may have approximately 200 to 300 substrates each. Some of the targets are downstream kinases which are activated through phosphorylation and further phosphorylate additional targets. RPS6KA5/MSK1 and RPS6KA4/MSK2 can directly phosphorylate and activate transcription factors such as CREB1, ATF1, the

NF-kappa-B isoform RELA/NFKB3, STAT1 and STAT3, but can also phosphorylate histone H3 and the nucleosomal protein HMGN1. RPS6KA5/MSK1 and RPS6KA4/MSK2 play important roles in the rapid induction of immediate-early genes in response to stress or mitogenic stimuli, either by inducing chromatin remodeling or by recruiting the transcription machinery. On the other hand, two other kinase targets, MAPKAPK2/MK2 and MAPKAPK3/MK3, participate in the control of gene expression mostly at the post-transcriptional level, by phosphorylating ZFP36 (tristetraprolin) and ELAVL1, and by regulating EEF2K, which is important for the elongation of mRNA during translation. MKNK1/MNK1 and MKNK2/MNK2, two other kinases activated by p38 MAPKs, regulate protein synthesis by phosphorylating the initiation factor EIF4E2. MAPK14 interacts also with casein kinase II, leading to its activation through autophosphorylation and further phosphorylation of TP53/p53. In the cytoplasm, the

p38 MAPK pathway is an important regulator of protein turnover. For example, CFLAR is an inhibitor of TNF-induced apoptosis whose proteasome-mediated degradation is regulated by p38 MAPK phosphorylation. In a similar way, MAPK14 phosphorylates the ubiquitin ligase SIAH2, regulating its activity towards EGLN3. MAPK14 may also inhibit the lysosomal degradation pathway of autophagy by interfering with the intracellular trafficking of the transmembrane protein ATG9. Another function of MAPK14 is to regulate the endocytosis of membrane receptors by different mechanisms that impinge on the small GTPase RAB5A. In addition, clathrin-mediated EGFR internalization induced by inflammatory cytokines and UV irradiation depends on MAPK14-mediated phosphorylation of EGFR itself as well as of RAB5A effectors. Ectodomain shedding of transmembrane proteins is regulated by p38 MAPKs as well. In response to inflammatory stimuli, p38 MAPKs phosphorylate the membrane-associated

metalloprotease ADAM17. Such phosphorylation is required for ADAM17-mediated ectodomain shedding of TGF-alpha family ligands, which results in the activation of EGFR signaling and cell proliferation. Another p38 MAPK substrate is FGFR1. FGFR1 can be translocated from the extracellular space into the cytosol and nucleus of target cells, and regulates processes such as rRNA synthesis and cell growth. FGFR1 translocation requires p38 MAPK activation. In the nucleus, many transcription factors are phosphorylated and activated by p38 MAPKs in response to different stimuli. Classical examples include ATF1, ATF2, ATF6, ELK1, PTPRH, DDIT3, TP53/p53 and MEF2C and MEF2A. The p38 MAPKs are emerging as important modulators of gene expression by regulating chromatin modifiers and remodelers. The promoters of several genes involved in the inflammatory response, such as IL6, IL8 and IL12B, display a p38 MAPK-dependent enrichment of histone H3 phosphorylation on 'Ser-10' (H3S10ph) in LPS-

	stimulated myeloid cells. This phosphorylation enhances the accessibility of the cryptic NF-kappa-B-binding sites marking promoters for increased NF-kappa-B recruitment. Phosphorylates CDC25B and CDC25C which is required for binding to 14-3-3 proteins and leads to initiation of a G2 delay after ultraviolet radiation. Phosphorylates TIAR following DNA damage, releasing TIAR from GADD45A mRNA and preventing mRNA degradation. The p38 MAPKs may also have kinase-independent roles, which are thought to be due to the binding to targets in the absence of phosphorylation. Protein O-Glc-N-acylation catalyzed by the OGT is regulated by MAPK14, and, although OGT does not seem to be phosphorylated by MAPK14, their interaction increases upon MAPK14 activation induced by glucose deprivation. This interaction may regulate OGT activity by recruiting it to specific targets such as neurofilament H, stimulating its O-Glc-N-acylation. Required in mid-fetal development for the growth of

					embryo-derived blood vessels in the labyrinth layer of the placenta. Also plays an essential role in developmental and stress-induced erythropoiesis, through regulation of EPO gene expression. Isoform MXI2 activation is stimulated by mitogens and oxidative stress and only poorly phosphorylates ELK1 and ATF2. Isoform EXIP may play a role in the early onset of apoptosis. Phosphorylates S100A9 at 'Thr-113'.
SLAP	MAPK14	q16539	Kinase	Mitogen-activated protein kinase 14	Serine/threonine kinase which acts as an essential component of the MAP kinase signal transduction pathway. MAPK14 is one of the four p38 MAPKs which play an important role in the cascades of cellular responses evoked by extracellular stimuli such as proinflammatory cytokines or physical stress leading to direct activation of transcription factors. Accordingly, p38 MAPKs phosphorylate a broad range of proteins and it has been estimated that they may have approximately 200 to 300 substrates each. Some of the targets are downstream kinases which are

	activated through phosphorylation and further phosphorylate additional targets. RPS6KA5/MSK1 and RPS6KA4/MSK2 can directly phosphorylate and activate transcription factors such as CREB1, ATF1, the NF-kappa-B isoform RELA/NFKB3, STAT1 and STAT3, but can also phosphorylate histone H3 and the nucleosomal protein HMGN1. RPS6KA5/MSK1 and RPS6KA4/MSK2 play important roles in the rapid induction of immediate-early genes in response to stress or mitogenic stimuli, either by inducing chromatin remodeling or by recruiting the transcription machinery. On the other hand, two other kinase targets, MAPKAPK2/MK2 and MAPKAPK3/MK3, participate in the control of gene expression mostly at the post-transcriptional level, by phosphorylating ZFP36 (tristetraprolin) and ELAVL1, and by regulating EEF2K, which is important for the elongation of mRNA during translation. MKNK1/MNK1 and MKNK2/MNK2, two other kinases activated by p38 MAPKs, regulate protein synthesis by

phosphorylating the initiation factor EIF4E2. MAPK14 interacts also with casein kinase II, leading to its activation through autophosphorylation and further phosphorylation of TP53/p53. In the cytoplasm, the p38 MAPK pathway is an important regulator of protein turnover. For example, CFLAR is an inhibitor of TNF-induced apoptosis whose proteasome-mediated degradation is regulated by p38 MAPK phosphorylation. In a similar way, MAPK14 phosphorylates the ubiquitin ligase SIAH2, regulating its activity towards EGLN3. MAPK14 may also inhibit the lysosomal degradation pathway of autophagy by interfering with the intracellular trafficking of the transmembrane protein ATG9. Another function of MAPK14 is to regulate the endocytosis of membrane receptors by different mechanisms that impinge on the small GTPase RAB5A. In addition, clathrin-mediated EGFR internalization induced by inflammatory cytokines and UV irradiation depends on MAPK14-mediated phosphorylation of EGFR itself

	as well as of RAB5A effectors. Ectodomain shedding of transmembrane proteins is regulated by p38 MAPKs as well. In response to inflammatory stimuli, p38 MAPKs phosphorylate the membrane-associated metalloprotease ADAM17. Such phosphorylation is required for ADAM17-mediated ectodomain shedding of TGF-alpha family ligands, which results in the activation of EGFR signaling and cell proliferation. Another p38 MAPK substrate is FGFR1. FGFR1 can be translocated from the extracellular space into the cytosol and nucleus of target cells, and regulates processes such as rRNA synthesis and cell growth. FGFR1 translocation requires p38 MAPK activation. In the nucleus, many transcription factors are phosphorylated and activated by p38 MAPKs in response to different stimuli. Classical examples include ATF1, ATF2, ATF6, ELK1, PTPRH, DDIT3, TP53/p53 and MEF2C and MEF2A. The p38 MAPKs are emerging as important modulators of gene expression by regulating chromatin modifiers and remodelers.

	The promoters of several genes involved in the inflammatory response, such as IL6, IL8 and IL12B, display a p38 MAPK-dependent enrichment of histone H3 phosphorylation on 'Ser-10' (H3S10ph) in LPS-stimulated myeloid cells. This phosphorylation enhances the accessibility of the cryptic NF-kappa-B-binding sites marking promoters for increased NF-kappa-B recruitment. Phosphorylates CDC25B and CDC25C which is required for binding to 14-3-3 proteins and leads to initiation of a G2 delay after ultraviolet radiation. Phosphorylates TIAR following DNA damage, releasing TIAR from GADD45A mRNA and preventing mRNA degradation. The p38 MAPKs may also have kinase-independent roles, which are thought to be due to the binding to targets in the absence of phosphorylation. Protein O-Glc-N-acylation catalyzed by the OGT is regulated by MAPK14, and, although OGT does not seem to be phosphorylated by MAPK14, their interaction increases upon MAPK14 activation induced by glucose

					deprivation. This interaction may regulate OGT activity by recruiting it to specific targets such as neurofilament H, stimulating its O-Glc-N-acylation. Required in mid-fetal development for the growth of embryo-derived blood vessels in the labyrinth layer of the placenta. Also plays an essential role in developmental and stress-induced erythropoiesis, through regulation of EPO gene expression. Isoform MXI2 activation is stimulated by mitogens and oxidative stress and only poorly phosphorylates ELK1 and ATF2. Isoform EXIP may play a role in the early onset of apoptosis. Phosphorylates S100A9 at 'Thr-113'.
STITCH	MAPK3	p27361	Kinase	Mitogen-activated protein kinase 3	Serine/threonine kinase which acts as an essential component of the MAP kinase signal transduction pathway. MAPK1/ERK2 and MAPK3/ERK1 are the 2 MAPKs which play an important role in the MAPK/ERK cascade. They participate also in a signaling cascade initiated by activated KIT and KITLG/SCF. Depending on the cellular context, the MAPK/ERK cascade

	mediates diverse biological functions such as cell growth, adhesion, survival and differentiation through the regulation of transcription, translation, cytoskeletal rearrangements. The MAPK/ERK cascade plays also a role in initiation and regulation of meiosis, mitosis, and postmitotic functions in differentiated cells by phosphorylating a number of transcription factors. About 160 substrates have already been discovered for ERKs. Many of these substrates are localized in the nucleus, and seem to participate in the regulation of transcription upon stimulation. However, other substrates are found in the cytosol as well as in other cellular organelles, and those are responsible for processes such as translation, mitosis and apoptosis. Moreover, the MAPK/ERK cascade is also involved in the regulation of the endosomal dynamics, including lysosome processing and endosome cycling through the perinuclear recycling compartment (PNRC); as well as in the fragmentation of the Golgi apparatus during mitosis. The substrates

					include transcription factors (such as ATF2, BCL6, ELK1, ERF, FOS, HSF4 or SPZ1), cytoskeletal elements (such as CANX, CTTN, GJA1, MAP2, MAPT, PXN, SORBS3 or STMN1), regulators of apoptosis (such as BAD, BTG2, CASP9, DAPK1, IER3, MCL1 or PPARG), regulators of translation (such as EIF4EBP1) and a variety of other signaling-related molecules (like ARHGEF2, FRS2 or GRB10). Protein kinases (such as RAF1, RPS6KA1/RSK1, RPS6KA3/RSK2, RPS6KA2/RSK3, RPS6KA6/RSK4, SYK, MKNK1/MNK1, MKNK2/MNK2, RPS6KA5/MSK1, RPS6KA4/MSK2, MAPKAPK3 or MAPKAPK5) and phosphatases (such as DUSP1, DUSP4, DUSP6 or DUSP16) are other substrates which enable the propagation the MAPK/ERK signal to additional cytosolic and nuclear targets, thereby extending the specificity of the cascade.
STITCH	MAPK8	p45983	Kinase	Mitogen-activated protein kinase 8	Serine/threonine-protein kinase involved in various processes such as cell proliferation, differentiation, migration, transformation and programmed cell death. Extracellular stimuli such as proinflammatory

	cytokines or physical stress stimulate the stress-activated protein kinase/c-Jun N-terminal kinase (SAP/JNK) signaling pathway. In this cascade, two dual specificity kinases MAP2K4/MKK4 and MAP2K7/MKK7 phosphorylate and activate MAPK8/JNK1. In turn, MAPK8/JNK1 phosphorylates a number of transcription factors, primarily components of AP-1 such as JUN, JDP2 and ATF2 and thus regulates AP-1 transcriptional activity. Phosphorylates the replication licensing factor CDT1, inhibiting the interaction between CDT1 and the histone H4 acetylase HBO1 to replication origins. Loss of this interaction abrogates the acetylation required for replication initiation. Promotes stressed cell apoptosis by phosphorylating key regulatory factors including p53/TP53 and Yes-associates protein YAP1. In T-cells, MAPK8 and MAPK9 are required for polarized differentiation of T-helper cells into Th1 cells. Contributes to the survival of erythroid cells by phosphorylating the antagonist of cell death BAD upon EPO stimulation. Mediates

	starvation-induced BCL2 phosphorylation, BCL2 dissociation from BECN1, and thus activation of autophagy. Phosphorylates STMN2 and hence regulates microtubule dynamics, controlling neurite elongation in cortical neurons. In the developing brain, through its cytoplasmic activity on STMN2, negatively regulates the rate of exit from multipolar stage and of radial migration from the ventricular zone. Phosphorylates several other substrates including heat shock factor protein 4 (HSF4), the deacetylase SIRT1, ELK1, or the E3 ligase ITCH. Phosphorylates the CLOCK-ARNTL/BMAL1 heterodimer and plays a role in the regulation of the circadian clock (PubMed:22441692). JNK1 isoforms display different binding patterns: beta-1 preferentially binds to c-Jun, whereas alpha-1, alpha-2, and beta-2 have a similar low level of binding to both c-Jun or ATF2. However, there is no correlation between binding and phosphorylation,

					which is achieved at about the same efficiency by all isoforms.
STITCH	MC2R	q01818	Receptor	Adrenocorticotropic hormone receptor	Receptor for corticotropin (ACTH). This receptor is mediated by G proteins (G(s)) which activate adenylate cyclase (cAMP).
STITCH	MDK	p21741	Signalling	Midkine	Developmentally regulated, secreted growth factor homologous to pleiotrophin (PTN), which has heparin binding activity. Binds anaplastic lymphoma kinase (ALK) which induces ALK activation and subsequent phosphorylation of the insulin receptor substrate (IRS1), followed by the activation of mitogen-activated protein kinase (MAPK) and PI3-kinase, and the induction of cell proliferation. Involved in neointima formation after arterial injury, possibly by mediating leukocyte recruitment. Also involved in early fetal adrenal gland development (By similarity).
STITCH	MGMT	p16455	Immune functions	Methylated-DNA--protein-cysteine methyltransferase	Involved in the cellular defense against the biological effects of O6-methylguanine (O6-MeG) in DNA. Repairs alkylated guanine in DNA by stoichiometrically transferring the alkyl group at the O-6 position to a

					cysteine residue in the enzyme. This is a suicide reaction: the enzyme is irreversibly inactivated.
STITCH	MLXIPL	q9np71	Regulator	Carbohydrate-responsive element-binding protein	Transcriptional repressor. Binds to the canonical and non-canonical E box sequences 5'-CACGTG-3' (By similarity).
SLAP	MMP1	p03956	Enzyme	Interstitial collagenase	Cleaves collagens of types I, II, and III at one site in the helical domain. Also cleaves collagens of types VII and X. In case of HIV infection, interacts and cleaves the secreted viral Tat protein, leading to a decrease in neuronal Tat's mediated neurotoxicity.
SLAP	MMP11	p24347		Stromelysin-3	May play an important role in the progression of epithelial malignancies.
SLAP	MMP13	p45452	Enzyme	Collagenase 3	Plays a role in the degradation of extracellular matrix proteins including fibrillar collagen, fibronectin, TNC and ACAN. Cleaves triple helical collagens, including type I, type II and type III collagen, but has the highest activity with soluble type II collagen. Can also degrade collagen type IV, type XIV and type X. May also function by activating or degrading key regulatory proteins, such as TGFB1 and CTGF. Plays a role in

					wound healing, tissue remodeling, cartilage degradation, bone development, bone mineralization and ossification. Required for normal embryonic bone development and ossification. Plays a role in the healing of bone fractures via endochondral ossification. Plays a role in wound healing, probably by a mechanism that involves proteolytic activation of TGFB1 and degradation of CTGF. Plays a role in keratinocyte migration during wound healing. May play a role in cell migration and in tumor cell invasion.
SLAP	MMP14	p50281	Regulator	Matrix metalloproteinase-14	Seems to specifically activate progelatinase A. May thus trigger invasion by tumor cells by activating progelatinase A on the tumor cell surface. May be involved in actin cytoskeleton reorganization by cleaving PTK7. Acts as a positive regulator of cell growth and migration via activation of MMP15. Involved in the formation of the fibrovascular tissues in association with pro-MMP2.
SLAP	MMP2	p08253		72 kDa type IV collagenase	Ubiquitinous metalloproteinase that is involved in diverse functions such as remodeling of the

	vasculature, angiogenesis, tissue repair, tumor invasion, inflammation, and atherosclerotic plaque rupture. As well as degrading extracellular matrix proteins, can also act on several nonmatrix proteins such as big endothelial 1 and beta-type CGRP promoting vasoconstriction. Also cleaves KISS at a Gly-|-Leu bond. Appears to have a role in myocardial cell death pathways. Contributes to myocardial oxidative stress by regulating the activity of GSK3beta. Cleaves GSK3beta in vitro. Involved in the formation of the fibrovascular tissues in association with MMP14.PEX, the C-terminal non-catalytic fragment of MMP2, posseses anti-angiogenic and anti-tumor properties and inhibits cell migration and cell adhesion to FGF2 and vitronectin. Ligand for integrinv/beta3 on the surface of blood vessels.Isoform 2: Mediates the proteolysis of CHUK/IKKA and initiates a primary innate immune response by inducing mitochondrial-nuclear stress signaling with activation of the pro-

					inflammatory NF-kappaB, NFAT and IRF transcriptional pathways.
SLAP	MMP3	p08254		Stromelysin-1	Can degrade fibronectin, laminin, gelatins of type I, III, IV, and V; collagens III, IV, X, and IX, and cartilage proteoglycans. Activates procollagenase.
Both	MMP7	p09237		Matrilysin	Degrades casein, gelatins of types I, III, IV, and V, and fibronectin. Activates procollagenase.
Both	MMP8	p22894		Neutrophil collagenase	Can degrade fibrillar type I, II, and III collagens.
Both	MMP9	p14780	Enzyme	Matrix metalloproteinase-9	May play an essential role in local proteolysis of the extracellular matrix and in leukocyte migration. Could play a role in bone osteoclastic resorption. Cleaves KiSS1 at a Gly-|-Leu bond. Cleaves type IV and type V collagen into large C-terminal three quarter fragments and shorter N-terminal one quarter fragments. Degrades fibronectin but not laminin or Pz-peptide
STITCH	MPO	p05164	Enzyme	Myeloperoxidase	Part of the host defense system of polymorphonuclear leukocytes. It is responsible for microbicidal activity against a wide range of organisms. In the stimulated PMN, MPO catalyzes the

					production of hypohalous acids, primarily hypochlorous acid in physiologic situations, and other toxic intermediates that greatly enhance PMN microbicidal activity.
STITCH	MTHFR	p42898	Enzyme	Methylenetetrahydrofolate reductase	Catalyzes the conversion of 5,10-methylenetetrahydrofolate to 5-methyltetrahydrofolate, a co-substrate for homocysteine remethylation to methionine.
STITCH	NAT2	p11245	Enzyme	Arylamine N-acetyltransferase 2	Participates in the detoxification of a plethora of hydrazine and arylamine drugs. Catalyzes the N- or O-acetylation of various arylamine and heterocyclic amine substrates and is able to bioactivate several known carcinogens.
Both	NFKB1	p19838	Regulator	Nuclear factor NF-kappa-B p105 subunit	NF-kappa-B is a pleiotropic transcription factor present in almost all cell types and is the endpoint of a series of signal transduction events that are initiated by a vast array of stimuli related to many biological processes such as inflammation, immunity, differentiation, cell growth, tumorigenesis and apoptosis. NF-kappa-B is a homo- or heterodimeric

	complex formed by the Rel-like domain-containing proteins RELA/p65, RELB, NFKB1/p105, NFKB1/p50, REL and NFKB2/p52 and the heterodimeric p65-p50 complex appears to be most abundant one. The dimers bind at kappa-B sites in the DNA of their target genes and the individual dimers have distinct preferences for different kappa-B sites that they can bind with distinguishable affinity and specificity. Different dimer combinations act as transcriptional activators or repressors, respectively. NF-kappa-B is controlled by various mechanisms of post-translational modification and subcellular compartmentalization as well as by interactions with other cofactors or corepressors. NF-kappa-B complexes are held in the cytoplasm in an inactive state complexed with members of the NF-kappa-B inhibitor (I-kappa-B) family. In a conventional activation pathway, I-kappa-B is phosphorylated by I-kappa-B kinases (IKKs) in response to different activators, subsequently degraded thus liberating the

	active NF-kappa-B complex which translocates to the nucleus. NF-kappa-B heterodimeric p65-p50 and RelB-p50 complexes are transcriptional activators. The NF-kappa-B p50-p50 homodimer is a transcriptional repressor, but can act as a transcriptional activator when associated with BCL3. NFKB1 appears to have dual functions such as cytoplasmic retention of attached NF-kappa-B proteins by p105 and generation of p50 by a cotranslational processing. The proteasome-mediated process ensures the production of both p50 and p105 and preserves their independent function, although processing of NFKB1/p105 also appears to occur post-translationally. p50 binds to the kappa-B consensus sequence 5'-GGRNNYYCC-3', located in the enhancer region of genes involved in immune response and acute phase reactions. In a complex with MAP3K8, NFKB1/p105 represses MAP3K8-induced MAPK signaling; active MAP3K8 is released by proteasome-dependent degradation of NFKB1/p105.

Both	NFKB2	q00653	Regulator	Nuclear factor NF-kappa-B p100 subunit	NF-kappa-B is a pleiotropic transcription factor present in almost all cell types and is the endpoint of a series of signal transduction events that are initiated by a vast array of stimuli related to many biological processes such as inflammation, immunity, differentiation, cell growth, tumorigenesis and apoptosis. NF-kappa-B is a homo- or heterodimeric complex formed by the Rel-like domain-containing proteins RELA/p65, RELB, NFKB1/p105, NFKB1/p50, REL and NFKB2/p52. The dimers bind at kappa-B sites in the DNA of their target genes and the individual dimers have distinct preferences for different kappa-B sites that they can bind with distinguishable affinity and specificity. Different dimer combinations act as transcriptional activators or repressors, respectively. NF-kappa-B is controlled by various mechanisms of post-translational modification and subcellular compartmentalization as well as by interactions with other cofactors or corepressors. NF-kappa-B complexes are held in the cytoplasm in an inactive

	state complexed with members of the NF-kappa-B inhibitor (I-kappa-B) family. In a conventional activation pathway, I-kappa-B is phosphorylated by I-kappa-B kinases (IKKs) in response to different activators, subsequently degraded thus liberating the active NF-kappa-B complex which translocates to the nucleus. In a non-canonical activation pathway, the MAP3K14-activated CHUK/IKKA homodimer phosphorylates NFKB2/p100 associated with RelB, inducing its proteolytic processing to NFKB2/p52 and the formation of NF-kappa-B RelB-p52 complexes. The NF-kappa-B heterodimeric RelB-p52 complex is a transcriptional activator. The NF-kappa-B p52-p52 homodimer is a transcriptional repressor. NFKB2 appears to have dual functions such as cytoplasmic retention of attached NF-kappa-B proteins by p100 and generation of p52 by a cotranslational processing. The proteasome-mediated process ensures the production of both p52 and p100 and preserves their independent function. p52 binds to the kappa-B

					consensus sequence 5'-GGRNNYYCC-3', located in the enhancer region of genes involved in immune response and acute phase reactions. p52 and p100 are respectively the minor and major form; the processing of p100 being relatively poor. Isoform p49 is a subunit of the NF-kappa-B protein complex, which stimulates the HIV enhancer in synergy with p65. In concert with RELB, regulates the circadian clock by repressing the transcriptional activator activity of the CLOCK-ARNTL/BMAL1 heterodimer.
STITCH	NFKBIA	p25963	Regulator	NF-kappa-B inhibitor alpha	Inhibits the activity of dimeric NF-kappa-B/REL complexes by trapping REL dimers in the cytoplasm through masking of their nuclear localization signals. On cellular stimulation by immune and proinflammatory responses, becomes phosphorylated promoting ubiquitination and degradation, enabling the dimeric RELA to translocate to the nucleus and activate transcription.
STITCH	NFKBIZ	q2byh8	Regulator	NF-kappa-B inhibitor zeta	Involved in regulation of NF-kappa-B transcription factor complexes. Inhibits NF-kappa-B activity without

					affecting its nuclear translocation upon stimulation. Inhibits DNA-binding of RELA and NFKB1/p50, and of the NF-kappa-B p65-p50 heterodimer and the NF-kappa-B p50-p50 homodimer. Seems also to activate NF-kappa-B-mediated transcription. In vitro, upon association with NFKB1/p50 has transcriptional activation activity and, together with NFKB1/p50 and RELA, is recruited to LCN2 promoters. Promotes transcription of LCN2 and DEFB4. Is recruited to IL-6 promoters and activates IL-6 but decreases TNF-alpha production in response to LPS. Seems to be involved in the induction of inflammatory genes activated through TLR/IL-1 receptor signaling. May promote apoptosis (By similarity)
SLAP	NISCH	q9y2i1	Receptor	Nischarin	Acts either as the functional imidazoline-1 receptor (I1R) candidate or as a membrane-associated mediator of the I1R signaling. Binds numerous imidazoline ligands that induces initiation of cell-signaling cascades triggering to cell survival, growth and migration. Its activation by the agonist

	rilmenidine induces an increase in phosphorylation of mitogen-activated protein kinases MAPK1 and MAPK3 in rostral ventrolateral medulla (RVLM) neurons that exhibited rilmenidine-evoked hypotension (By similarity). Blocking its activation with efaroxan abolished rilmenidine-induced mitogen-activated protein kinase phosphorylation in RVLM neurons (By similarity). Acts as a modulator of Rac-regulated signal transduction pathways (By similarity). Suppresses Rac1-stimulated cell migration by interacting with PAK1 and inhibiting its kinase activity (By similarity). Also blocks Pak-independent Rac signaling by interacting with RAC1 and inhibiting Rac1-stimulated NF-kB response element and cyclin D1 promoter activation (By similarity). Inhibits also LIMK1 kinase activity by reducing LIMK1 'Tyr-508' phosphorylation (By similarity). Inhibits Rac-induced cell migration and invasion in breast and colon epithelial cells (By similarity). Inhibits lamellipodia formation, when overexpressed (By similarity). Plays a role in

					protection against apoptosis. Involved in association with IRS4 in the enhancement of insulin activation of MAPK1 and MAPK3. When overexpressed, induces a redistribution of cell surface ITGA5 integrin to intracellular endosomal structures.
STITCH	NOS1	p29475	Enzyme	Nitric oxide synthase, brain	Produces nitric oxide (NO) which is a messenger molecule with diverse functions throughout the body. In the brain and peripheral nervous system, NO displays many properties of a neurotransmitter. Probably has nitrosylase activity and mediates cysteine S-nitrosylation of cytoplasmic target proteins such SRR.
STITCH	NOS2	p35228	Enzyme	Nitric oxide synthase, inducible	Produces nitric oxide (NO) which is a messenger molecule with diverse functions throughout the body. In macrophages, NO mediates tumoricidal and bactericidal actions. Also has nitrosylase activity and mediates cysteine S-nitrosylation of cytoplasmic target proteins such COX2.
STITCH	NOS3	p60323	Regulator	Nanos homolog 3	Plays a role in the maintenance of the undifferentiated state of germ cells regulating the

					spermatogonia cell cycle and inducing a prolonged transit in G1 phase. Affects cell proliferation probably by repressing translation of specific mRNAs. Maintains the germ cell lineage by suppressing both Bax-dependent and -independent apoptotic pathways. Essential in the early stage embryo to protect the migrating primordial germ cells (PGCs) from apoptosis.
Both	NR1I2	o75469	Regulator	Nuclear receptor subfamily 1 group I member 2	Nuclear receptor that binds and is activated by variety of endogenous and xenobiotic compounds. Transcription factor that activates the transcription of multiple genes involved in the metabolism and secretion of potentially harmful xenobiotics, drugs and endogenous compounds. Activated by the antibiotic rifampicin and various plant metabolites, such as hyperforin, guggulipid, colupulone, and isoflavones. Response to specific ligands is species-specific. Activated by naturally occurring steroids, such as pregnenolone and progesterone. Binds to a

					response element in the promoters of the CYP3A4 and ABCB1/MDR1 genes.
Both	NR1I3	q14994	Enzyme	Nuclear receptor subfamily 1 group I member 3	Binds and transactivates the retinoic acid response elements that control expression of the retinoic acid receptor beta 2 and alcohol dehydrogenase 3 genes. Transactivates both the phenobarbital responsive element module of the human CYP2B6 gene and the CYP3A4 xenobiotic response element.
Both	NR3C1	p04150	Receptor	Glucocorticoid receptor	Receptor for glucocorticoids (GC). Has a dual mode of action: as a transcription factor that binds to glucocorticoid response elements (GRE), both for nuclear and mitochondrial DNA, and as a modulator of other transcription factors. Affects inflammatory responses, cellular proliferation and differentiation in target tissues. Could act as a coactivator for STAT5-dependent transcription upon growth hormone (GH) stimulation and could reveal an essential role of hepatic GR in the control of body growth. Involved in chromatin remodeling. May play a negative role in

					adipogenesis through the regulation of lipolytic and antilipogenic genes expression.
SLAP	NR3C2	p08235	Receptor	Mineralocorticoid receptor	Receptor for both mineralocorticoids (MC) such as aldosterone and glucocorticoids (GC) such as corticosterone or cortisol. Binds to mineralocorticoid response elements (MRE) and transactivates target genes. The effect of MC is to increase ion and water transport and thus raise extracellular fluid volume and blood pressure and lower potassium levels
STITCH	ODC1	p11926	Enzyme	Ornithine decarboxylase	Key enzyme of polyamine biosynthesis that converts ornithine into putrescine, which is the precursor for the polyamines, spermidine and spermine
SLAP	OPRK1	p41145	Receptor	Kappa-type opioid receptor	G-protein coupled opioid receptor that functions as receptor for endogenous alpha-neoendorphins and dynorphins, but has low affinity for beta-endorphins. Also functions as receptor for various synthetic opioids and for the psychoactive diterpene salvinorin A. Ligand binding causes a conformation change that triggers signaling via guanine nucleotide-binding proteins (G proteins) and modulates the activity of

					down-stream effectors, such as adenylate cyclase. Signaling leads to the inhibition of adenylate cyclase activity. Inhibits neurotransmitter release by reducing calcium ion currents and increasing potassium ion conductance. Plays a role in the perception of pain. Plays a role in mediating reduced physical activity upon treatment with synthetic opioids. Plays a role in the regulation of salivation in response to synthetic opioids. May play a role in arousal and regulation of autonomic and neuroendocrine functions.
SLAP	OPRM1	p35372	Receptor	Mu-type opioid receptor	Receptor for endogenous opioids such as beta-endorphin and endomorphin. Receptor for natural and synthetic opioids including morphine, heroin, DAMGO, fentanyl, etorphine, buprenorphin and methadone. Agonist binding to the receptor induces coupling to an inactive GDP-bound heterotrimeric G-protein complex and subsequent exchange of GDP for GTP in the G-protein alpha subunit leading to dissociation of the G-protein complex with the free GTP-bound G-protein alpha and the G-protein beta-

	gamma dimer activating downstream cellular effectors. The agonist- and cell type-specific activity is predominantly coupled to pertussis toxin-sensitive G(i) and G(o) G alpha proteins, GNAI1, GNAI2, GNAI3 and GNAO1 isoforms Alpha-1 and Alpha-2, and to a lesser extend to pertussis toxin-insensitive G alpha proteins GNAZ and GNA15. They mediate an array of downstream cellular responses, including inhibition of adenylate cyclase activity and both N-type and L-type calcium channels, activation of inward rectifying potassium channels, mitogen-activated protein kinase (MAPK), phospholipase C (PLC), phosphoinositide/protein kinase (PKC), phosphoinositide 3-kinase (PI3K) and regulation of NF-kappa-B. Also couples to adenylate cyclase stimulatory G alpha proteins. The selective temporal coupling to G-proteins and subsequent signaling can be regulated by RGSZ proteins, such as RGS9, RGS17 and RGS4. Phosphorylation by members of the GPRK subfamily of Ser/Thr protein kinases and association

	with beta-arrestins is involved in short-term receptor desensitization. Beta-arrestins associate with the GPRK-phosphorylated receptor and uncouple it from the G-protein thus terminating signal transduction. The phosphorylated receptor is internalized through endocytosis via clathrin-coated pits which involves beta-arrestins. The activation of the ERK pathway occurs either in a G-protein-dependent or a beta-arrestin-dependent manner and is regulated by agonist-specific receptor phosphorylation. Acts as a class A G-protein coupled receptor (GPCR) which dissociates from beta-arrestin at or near the plasma membrane and undergoes rapid recycling. Receptor down-regulation pathways are varying with the agonist and occur dependent or independent of G-protein coupling. Endogenous ligands induce rapid desensitization, endocytosis and recycling whereas morphine induces only low desensitization and endocytosis. Heterooligomerization with other GPCRs can modulate agonist binding, signaling and

					trafficking properties. Involved in neurogenesis. Isoform 12 couples to GNAS and is proposed to be involved in excitatory effects. Isoform 16 and isoform 17 do not bind agonists but may act through oligomerization with binding-competent OPRM1 isoforms and reduce their ligand binding activity.
STITCH	ORM1	p02763	Transport	Alpha-1-acid glycoprotein 1	Functions as transport protein in the blood stream. Binds various ligands in the interior of its beta-barrel domain. Also binds synthetic drugs and influences their distribution and availability in the body. Appears to function in modulating the activity of the immune system during the acute-phase reaction.
STITCH	ORM2	p19652	Transport	Alpha-1-acid glycoprotein 2	Functions as transport protein in the blood stream. Binds various hydrophobic ligands in the interior of its beta-barrel domain. Also binds synthetic drugs and influences their distribution and availability. Appears to function in modulating the activity of the immune system during the acute-phase reaction
STITCH	PARP1	p09874	Enzyme	Poly [ADP-ribose] polymerase 1	Involved in the base excision repair (BER) pathway, by catalyzing the poly(ADP-ribosyl)ation of a limited

					number of acceptor proteins involved in chromatin architecture and in DNA metabolism. This modification follows DNA damages and appears as an obligatory step in a detection/signaling pathway leading to the reparation of DNA strand breaks. Mediates the poly(ADP-ribosyl)ation of APLF and CHFR. Positively regulates the transcription of MTUS1 and negatively regulates the transcription of MTUS2/TIP150. With EEF1A1 and TXK, forms a complex that acts as a T-helper 1 (Th1) cell-specific transcription factor and binds the promoter of IFN-gamma to directly regulate its transcription, and is thus involved importantly in Th1 cytokine production. Required for PARP9 and DTX3L recruitment to DNA damage sites. PARP1-dependent PARP9-DTX3L-mediated ubiquitination promotes the rapid and specific recruitment of 53BP1/TP53BP1, UIMC1/RAP80, and BRCA1 to DNA damage sites.
STITCH	PCNA	p12004	Regulator	Proliferating cell nuclear antigen	Auxiliary protein of DNA polymerase delta and is involved in the control of eukaryotic DNA replication

	by increasing the polymerase's processibility during elongation of the leading strand. Induces a robust stimulatory effect on the 3'-5' exonuclease and 3'-phosphodiesterase, but not apurinic-apyrimidinic (AP) endonuclease, APEX2 activities. Has to be loaded onto DNA in order to be able to stimulate APEX2. Plays a key role in DNA damage response (DDR) by being conveniently positioned at the replication fork to coordinate DNA replication with DNA repair and DNA damage tolerance pathways. Acts as a loading platform to recruit DDR proteins that allow completion of DNA replication after DNA damage and promote postreplication repair: Monoubiquitinated PCNA leads to recruitment of translesion (TLS) polymerases, while 'Lys-63'-linked polyubiquitination of PCNA is involved in error-free pathway and employs recombination mechanisms to synthesize across the lesion.

Both	PDPK1	o15530	Kinase	3-phosphoinositide-dependent protein kinase 1	Serine/threonine kinase which acts as a master kinase, phosphorylating and activating a subgroup of the AGC family of protein kinases. Its targets include: protein kinase B (PKB/AKT1, PKB/AKT2, PKB/AKT3), p70 ribosomal protein S6 kinase (RPS6KB1), p90 ribosomal protein S6 kinase (RPS6KA1, RPS6KA2 and RPS6KA3), cyclic AMP-dependent protein kinase (PRKACA), protein kinase C (PRKCD and PRKCZ), serum and glucocorticoid-inducible kinase (SGK1, SGK2 and SGK3), p21-activated kinase-1 (PAK1), protein kinase PKN (PKN1 and PKN2). Plays a central role in the transduction of signals from insulin by providing the activating phosphorylation to PKB/AKT1, thus propagating the signal to downstream targets controlling cell proliferation and survival, as well as glucose and amino acid uptake and storage. Negatively regulates the TGF-beta-induced signaling by: modulating the association of SMAD3 and SMAD7 with TGF-beta receptor, phosphorylating SMAD2, SMAD3, SMAD4 and SMAD7, preventing the nuclear

	translocation of SMAD3 and SMAD4 and the translocation of SMAD7 from the nucleus to the cytoplasm in response to TGF-beta. Activates PPARG transcriptional activity and promotes adipocyte differentiation. Activates the NF-kappa-B pathway via phosphorylation of IKKB. The tyrosine phosphorylated form is crucial for the regulation of focal adhesions by angiotensin II. Controls proliferation, survival, and growth of developing pancreatic cells. Participates in the regulation of Ca2+ entry and Ca2+-activated K+ channels of mast cells. Essential for the motility of vascular endothelial cells (ECs) and is involved in the regulation of their chemotaxis. Plays a critical role in cardiac homeostasis by serving as a dual effector for cell survival and beta-adrenergic response. Plays an important role during thymocyte development by regulating the expression of key nutrient receptors on the surface of pre-T cells and mediating Notch-induced cell growth and proliferative responses. Provides negative feedback inhibition to toll-like

					receptor-mediated NF-kappa-B activation in macrophages. Isoform 3 is catalytically inactive.
SLAP	PGR	*uncertain*			
SLAP	PLA2G4A	p47712	Enzyme	Cytosolic phospholipase A2	Selectively hydrolyzes arachidonyl phospholipids in the sn-2 position releasing arachidonic acid. Together with its lysophospholipid activity, it is implicated in the initiation of the inflammatory response.
STITCH	PLAU	p00749	Enzyme	Urokinase-type plasminogen activator	Specifically cleaves the zymogen plasminogen to form the active enzyme plasmin.
SLAP	PNMT	p11086	Enzyme	Phenylethanolamine N-methyltransferase	Converts noradrenaline to adrenaline.
STITCH	PNP	p00491	Enzyme	Purine nucleoside phosphorylase	The purine nucleoside phosphorylases catalyze the phosphorolytic breakdown of the N-glycosidic bond in the beta-(deoxy)ribonucleoside molecules, with the formation of the corresponding free purine bases and pentose-1-phosphate
STITCH	POMC	p01189	Signalling	Pro-opiomelanocortin	ACTH stimulates the adrenal glands to release cortisol.

					MSH (melanocyte-stimulating hormone) increases the pigmentation of skin by increasing melanin production in melanocytes. Beta-endorphin and Met-enkephalin are endogenous opiates.
SLAP	PPARA	q07869	Regulator	Peroxisome proliferator-activated receptor alpha	Ligand-activated transcription factor. Key regulator of lipid metabolism. Activated by the endogenous ligand 1-palmitoyl-2-oleoyl-sn-glycerol-3-phosphocholine (16:0/18:1-GPC). Activated by oleylethanolamide, a naturally occurring lipid that regulates satiety. Receptor for peroxisome proliferators such as hypolipidemic drugs and fatty acids. Regulates the peroxisomal beta-oxidation pathway of fatty acids. Functions as transcription activator for the ACOX1 and P450 genes. Transactivation activity requires heterodimerization with RXRA and is antagonized by NR2C2. May be required for the propagation of clock information to metabolic pathways regulated by PER2.

Both	PPARD	q03181	Receptor	Peroxisome proliferator-activated receptor delta	Ligand-activated transcription factor. Receptor that binds peroxisome proliferators such as hypolipidemic drugs and fatty acids. Has a preference for poly-unsaturated fatty acids, such as gamma-linoleic acid and eicosapentanoic acid. Once activated by a ligand, the receptor binds to promoter elements of target genes. Regulates the peroxisomal beta-oxidation pathway of fatty acids. Functions as transcription activator for the acyl-CoA oxidase gene. Decreases expression of NPC1L1 once activated by a ligand.
Both	PPARG	p37231	Regulator	Peroxisome proliferator-activated receptor gamma	Nuclear receptor that binds peroxisome proliferators such as hypolipidemic drugs and fatty acids. Once activated by a ligand, the nuclear receptor binds to DNA specific PPAR response elements (PPRE) and modulates the transcription of its target genes, such as acyl-CoA oxidase. It therefore controls the peroxisomal beta-oxidation pathway of fatty acids. Key regulator of adipocyte differentiation and glucose homeostasis. ARF6 acts as a key regulator of the tissue-specific adipocyte P2 (aP2) enhancer. Acts as a

					critical regulator of gut homeostasis by suppressing NF-kappa-B-mediated proinflammatory responses. Plays a role in the regulation of cardiovascular circadian rhythms by regulating the transcription of ARNTL/BMAL1 in the blood vessels (By similarity)
STITCH	PPIG	q13427	Regulator	Peptidyl-prolyl cis-trans isomerase G	PPIases accelerate the folding of proteins. It catalyzes the cis-trans isomerization of proline imidic peptide bonds in oligopeptides. May be implicated in the folding, transport, and assembly of proteins. May play an important role in the regulation of pre-mRNA splicing.
STITCH	PRB3	q04118	Receptor	Basic salivary proline-rich protein 3	Acts as a receptor for the Gram-negative bacterium F.nucleatum.
SLAP	PRKACA	p17612	Kinase	cAMP-dependent protein kinase catalytic subunit alpha	Phosphorylates a large number of substrates in the cytoplasm and the nucleus. Regulates the abundance of compartmentalized pools of its regulatory subunits through phosphorylation of PJA2 which binds and ubiquitinates these subunits, leading to their subsequent proteolysis. Phosphorylates CDC25B, ABL1, NFKB1, CLDN3, PSMC5/RPT6, PJA2, RYR2, RORA

	and VASP. RORA is activated by phosphorylation. Required for glucose-mediated adipogenic differentiation increase and osteogenic differentiation inhibition from osteoblasts. Involved in the regulation of platelets in response to thrombin and collagen; maintains circulating platelets in a resting state by phosphorylating proteins in numerous platelet inhibitory pathways when in complex with NF-kappa-B (NFKB1 and NFKB2) and I-kappa-B-alpha (NFKBIA), but thrombin and collagen disrupt these complexes and free active PRKACA stimulates platelets and leads to platelet aggregation by phosphorylating VASP. Prevents the antiproliferative and anti-invasive effects of alpha-difluoromethylornithine in breast cancer cells when activated. RYR2 channel activity is potentiated by phosphorylation in presence of luminal Ca2+, leading to reduced amplitude and increased frequency of store overload-induced Ca2+ release (SOICR) characterized by an increased rate of Ca2+ release and propagation velocity of spontaneous Ca2+

					waves, despite reduced wave amplitude and resting cytosolic Ca2+. PSMC5/RPT6 activation by phosphorylation stimulates proteasome. Negatively regulates tight junctions (TJs) in ovarian cancer cells via CLDN3 phosphorylation. NFKB1 phosphorylation promotes NF-kappa-B p50-p50 DNA binding. Involved in embryonic development by down-regulating the Hedgehog (Hh) signaling pathway that determines embryo pattern formation and morphogenesis. Prevents meiosis resumption in prophase-arrested oocytes via CDC25B inactivation by phosphorylation. May also regulate rapid eye movement (REM) sleep in the pedunculopontine tegmental (PPT). Phosphorylates APOBEC3G and AICDA. Isoform 2 phosphorylates and activates ABL1 in sperm flagellum to promote spermatozoa capacitation.
STITCH	PTEN	p60484	Enzyme	Phosphatidylinositol 3,4,5-trisphosphate 3-phosphatase and dual-	Tumor suppressor. Acts as a dual-specificity protein phosphatase, dephosphorylating tyrosine-, serine- and threonine-phosphorylated proteins. Also acts as a lipid phosphatase, removing the phosphate in the D3

	specificity protein phosphatase	position of the inositol ring from phosphatidylinositol 3,4,5-trisphosphate, phosphatidylinositol 3,4-diphosphate, phosphatidylinositol 3-phosphate and inositol 1,3,4,5-tetrakisphosphate with order of substrate preference in vitro PtdIns(3,4,5)P3 > PtdIns(3,4)P2 > PtdIns3P > Ins(1,3,4,5)P4. The lipid phosphatase activity is critical for its tumor suppressor function. Antagonizes the PI3K-AKT/PKB signaling pathway by dephosphorylating phosphoinositides and thereby modulating cell cycle progression and cell survival. The unphosphorylated form cooperates with AIP1 to suppress AKT1 activation. Dephosphorylates tyrosine-phosphorylated focal adhesion kinase and inhibits cell migration and integrin-mediated cell spreading and focal adhesion formation. Plays a role as a key modulator of the AKT-mTOR signaling pathway controlling the tempo of the process of newborn neurons integration during adult neurogenesis, including correct neuron positioning, dendritic

					development and synapse formation. May be a negative regulator of insulin signaling and glucose metabolism in adipose tissue. The nuclear monoubiquitinated form possesses greater apoptotic potential, whereas the cytoplasmic nonubiquitinated form induces less tumor suppressive ability. In motile cells, suppresses the formation of lateral pseudopods and thereby promotes cell polarization and directed movement. Isoform alpha: Functional kinase, like isoform 1 it antagonizes the PI3K-AKT/PKB signaling pathway. Plays a role in mitochondrial energetic metabolism by promoting COX activity and ATP production, via collaboration with isoform 1 in increasing protein levels of PINK1.
SLAP	PTGER1	p34995	Receptor	Prostaglandin E2 receptor EP1 subtype	Receptor for prostaglandin E2 (PGE2). The activity of this receptor is mediated by G(q) proteins which activate a phosphatidylinositol-calcium second messenger system. May play a role as an important modulator of renal function. Implicated the smooth

					muscle contractile response to PGE2 in various tissues.
SLAP	PTGER2	p43116	Receptor	Prostaglandin E2 receptor EP2 subtype	Receptor for prostaglandin E2 (PGE2). The activity of this receptor is mediated by G(s) proteins that stimulate adenylate cyclase. The subsequent raise in intracellular cAMP is responsible for the relaxing effect of this receptor on smooth muscle.
SLAP	PTGER3	p43115	Receptor	Prostaglandin E2 receptor EP3 subtype	Receptor for prostaglandin E2 (PGE2); the EP3 receptor may be involved in inhibition of gastric acid secretion, modulation of neurotransmitter release in central and peripheral neurons, inhibition of sodium and water reabsorption in kidney tubulus and contraction in uterine smooth muscle. The activity of this receptor can couple to both the inhibition of adenylate cyclase mediated by G-I proteins, and to an elevation of intracellular calcium. The various isoforms have identical ligand binding properties but can interact with different second messenger systems (By similarity).

Both	PTGER4	p35408	Receptor	Prostaglandin E2 receptor EP4 subtype	Receptor for prostaglandin E2 (PGE2). The activity of this receptor is mediated by G(s) proteins that stimulate adenylate cyclase. Has a relaxing effect on smooth muscle. May play an important role in regulating renal hemodynamics, intestinal epithelial transport, adrenal aldosterone secretion, and uterine function.
Both	PTGS1	p23219	Enzyme	Prostaglandin G/H synthase 1	Converts arachidonate to prostaglandin H2 (PGH2), a committed step in prostanoid synthesis. Involved in the constitutive production of prostanoids in particular in the stomach and platelets. In gastric epithelial cells, it is a key step in the generation of prostaglandins, such as prostaglandin E2 (PGE2), which plays an important role in cytoprotection. In platelets, it is involved in the generation of thromboxane A2 (TXA2), which promotes platelet activation and aggregation, vasoconstriction and proliferation of vascular smooth muscle cells.
Both	PTGS2	p35354	Enzyme	Prostaglandin G/H synthase 2	Converts arachidonate to prostaglandin H2 (PGH2), a committed step in prostanoid synthesis. Constitutively

					expressed in some tissues in physiological conditions, such as the endothelium, kidney and brain, and in pathological conditions, such as in cancer. PTGS2 is responsible for production of inflammatory prostaglandins. Up-regulation of PTGS2 is also associated with increased cell adhesion, phenotypic changes, resistance to apoptosis and tumor angiogenesis. In cancer cells, PTGS2 is a key step in the production of prostaglandin E2 (PGE2), which plays important roles in modulating motility, proliferation and resistance to apoptosis.
STITCH	PTH	p01270	Hormone	Parathyroid hormone	PTH elevates calcium level by dissolving the salts in bone and preventing their renal excretion. Stimulates [1-14C]-2-deoxy-D-glucose (2DG) transport and glycogen synthesis in osteoblastic cells.
STITCH	RALBP1	q15311	Structural	RalA-binding protein 1	Can activate specifically hydrolysis of GTP bound to RAC1 and CDC42, but not RALA. Mediates ATP-dependent transport of S-(2,4-dinitrophenyl)-glutathione (DNP-SG) and doxorubicin (DOX) and is the major ATP-dependent transporter of glutathione

					conjugates of electrophiles (GS-E) and DOX in erythrocytes. Can catalyze transport of glutathione conjugates and xenobiotics, and may contribute to the multidrug resistance phenomenon. Serves as a scaffold protein that brings together proteins forming an endocytotic complex during interphase and also with CDK1 to switch off endocytosis, One of its substrates would be EPN1/Epsin.
STITCH	RELA	q04206	Regulator	Transcription factor p65	NF-kappa-B is a pleiotropic transcription factor present in almost all cell types and is the endpoint of a series of signal transduction events that are initiated by a vast array of stimuli related to many biological processes such as inflammation, immunity, differentiation, cell growth, tumorigenesis and apoptosis. NF-kappa-B is a homo- or heterodimeric complex formed by the Rel-like domain-containing proteins RELA/p65, RELB, NFKB1/p105, NFKB1/p50, REL and NFKB2/p52 and the heterodimeric p65-p50 complex appears to be most abundant one. The dimers bind at kappa-B sites in the DNA of their target

genes and the individual dimers have distinct preferences for different kappa-B sites that they can bind with distinguishable affinity and specificity. Different dimer combinations act as transcriptional activators or repressors, respectively. NF-kappa-B is controlled by various mechanisms of post-translational modification and subcellular compartmentalization as well as by interactions with other cofactors or corepressors. NF-kappa-B complexes are held in the cytoplasm in an inactive state complexed with members of the NF-kappa-B inhibitor (I-kappa-B) family. In a conventional activation pathway, I-kappa-B is phosphorylated by I-kappa-B kinases (IKKs) in response to different activators, subsequently degraded thus liberating the active NF-kappa-B complex which translocates to the nucleus. NF-kappa-B heterodimeric p65-p50 and p65-c-Rel complexes are transcriptional activators. The NF-kappa-B p65-p65 complex appears to be involved in invasin-mediated activation of IL-8 expression. The

					inhibitory effect of I-kappa-B upon NF-kappa-B the cytoplasm is exerted primarily through the interaction with p65. p65 shows a weak DNA-binding site which could contribute directly to DNA binding in the NF-kappa-B complex. Associates with chromatin at the NF-kappa-B promoter region via association with DDX1. Essential for cytokine gene expression in T-cells (PubMed:15790681).
STITCH	REN	p00797	Enzyme	Renin	Renin is a highly specific endopeptidase, whose only known function is to generate angiotensin I from angiotensinogen in the plasma, initiating a cascade of reactions that produce an elevation of blood pressure and increased sodium retention by the kidney.
SLAP	ROCK1	q13464	Kinase	Rho-associated protein kinase 1	Protein kinase which is a key regulator of actin cytoskeleton and cell polarity. Involved in regulation of smooth muscle contraction, actin cytoskeleton organization, stress fiber and focal adhesion formation, neurite retraction, cell adhesion and motility via phosphorylation of DAPK3, GFAP, LIMK1, LIMK2, MYL9/MLC2, PFN1 and PPP1R12A.

					Phosphorylates FHOD1 and acts synergistically with it to promote SRC-dependent non-apoptotic plasma membrane blebbing. Phosphorylates JIP3 and regulates the recruitment of JNK to JIP3 upon UVB-induced stress. Acts as a suppressor of inflammatory cell migration by regulating PTEN phosphorylation and stability. Acts as a negative regulator of VEGF-induced angiogenic endothelial cell activation. Required for centrosome positioning and centrosome-dependent exit from mitosis. Plays a role in terminal erythroid differentiation. May regulate closure of the eyelids and ventral body wall by inducing the assembly of actomyosin bundles. Promotes keratinocyte terminal differentiation. Involved in osteoblast compaction through the fibronectin fibrillogenesis cell-mediated matrix assembly process, essential for osteoblast mineralization.
SLAP	ROCK2	o75116	Kinase	Rho-associated protein kinase 2	Protein kinase which is a key regulator of actin cytoskeleton and cell polarity. Involved in regulation of smooth muscle contraction, actin cytoskeleton

	organization, stress fiber and focal adhesion formation, neurite retraction, cell adhesion and motility via phosphorylation of ADD1, BRCA2, CNN1, EZR, DPYSL2, EP300, MSN, MYL9/MLC2, NPM1, RDX, PPP1R12A and VIM. Phosphorylates SORL1 and IRF4. Acts as a negative regulator of VEGF-induced angiogenic endothelial cell activation. Positively regulates the activation of p42/MAPK1-p44/MAPK3 and of p90RSK/RPS6KA1 during myogenic differentiation. Plays an important role in the timely initiation of centrosome duplication. Inhibits keratinocyte terminal differentiation. May regulate closure of the eyelids and ventral body wall through organization of actomyosin bundles. Plays a critical role in the regulation of spine and synaptic properties in the hippocampus. Plays an important role in generating the circadian rhythm of the aortic myofilament Ca^{2+} sensitivity and vascular contractility by modulating the myosin light chain phosphorylation.

STITCH	S100A4	p26447		Protein S100-A4	calcium ion binding; RAGE receptor binding; poly(A) RNA binding
STITCH	SAT1	p21673	Enzyme	Diamine acetyltransferase 1	Enzyme which catalyzes the acetylation of polyamines. Substrate specificity: norspermidine = spermidine >> spermine > N(1)-acetylspermine > putrescine. This highly regulated enzyme allows a fine attenuation of the intracellular concentration of polyamines. Also involved in the regulation of polyamine transport out of cells. Acts on 1,3-diaminopropane, 1,5-diaminopentane, putrescine, spermidine (forming N(1)- and N(8)-acetylspermidine), spermine, N(1)-acetylspermidine and N(8)-acetylspermidine.
Both	SCN10A	q9y5y9	Ion channel	Sodium channel protein type 10 subunit alpha	Tetrodotoxin-resistant channel that mediates the voltage-dependent sodium ion permeability of excitable membranes. Assuming opened or closed conformations in response to the voltage difference across the membrane, the protein forms a sodium-selective channel through which sodium ions may pass in accordance with their electrochemical

					gradient. Plays a role in neuropathic pain mechanisms.
Both	SCN11A	q9ui33	Ion channel	Sodium channel protein type 11 subunit alpha	This protein mediates the voltage-dependent sodium ion permeability of excitable membranes. Assuming opened or closed conformations in response to the voltage difference across the membrane, the protein forms a sodium-selective channel through which sodium ions may pass in accordance with their electrochemical gradient. It is a tetrodotoxin-resistant sodium channel isoform. Also involved, with the contribution of the receptor tyrosine kinase NTRK2, in rapid BDNF-evoked neuronal depolarization.
Both	SCN1A	p35498	Ion channel	Sodium channel protein type 1 subunit alpha	Mediates the voltage-dependent sodium ion permeability of excitable membranes. Assuming opened or closed conformations in response to the voltage difference across the membrane, the protein forms a sodium-selective channel through which Na^+ ions may pass in accordance with their electrochemical gradient.

Both	SCN1B	q079699	Ion channel	Sodium channel subunit beta-1	Crucial in the assembly, expression, and functional modulation of the heterotrimeric complex of the sodium channel. The subunit beta-1 can modulate multiple alpha subunit isoforms from brain, skeletal muscle, and heart. Its association with neurofascin may target the sodium channels to the nodes of Ranvier of developing axons and retain these channels at the nodes in mature myelinated axons. Isoform 2: Cell adhesion molecule that plays a critical role in neuronal migration and pathfinding during brain development. Stimulates neurite outgrowth.
Both	SCN2A	q99250	Ion channel	Sodium channel protein type 2 subunit alpha	Mediates the voltage-dependent sodium ion permeability of excitable membranes. Assuming opened or closed conformations in response to the voltage difference across the membrane, the protein forms a sodium-selective channel through which Na^+ ions may pass in accordance with their electrochemical gradient.
Both	SCN2B	o60939	Ion channel	Sodium channel subunit beta-2	Crucial in the assembly, expression, and functional modulation of the heterotrimeric complex of the

					sodium channel. The subunit beta-2 causes an increase in the plasma membrane surface area and in its folding into microvilli. Interacts with TNR may play a crucial role in clustering and regulation of activity of sodium channels at nodes of Ranvier (By similarity).
Both	SCN3A	q9ny46	Ion channel	Sodium channel protein type 3 subunit alpha	Mediates the voltage-dependent sodium ion permeability of excitable membranes. Assuming opened or closed conformations in response to the voltage difference across the membrane, the protein forms a sodium-selective channel through which Na^+ ions may pass in accordance with their electrochemical gradient.
SLAP	SCN3B	q9ny72	Ion channel	Sodium channel subunit beta-3	Modulates channel gating kinetics. Causes unique persistent sodium currents. Inactivates the sodium channel opening more slowly than the subunit beta-1. Its association with neurofascin may target the sodium channels to the nodes of Ranvier of developing axons and retain these channels at the nodes in mature myelinated axons (By similarity).

Both	SCN4A	p35499	Ion channel	Sodium channel protein type 4 subunit alpha	This protein mediates the voltage-dependent sodium ion permeability of excitable membranes. Assuming opened or closed conformations in response to the voltage difference across the membrane, the protein forms a sodium-selective channel through which Na^+ ions may pass in accordance with their electrochemical gradient. This sodium channel may be present in both denervated and innervated skeletal muscle.
SLAP	SCN4B	q8iwt1	Ion channel	Sodium channel subunit beta-4	Modulates channel gating kinetics. Causes negative shifts in the voltage dependence of activation of certain alpha sodium channels, but does not affect the voltage dependence of inactivation. Modulates the suceptibility of the sodium channel to inhibition by toxic peptides from spider, scorpion, wasp and sea anemone venom.
Both	SCN5A	q14524	Ion channel	Sodium channel protein type 5 subunit alpha	This protein mediates the voltage-dependent sodium ion permeability of excitable membranes. Assuming opened or closed conformations in response to the voltage difference across the membrane, the protein

					forms a sodium-selective channel through which Na^+ ions may pass in accordance with their electrochemical gradient. It is a tetrodotoxin-resistant Na^+ channel isoform. This channel is responsible for the initial upstroke of the action potential. Channel inactivation is regulated by intracellular calcium levels.
STITCH	SCN7A	q01118	Ion channel	Sodium channel protein type 7 subunit alpha	Mediates the voltage-dependent sodium ion permeability of excitable membranes. Assuming opened or closed conformations in response to the voltage difference across the membrane, the protein forms a sodium-selective channel through which Na^+ ions may pass in accordance with their electrochemical gradient.
STITCH	SCN8A	q9uqd0	Ion channel	Sodium channel protein type 8 subunit alpha	Mediates the voltage-dependent sodium ion permeability of excitable membranes. Assuming opened or closed conformations in response to the voltage difference across the membrane, the protein forms a sodium-selective channel through which Na+ ions may pass in accordance with their

					electrochemical gradient. In macrophages and melanoma cells, isoform 5 may participate in the control of podosome and invadopodia formation
Both	SCN9A	q15858	Ion channel	Sodium channel protein type 9 subunit alpha	Mediates the voltage-dependent sodium ion permeability of excitable membranes. Assuming opened or closed conformations in response to the voltage difference across the membrane, the protein forms a sodium-selective channel through which Na^+ ions may pass in accordance with their electrochemical gradient. It is a tetrodotoxin-sensitive Na^+ channel isoform. Plays a role in pain mechanisms, especially in the development of inflammatory pain (By similarity).
STITCH	SERPINA7	p05543	Transport	Thyroxine-binding globulin	Major thyroid hormone transport protein in serum.
STITCH	SHBG	p04278	Transport	Sex hormone-binding globulin	Functions as an androgen transport protein, but may also be involved in receptor mediated processes. Each dimer binds one molecule of steroid. Specific for 5-alpha-dihydrotestosterone, testosterone, and 17-beta-estradiol. Regulates the plasma metabolic

					clearance rate of steroid hormones by controlling their plasma concentration.
SLAP	SLC12A1	q13621	Transport	Solute carrier family 12 member 1	Electrically silent transporter system. Mediates sodium and chloride reabsorption. Plays a vital role in the regulation of ionic balance and cell volume.
SLAP	SLC12A3	p55017	Transport	Solute carrier family 12 member 3	Key mediator of sodium and chloride reabsorption in this nephron segment, accounting for a significant fraction of renal sodium reabsorption.
STITCH	SLC22A1	o15245	Transport	Solute carrier family 22 member 1	Translocates a broad array of organic cations with various structures and molecular weights including the model compounds 1-methyl-4-phenylpyridinium (MPP), tetraethylammonium (TEA), N-1-methylnicotinamide (NMN), 4-(4-(dimethylamino)styryl)-N-methylpyridinium (ASP), the endogenous compounds choline, guanidine, histamine, epinephrine, adrenaline, noradrenaline and dopamine, and the drugs quinine, and metformin. The transport of organic cations is inhibited by a broad array of compounds like tetramethylammonium (TMA), cocaine, lidocaine,

					NMDA receptor antagonists, atropine, prazosin, cimetidine, TEA and NMN, guanidine, cimetidine, choline, procainamide, quinine, tetrabutylammonium, and tetrapentylammonium. Translocates organic cations in an electrogenic and pH-independent manner. Translocates organic cations across the plasma membrane in both directions. Transports the polyamines spermine and spermidine. Transports pramipexole across the basolateral membrane of the proximal tubular epithelial cells. The choline transport is activated by MMTS. Regulated by various intracellular signaling pathways including inhibition by protein kinase A activation, and endogenously activation by the calmodulin complex, the calmodulin-dependent kinase II and LCK tyrosine kinase.
STITCH	SLC22A11	q9nsa0	Transport	Solute carrier family 22 member 11	Mediates saturable uptake of estrone sulfate, dehydroepiandrosterone sulfate and related compounds.
STITCH	SLC22A2	o15244	Transport	Solute carrier family 22 member 2	Mediates tubular uptake of organic compounds from circulation. Mediates the influx of agmatine,

					dopamine, noradrenaline (norepinephrine), serotonin, choline, famotidine, ranitidine, histamin, creatinine, amantadine, memantine, acriflavine, 4-[4-(dimethylamino)-styryl]-N-methylpyridinium ASP, amiloride, metformin, N-1-methylnicotinamide (NMN), tetraethylammonium (TEA), 1-methyl-4-phenylpyridinium (MPP), cimetidine, cisplatin and oxaliplatin. Cisplatin may develop a nephrotoxic action. Transport of creatinine is inhibited by fluoroquinolones such as DX-619 and LVFX. This transporter is a major determinant of the anticancer activity of oxaliplatin and may contribute to antitumor specificity.
Both	SLC22A6	q4u2r8	Transport	Solute carrier family 22 member 6	Involved in the renal elimination of endogenous and exogenous organic anions. Functions as organic anion exchanger when the uptake of one molecule of organic anion is coupled with an efflux of one molecule of endogenous dicarboxylic acid (glutarate, ketoglutarate, etc). Mediates the sodium-independent uptake of 2,3-dimercapto-1-

	propanesulfonic acid (DMPS) (By similarity). Mediates the sodium-independent uptake of p-aminohippurate (PAH), ochratoxin (OTA), acyclovir (ACV), 3'-azido-3-'deoxythymidine (AZT), cimetidine (CMD), 2,4-dichloro-phenoxyacetate (2,4-D), hippurate (HA), indoleacetate (IA), indoxyl sulfate (IS) and 3-carboxy-4-methyl-5-propyl-2-furanpropionate (CMPF), cidofovir, adefovir, 9-(2-phosphonylmethoxyethyl) guanine (PMEG), 9-(2-phosphonylmethoxyethyl) diaminopurine (PMEDAP) and edaravone sulfate. PAH uptake is inhibited by p-chloromercuribenzenesulphonate (PCMBS), diethyl pyrocarbonate (DEPC), sulindac, diclofenac, carprofen, glutarate and okadaic acid (By similarity). PAH uptake is inhibited by benzothiazolylcysteine (BTC), S-chlorotrifluoroethylcysteine (CTFC), cysteine S-conjugates S-dichlorovinylcysteine (DCVC), furosemide, steviol, phorbol 12-myristate 13-acetate (PMA), calcium ionophore A23187, benzylpenicillin, furosemide, indomethacin, bumetamide, losartan,

					probenecid, phenol red, urate, and alpha-ketoglutarate.
STITCH	SLC22A7	q9y694	Transport	Solute carrier family 22 member 7	Mediates sodium-independent multispecific organic anion transport. Transport of prostaglandin E2, prostaglandin F2, tetracycline, bumetanide, estrone sulfate, glutarate, dehydroepiandrosterone sulfate, allopurinol, 5-fluorouracil, paclitaxel, L-ascorbic acid, salicylate, ethotrexate, and alpha-ketoglutarate.
STITCH	SLC22A8	q8tcc7	Transport	Solute carrier family 22 member 8	Plays an important role in the excretion/detoxification of endogenous and exogenous organic anions, especially from the brain and kidney. Involved in the transport basolateral of steviol, fexofenadine. Transports benzylpenicillin (PCG), estrone-3-sulfate (E1S), cimetidine (CMD), 2,4-dichloro-phenoxyacetate (2,4-D), p-amino-hippurate (PAH), acyclovir (ACV) and ochratoxin (OTA).
STITCH	SLC2A6	q9ugq3	Transport	Solute carrier family 2, facilitated glucose transporter member 6	Facilitative glucose transporter; binds cytochalasin B with low affinity.

STITCH	SLC2A9	q9nrm0	Transport	Solute carrier family 2, facilitated glucose transporter member 9	Transport urate and fructose. May have a role in the urate reabsorption by proximal tubules. Also transports glucose at low rate
STITCH	SLC46A1	q96nt5	Transport	Proton-coupled folate transporter	Has been shown to act both as an intestinal proton-coupled high-affinity folate transporter and as an intestinal heme transporter which mediates heme uptake from the gut lumen into duodenal epithelial cells. The iron is then released from heme and may be transported into the bloodstream. Dietary heme iron is an important nutritional source of iron. Shows a higher affinity for folate than heme.
SLAP	SLC6A2	p23975	Transport	Sodium-dependent noradrenaline transporter	Amine transporter. Terminates the action of noradrenaline by its high affinity sodium-dependent reuptake into presynaptic terminals.
SLAP	SLC6A3	q01959	Transport	Sodium-dependent dopamine transporter	Amine transporter. Terminates the action of dopamine by its high affinity sodium-dependent reuptake into presynaptic terminals.
SLAP	SLC6A4	p31645	Transport	Sodium-dependent serotonin transporter	Serotonin transporter whose primary function in the central nervous system involves the regulation of serotonergic signaling via transport of serotonin

					molecules from the synaptic cleft back into the pre-synaptic terminal for re-utilization. Plays a key role in mediating regulation of the availability of serotonin to other receptors of serotonergic systems. Terminates the action of serotonin and recycles it in a sodium-dependent manner.
STITCH	SLC7A11	q9upy5	Transport	Cystine/glutamate transporter	Sodium-independent, high-affinity exchange of anionic amino acids with high specificity for anionic form of cystine and glutamate.
STITCH	SLCO1C1	q9nyb5	Transport	Solute carrier organic anion transporter family member 1C1	Mediates the Na^+-independent high affinity transport of organic anions such as the thyroid hormones thyroxine (T4) and rT3. Other potential substrates, such as triiodothyronine (T3), 17-beta-glucuronosyl estradiol, estrone-3-sulfate and sulfobromophthalein (BSP) are transported with much lower efficiency. May play a signifiant role in regulating T4 flux into and out of the brain (By similarity)
STITCH	SP1	p08047	Regulator	Transcription factor Sp1	Transcription factor that can activate or repress transcription in response to physiological and pathological stimuli. Binds with high affinity to GC-rich

					motifs and regulates the expression of a large number of genes involved in a variety of processes such as cell growth, apoptosis, differentiation and immune responses. Highly regulated by post-translational modifications (phosphorylations, sumoylation, proteolytic cleavage, glycosylation and acetylation). Binds also the PDGFR-alpha G-box promoter. May have a role in modulating the cellular response to DNA damage. Implicated in chromatin remodeling. Plays a role in the recruitment of SMARCA4/BRG1 on the c-FOS promoter. Plays an essential role in the regulation of FE65 gene expression. In complex with ATF7IP, maintains telomerase activity in cancer cells by inducing TERT and TERC gene expression. Isoform 3 is a stronger activator of transcription than isoform 1. Positively regulates the transcription of the core clock component ARNTL/BMAL1.
STITCH	SRC	p12931	Kinase	Proto-oncogene tyrosine-protein kinase Src	Non-receptor protein tyrosine kinase which is activated following engagement of many different classes of cellular receptors including immune

	response receptors, integrins and other adhesion receptors, receptor protein tyrosine kinases, G protein-coupled receptors as well as cytokine receptors. Participates in signaling pathways that control a diverse spectrum of biological activities including gene transcription, immune response, cell adhesion, cell cycle progression, apoptosis, migration, and transformation. Due to functional redundancy between members of the SRC kinase family, identification of the specific role of each SRC kinase is very difficult. SRC appears to be one of the primary kinases activated following engagement of receptors and plays a role in the activation of other protein tyrosine kinase (PTK) families. Receptor clustering or dimerization leads to recruitment of SRC to the receptor complexes where it phosphorylates the tyrosine residues within the receptor cytoplasmic domains. Plays an important role in the regulation of cytoskeletal organization through phosphorylation of specific substrates such as AFAP1. Phosphorylation of

	AFAP1 allows the SRC SH2 domain to bind AFAP1 and to localize to actin filaments. Cytoskeletal reorganization is also controlled through the phosphorylation of cortactin (CTTN). When cells adhere via focal adhesions to the extracellular matrix, signals are transmitted by integrins into the cell resulting in tyrosine phosphorylation of a number of focal adhesion proteins, including PTK2/FAK1 and paxillin (PXN). In addition to phosphorylating focal adhesion proteins, SRC is also active at the sites of cell-cell contact adherens junctions and phosphorylates substrates such as beta-catenin (CTNNB1), delta-catenin (CTNND1), and plakoglobin (JUP). Another type of cell-cell junction, the gap junction, is also a target for SRC, which phosphorylates connexin-43 (GJA1). SRC is implicated in regulation of pre-mRNA-processing and phosphorylates RNA-binding proteins such as KHDRBS1. Also plays a role in PDGF-mediated tyrosine phosphorylation of both STAT1 and STAT3, leading to

	increased DNA binding activity of these transcription factors. Involved in the RAS pathway through phosphorylation of RASA1 and RASGRF1. Plays a role in EGF-mediated calcium-activated chloride channel activation. Required for epidermal growth factor receptor (EGFR) internalization through phosphorylation of clathrin heavy chain (CLTC and CLTCL1) at 'Tyr-1477'. Involved in beta-arrestin (ARRB1 and ARRB2) desensitization through phosphorylation and activation of ADRBK1, leading to beta-arrestin phosphorylation and internalization. Has a critical role in the stimulation of the CDK20/MAPK3 mitogen-activated protein kinase cascade by epidermal growth factor. Might be involved not only in mediating the transduction of mitogenic signals at the level of the plasma membrane but also in controlling progression through the cell cycle via interaction with regulatory proteins in the nucleus. Plays an important role in osteoclastic bone resorption in conjunction with PTK2B/PYK2. Both the

					formation of a SRC-PTK2B/PYK2 complex and SRC kinase activity are necessary for this function. Recruited to activated integrins by PTK2B/PYK2, thereby phosphorylating CBL, which in turn induces the activation and recruitment of phosphatidylinositol 3-kinase to the cell membrane in a signaling pathway that is critical for osteoclast function. Promotes energy production in osteoclasts by activating mitochondrial cytochrome C oxidase. Phosphorylates DDR2 on tyrosine residues, thereby promoting its subsequent autophosphorylation. Phosphorylates RUNX3 and COX2 on tyrosine residues, TNK2 on 'Tyr-284' and CBL on 'Tyr-731'. Enhances DDX58/RIG-I-elicited antiviral signaling. Phosphorylates PDPK1 at 'Tyr-9', 'Tyr-373' and 'Tyr-376'. Phosphorylates BCAR1 at 'Tyr-128'. Phosphorylates CBLC at multiple tyrosine residues, phosphorylation at 'Tyr-341' activates CBLC E3 activity.
STITCH	SST	p61278	Hormone	Somatostatin	Somatostatin inhibits the release of somatotropin.

STITCH	ST6GAL1	p15907	Transport	Beta-galactoside alpha-2,6-sialyltransferase 1	Transfers sialic acid from CMP-sialic acid to galactose-containing acceptor substrates.
STITCH	STAR	p49675	Regulator	Steroidogenic acute regulatory protein, mitochondrial	Plays a key role in steroid hormone synthesis by enhancing the metabolism of cholesterol into pregnenolone. Mediates the transfer of cholesterol from the outer mitochondrial membrane to the inner mitochondrial membrane where it is cleaved to pregnenolone.
STITCH	STAT3	p40763	Immune functions	Signal transducer and activator of transcription 3	Signal transducer and transcription activator that mediates cellular responses to interleukins, KITLG/SCF and other growth factors. May mediate cellular responses to activated FGFR1, FGFR2, FGFR3 and FGFR4. Binds to the interleukin-6 (IL-6)-responsive elements identified in the promoters of various acute-phase protein genes. Activated by IL31 through IL31RA. Cytoplasmic STAT3 represses macroautophagy by inhibiting EIF2AK2/PKR activity. Plays an important role in host defense in methicillin-resistant S.aureus lung infection by regulating the

					expression of the antimicrobial lectin REG3G (By similarity).
STITCH	SULT1E1	p49888	Enzyme	Estrogen sulfotransferase	Sulfotransferase that utilizes 3'-phospho-5'-adenylyl sulfate (PAPS) as sulfonate donor to catalyze the sulfate conjugation of estradiol and estrone. May play a role in the regulation of estrogen receptor activity by metabolizing free estradiol. Maximally sulfates beta-estradiol and estrone at concentrations of 20 nM. Also sulfates dehydroepiandrosterone, pregnenolone, ethinylestradiol, equalenin, diethylstilbesterol and 1-naphthol, at significantly higher concentrations; however, cortisol, testosterone and dopamine are not sulfated.
STITCH	TAS2R1	q9nyw7	Receptor	Taste receptor type 2 member 1	Receptor that may play a role in the perception of bitterness and is gustducin-linked. May play a role in sensing the chemical composition of the gastrointestinal content. The activity of this receptor may stimulate alpha gustducin, mediate PLC-beta-2 activation and lead to the gating of TRPM5.

STITCH	TAS2R10	q9ntw0	Receptor	Taste receptor type 2 member 10	Gustducin-coupled strychnine receptor implicated in the perception of bitter compounds in the oral cavity and the gastrointestinal tract. Signals through PLCB2 and the calcium-regulated cation channel TRPM5.
STITCH	TAS2R14	q9nyv8	Receptor	Taste receptor type 2 member 14	Receptor that may play a role in the perception of bitterness and is gustducin-linked. May play a role in sensing the chemical composition of the gastrointestinal content. The activity of this receptor may stimulate alpha gustducin, mediate PLC-beta-2 activation and lead to the gating of TRPM5 (By similarity).
STITCH	TAS2R30	p59541	Receptor	Taste receptor type 2 member 30	Receptor that may play a role in the perception of bitterness and is gustducin-linked. May play a role in sensing the chemical composition of the gastrointestinal content. The activity of this receptor may stimulate alpha gustducin, mediate PLC-beta-2 activation and lead to the gating of TRPM5 (By similarity).
STITCH	TAS2R38	p59533	Receptor	Taste receptor type 2 member 38	Receptor that may play a role in the perception of bitterness and is gustducin-linked. May play a role in

					sensing the chemical composition of the gastrointestinal content. The activity of this receptor may stimulate alpha gustducin, mediate PLC-beta-2 activation and lead to the gating of TRPM5 (By similarity).
STITCH	TAS2R4	q9nyw5	Receptor	Taste receptor type 2 member 4	Gustducin-coupled receptor for denatonium and N(6)-propyl-2-thiouracil implicated in the perception of bitter compounds in the oral cavity and the gastrointestinal tract. Signals through PLCB2 and the calcium-regulated cation channel TRPM5. In airway epithelial cells, binding of denatonium increases the intracellular calcium ion concentration and stimulates ciliary beat frequency.
STITCH	TBXAS1	p24557	Enzyme	Thromboxane-A synthase	heme binding; monooxygenase activity; thromboxane-A synthase activity; iron ion binding; oxidoreductased activity, actining on paired donors, with incorporation or reduction of molecular oxygen
STITCH	TFAP2A	p05549	Regulator	Transcription factor AP-2-alpha	Sequence-specific DNA-binding protein that interacts with inducible viral and cellular enhancer elements to regulate transcription of selected genes. AP-2 factors

					bind to the consensus sequence 5'-GCCNNNGGC-3' and activate genes involved in a large spectrum of important biological functions including proper eye, face, body wall, limb and neural tube development. They also suppress a number of genes including MCAM/MUC18, C/EBP alpha and MYC. AP-2-alpha is the only AP-2 protein required for early morphogenesis of the lens vesicle. Together with the CITED2 coactivator, stimulates the PITX2 P1 promoter transcription activation. Associates with chromatin to the PITX2 P1 promoter region.
STITCH	TG	p01266		Thyroglobulin	Precursor of the iodinated thyroid hormones thyroxine (T4) and triiodothyronine (T3).
STITCH	THRA	p10827	Receptor	Thyroid hormone receptor alpha	Nuclear hormone receptor that can act as a repressor or activator of transcription. High affinity receptor for thyroid hormones, including triiodothyronine and thyroxine.
STITCH	TMSB10	p63313	Structural	Thymosin beta-10	Plays an important role in the organization of the cytoskeleton. Binds to and sequesters actin

					monomers (G actin) and therefore inhibits actin polymerization (By similarity)
Both	TNF	p01375	Signalling	Tumor necrosis factor	Cytokine that binds to TNFRSF1A/TNFR1 and TNFRSF1B/TNFBR. It is mainly secreted by macrophages and can induce cell death of certain tumor cell lines. It is potent pyrogen causing fever by direct action or by stimulation of interleukin-1 secretion and is implicated in the induction of cachexia, Under certain conditions it can stimulate cell proliferation and induce cell differentiation. Impairs regulatory T-cells (Treg) function in individuals with rheumatoid arthritis via FOXP3 dephosphorylation. Upregulates the expression of protein phosphatase 1 (PP1), which dephosphorylates the key 'Ser-418' residue of FOXP3, thereby inactivating FOXP3 and rendering Treg cells functionally defective (PubMed:23396208). The TNF intracellular domain (ICD) form induces IL12 production in dendritic cells.

STITCH	TNFRSF10B	o14763	Receptor	Tumour necrosis factor receptor superfamily member 10B	Receptor for the cytotoxic ligand TNFSF10/TRAIL. The adapter molecule FADD recruits caspase-8 to the activated receptor. The resulting death-inducing signaling complex (DISC) performs caspase-8 proteolytic activation which initiates the subsequent cascade of caspases (aspartate-specific cysteine proteases) mediating apoptosis. Promotes the activation of NF-kappa-B. Essential for ER stress-induced apoptosis.
STITCH	TNFRSF1B	p20333	Receptor	Tumour necrosis factor receptor superfamily member 1B	Receptor with high affinity for TNFSF2/TNF-alpha and approximately 5-fold lower affinity for homotrimeric TNFSF1/lymphotoxin-alpha. The TRAF1/TRAF2 complex recruits the apoptotic suppressors BIRC2 and BIRC3 to TNFRSF1B/TNFR2. This receptor mediates most of the metabolic effects of TNF-alpha. Isoform 2 blocks TNF-alpha-induced apoptosis, which suggests that it regulates TNF-alpha function by antagonizing its biological activity.

STITCH	TNFSF10	p50591	Signalling	Tumour necrosis factor ligand superfamily member 10	Cytokine that binds to TNFRSF10A/TRAILR1, TNFRSF10B/TRAILR2, TNFRSF10C/TRAILR3, TNFRSF10D/TRAILR4 and possibly also to TNFRSF11B/OPG. Induces apoptosis. Its activity may be modulated by binding to the decoy receptors TNFRSF10C/TRAILR3, TNFRSF10D/TRAILR4 and TNFRSF11B/OPG that cannot induce apoptosis.
SLAP	TP53	p04637	Regulator	Cellular tumor antigen p53	Acts as a tumor suppressor in many tumor types; induces growth arrest or apoptosis depending on the physiological circumstances and cell type. Involved in cell cycle regulation as a trans-activator that acts to negatively regulate cell division by controlling a set of genes required for this process. One of the activated genes is an inhibitor of cyclin-dependent kinases. Apoptosis induction seems to be mediated either by stimulation of BAX and FAS antigen expression, or by repression of Bcl-2 expression. In cooperation with mitochondrial PPIF is involved in activating oxidative stress-induced necrosis; the function is largely independent of transcription. Induces the

					transcription of long intergenic non-coding RNA p21 (lincRNA-p21) and lincRNA-Mkln1. LincRNA-p21 participates in TP53-dependent transcriptional repression leading to apoptosis and seem to have to effect on cell-cycle regulation. Implicated in Notch signalling cross-over. Prevents CDK7 kinase activity when associated to CAK complex in response to DNA damage, thus stopping cell cycle progression. Isoform 2 enhances the transactivation activity of isoform 1 from some but not all TP53-inducible promoters. Isoform 4 suppresses transactivation activity and impairs growth suppression mediated by isoform 1. Isoform 7 inhibits isoform 1-mediated apoptosis. Regulates the circadian clock by repressing CLOCK-ARNTL/BMAL1-mediated transcriptional activation of PER2
SLAP	TPH1	p17752	Enzyme	Tryptophan 5-hydroxylase 1	amino acid binding; iron ion binding; tryptophan 5-monoxygenase activity

STITCH	TPO	p07202	Enzyme	Thyroid peroxidase	Iodination and coupling of the hormonogenic tyrosines in thyroglobulin to yield the thyroid hormones T_3 and T_4.
STITCH	TRH	p20396	Regulator	Pro-thyrotropin-releasing hormone	Functions as a regulator of the biosynthesis of TSH in the anterior pituitary gland and as a neurotransmitter/ neuromodulator in the central and peripheral nervous systems. May promote hair shaft elongation, prolong the hair cycle growth phase (anagen) and antagonized its termination by TGFB2. May also increase proliferation and inhibited apoptosis of hair matrix keratinocytes
STITCH	TSHR	p16473	Receptor	Thyrotropin receptor	Receptor for thyrothropin. Plays a central role in controlling thyroid cell metabolism. The activity of this receptor is mediated by G proteins which activate adenylate cyclase. Also acts as a receptor for thyrostimulin (GPA2+GPB5).
STITCH	UGT1A3	p35503	Metabolism	UDP-glucuronosyltransferase 1-3	UDPGT is of major importance in the conjugation and subsequent elimination of potentially toxic xenobiotics and endogenous compounds. Isoform 2

					lacks transferase activity but acts as a negative regulator of isoform 1.
STITCH	UGT1A4	p22310	Metabolism	UDP-glucuronosyltransferase 1-4	UDPGT is of major importance in the conjugation and subsequent elimination of potentially toxic xenobiotics and endogenous compounds. This isoform glucuronidates bilirubin IX-alpha to form both the IX-alpha-C8 and IX-alpha-C12 monoconjugates and diconjugate. Isoform 2 lacks transferase activity but acts as a negative regulator of isoform 1 (By similarity).
STITCH	UGT2B7	p16662	Metabolism	UDP-glucuronosyltransferase 2B7	UDPGT is of major importance in the conjugation and subsequent elimination of potentially toxic xenobiotics and endogenous compounds. Its unique specificity for 3,4-catechol oestrogens and oestriol suggests it may play an important role in regulating the level and activity of these potent and active oestrogen metabolites. Is also active with androsterone, hyodeoxycholic acid and tetrachlorocatechol (in vitro).

STITCH	VEGFA	p15692	Vascular endothelial growth factor A	Growth factor active in angiogenesis, vasculogenesis and endothelial cell growth. Induces endothelial cell proliferation, promotes cell migration, inhibits apoptosis and induces permeabilisation of blood vessels. Binds to the FLT1/VEGFR1 and KDR/VEGFR2 receptors, heparan sulfate and heparin. NRP1/Neuropilin-1 binds isoforms VEGF-165 and VEGF-145. Isoform VEGF165B binds to KDR but does not activate downstream signalling pathways, does not activate angiogenesis and inhibits tumour growth.
STITCH	VEGFC	p49767	Vascular endothelial growth factor C	Growth factor active in angiogenesis, and endothelial cell growth, stimulating their proliferation and migration and also has effects on the permeability of blood vessels. May function in angiogenesis of the venous and lymphatic vascular systems during embryogenesis, and also in the maintenance of differentiated lymphatic endothelium in adults. Binds and activates VEGFR-2 (KDR/FLK1) and VEGFR-3 (FLT4) receptors.

STITCH	XDH	p47989	Regulator	Xanthine dehydrogenase/oxidase	Key enzyme in purine degradation. Catalyses the oxidation of hypoxanthine to xanthine. Catalyses the oxidation of xanthine to uric acid. Contributes to the generation of reactive oxygen species. Has also low oxidase activity towards aldehydes (in vitro).
STITCH	YWHAE	p62258	Regulator	14-3-3 protein epsilon	Adapter protein implicated in the regulation of a large spectrum of both general and specialized signaling pathways. Binds to a large number of partners, usually by recognition of a phosphoserine or phosphothreonine motif. Binding generally results in the modulation of the activity of the binding partner.

Appendix 3: Results of SLAP

11.1 Allopurinol

target	p value
IL1B	0.7284

11.2 Carbamazepine

target	p value
HTR2B	5.5773114665e-05
HTR2A	8.22392383655e-05
DRD2	9.20315383451e-05
CYP2C9	1e-04
SCN2A	1e-04
SCN3A	1e-04
CYP3A4	2e-04
DRD3	2e-04
HTR2C	2e-04
CYP1A2	3e-04
DRD5	3e-04
ABCC1	4e-04
DRD4	4e-04
ABCB1	5e-04
HTR7	5e-04
DRD1	6e-04
PGR	6e-04
CYP2A6	8e-04
ABCC2	0.001
HTR1A	0.001
CYP2B6	0.0011
CYP2C8	0.0011
NR3C2	0.0011

target	p value
KCNH2	0.0012
HTR1B	0.0013
HTR1F	0.0013
HTR1D	0.0017
AR	0.0018
SCN10A	0.0018
HTR4	0.0019
ABCG2	0.0023
HRH1	0.0023
SCN5A	0.0029
NR1I2	0.003
SLC6A4	0.0032
CYP2C18	0.0037
JUN	0.0037
SCN4A	0.0037
FPR1	0.0038
CYP17A1	0.0039
GSTA1	0.0041
GSTM1	0.0042
SCN1A	0.0043
HTR1E	0.0047
NFKB1	0.0049
CHRNA7	0.005
ESR1	0.0054
HTR3A	0.0062
EPHX2	0.0064
TP53	0.0064
CYP19A1	0.0069
NR1I3	0.0069
NFKB2	0.007
PTGS2	0.0075
ADRA2A	0.0081

target	p value
CYP11B1	0.0084
PTGS1	0.0087
GSTP1	0.0092
HTR6	0.0094
SCN9A	0.0094
MAOA	0.0095
ABCB11	0.0099
NR3C1	0.0099

11.3 Celecoxib

target	p value
CA1	3.19476265354e-06
CA2	5.55073451469e-06
PTGS2	1.40995423594e-05
CA9	1.49023706417e-05
CA12	2.40337858337e-05
CA14	2.50867494557e-05
CA4	2.59960900877e-05
CA5A	3.12292726893e-05
CA5B	3.1998151108e-05
CA7	3.60611733822e-05
CA13	5.50738672461e-05
PTGS1	6.04181918484e-05
PPARA	6.31778502987e-05
ADRA2A	6.45500039546e-05
HTR1D	6.99928488774e-05
ADRA2C	7.52018764707e-05
ADRA2B	7.59544860616e-05
HTR1B	7.66886409999e-05
AKT2	1e-04

CA3	1e-04
CASP7	1e-04
CDK4	1e-04
CNR1	1e-04
DRD2	1e-04
HTR1F	1e-04
HTR2A	1e-04
HTR2C	1e-04
CHRM3	2e-04
CHRM4	2e-04
DRD1	2e-04
DRD3	2e-04
DRD5	2e-04
CNR2	3e-04
DRD4	3e-04
HRH1	3e-04
HTR1A	3e-04
HTR7	3e-04
CASP1	4e-04
CDK2	4e-04
CHRM1	4e-04
HTR2B	4e-04
HRH2	5e-04
PPARD	5e-04
ALOX5	6e-04
MMP2	6e-04
CYP3A4	8e-04
CHRM2	9e-04
HTR1E	9e-04
HTR6	9e-04
MMP1	9e-04
HRH4	0.001
HTR4	0.0011

KCNH2	0.0011
MMP8	0.0011
PTGER4	0.0011
NISCH	0.0014
ADRA1A	0.0017
MAPK12	0.0017
CYP1A2	0.0018
PNMT	0.0018
BCL2	0.0019
CA11	0.0019
CYP2C9	0.0019
HTR3A	0.002
MMP13	0.0021
MMP3	0.0022
CA8	0.0023
PTGER3	0.0023
ADAM17	0.0026
PTGER1	0.0027
SLC6A4	0.0027
CA10	0.0028
HRH3	0.0028
TPH1	0.0029
NFKB1	0.003
MMP14	0.0038
ADRA1B	0.0039
TP53	0.0039
BCL2L1	0.0044
ABCC2	0.0045
NFKB2	0.0045
ADRA1D	0.0046
ABCB1	0.0047
ROCK1	0.0051
ADRB2	0.0053

SLC22A6	0.0055
ADRB1	0.0061
CHRM5	0.0061
CYP2C8	0.0061
AKT1	0.0064
FGF1	0.0065
CHRNA7	0.0066
SLC12A1	0.0066
ASL	0.0067
CCND1	0.0068
CYP2B6	0.0068
PRKACA	0.0068
CASP3	0.007
FGF2	0.0073
PGR	0.0077
TNF	0.008
MAPK1	0.0082
MMP7	0.0082
SLC12A3	0.0082
IL1B	0.0083
MMP11	0.0083
KCNMA1	0.0091
ROCK2	0.0091
DDC	0.0096
HNMT	0.0097
SCN1A	0.0099
PLA2G4A	0.01
CYP19A1	0.0115
PDPK1	0.0131
MMP9	0.0136
PPARG	0.017
CCL2	0.0181
SLC6A3	0.0183

GSTP1	0.0213
CCR5	0.022
AR	0.0269
MAPK14	0.0287
PTGER2	0.0288
ABCC4	0.0355
OPRM1	0.0492
OPRK1	0.0692

11.4 Clavulanic acid

No Targets Predicted

11.5 Flucloxacillin

No Targets Predicted

11.6 Lamotrigine

target	p value
SCN2A	9.70053876914e-06
SCN1A	1.21165483008e-05
SCN3A	1.26338520879e-05
SCN5A	1e-04
SCN10A	7e-04
SCN4A	8e-04
SCN9A	0.0011
SCN4B	0.0014
CYP3A4	0.0015
SCN2B	0.0016
SCN1B	0.0017
HRH1	0.0018
SCN11A	0.0019
SCN3B	0.0021
HRH3	0.0024

HTR2A	0.0024
CACNA1I	0.0027
ABCC1	0.0028
KCNH2	0.0028
CACNA1C	0.0039
CACNA1H	0.0041
ABCB1	0.0043
CACNA1G	0.0049
SLC6A4	0.0049
DRD2	0.0053
HTR2C	0.0056
SLC6A2	0.0059
CACNA1D	0.007
GRIN2B	0.0076
ABCC2	0.0077
CCR5	0.0082
CACNA1S	0.0083
SLC6A3	0.0087
ABCG2	0.0088
DRD1	0.0088
ADRA1A	0.0091
CALM1	0.0093
FPR1	0.0093
CACNA1F	0.0094
KCNQ1	0.0098
DHFR	0.4712

11.7 Nevirapine

No targets predicted

11.8 Phenytoin

target	p value

SCN2A	2.31001566489e-05
SCN1A	3.03887677753e-05
SCN3A	3.21342523509e-05
CYP3A4	7.26175587376e-05
CYP2C9	1e-04
SCN5A	2e-04
CYP1A2	3e-04
ABCC1	9e-04
CYP2B6	9e-04
ABCB1	0.0011
CYP2A6	0.0012
SCN10A	0.0014
SCN4A	0.0015
KCNH2	0.0018
SCN4B	0.0018
SCN2B	0.0019
SCN1B	0.002
CYP2C8	0.0021
SCN3B	0.0023
SCN9A	0.0023
ABCC2	0.0036
HRH1	0.0042
PGR	0.0047
SCN11A	0.0047
ABCG2	0.0052
EPHX2	0.0053
CACNA1H	0.0069
CACNA1I	0.0075
CACNA1C	0.0079
NR1I2	0.008
CYP19A1	0.0085
CYP4A11	0.0085
CACNA1G	0.0087

FPR1	0.0088
CYP17A1	0.0092

11.9 Propylthiouracil

No targets predicted.

11.10 Sulfasalazine

target	p value
CA4	1.61694131162e-06
CA2	4.98441516594e-06
CA1	6.0048935786e-06
CA9	7.60332405514e-06
CA12	5.53898608426e-05
CA5A	2e-04
CA5B	2e-04
NFKB1	2e-04
CA14	3e-04
CA7	6e-04
CA13	8e-04
JUN	0.001
CA3	0.0021
TPH1	0.0067
CA11	0.0079
MMP8	0.0093
IL1B	0.0846
NFKB2	0.4083

11.11 Sulindac

No targets predicted.

Appendix 4: Results from STITCH 4.0

12.1 Allopurinol

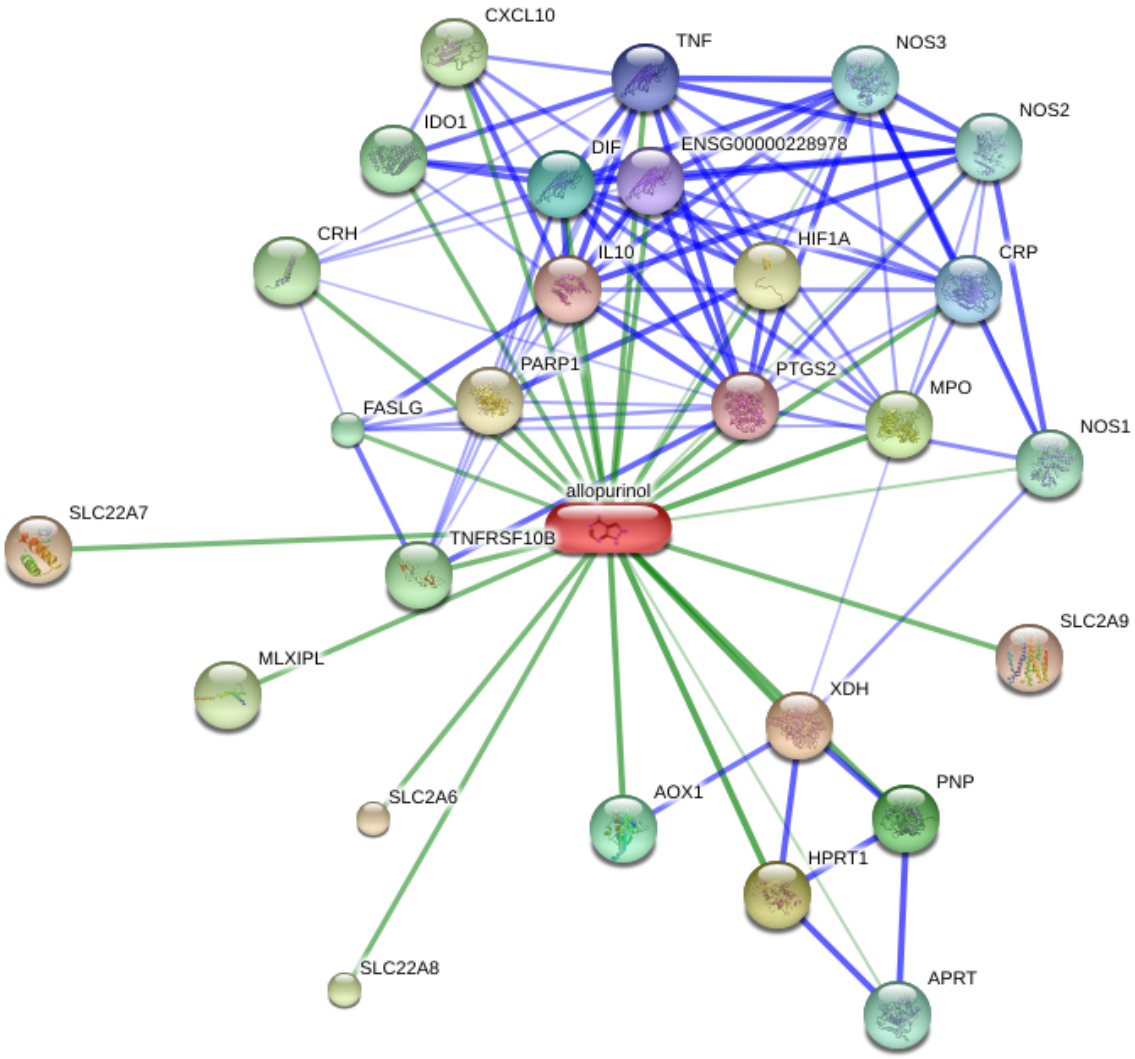

Predicted Functional Partners:

	XDH	xanthine dehydrogenase; This enzyme can be converted from the dehydrogenase form (D) to the oxi [...] (1333 aa)	0.996
	HPRT1	hypoxanthine phosphoribosyltransferase 1 (218 aa)	0.988
	MPO	myeloperoxidase; Part of the host defense system of polymorphonuclear leukocytes. It is respons [...] (745 aa)	0.915
	PNP	purine nucleoside phosphorylase (289 aa)	0.914

AOX1	aldehyde oxidase 1 (1338 aa)	0.905
DIF	Tumor necrosis factor Precursor (TNF-alpha)(Tumor necrosis factor ligand superfamily member 2)([...] (233 aa)	0.835
CRP	C-reactive protein, pentraxin-related; Displays several functions associated with host defense- [...] (224 aa)	0.834
TNF	tumor necrosis factor (TNF superfamily, member 2); Cytokine that binds to TNFRSF1A/TNFR1 and TN [...] (233 aa)	0.827
ENSG00000228978	Tumor necrosis factor (TNF superfamily, member 2) Fragment (171 aa)	0.825
PTGS2	prostaglandin-endoperoxide synthase 2 (prostaglandin G/H synthase and cyclooxygenase); May have [...] (604 aa)	0.823
IL10	interleukin 10; Inhibits the synthesis of a number of cytokines, including IFN-gamma, IL-2, IL- [...] (178 aa)	0.819
SLC2A9	solute carrier family 2 (facilitated glucose transporter), member 9; Transport urate and fructo [...] (540 aa)	0.819
SLC22A7	solute carrier family 22 (organic anion transporter), member 7; Mediates sodium-independent mul [...] (548 aa)	0.800
SLC2A6	solute carrier family 2 (facilitated glucose transporter), member 6; Facilitative glucose trans [...] (507 aa)	0.800
PARP1	poly (ADP-ribose) polymerase 1; Involved in the base excision repair (BER) pathway, by catalyzi [...] (1014 aa)	0.800
HIF1A	hypoxia inducible factor 1, alpha subunit (basic helix-loop-helix transcription factor); Functi [...] (826 aa)	0.800
SLC22A8	solute carrier family 22 (organic anion transporter), member 8; Plays an important role in the [...] (542 aa)	0.800
MLXIPL	MLX interacting protein-like; Transcriptional repressor. Binds to the canonical and non-canonic [...] (852 aa)	0.800
CXCL10	chemokine (C-X-C motif) ligand 10; Chemotactic for monocytes and T-lymphocytes. Binds to CXCR3 (98 aa)	0.800

CRH	corticotropin releasing hormone; This hormone from hypothalamus regulates the release of cortic [...] (196 aa)	0.800
TNFRSF10B	tumor necrosis factor receptor superfamily, member 10b; Receptor for the cytotoxic ligand TNFSF [...] (440 aa)	0.800
IDO1	indoleamine 2,3-dioxygenase 1; Catalyzes the cleavage of the pyrrol ring of tryptophan and inco [...] (403 aa)	0.800
FASLG	Fas ligand (TNF superfamily, member 6); Cytokine that binds to TNFRSF6/FAS, a receptor that tra [...] (281 aa)	0.719
NOS1	nitric oxide synthase 1 (neuronal); Produces nitric oxide (NO) which is a messenger molecule wi [...] (1434 aa)	0.504
APRT	adenine phosphoribosyltransferase; Catalyzes a salvage reaction resulting in the formation of A [...] (180 aa)	0.453
NOS2	nitric oxide synthase 2, inducible; Produces nitric oxide (NO) which is a messenger molecule wi [...] (1153 aa)	0.446
NOS3	nitric oxide synthase 3 (endothelial cell); Produces nitric oxide (NO) which is implicated in v [...] (1203 aa)	0.420

12.2 Carbamazepine

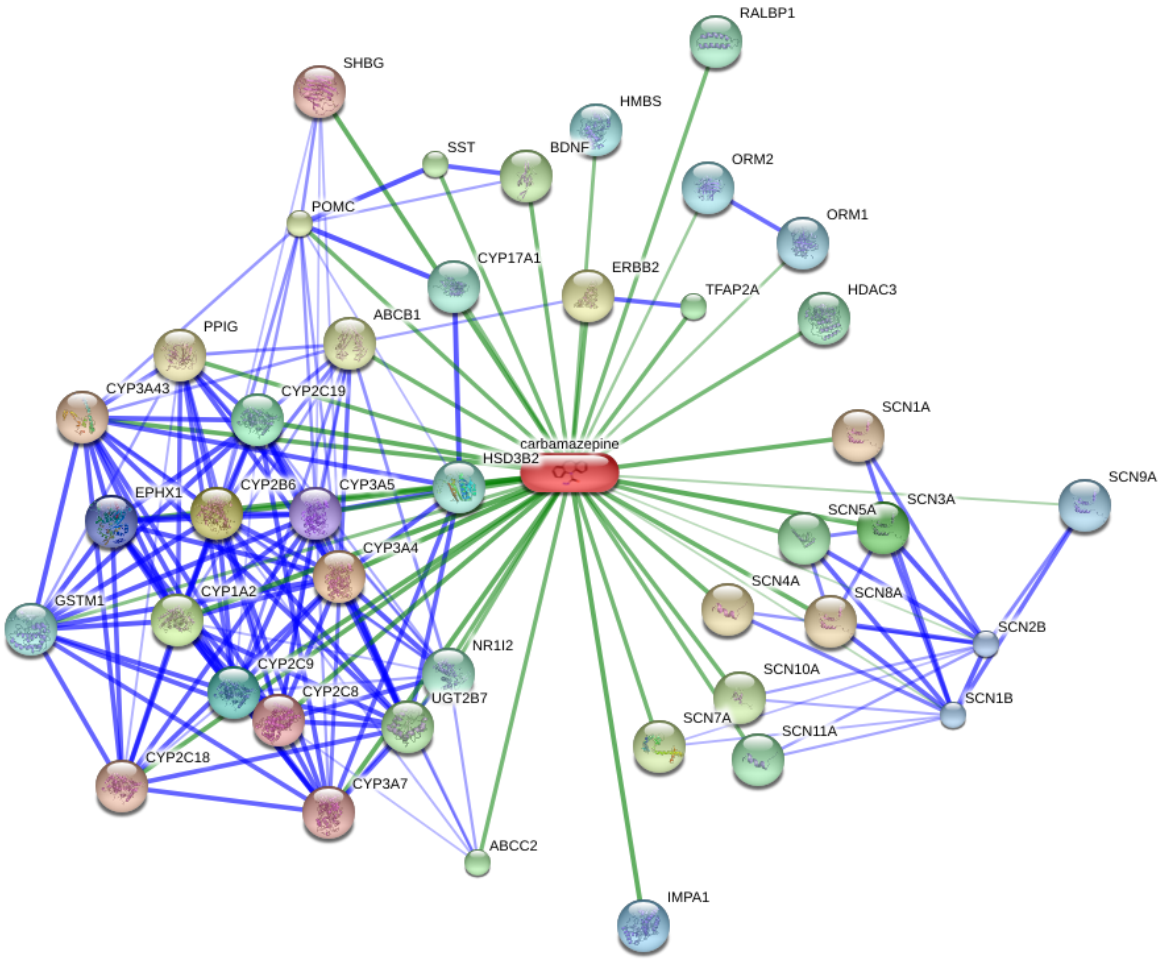

Predicted Functional Partners:

●	CYP3A4	cytochrome P450, family 3, subfamily A, polypeptide 4; Cytochromes P450 are a group of heme-thi [...] (503 aa)	0.989
●	CYP2B6	cytochrome P450, family 2, subfamily B, polypeptide 6; Cytochromes P450 are a group of heme-thi [...] (491 aa)	0.984
●	CYP1A2	cytochrome P450, family 1, subfamily A, polypeptide 2; Cytochromes P450 are a group of heme-thi [...] (516 aa)	0.969
●	SCN3A	sodium channel, voltage-gated, type III, alpha subunit; Mediates the voltage-dependent sodium i [...] (2000 aa)	0.951
●	CYP2C19	cytochrome P450, family 2, subfamily C, polypeptide 19; Responsible for the metabolism of a num [...] (490 aa)	0.930

CYP2C9	cytochrome P450, family 2, subfamily C, polypeptide 9; Cytochromes P450 are a group of heme-thi [...] (490 aa)	0.930
IMPA1	inositol(myo)-1(or 4)-monophosphatase 1; Responsible for the provision of inositol required for [...] (336 aa)	0.929
EPHX1	epoxide hydrolase 1, microsomal (xenobiotic); Biotransformation enzyme that catalyzes the hydro [...] (455 aa)	0.927
CYP3A5	cytochrome P450, family 3, subfamily A, polypeptide 5; Cytochromes P450 are a group of heme-thi [...] (502 aa)	0.921
CYP2C8	cytochrome P450, family 2, subfamily C, polypeptide 8; Cytochromes P450 are a group of heme-thi [...] (490 aa)	0.921
CYP3A7	cytochrome P450, family 3, subfamily A, polypeptide 7; Cytochromes P450 are a group of heme-thi [...] (503 aa)	0.912
SHBG	sex hormone-binding globulin; Functions as an androgen transport protein, but may also be invol [...] (402 aa)	0.911
CYP2C18	cytochrome P450, family 2, subfamily C, polypeptide 18; Cytochromes P450 are a group of heme-th [...] (490 aa)	0.900
CYP3A43	cytochrome P450, family 3, subfamily A, polypeptide 43; Exhibits low testosterone 6-beta-hydrox [...] (504 aa)	0.900
SCN1A	sodium channel, voltage-gated, type I, alpha subunit; Mediates the voltage-dependent sodium ion [...] (1998 aa)	0.880
SCN8A	sodium channel, voltage gated, type VIII, alpha subunit; Mediates the voltage-dependent sodium [...] (1980 aa)	0.873
SCN4A	sodium channel, voltage-gated, type IV, alpha subunit; This protein mediates the voltage-depend [...] (1836 aa)	0.860
PPIG	peptidylprolyl isomerase G (cyclophilin G); PPIases accelerate the folding of proteins. It cata [...] (754 aa)	0.860
ERBB2	v-erb-b2 erythroblastic leukemia viral oncogene homolog 2, neuro/glioblastoma derived oncogene [...] (1255 aa)	0.840
ABCB1	ATP-binding cassette, sub-family B (MDR/TAP), member 1; Energy-dependent efflux pump responsibl [...] (1280 aa)	0.836
POMC	proopiomelanocortin; ACTH stimulates the adrenal glands to release cortisol (267 aa)	0.831

SCN7A	sodium channel, voltage-gated, type VII, alpha; Mediates the voltage-dependent sodium ion perme [...] (1682 aa)	0.828
SCN10A	sodium channel, voltage-gated, type X, alpha subunit; This protein mediates the voltage-depende [...] (1956 aa)	0.827
BDNF	brain-derived neurotrophic factor; During development, promotes the survival and differentiatio [...] (329 aa)	0.827
SST	somatostatin; Somatostatin inhibits the release of somatotropin (116 aa)	0.823
UGT2B7	UDP glucuronosyltransferase 2 family, polypeptide B7; UDPGT is of major importance in the conju [...] (529 aa)	0.819
ABCC2	ATP-binding cassette, sub-family C (CFTR/MRP), member 2; Mediates hepatobiliary excretion of nu [...] (1545 aa)	0.818
TFAP2A	transcription factor AP-2 alpha (activating enhancer binding protein 2 alpha); Sequence-specifi [...] (437 aa)	0.814
SCN5A	sodium channel, voltage-gated, type V, alpha subunit; This protein mediates the voltage-depende [...] (2016 aa)	0.813
SCN11A	sodium channel, voltage-gated, type XI, alpha subunit; This protein mediates the voltage-depend [...] (1791 aa)	0.800
HDAC3	histone deacetylase 3; Responsible for the deacetylation of lysine residues on the N-terminal p [...] (428 aa)	0.800
RALBP1	ralA binding protein 1; Can activate specifically hydrolysis of GTP bound to RAC1 and CDC42, bu [...] (655 aa)	0.800
NR1I2	nuclear receptor subfamily 1, group I, member 2; Nuclear receptor that binds and is activated b [...] (473 aa)	0.742
CYP17A1	cytochrome P450, family 17, subfamily A, polypeptide 1; Conversion of pregnenolone and progeste [...] (508 aa)	0.700
HSD3B2	hydroxy-delta-5-steroid dehydrogenase, 3 beta- and steroid delta-isomerase 2; 3-beta-HSD is a b [...] (372 aa)	0.700
GSTM1	glutathione S-transferase mu 1; Conjugation of reduced glutathione to a wide number of exogenou [...] (218 aa)	0.700
HMBS	hydroxymethylbilane synthase; Tetrapolymerization of the monopyrrole PBG into the hydroxymethyl [...] (361 aa)	0.700

●	ORM2	orosomucoid 2; Appears to function in modulating the activity of the immune system during the a [...] (201 aa)	0.583
●	ORM1	orosomucoid 1; Appears to function in modulating the activity of the immune system during the a [...] (201 aa)	0.583
●	SCN9A	sodium channel, voltage-gated, type IX, alpha subunit; Mediates the voltage-dependent sodium io [...] (1977 aa)	0.489
●	SCN1B	sodium channel, voltage-gated, type I, beta; Crucial in the assembly, expression, and functiona [...] (268 aa)	0.432
●	SCN2B	sodium channel, voltage-gated, type II, beta; Crucial in the assembly, expression, and function [...] (215 aa)	0.413

12.3 Celecoxib

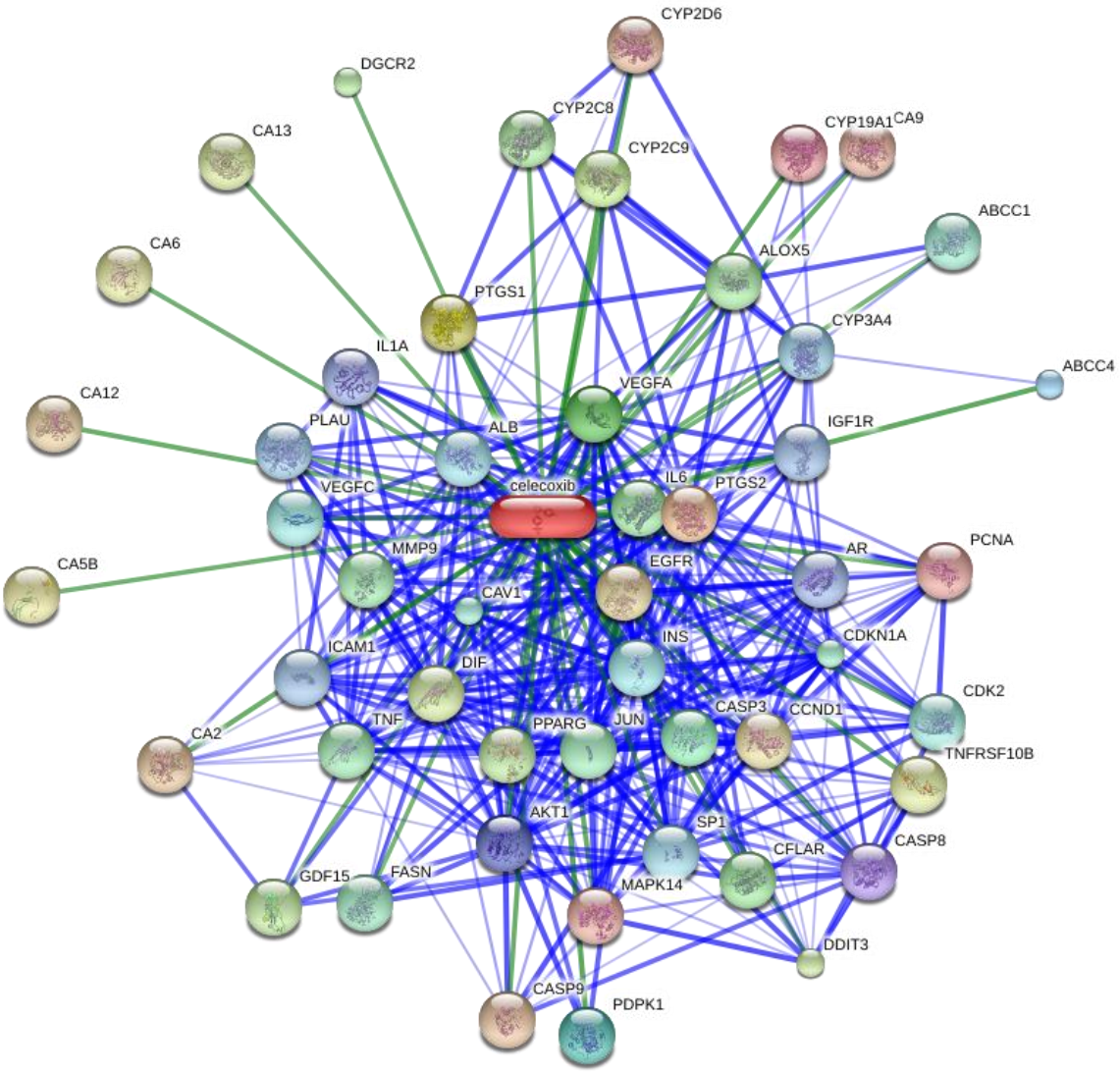

Predicted Functional Partners:

PTGS2	prostaglandin-endoperoxide synthase 2 (prostaglandin G/H synthase and cyclooxygenase); May have [...] (604 aa)	0.999
PTGS1	prostaglandin-endoperoxide synthase 1 (prostaglandin G/H synthase and cyclooxygenase); May play [...] (599 aa)	0.997
CYP2C9	cytochrome P450, family 2, subfamily C, polypeptide 9; Cytochromes P450 are a group of heme-thi [...] (490 aa)	0.987
VEGFA	vascular endothelial growth factor A; Growth factor active in angiogenesis, vasculogenesis and [...] (412 aa)	0.984
CASP3	caspase 3, apoptosis-related cysteine peptidase; Involved in the activation cascade of caspases [...] (277 aa)	0.983
PDPK1	3-phosphoinositide dependent protein kinase-1; Phosphorylates and activates not only PKB/AKT, b [...] (556 aa)	0.968
ABCC4	ATP-binding cassette, sub-family C (CFTR/MRP), member 4; May be an organic anion pump relevant [...] (1325 aa)	0.958
AKT1	v-akt murine thymoma viral oncogene homolog 1; General protein kinase capable of phosphorylatin [...] (480 aa)	0.956
CASP8	caspase 8, apoptosis-related cysteine peptidase; Most upstream protease of the activation casca [...] (538 aa)	0.951
CYP19A1	cytochrome P450, family 19, subfamily A, polypeptide 1; Catalyzes the formation of aromatic C18 [...] (503 aa)	0.941
PCNA	proliferating cell nuclear antigen; This protein is an auxiliary protein of DNA polymerase delt [...] (261 aa)	0.914
MAPK14	mitogen-activated protein kinase 14; Responds to activation by environmental stress, pro- infla [...] (360 aa)	0.908
CA9	carbonic anhydrase IX; Reversible hydration of carbon dioxide. Participates in pH regulation. M [...] (459 aa)	0.907
CYP2D6	cytochrome P450, family 2, subfamily D, polypeptide 6; Responsible for the metabolism of many d [...] (497 aa)	0.906
CASP9	caspase 9, apoptosis-related cysteine peptidase; Involved in the activation cascade of caspases [...] (416 aa)	0.900

CA2	carbonic anhydrase II; Essential for bone resorption and osteoclast differentiation (By similar [...] (260 aa)	0.900
CA12	carbonic anhydrase XII; Reversible hydration of carbon dioxide (354 aa)	0.900
EGFR	epidermal growth factor receptor (erythroblastic leukemia viral (v-erb-b) oncogene homolog, avi [...] (1210 aa)	0.873
CCND1	cyclin D1; Essential for the control of the cell cycle at the G1/S (start) transition (295 aa)	0.865
CA5B	inactivation escape 2 (non-protein coding); Reversible hydration of carbon dioxide (317 aa)	0.858
CA6	carbonic anhydrase VI; Reversible hydration of carbon dioxide. Its role in saliva is unknown (308 aa)	0.857
TNFRSF10B	tumor necrosis factor receptor superfamily, member 10b; Receptor for the cytotoxic ligand TNFSF [...] (440 aa)	0.852
CA13	carbonic anhydrase XIII; Reversible hydration of carbon dioxide (262 aa)	0.852
DIF	Tumor necrosis factor Precursor (TNF-alpha)(Tumor necrosis factor ligand superfamily member 2)([...] (233 aa)	0.846
DDIT3	DNA-damage-inducible transcript 3; Inhibits the DNA-binding activity of C/EBP and LAP by formin [...] (169 aa)	0.845
GDF15	growth differentiation factor 15 (308 aa)	0.845
PPARG	peroxisome proliferator-activated receptor gamma; Receptor that binds peroxisome proliferators [...] (505 aa)	0.845
DGCR2	DiGeorge syndrome critical region gene 2; Putative adhesion receptor, that could be involved in [...] (550 aa)	0.844
CYP2C8	cytochrome P450, family 2, subfamily C, polypeptide 8; Cytochromes P450 are a group of heme-thi [...] (490 aa)	0.839
ALOX5	arachidonate 5-lipoxygenase; Catalyzes the first step in leukotriene biosynthesis, and thereby [...] (674 aa)	0.839
CFLAR	CASP8 and FADD-like apoptosis regulator; Apoptosis regulator protein which may function as a cr [...] (480 aa)	0.838
IL6	interleukin 6 (interferon, beta 2); Cytokine with a wide variety of biological functions. It is [...] (212 aa)	0.834

MMP9	matrix metallopeptidase 9 (gelatinase B, 92kDa gelatinase, 92kDa type IV collagenase); May play [...] (707 aa)	0.833
TNF	tumor necrosis factor (TNF superfamily, member 2); Cytokine that binds to TNFRSF1A/TNFR1 and TN [...] (233 aa)	0.831
JUN	jun oncogene; Transcription factor that recognizes and binds to the enhancer heptamer motif 5'- [...] (331 aa)	0.828
FASN	fatty acid synthase; Fatty acid synthetase catalyzes the formation of long- chain fatty acids f [...] (2511 aa)	0.827
CDKN1A	cyclin-dependent kinase inhibitor 1A (p21, Cip1); May be the important intermediate by which p5 [...] (164 aa)	0.827
ABCC1	ATP-binding cassette, sub-family C (CFTR/MRP), member 1; Mediates export of organic anions and [...] (1531 aa)	0.824
CAV1	caveolin 1, caveolae protein, 22kDa; May act as a scaffolding protein within caveolar membranes [...] (178 aa)	0.824
CDK2	cyclin-dependent kinase 2; Involved in the control of the cell cycle. Interacts with cyclins A, [...] (298 aa)	0.824
VEGFC	vascular endothelial growth factor C; Growth factor active in angiogenesis, and endothelial cel [...] (420 aa)	0.823
INS	insulin; Insulin decreases blood glucose concentration. It increases cell permeability to monos [...] (200 aa)	0.822
ALB	albumin; Serum albumin, the main protein of plasma, has a good binding capacity for water, Ca(2 [...] (609 aa)	0.819
SP1	Sp1 transcription factor; Transcription factor that can activate or repress transcription in re [...] (785 aa)	0.819
CYP3A4	cytochrome P450, family 3, subfamily A, polypeptide 4; Cytochromes P450 are a group of heme-thi [...] (503 aa)	0.818
PLAU	plasminogen activator, urokinase; Specifically cleave the zymogen plasminogen to form the activ [...] (431 aa)	0.817
ICAM1	intercellular adhesion molecule 1; ICAM proteins are ligands for the leukocyte adhesion protein [...] (532 aa)	0.817
IGF1R	insulin-like growth factor 1 receptor; This receptor binds insulin-like growth factor 1 (IGF1) [...] (1367 aa)	0.816

	AR	androgen receptor; Steroid hormone receptors are ligand-activated transcription factors that re [...] (920 aa)	0.814
	IL1A	interleukin 1, alpha; Produced by activated macrophages, IL-1 stimulates thymocyte proliferatio [...] (271 aa)	0.814

12.4 Clavulanic acid

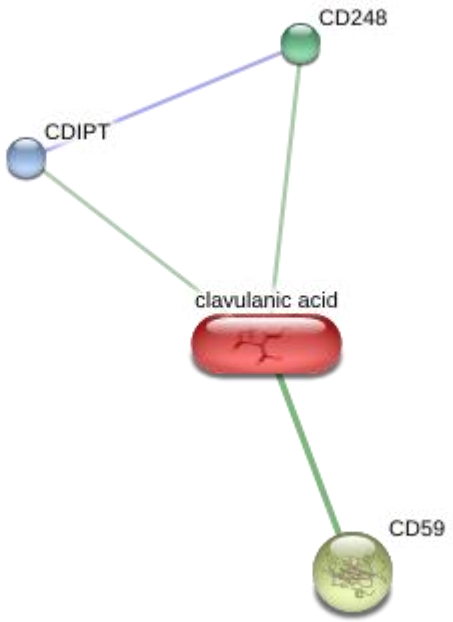

Predicted Functional Partners:

	CD59	CD59 molecule, complement regulatory protein; Potent inhibitor of the complement membrane attac [...] (128 aa)	0.800
	CD248	CD248 molecule, endosialin; May play a role in tumor angiogenesis (757 aa)	0.544
	CDIPT	CDP-diacylglycerol--inositol 3-phosphatidyltransferase (phosphatidylinositol synthase); Catalyz [...] (213 aa)	0.522

12.5 Flucloxacillin

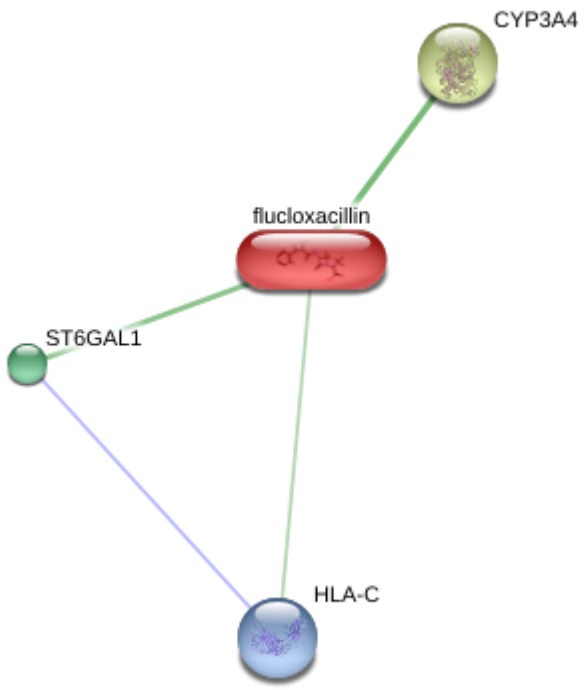

Predicted Functional Partners:

●	CYP3A4	cytochrome P450, family 3, subfamily A, polypeptide 4; Cytochromes P450 are a group of heme-thi [...] (503 aa)	0.800
●	ST6GAL1	ST6 beta-galactosamide alpha-2,6-sialyltranferase 1; Transfers sialic acid from the donor of su [...] (406 aa)	0.671
●	HLA-C	major histocompatibility complex, class I, C; Involved in the presentation of foreign antigens [...] (366 aa)	0.445

12.6 Lamotrigine

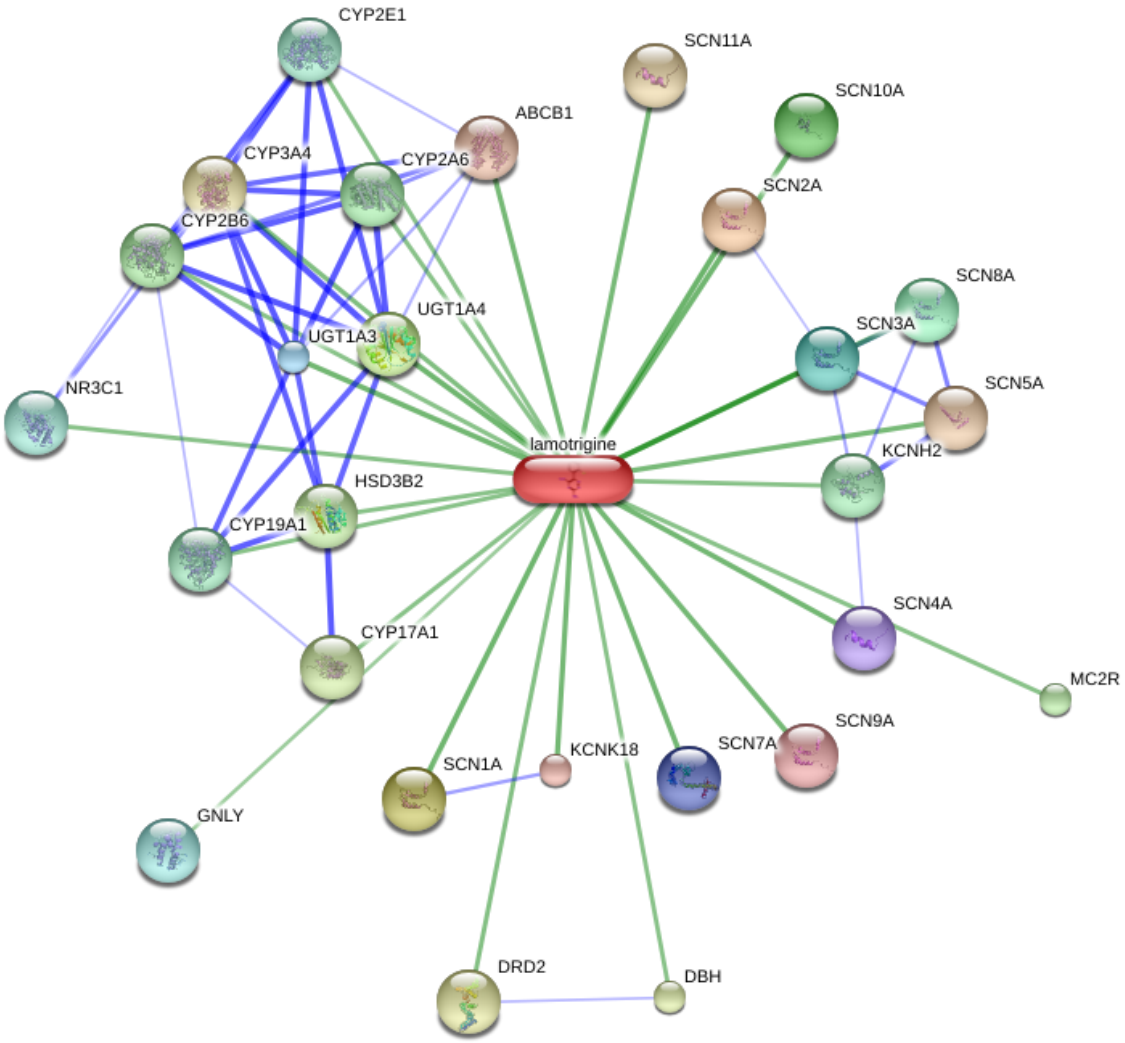

Predicted Functional Partners:

●	SCN2A	sodium channel, voltage-gated, type II, alpha subunit; Mediates the voltage-dependent sodium io [...] (2005 aa)	0.870
●	SCN1A	sodium channel, voltage-gated, type I, alpha subunit; Mediates the voltage-dependent sodium ion [...] (1998 aa)	0.849
●	UGT1A4	UDP glucuronosyltransferase 1 family, polypeptide A4; UDPGT is of major importance in the conju [...] (534 aa)	0.847
●	SCN10A	sodium channel, voltage-gated, type X, alpha subunit; This protein mediates the voltage-depende [...] (1956 aa)	0.840

	SCN8A	sodium channel, voltage gated, type VIII, alpha subunit; Mediates the voltage-dependent sodium [...] (1980 aa)	0.836
	SCN3A	sodium channel, voltage-gated, type III, alpha subunit; Mediates the voltage-dependent sodium i [...] (2000 aa)	0.835
	UGT1A3	UDP glucuronosyltransferase 1 family, polypeptide A3; UDPGT is of major importance in the conju [...] (534 aa)	0.831
	SCN7A	sodium channel, voltage-gated, type VII, alpha; Mediates the voltage-dependent sodium ion perme [...] (1682 aa)	0.828
	SCN4A	sodium channel, voltage-gated, type IV, alpha subunit; This protein mediates the voltage-depend [...] (1836 aa)	0.827
	SCN9A	sodium channel, voltage-gated, type IX, alpha subunit; Mediates the voltage-dependent sodium io [...] (1977 aa)	0.820
	KCNK18	potassium channel, subfamily K, member 18; Outward rectifying potassium channel. Produces rapid [...] (384 aa)	0.819
	ABCB1	ATP-binding cassette, sub-family B (MDR/TAP), member 1; Energy-dependent efflux pump responsibl [...] (1280 aa)	0.814
	SCN5A	sodium channel, voltage-gated, type V, alpha subunit; This protein mediates the voltage-depende [...] (2016 aa)	0.800
	SCN11A	sodium channel, voltage-gated, type XI, alpha subunit; This protein mediates the voltage-depend [...] (1791 aa)	0.800
	CYP3A4	cytochrome P450, family 3, subfamily A, polypeptide 4; Cytochromes P450 are a group of heme-thi [...] (503 aa)	0.750
	DRD2	dopamine receptor D2; This is one of the five types (D1 to D5) of receptors for dopamine. The a [...] (443 aa)	0.729
	DBH	dopamine beta-hydroxylase (dopamine beta-monooxygenase); Conversion of dopamine to noradrenalin [...] (617 aa)	0.700
	CYP17A1	cytochrome P450, family 17, subfamily A, polypeptide 1; Conversion of pregnenolone and progeste [...] (508 aa)	0.700
	HSD3B2	hydroxy-delta-5-steroid dehydrogenase, 3 beta- and steroid delta-isomerase 2; 3-beta-HSD is a b [...] (372 aa)	0.700
	MC2R	melanocortin 2 receptor (adrenocorticotropic hormone); Receptor for ACTH. This receptor is medi [...] (297 aa)	0.700

	CYP2B6	cytochrome P450, family 2, subfamily B, polypeptide 6; Cytochromes P450 are a group of heme-thi [...] (491 aa)	0.700
	CYP2A6	cytochrome P450, family 2, subfamily A, polypeptide 7; Cytochromes P450 are a group of heme-thi [...] (494 aa)	0.700
	KCNH2	potassium voltage-gated channel, subfamily H (eag-related), member 2; Pore-forming (alpha) subu [...] (1159 aa)	0.700
	CYP19A1	cytochrome P450, family 19, subfamily A, polypeptide 1; Catalyzes the formation of aromatic C18 [...] (503 aa)	0.700
	CYP2E1	cytochrome P450, family 2, subfamily E, polypeptide 1; Metabolizes several precarcinogens, drug [...] (493 aa)	0.700
	NR3C1	nuclear receptor subfamily 3, group C, member 1 (glucocorticoid receptor); Receptor for glucoco [...] (778 aa)	0.700
	GNLY	granulysin; Antimicrobial protein that kills intracellular pathogens. Active against a broad ra [...] (145 aa)	0.587

12.7 Nevirapine

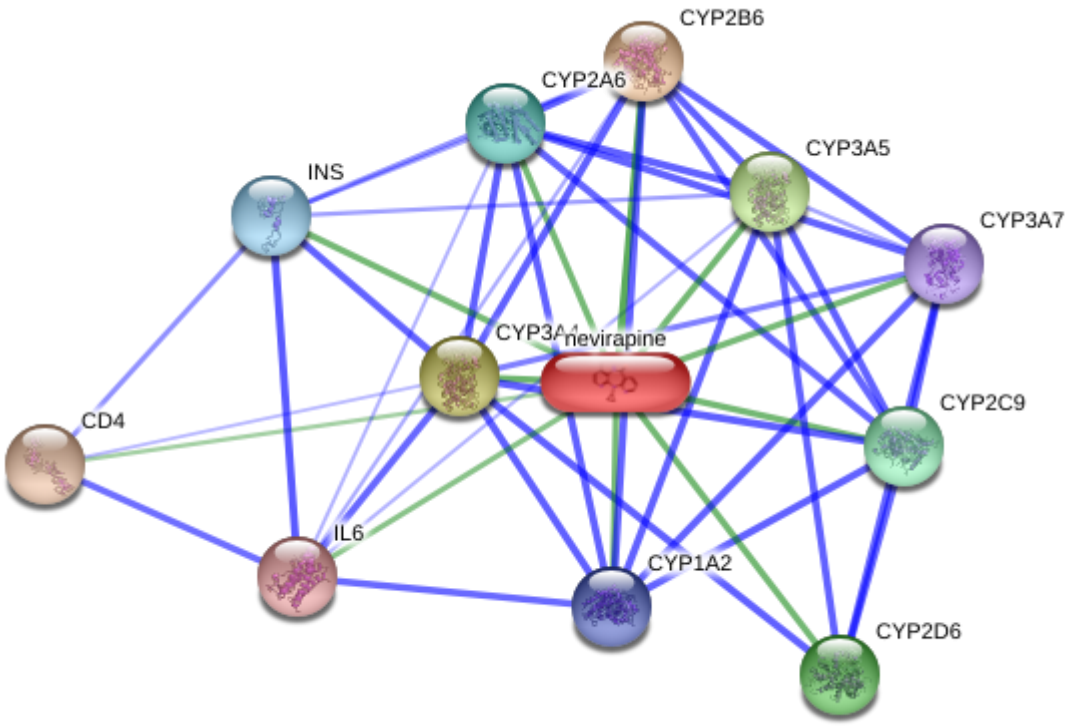

Predicted Functional Partners:

	CYP2B6	cytochrome P450, family 2, subfamily B, polypeptide 6; Cytochromes P450 are a group of heme-thi [...] (491 aa)	0.969
	CYP3A4	cytochrome P450, family 3, subfamily A, polypeptide 4; Cytochromes P450 are a group of heme-thi [...] (503 aa)	0.862
	CYP3A5	cytochrome P450, family 3, subfamily A, polypeptide 5; Cytochromes P450 are a group of heme-thi [...] (502 aa)	0.831
	CYP2D6	cytochrome P450, family 2, subfamily D, polypeptide 6; Responsible for the metabolism of many d [...] (497 aa)	0.825
	CYP2C9	cytochrome P450, family 2, subfamily C, polypeptide 9; Cytochromes P450 are a group of heme-thi [...] (490 aa)	0.823
	CYP2A6	cytochrome P450, family 2, subfamily A, polypeptide 7; Cytochromes P450 are a group of heme-thi [...] (494 aa)	0.814
	INS	insulin; Insulin decreases blood glucose concentration. It increases cell permeability to monos [...] (200 aa)	0.814
	CYP1A2	cytochrome P450, family 1, subfamily A, polypeptide 2; Cytochromes P450 are a group of heme-thi [...] (516 aa)	0.813
	CYP3A7	cytochrome P450, family 3, subfamily A, polypeptide 7; Cytochromes P450 are a group of heme-thi [...] (503 aa)	0.800
	IL6	interleukin 6 (interferon, beta 2); Cytokine with a wide variety of biological functions. It is [...] (212 aa)	0.700
	CD4	CD4 molecule; Accessory protein for MHC class-II antigen/T-cell receptor interaction. May regul [...] (458 aa)	0.549

12.8 Phenytoin

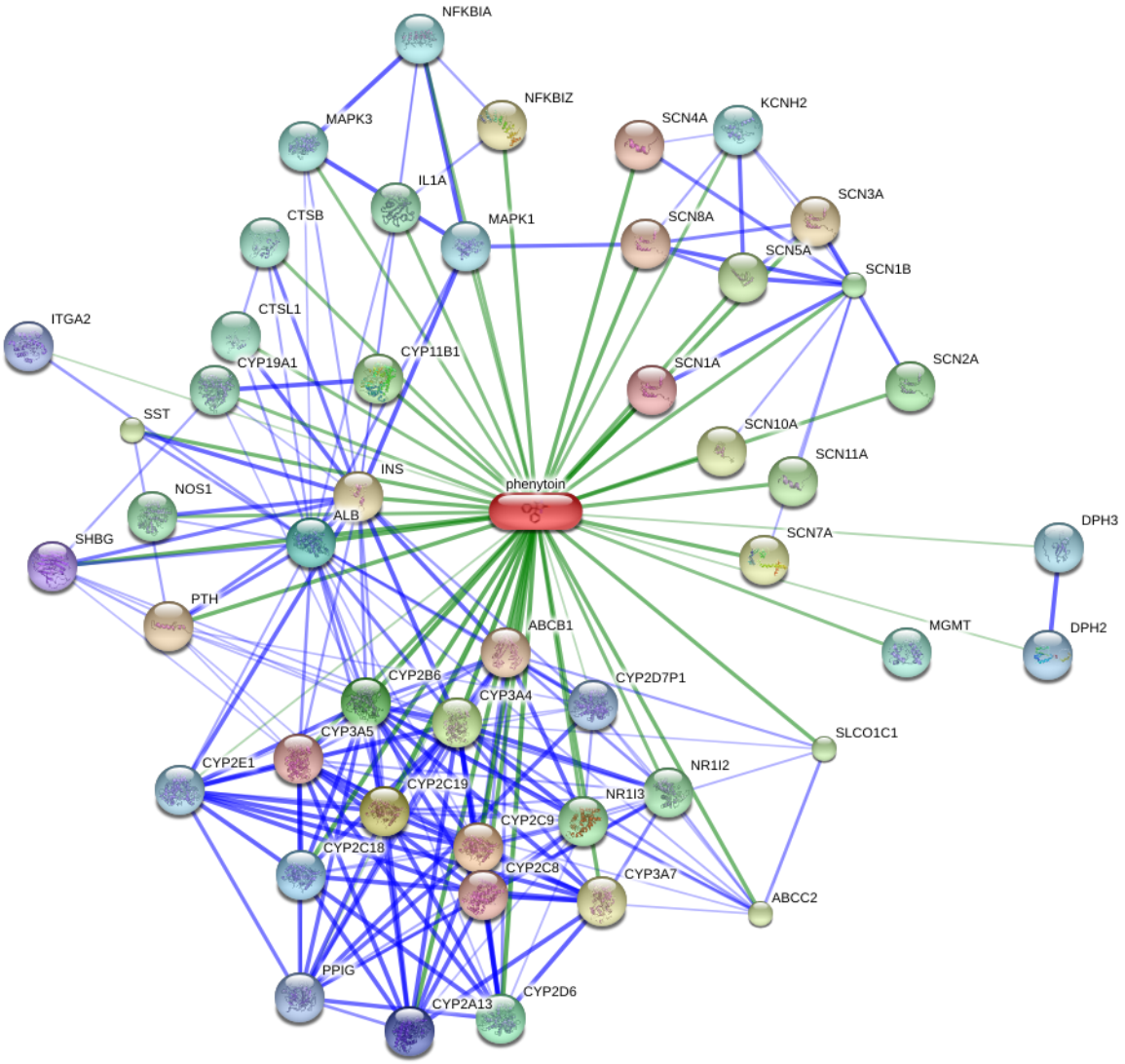

Predicted Functional Partners:

●	CYP2C9	cytochrome P450, family 2, subfamily C, polypeptide 9; Cytochromes P450 are a group of heme-thi [...] (490 aa)	0.992
●	CYP2C19	cytochrome P450, family 2, subfamily C, polypeptide 19; Responsible for the metabolism of a num [...] (490 aa)	0.989
●	CYP3A4	cytochrome P450, family 3, subfamily A, polypeptide 4; Cytochromes P450 are a group of heme-thi [...] (503 aa)	0.987
●	CYP2B6	cytochrome P450, family 2, subfamily B, polypeptide 6; Cytochromes P450 are a group of heme-thi [...] (491 aa)	0.971

	CYP2D6	cytochrome P450, family 2, subfamily D, polypeptide 6; Responsible for the metabolism of many d [...] (497 aa)	0.940
	ALB	albumin; Serum albumin, the main protein of plasma, has a good binding capacity for water, Ca(2 [...] (609 aa)	0.925
	CYP2C18	cytochrome P450, family 2, subfamily C, polypeptide 18; Cytochromes P450 are a group of heme-th [...] (490 aa)	0.925
	CYP2A13	cytochrome P450, family 2, subfamily A, polypeptide 13; Exhibits a coumarin 7-hydroxylase activ [...] (494 aa)	0.913
	SHBG	sex hormone-binding globulin; Functions as an androgen transport protein, but may also be invol [...] (402 aa)	0.909
	SCN1A	sodium channel, voltage-gated, type I, alpha subunit; Mediates the voltage-dependent sodium ion [...] (1998 aa)	0.879
	CYP3A5	cytochrome P450, family 3, subfamily A, polypeptide 5; Cytochromes P450 are a group of heme-thi [...] (502 aa)	0.861
	CYP2C8	cytochrome P450, family 2, subfamily C, polypeptide 8; Cytochromes P450 are a group of heme-thi [...] (490 aa)	0.860
	SCN4A	sodium channel, voltage-gated, type IV, alpha subunit; This protein mediates the voltage-depend [...] (1836 aa)	0.856
	SCN8A	sodium channel, voltage gated, type VIII, alpha subunit; Mediates the voltage-dependent sodium [...] (1980 aa)	0.850
	ABCB1	ATP-binding cassette, sub-family B (MDR/TAP), member 1; Energy-dependent efflux pump responsibl [...] (1280 aa)	0.850
	PTH	parathyroid hormone; PTH elevates calcium level by dissolving the salts in bone and preventing [...] (115 aa)	0.849
	SCN3A	sodium channel, voltage-gated, type III, alpha subunit; Mediates the voltage-dependent sodium i [...] (2000 aa)	0.841
	INS	insulin; Insulin decreases blood glucose concentration. It increases cell permeability to monos [...] (200 aa)	0.836
	NFKBIZ	nuclear factor of kappa light polypeptide gene enhancer in B-cells inhibitor, zeta; Involved in [...] (718 aa)	0.833
	CYP3A7	cytochrome P450, family 3, subfamily A, polypeptide 7; Cytochromes P450 are a group of heme-thi [...] (503 aa)	0.825

	SCN7A	sodium channel, voltage-gated, type VII, alpha; Mediates the voltage-dependent sodium ion perme [...] (1682 aa)	0.824
	SCN10A	sodium channel, voltage-gated, type X, alpha subunit; This protein mediates the voltage-depende [...] (1956 aa)	0.819
	ABCC2	ATP-binding cassette, sub-family C (CFTR/MRP), member 2; Mediates hepatobiliary excretion of nu [...] (1545 aa)	0.819
	SST	somatostatin; Somatostatin inhibits the release of somatotropin (116 aa)	0.819
	SCN5A	sodium channel, voltage-gated, type V, alpha subunit; This protein mediates the voltage-depende [...] (2016 aa)	0.813
	SLCO1C1	solute carrier organic anion transporter family, member 1C1; Mediates the Na(+)-independent hig [...] (712 aa)	0.810
	SCN11A	sodium channel, voltage-gated, type XI, alpha subunit; This protein mediates the voltage-depend [...] (1791 aa)	0.800
	CYP11B1	cytochrome P450, family 11, subfamily B, polypeptide 1; Has steroid 11-beta-hydroxylase activit [...] (503 aa)	0.800
	SCN1B	sodium channel, voltage-gated, type I, beta; Crucial in the assembly, expression, and functiona [...] (268 aa)	0.789
	SCN2A	sodium channel, voltage-gated, type II, alpha subunit; Mediates the voltage-dependent sodium io [...] (2005 aa)	0.770
	NR1I3	nuclear receptor subfamily 1, group I, member 3; Binds and transactivates the retinoic acid res [...] (357 aa)	0.764
	NR1I2	nuclear receptor subfamily 1, group I, member 2; Nuclear receptor that binds and is activated b [...] (473 aa)	0.747
	NOS1	nitric oxide synthase 1 (neuronal); Produces nitric oxide (NO) which is a messenger molecule wi [...] (1434 aa)	0.738
	IL1A	interleukin 1, alpha; Produced by activated macrophages, IL-1 stimulates thymocyte proliferatio [...] (271 aa)	0.733
	CYP19A1	cytochrome P450, family 19, subfamily A, polypeptide 1; Catalyzes the formation of aromatic C18 [...] (503 aa)	0.716
	CTSL1	cathepsin L1; Important for the overall degradation of proteins in lysosomes (333 aa)	0.700

	CTSB	cathepsin B; Thiol protease which is believed to participate in intracellular degradation and t [...] (339 aa)	0.700
	MGMT	O-6-methylguanine-DNA methyltransferase; Involved in the cellular defense against the biologica [...] (238 aa)	0.700
	MAPK3	mitogen-activated protein kinase 3; Involved in both the initiation and regulation of meiosis, [...] (379 aa)	0.700
	KCNH2	potassium voltage-gated channel, subfamily H (eag-related), member 2; Pore-forming (alpha) subu [...] (1159 aa)	0.700
	NFKBIA	nuclear factor of kappa light polypeptide gene enhancer in B-cells inhibitor, alpha; Inhibits t [...] (317 aa)	0.700
	MAPK1	mitogen-activated protein kinase 1; Involved in both the initiation and regulation of meiosis, [...] (360 aa)	0.700
	DPH3	DPH3, KTI11 homolog (S. cerevisiae); Essential for the first step in the synthesis of diphthami [...] (82 aa)	0.464
	CYP2E1	cytochrome P450, family 2, subfamily E, polypeptide 1; Metabolizes several precarcinogens, drug [...] (493 aa)	0.455
	DPH2	DPH2 homolog (S. cerevisiae); Required for the first step in the synthesis of diphthamide, a po [...] (489 aa)	0.454
	CYP2D7P1	cytochrome P450, family 2, subfamily D, polypeptide 7 pseudogene 1 (497 aa)	0.422
	PPIG	peptidylprolyl isomerase G (cyclophilin G); PPIases accelerate the folding of proteins. It cata [...] (754 aa)	0.416
	ITGA2	integrin, alpha 2 (CD49B, alpha 2 subunit of VLA-2 receptor); Integrin alpha-2/beta-1 is a rece [...] (1181 aa)	0.404

12.9 Propylthiouracil

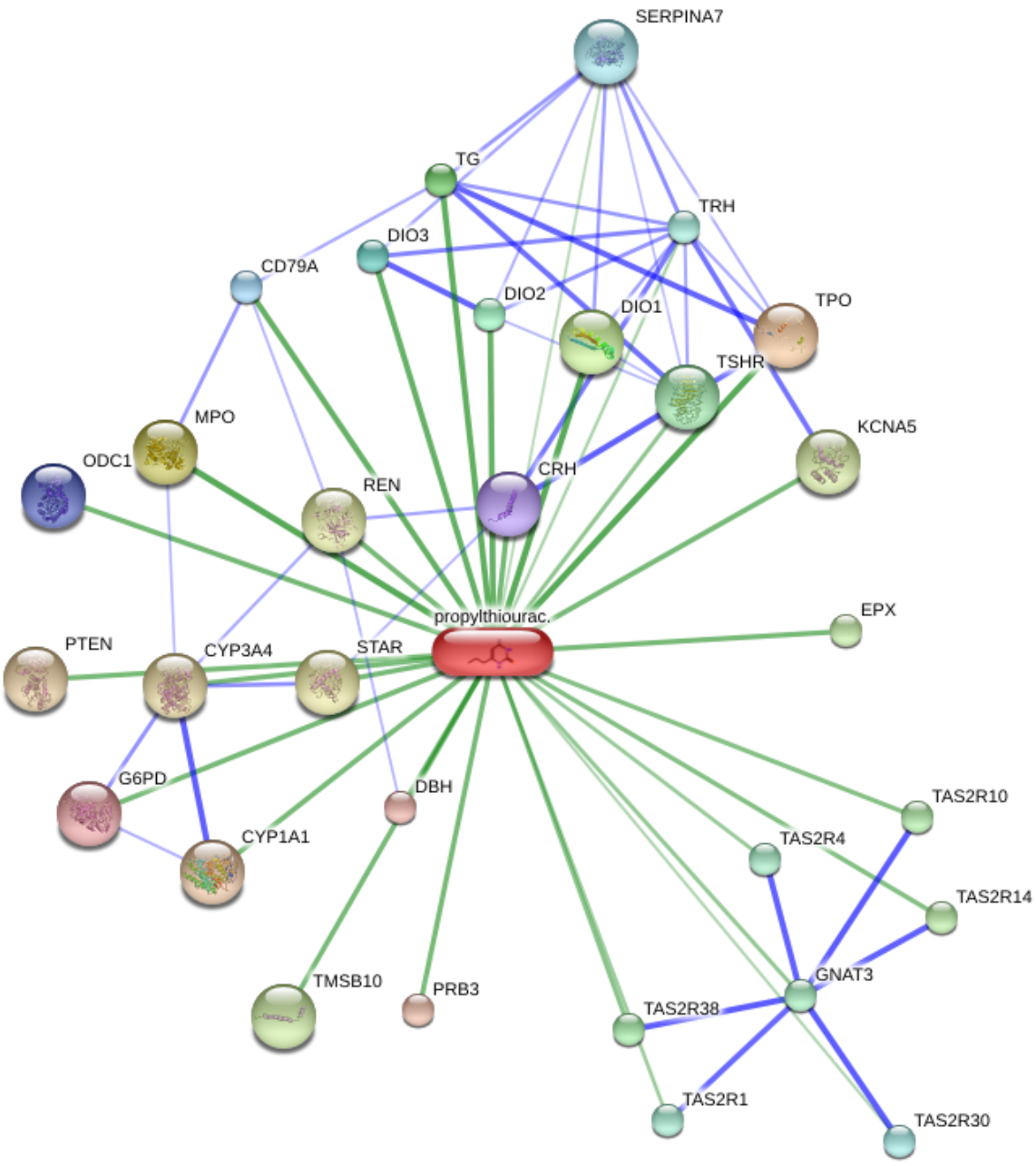

Predicted Functional Partners:

●	TPO	thyroid peroxidase; Iodination and coupling of the hormonogenic tyrosines in thyroglobulin to y [...] (933 aa)	0.987
●	MPO	myeloperoxidase; Part of the host defense system of polymorphonuclear leukocytes. It is respons [...] (745 aa)	0.984

	DIO1	deiodinase, iodothyronine, type I; Responsible for the deiodination of T4 (3,5,3',5'- tetraiodo [...] (249 aa)	0.978
	TG	thyroglobulin; Precursor of the iodinated thyroid hormones thyroxine (T4) and triiodothyronine [...] (2768 aa)	0.932
	DIO2	deiodinase, iodothyronine, type II; Responsible for the deiodination of T4 (3,5,3',5'- tetraiod [...] (273 aa)	0.904
	DIO3	deiodinase, iodothyronine, type III; Responsible for the deiodination of T4 (3,5,3',5'- tetraio [...] (278 aa)	0.903
	CD79A	CD79a molecule, immunoglobulin-associated alpha; Required in cooperation with CD79B for initiat [...] (226 aa)	0.900
	ODC1	ornithine decarboxylase 1 (461 aa)	0.818
	CRH	corticotropin releasing hormone; This hormone from hypothalamus regulates the release of cortic [...] (196 aa)	0.810
	G6PD	glucose-6-phosphate dehydrogenase; Produces pentose sugars for nucleic acid synthesis and main [...] (545 aa)	0.800
	DBH	dopamine beta-hydroxylase (dopamine beta-monooxygenase); Conversion of dopamine to noradrenalin [...] (617 aa)	0.800
	PRB3	proline-rich protein BstNI subfamily 3; Acts as a receptor for the Gram-negative bacterium F.nu [...] (309 aa)	0.800
	CYP1A1	cytochrome P450, family 1, subfamily A, polypeptide 1; Cytochromes P450 are a group of heme-thi [...] (512 aa)	0.800
	PTEN	phosphatase and tensin homolog; Tumor suppressor. Acts as a dual-specificity protein phosphatas [...] (403 aa)	0.800
	CYP3A4	cytochrome P450, family 3, subfamily A, polypeptide 4; Cytochromes P450 are a group of heme-thi [...] (503 aa)	0.800
	STAR	steroidogenic acute regulatory protein; Plays a key role in steroid hormone synthesis by enhanc [...] (285 aa)	0.800
	REN	renin; Renin is a highly specific endopeptidase, whose only known function is to generate angio [...] (406 aa)	0.800
	KCNA5	potassium voltage-gated channel, shaker-related subfamily, member 5; Mediates the voltage-depen [...] (613 aa)	0.800
	TMSB10	thymosin beta 10; Plays an important role in the organization of the cytoskeleton. Binds to and [...] (44 aa)	0.800

	EPX	eosinophil peroxidase; Mediates tyrosine nitration of secondary granule proteins in mature rest [...] (715 aa)	0.800
	TAS2R14	taste receptor, type 2, member 14; Receptor that may play a role in the perception of bitternes [...] (317 aa)	0.728
	TAS2R10	taste receptor, type 2, member 10; Gustducin-coupled strychnine receptor implicated in the perc [...] (307 aa)	0.716
	TAS2R38	taste receptor, type 2, member 38; Receptor that may play a role in the perception of bitternes [...] (333 aa)	0.690
	TSHR	thyroid stimulating hormone receptor; Receptor for thyrothropin. Plays a central role in contro [...] (764 aa)	0.653
	GNAT3	guanine nucleotide binding protein, alpha transducing 3; Guanine nucleotide-binding protein (G [...] (354 aa)	0.637
	TAS2R4	taste receptor, type 2, member 4; Gustducin-coupled receptor for denatonium and N(6)- propyl-2- [...] (299 aa)	0.604
	TAS2R1	taste receptor, type 2, member 1; Receptor that may play a role in the perception of bitterness [...] (299 aa)	0.576
	TRH	thyrotropin-releasing hormone; Functions as a regulator of the biosynthesis of TSH in the anter [...] (242 aa)	0.503
	TAS2R30	taste receptor, type 2, member 46; Receptor that may play a role in the perception of bitternes [...] (299 aa)	0.476
	SERPINA7	serpin peptidase inhibitor, clade A (alpha-1 antiproteinase, antitrypsin), member 7; Major thyr [...] (415 aa)	0.424

12.10 Sulfasalazine

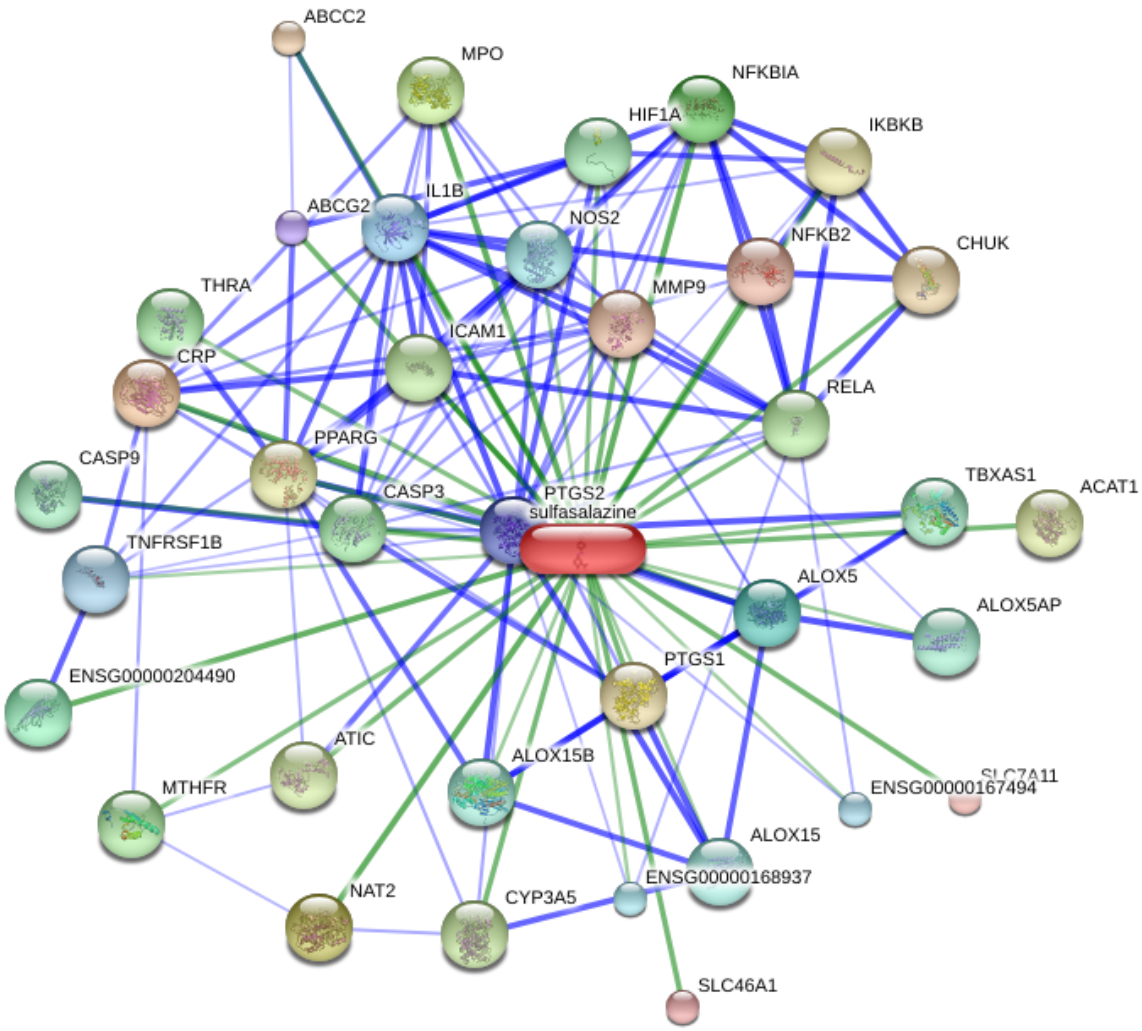

Predicted Functional Partners:

●	CRP	C-reactive protein, pentraxin-related; Displays several functions associated with host defense- [...] (224 aa)	0.931
●	NAT2	N-acetyltransferase 2 (arylamine N-acetyltransferase); Participates in the detoxification of a [...] (290 aa)	0.917
●	MPO	myeloperoxidase; Part of the host defense system of polymorphonuclear leukocytes. It is respons [...] (745 aa)	0.915
●	NFKBIA	nuclear factor of kappa light polypeptide gene enhancer in B-cells inhibitor, alpha; Inhibits t [...] (317 aa)	0.915

	ENSG00000204490	Tumor necrosis factor Precursor (TNF-alpha)(Tumor necrosis factor ligand superfamily member 2)([...] (233 aa)	0.900
	ALOX5	arachidonate 5-lipoxygenase; Catalyzes the first step in leukotriene biosynthesis, and thereby [...] (674 aa)	0.900
	IL1B	interleukin 1, beta; Produced by activated macrophages, IL-1 stimulates thymocyte proliferation [...] (269 aa)	0.852
	PTGS2	prostaglandin-endoperoxide synthase 2 (prostaglandin G/H synthase and cyclooxygenase); May have [...] (604 aa)	0.831
	ABCG2	ATP-binding cassette, sub-family G (WHITE), member 2; Xenobiotic transporter that may play an i [...] (655 aa)	0.831
	SLC46A1	solute carrier family 46 (folate transporter), member 1; Has been shown to act both as an intes [...] (459 aa)	0.817
	SLC7A11	solute carrier family 7, (cationic amino acid transporter, y+ system) member 11; Sodium-indepen [...] (501 aa)	0.816
	NFKB2	nuclear factor of kappa light polypeptide gene enhancer in B-cells 2 (p49/p100); NF-kappa-B is [...] (900 aa)	0.814
	MMP9	matrix metallopeptidase 9 (gelatinase B, 92kDa gelatinase, 92kDa type IV collagenase); May play [...] (707 aa)	0.809
	ABCC2	ATP-binding cassette, sub-family C (CFTR/MRP), member 2; Mediates hepatobiliary excretion of nu [...] (1545 aa)	0.800
	CHUK	conserved helix-loop-helix ubiquitous kinase; Acts as part of the IKK complex in the convention [...] (745 aa)	0.800
	PTGS1	prostaglandin-endoperoxide synthase 1 (prostaglandin G/H synthase and cyclooxygenase); May play [...] (599 aa)	0.800
	IKBKB	inhibitor of kappa light polypeptide gene enhancer in B-cells, kinase beta; Acts as part of the [...] (756 aa)	0.800

PPARG	peroxisome proliferator-activated receptor gamma; Receptor that binds peroxisome proliferators [...] (505 aa)	0.800
ACAT1	acetyl-Coenzyme A acetyltransferase 1; Plays a major role in ketone body metabolism (427 aa)	0.800
ATIC	5-aminoimidazole-4-carboxamide ribonucleotide formyltransferase/IMP cyclohydrolase; Bifunctiona [...] (592 aa)	0.800
CYP3A5	cytochrome P450, family 3, subfamily A, polypeptide 5; Cytochromes P450 are a group of heme-thi [...] (502 aa)	0.800
ICAM1	intercellular adhesion molecule 1; ICAM proteins are ligands for the leukocyte adhesion protein [...] (532 aa)	0.787
RELA	v-rel reticuloendotheliosis viral oncogene homolog A (avian); NF-kappa-B is a pleiotropic trans [...] (551 aa)	0.751
MTHFR	5,10-methylenetetrahydrofolate reductase (NADPH); Catalyzes the conversion of 5,10- methylenete [...] (656 aa)	0.729
THRA	thyroid hormone receptor, alpha (erythroblastic leukemia viral (v-erb-a) oncogene homolog, avia [...] (490 aa)	0.719
CASP3	caspase 3, apoptosis-related cysteine peptidase; Involved in the activation cascade of caspases [...] (277 aa)	0.715
HIF1A	hypoxia inducible factor 1, alpha subunit (basic helix-loop-helix transcription factor); Functi [...] (826 aa)	0.700
CASP9	caspase 9, apoptosis-related cysteine peptidase; Involved in the activation cascade of caspases [...] (416 aa)	0.700
TBXAS1	thromboxane A synthase 1 (platelet) (534 aa)	0.700
ALOX5AP	arachidonate 5-lipoxygenase-activating protein; Required for leukotriene biosynthesis by ALOX5 [...] (161 aa)	0.583
ALOX15B	arachidonate 15-lipoxygenase, type B; Converts arachidonic acid exclusively to 15S- hydroperoxy [...] (676 aa)	0.583
ALOX15	arachidonate 15-lipoxygenase; Converts arachidonic acid to 15S- hydroperoxyeicosatetraenoic aci [...] (662 aa)	0.583

	NOS2	nitric oxide synthase 2, inducible; Produces nitric oxide (NO) which is a messenger molecule wi [...] (1153 aa)	0.561
	ENSG00000168937	Putative uncharacterized protein ENSP00000305638 Fragment (68 aa)	0.561
	ENSG00000167494	Putative uncharacterized protein ENSP00000300983 Fragment (115 aa)	0.561
	TNFRSF1B	tumor necrosis factor receptor superfamily, member 1B; Receptor with high affinity for TNFSF2/T [...] (461 aa)	0.529

12.11 Sulindac

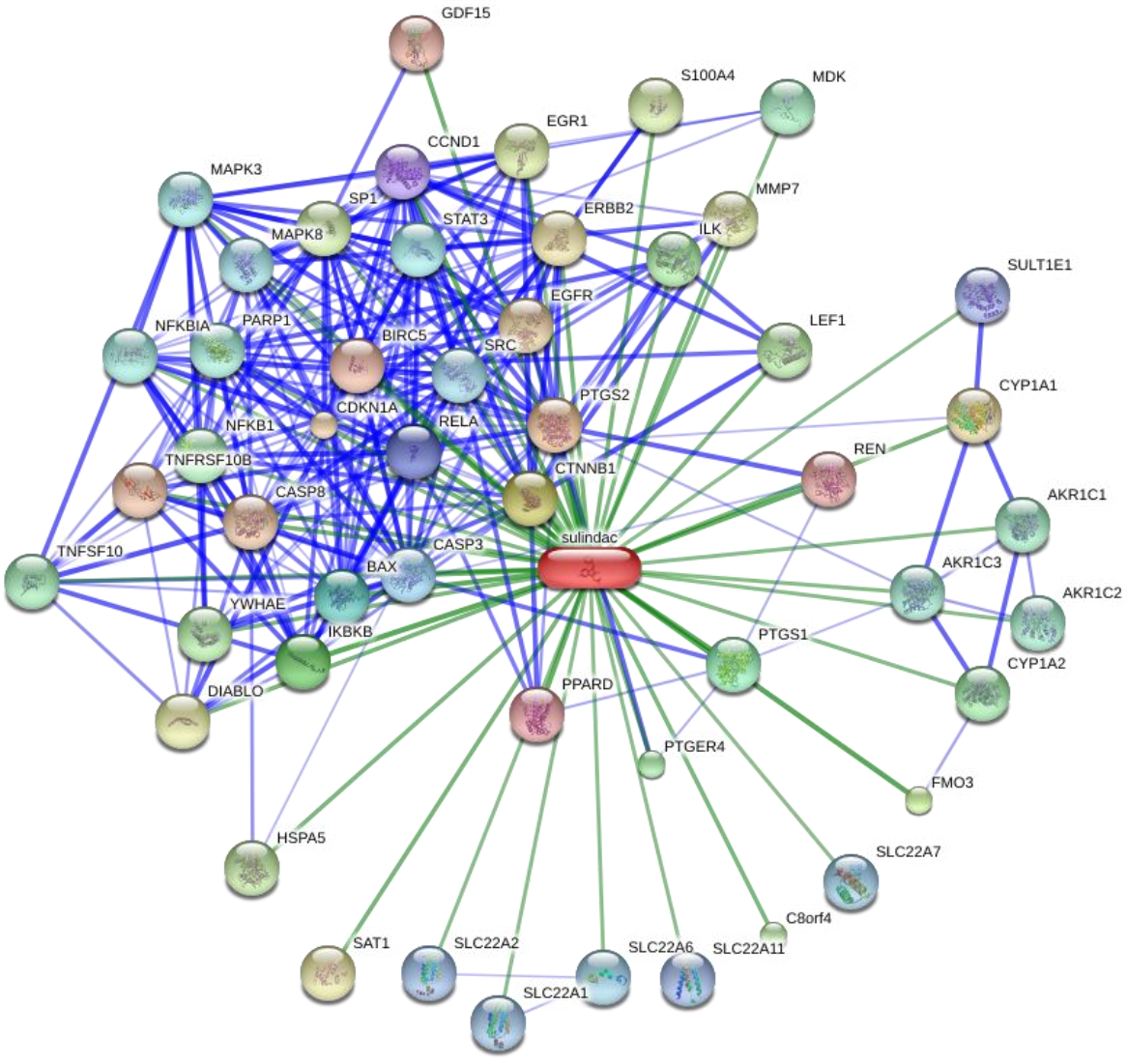

Predicted Functional Partners:

	PTGS2	prostaglandin-endoperoxide synthase 2 (prostaglandin G/H synthase and cyclooxygenase); May have [...] (604 aa)	0.996
	CTNNB1	catenin (cadherin-associated protein), beta 1, 88kDa; Involved in the regulation of cell adhesi [...] (781 aa)	0.984
	FMO3	flavin containing monooxygenase 3; Involved in the oxidative metabolism of a variety of xenobio [...] (532 aa)	0.981
	IKBKB	inhibitor of kappa light polypeptide gene enhancer in B-cells, kinase beta; Acts as part of the [...] (756 aa)	0.979
	PTGS1	prostaglandin-endoperoxide synthase 1 (prostaglandin G/H synthase and cyclooxygenase); May play [...] (599 aa)	0.972
	BAX	BCL2-associated X protein; Accelerates programmed cell death by binding to, and antagonizing th [...] (218 aa)	0.950
	CASP3	caspase 3, apoptosis-related cysteine peptidase; Involved in the activation cascade of caspases [...] (277 aa)	0.924
	RELA	v-rel reticuloendotheliosis viral oncogene homolog A (avian); NF-kappa-B is a pleiotropic trans [...] (551 aa)	0.921
	CCND1	cyclin D1; Essential for the control of the cell cycle at the G1/S (start) transition (295 aa)	0.921
	PPARD	peroxisome proliferator-activated receptor delta; Ligand-activated transcription factor. Recept [...] (441 aa)	0.911
	REN	renin; Renin is a highly specific endopeptidase, whose only known function is to generate angio [...] (406 aa)	0.909
	GDF15	growth differentiation factor 15 (308 aa)	0.855
	BIRC5	baculoviral IAP repeat-containing 5; Component of the chromosomal passenger complex (CPC), a co [...] (165 aa)	0.852
	TNFRSF10B	tumor necrosis factor receptor superfamily, member 10b; Receptor for the cytotoxic ligand TNFSF [...] (440 aa)	0.852
	CASP8	caspase 8, apoptosis-related cysteine peptidase; Most upstream protease of the activation casca [...] (538 aa)	0.843
	CDKN1A	cyclin-dependent kinase inhibitor 1A (p21, Cip1); May be the important intermediate by which p5 [...] (164 aa)	0.833

	EGFR	epidermal growth factor receptor (erythroblastic leukemia viral (v-erb-b) oncogene homolog, avi [...] (1210 aa)	0.831
	CYP1A1	cytochrome P450, family 1, subfamily A, polypeptide 1; Cytochromes P450 are a group of heme-thi [...] (512 aa)	0.824
	ERBB2	v-erb-b2 erythroblastic leukemia viral oncogene homolog 2, neuro/glioblastoma derived oncogene [...] (1255 aa)	0.823
	SAT1	spermidine/spermine N1-acetyltransferase 1; Enzyme which catalyzes the acetylation of polyamine [...] (171 aa)	0.818
	DIABLO	diablo homolog (Drosophila); Promotes apoptosis by activating caspases in the cytochrome c/Apaf [...] (239 aa)	0.818
	MMP7	matrix metallopeptidase 7 (matrilysin, uterine); Degrades casein, gelatins of types I, III, IV, [...] (267 aa)	0.816
	EGR1	early growth response 1; Transcriptional regulator. Recognizes and binds to the DNA sequence 5' [...] (543 aa)	0.812
	S100A4	S100 calcium binding protein A4 (101 aa)	0.800
	SP1	Sp1 transcription factor; Transcription factor that can activate or repress transcription in re [...] (785 aa)	0.800
	HSPA5	heat shock 70kDa protein 5 (glucose-regulated protein, 78kDa); Probably plays a role in facilit [...] (654 aa)	0.800
	C8orf4	Uncharacterized protein C8orf4 (Thyroid cancer protein 1)(TC-1); May decrease apoptosis (106 aa)	0.800
	LEF1	lymphoid enhancer-binding factor 1; Participates in the Wnt signaling pathway. Activates transc [...] (399 aa)	0.800
	YWHAE	tyrosine 3-monooxygenase/tryptophan 5-monooxygenase activation protein, epsilon polypeptide; Ad [...] (255 aa)	0.800
	ILK	integrin-linked kinase; Receptor-proximal protein kinase regulating integrin- mediated signal t [...] (452 aa)	0.770
	PTGER4	prostaglandin E receptor 4 (subtype EP4); Receptor for prostaglandin E2 (PGE2). The activity of [...] (488 aa)	0.757
	CYP1A2	cytochrome P450, family 1, subfamily A, polypeptide 2; Cytochromes P450 are a group of heme-thi [...] (516 aa)	0.754
	NFKB1	nuclear factor of kappa light polypeptide gene enhancer in B-cells 1; NF-kappa-B is a pleiotrop [...] (969 aa)	0.748

	TNFSF10	tumor necrosis factor (ligand) superfamily, member 10; Cytokine that binds to TNFRSF10A/TRAILR1 [...] (281 aa)	0.747
	MDK	midkine (neurite growth-promoting factor 2); Has heparin binding activity, and growth promoting [...] (143 aa)	0.737
	AKR1C1	aldo-keto reductase family 1, member C1 (dihydrodiol dehydrogenase 1; 20-alpha (3-alpha)-hydrox [...] (323 aa)	0.731
	AKR1C2	aldo-keto reductase family 1, member C2 (dihydrodiol dehydrogenase 2; bile acid binding protein [...] (323 aa)	0.731
	AKR1C3	aldo-keto reductase family 1, member C3 (3-alpha hydroxysteroid dehydrogenase, type II); Cataly [...] (323 aa)	0.731
	PARP1	poly (ADP-ribose) polymerase 1; Involved in the base excision repair (BER) pathway, by catalyzi [...] (1014 aa)	0.728
	NFKBIA	nuclear factor of kappa light polypeptide gene enhancer in B-cells inhibitor, alpha; Inhibits t [...] (317 aa)	0.728
	MAPK3	mitogen-activated protein kinase 3; Involved in both the initiation and regulation of meiosis, [...] (379 aa)	0.727
	STAT3	signal transducer and activator of transcription 3 (acute-phase response factor); Transcription [...] (770 aa)	0.726
	MAPK8	mitogen-activated protein kinase 8; Responds to activation by environmental stress and pro- inf [...] (427 aa)	0.724
	SRC	v-src sarcoma (Schmidt-Ruppin A-2) viral oncogene homolog (avian) (536 aa)	0.722
	SLC22A6	solute carrier family 22 (organic anion transporter), member 6; Involved in the renal eliminati [...] (563 aa)	0.712
	SLC22A7	solute carrier family 22 (organic anion transporter), member 7; Mediates sodium-independent mul [...] (548 aa)	0.712
	SLC22A1	solute carrier family 22 (organic cation transporter), member 1; Translocates a broad array of [...] (554 aa)	0.712
	SLC22A2	solute carrier family 22 (organic cation transporter), member 2; Mediates tubular uptake of org [...] (555 aa)	0.712
	SLC22A11	solute carrier family 22 (organic anion/urate transporter), member 11; Mediates saturable uptak [...] (550 aa)	0.712

	SULT1E1	sulfotransferase family 1E, estrogen-preferring, member 1; May control the level of the estroge [...] (294 aa)	0.710

Appendix 5: SMARTS notation primitives

Table 13.1 SMARTS Atomic Primitives, taken from the SMARTS theory manual(204).

Symbol	Symbol name	Atomic property requirements	Default
*	wildcard	any atom	(no default)
a	aromatic	aromatic	(no default)
A	aliphatic	aliphatic	(no default)
D<n>	degree	<n> explicit connections	exactly one
H<n>	total-H-count	<n> attached hydrogens	exactly one[1]
h<n>	implicit-H-count	<n> implicit hydrogens	at least one
R<n>	ring membership	in <n> SSSR rings	any ring atom
r<n>	ring size	in smallest SSSR ring of size <n>	any ring atom
v<n>	valence	total bond order <n>	exactly one[2]
X<n>	connectivity	<n> total connections	exactly one[2]
x<n>	ring connectivity	<n> total ring connections	at least one[2]
- <n>	negative charge	-<n> charge	-1 charge (-- is -2, etc)
+<n>	positive charge	+<n> formal charge	+1 charge (++ is +2, etc)
#n	atomic number	atomic number <n>	(no default)[2]
@	chirality	anticlockwise	anticlockwise, default class[2]
@@	chirality	clockwise	clockwise, default class[2]
@<c><n>	chirality	chiral class <c> chirality <n>	(nodefault)
@<c><n>?	chiral or unspec	chirality <c><n> or unspecified	(no default)
<n>	atomic mass	explicit atomic mass	unspecified mass

Table 13.2 SMARTS Bond Primitives, taken from the SMARTS theory manual(204).

Symbol	Atomic property requirements

-	single bond (aliphatic)
/	directional bond "up"
\	directional bond "down"
/?	directional bond "up or unspecified"
\?	directional bond "down or unspecified"
=	double bond
#	triple bond
:	aromatic bond
~	any bond (wildcard)
@	any ring bond

Table 13.3 SMARTS Logical Operators, taken from the SMARTS theory manual(204).

Symbol	Expression	Meaning
exclamation	!e1	not e1
ampersand	e1&e2	a1 and e2 (high precedence)
comma	e1,e2	e1 or e2
semicolon	e1;e2	a1 and e2 (low precedence)

Appendix 6: Definitions of the pharmacophore features included in the genernation of pharmacophore hypotheses.

Feature group	Feature definition (SMARTS)		Feature type
Hydrogen bond acceptor	[N;X1]#[#6]		vector
	[N;X1]#CC	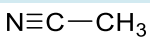	vector
	[N;X2](=C~[C,c])C	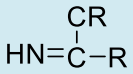	vector
	[N;X2](O)=N[a]	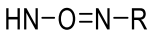	vector
	[N;X2](=N-O)[a]	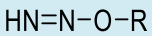	vector
	[n;X2]1ccccc1	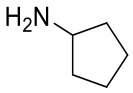	vector
	[n;X2]([a])([a])		vector
	[N;X2](=C~[C,c])(~[*])	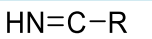	vector
	[N;X3](C)(C)[N;X3]C	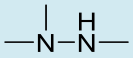	vector
	[N;X2](=C)(~[*])	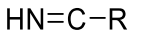	vector
	[N;X2](~[C,c])=[N;X2]	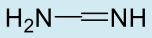	vector
	[n;X2]1c[nH]cc1		vector
	O=[S;X4](=O)([!#8])([!#8])		vector
	[O;X2]C		vector
	[O;X2]N		vector
	[O;X1]=[C,c]		vector
	o		vector
	[O;X2](C)C		vector
	[O;X2]c1ncccc1		vector
	[O;X2]~[a]		vector
	O=PO([!#1])		vector
	[O;X2]		vector
	[S;X2](C)C		vector
	[S;X2](=C)N		vector
	O=C[O-,OH]		point
	[O-,OH]C(=O)		point

Appendix 6: Definitions of the pharmacophore features included in the genernation of pharmacophore hypotheses.

Feature group	Feature definition (SMARTS)	Feature type
	[nH]([a])[a]	point
	[#7;X3][*]=[O,S]	point
	[N;X3](C)(C)[C;X3]	point
	[N;X3][a]	point
	N(=N=N)[#6]	point
	[NH2](C(=O)[NH2])	point
	[NH](C=O)(C=O)	point
	[NH2](S(=O)(=O)[#6])[#6]	point
	[NH](S(=O)(=O)[#6])[#6]	point
	n1c([NH2])ccnc1([NH2])	point
Hydrogen bond donor	[#1][O;X2]	vector
	[#1]S[#6]	vector
	[#1][C;X2]#[C;X2]	vector
	[#1][NX3]C(=[NX2])[#6]	vector
	[#1][#7]	vector
	[#1]OC(=O)	point
	[#1]O[S;X3]=O	point
	[#1]O[S;X4](=O)(=O)	point
	[#1]O[P;X3]=O	point
	[#1]O[P;X4]=O	point
	[#1]n1nnnc1	point
	[#1]N([S;X4](=O)(=O))(C(F)(F)(F))	point
	[#1]([NH2;X3,NH3]([#6;X4]))	point
	[#1]([NH;X3,NH2]([#6;X4])([#6;X4]))	point
	[#1]([NH;X4]([#6;X4])([#6;X4])([#6;X4]))	point
	[#1][NX3]C(=[NX2])[NX3]	point
	[#1][NX3]C(=[NX3+])	point
	[#1][NX3+]=C[NH2]	point
	[#1][NX3]C(=[NX2])	point
	[#1][NX3][#6](=[NX2,NX3+])[#6]	point
Hydrophobic	[a]F	group
	[a]Cl	group
	[a]Br	group
	[a]I	group
	[a]C(F)(F)(F)	group
	[a][CH2]C(F)(F)(F)	group

Appendix 6: Definitions of the pharmacophore features included in the genernation of pharmacophore hypotheses.

Feature group	Feature definition (SMARTS)	Feature type
	[a]O[CH3]	group
	[a]S[CH3]	group
	[a]OC(F)(F)(F)	group
	C(F)(F)(F)	group
	F	group
	Cl	group
	Br	group
	I	group
	default_aromatic_surface	group
	default_aliphatic_surface	group
	C[S;X2]C	group
	[S;X2]CC	group
	[S;X2]C	group
Positive	[NX3][#6](=[NX2,NX3+])[#6]	group
	[NX2,NX3+]=[#6]([NH;X3])([NH;X3])	group
	[NX2,NX3+]=[#6]([NX3])([NX3])	group
	n1c([NH2])ccnc1([NH2])	group
	[NX2,NX3+]=C([NX3])c1ccccc1	group
	[NH2;X3,NH3]([#6;X4])	group
	[NH;X3,NH2]([#6;X4])([#6;X4])	group
	[NX3,NH]([#6;X4])([#6;X4])([#6;X4])	group
	N1CCCCC1	group
	[+]	group
Negative	O=C[O-]	group
	O=C[OH]	group
	[S;X4](=O)(=O)([OH])	group
	[S;X4](=O)(=O)([O-])	group
	[S;X3](=O)([OH])	group
	[S;X3](=O)([O-])	group
	[P;X4](=O)([OH])([OH])	group
	[P;X4](=O)([OH])([O-])	group
	[P;X4](=O)([O-])	group
	[P;X4](=O)([OH])	group
	n1nc[nH]n1	group
	n1ncnn1	group
	[#1]N([S;X4](=O)(=O))(C(F)(F)(F))	group

Appendix 6: Definitions of the pharmacophore features included in the genernation of pharmacophore hypotheses.

Feature group	Feature definition (SMARTS)	Feature type
	[-]	group
Armomatic ring	default_aromatic_vector	group
	default_aromatic_surface	group

Appendix 7: List of DrugBank molecules which match the toxicophore hypothesis

Table 15.1 List of DrugBank molecules that match the toxicophore hypothesis as determined by the Phase Advanced Pharmacophore Screening tool using an Intersite Distance Matching Tolerance of 0.5Å.

Drug name
(1n)-4-n-butoxyphenylsulfonyl-(2r)-n-hydroxycarboxamido-(4s)-methanesulfonylamino-pyrrolidine
(1r)-n,6-dihydroxy-7-methoxy-2-[(4-methoxyphenyl)sulfonyl]-1,2,3,4-tetrahydroisoquinoline-1-carboxamide
(2e)-3-(3,4-dihydroxyphenyl)-n-[2-(4-hydroxyphenyl)ethyl]acrylamide
(2r)-({4-[amino(imino)methyl]phenyl}amino){5-ethoxy-2-fluoro-3-[(3r)-tetrahydrofuran-3-yloxy]phenyl}aceticacid
(2r)-2-amino-3,3,3-trifluoro-n-hydroxy-2-{[(4-phenoxyphenyl)sulfonyl]methyl}propanamide
(2r)-amino(3,5-dihydroxyphenyl)acetic acid
(2r)-amino(4-hydroxyphenyl)acetic acid
(2s)-2-({6-[(3-amino-5-chlorophenyl)amino]-9-isopropyl-9h-purin-2-yl}amino)-3-methylbutan-1-ol
(2s)-2-{[3-(3-aminophenyl)imidazo[1,2-b]pyridazin-6-yl]amino}-3-methylbutan-1-ol
(2s)-amino(4-hydroxyphenyl)acetic acid
(2s)-hydroxy(4-hydroxyphenyl)ethanoic acid
(2s,3s)-3-formyl-2-({[(4-nitrophenyl)sulfonyl]amino}methyl)pentanoic acid
(2s,3s)-trans-dihydroquercetin
(2-sulfanyl-3-phenylpropanoyl)-phe-tyr
(3r,5z,8s,9s,11e)-8,9,16-trihydroxy-14-methoxy-3-methyl-3,4,9,10-tetrahydro-1h-2-benzoxacyclotetradecine-1,7(8h)-dione
(3s,6s)-3,6-bis(4-hydroxybenzyl)piperazine-2,5-dione
(4-hydroxymaltosephenyl)glycine
(4r)-4-(3-butoxy-4-methoxybenzyl)imidazolidin-2-one
(4r,5r)-5-amino-1-[2-(1,3-benzodioxol-5-yl)ethyl]-4-(2,4,5-trifluorophenyl)piperidin-2-one

Drug name
(5-{3-[5-(piperidin-1-ylmethyl)-1h-indol-2-yl]-1h-indazol-6-yl}-2h-1,2,3-triazol-4-yl)methanol
(5-methyl-6-oxo-1,6-dihydro-pyridin-3-yl)-1,2-dideoxy-ribofuranose-5-monophosphate
(r)-1-para-nitro-phenyl-2-azido-ethanol
[(2r,3s,4r,5r)-5-(6-amino-9h-purin-9-yl)-3,4-dihydroxytetrahydro-2-furanyl]methyl sulfamate
[2-cytidylate-o'-phosphonyloxyl]-ethyl-trimethyl-ammonium
[4-(4-hydroxy-benzyl)-2-(2-hydroxy-1-methyl-ethyl)-5-oxo-imidazolidin-1-yl]-acetic acid
[4-(4-phenyl-piperidin-1-yl)-benzenesulfonylamino]-acetic acid
{(2z)-4-amino-2-[(4-methoxyphenyl)imino]-2,3-dihydro-1,3-thiazol-5-yl}(4-methoxyphenyl)methanone
1-((2-hydroxyethoxy)methyl)-5-(3-(benzyloxy)benzyl)pyrimidine-2,4(1h,3h)-dione
1-((2-hydroxyethoxy)methyl)-5-(phenylthio)pyrimidine-2,4(1h,3h)-dione
1-(2-hydroxyethyloxymethyl)-6-phenyl thiothymine
1-(3-o-phosphono-beta-l-arabinofuranosyl)pyrimidine-2,4(1h,3h)-dione
1-(5-chloro-2,4-dimethoxyphenyl)-3-(5-cyanopyrazin-2-yl)urea
1-(5-chloro-2-methoxyphenyl)-3-{6-[2-(dimethylamino)-1-methylethoxy]pyrazin-2-yl}urea
1-(5'-phospho-beta-d-ribofuranosyl)barbituric acid
1-[2-(4-ethoxy-3-fluoropyridin-2-yl)ethyl]-3-(5-methylpyridin-2-yl)thiourea
10-propargyl-5,8-dideazafolic acid
1-benzyl-3-(4-methoxy-benzenesulfonyl)-6-oxo-hexahydro-pyrimidine-4-carboxylic acid hydroxyamide
1-deaza-adenosine
1-o-[p-nitrophenyl]-beta-d-galactopyranose
2-({[4-(trifluoromethoxy)phenyl]sulfonyl}amino)ethyl dihydrogen phosphate
2,4-dinitrophenyl 2-deoxy-2-fluoro-beta-d-allopyranoside
2-[2-(4-chloro-phenylsulfanyl)-acetylamino]-3-(4-guanidino-phenyl)-propionamide
2-[5-methanesulfonylamino-2-(4-aminophenyl)-6-oxo-1,6-dihydro-1-pyrimidinyl]-n-(3,3,3-trifluoro-1-isopropyl-2-oxopropyl)acetamide

Drug name
2-{1-[2-(2-amino-thiazol-4-yl)-2-methoxyimino-acetylamino]-2-oxo-ethyl}-5,5-dimethyl-thiazolidine-4-carboxylic acid
2-{1-[2-amino-2-(4-hydroxy-phenyl)-acetylamino]-2-oxo-ethyl}-5,5-dimethyl-thiazolidine-4-carboxylic acid
2-{4-[4-(4-chloro-phenoxy)-benzenesulfonyl]-tetrahydro-pyran-4-yl}-n-hydroxy-acetamide
2'-5'dideoxyuridine
2-amino-3-(1-hydroperoxy-1h-indol-3-yl)propan-1-ol
2-amino-adenosine
2-chlorodideoxyadenosine
2'-deoxycytidine
2'-deoxycytidine-5'-monophosphate
2'-deoxycytidine-5'-triphosphate
2'-deoxyuridine
2'-deoxyuridine 5'-alpha,beta-imido-diphosphate
2'-deoxyuridine 5'-alpha,beta-imido-triphosphate
2-fluoro-2'-deoxyadenosine
2-fluoro-6-{[2-({2-methoxy-4-[(methylsulfonyl)methyl]phenyl}amino)-7h-pyrrolo[2,3-d]pyrimidin-4-yl]amino}benzamide
2-hydroxy-5-({1-[(2-naphthyloxy)methyl]-3-oxoprop-1-enyl}amino)tyrosine
2-hydroxy-5-({1-[(4-methylphenoxy)methyl]-3-oxoprop-1-enyl}amino)-l-tyrosine
2-hydroxy-5-(2-mercapto-ethylsulfamoyl)-benzoic acid
2-hydroxy-5-{[(1e)-2-phenylethylidene]amino}-l-tyrosine
2-mercapto-n-[1,2,3,10-tetramethoxy-9-oxo-5,6,7,9-tetrahydro-benzo[a]heptalen-7-yl]acetamide
2-methyl-2-(4-{[({4-methyl-2-[4-(trifluoromethyl)phenyl]-1,3-thiazol-5-yl}carbonyl)amino]methyl}phenoxy)propanoic acid
2-methylthio-n6-isopentenyl-adenosine-5'-monophosphate
2-ribofuranosyl-3-iodo-2,3-dihydro-1h-pyrazolo[3,4-d]pyrimidin-4-ylamine
3-(4-hydroxyphenyl)-1-(2,4,6-trihydroxyphenyl)propan-1-one

Drug name
3-{[4-([amino(imino)methyl]aminosulfonyl)anilino]methylene}-2-oxo-2,3-dihydro-1h-indole
3-amino-6-hydroxy-tyrosine
3-chloro-4-hydroxyphenylglycine
3-deaza-adenosine
3-deazacytidine
3'-deoxy 3'-amino adenosine-5'-diphosphate
3-deoxyguanosine
3-fluorotyrosine
3-iodo-tyrosine
3'-oxo-adenosine
3'-uridinemonophosphate
4-[(7-oxo-7h-thiazolo[5,4-e]indol-8-ylmethyl)-amino]-n-pyridin-2-yl-benzenesulfonamide
4-{[(1r,2s)-1,2-dihydroxy-2-methyl-3-(4-nitrophenoxy)propyl]amino}-2-(trifluoromethyl)benzonitrile
4-amino-n-[(2-sulfanylethyl)carbamoyl]benzenesulfonamide
4-hydroxyphenylglycine
4-methylumbelliferyl-alpha-d-glucose
4-nitrophenyl-ara
5-(6-amino-9h-purin-9-yl)-4-hydroxytetrahydrofuran-3-yl dihydrogen phosphate
5'-[[2-(aminooxy)ethyl]methylsulfonio]-5'-deoxy-adenosine
5-[4-(1-carboxymethyl-2-oxo-propylcarbamoyl)-benzylsulfamoyl]-2-hydroxy-benzoic acid
5'-{[4-(aminooxy)butyl](methyl)amino}-5'-deoxy-8-ethenyladenosine
5-{3-[3-(2,4-dichloro-benzoyl)-ureido]-2-methyl-phenoxy}-pentanoic acid
5-bromo-2'-deoxyuridine-5'-monophosphate
5-bromo-cytidinemonophosphate
5-bromo-n[2-(dimethylamino)ethyl]-9-aminoacridine-4-carboxamide
5-bromovinyldeoxyuridine
5-chloro-n-((1r,2s)-2-(4-(2-oxopyridin-1(2h)-yl)benzamido) cyclopentyl)thiophene-2-carboxamide

Drug name
5-chloro-n-{4-[(1r)-1,2-dihydroxyethyl]phenyl}-1h-indole-2-carboxamide
5'-deoxy-5'-(methylthio)-tubercidin
5-fluoro-2'-deoxyuridine-5'-monophosphate
5-fluorouridine
5-formyl-6-hydrofolic acid
5-hydroxynaphthalene-1-sulfonamide
5-iodo-2'-deoxyuridine-5'-monophosphate
5-iodotubercidin
5-methyl-2'-deoxypseudouridine
5-methylcytidine-5'-monophosphate
5-methyluridine 5'-monophosphate
5--monophosphate-9-beta-d-ribofuranosyl xanthine
'5'-o-(n-(l-alanyl)-sulfamoyl)adenosine
5'-o-(n-(l-cysteinyl)-sulfamoyl)adenosine
5'-o-(n-(l-threonyl)-sulfamoyl)adenosine
5'-o-(n-ethyl-sulfamoyl)adenosine
5'-s-ethyl-5'-thioadenosine
6-(2,6-dibromophenyl)pyrido[2,3-d]pyrimidine-2,7-diamine
6-(2,6-dichlorophenyl)-2-{[3-(hydroxymethyl)phenyl]amino}-8-methylpyrido[2,3-d]pyrimidin-7(8h)-one
6-(2,6-dimethoxyphenyl)pyrido[2,3-d]pyrimidine-2,7-diamine
6,7-dioxo-5h-8-ribitylaminolumazine
6-aza-ump
6-carbamimidoyl-4-(3-hydroxy-2-methyl-benzoylamino)-naphthalene-2-carboxylic acid methyl ester
6-chloro-n-pyrimidin-5-yl-3-{[3-(trifluoromethyl)phenyl]amino}-1,2-benzisoxazole-7-carboxamide
6-hydroxy-7,8-dihydro purine nucleoside
6-o-phosphoryl inosine monophosphate
7-(2,5-dihydropyrrol-1-yl)-6-phenyl-pyrido[6,5-d]pyrimidin-2-amine

Drug name
7-(5-deoxy-beta-d-ribofuranosyl)-5-iodo-7h-pyrrolo[2,3-d]pyrimidin-4-amine
7-alpha-d-ribofuranosyl-2-aminopurine-5'-phosphate
7-alpha-d-ribofuranosyl-purine-5'-phosphate
7-amino-2-tert-butyl-4-{[2-(1h-imidazol-4-yl)ethyl]amino}pyrido[2,3-d]pyrimidine-6-carboxamide
7-carboxy-5-hydroxy-12,13-dihydro-6h-indolo[2,3-a]pyrrolo[3,4-c]carbazole
7-methylguanosine
7n-methyl-8-hydroguanosine-5'-monophosphate
8-bromo-adenosine-5'-monophosphate
8-oxo-2'-deoxy-guanosine-5'-monophosphate
9-beta-d-xylofuranosyl-adenine
Acebutolol
Acyclovir
Acylated ceftazidime
Adamantane-1-carboxylic acid-5-dimethylamino-naphthalene-1-sulfonylamino-butyl-amide
Adenosine
Adenosine monophosphate
Adenosine phosphonoacetic acid
Adenosine-3'-5'-diphosphate
Adenosine-5'-(dithio)phosphate
Adenosine-5'-phosphosulfate
Adenosine-5'-propylphosphate
Adenosyl-ornithine
Adenylosuccinic acid
Al5927
Alizapride
Alpha-adenosine monophosphate
Alpha-methylene adenosine monophosphate
Alpha-n-dichloroacetyl-p-aminophenylserinol

Drug name
Amiloride
Aminacrine
Aminophosphonic acid-guanylate ester
Amoxicillin
Anisomycin
Arbutamine
Arformoterol
Aspartyl-adenosine-5'-monophosphate
Balanol analog 1
Balanol analog 2
Balsalazide
Bambuterol
Bentiromide
Benzoyl-tyrosine-alanine-methyl ketone
Biopterin
Bitolterol
Bromamphenicol
Bvdu-mp
Capecitabine
Carbidopa
Carteolol
Cefadroxil
Cefdinir
Cefotaxime group
Cefprozil
Ceftibuten
Chloramphenicol
Chloramphenicol succinate
Chloroprocaine
Cidofovir

Drug name
Clenbuterol
Cordycepin triphosphate
Cp-coeleneterazine
Cyclic adenosine monophosphate
Cyclouridine
Cytarabine
Cytidine 5'-diphosphoglycerol
Cytidine-2'-monophosphate
Cytidine-3'-monophosphate
Cytidine-5'-diphosphate
Cytidine-5'-monophosphate
Cytidine-5'-triphosphate
Cytosine arabinose-5'-phosphate
Dansylamide
Deoxythymidine
Deoxyuridine-5'-diphosphate
Deoxyuridine-5'-triphosphate
Dibucaine
Didanosine
Dipivefrin
Droxidopa
D-tyrosine
Dyphylline
Emtricitabine
Epinephrine
Esomeprazole
Fenoterol
Flavoxate
Floxuridine
Fludarabine

Drug name
Folic acid
Formoterol
Ganciclovir
Guanosine-3'-monophosphate
Guanosine-5'-diphosphate
Histidyl-adenosine monophosphate
Honh-benzylmalonyl-l-alanylglycine-p-nitroanilide
Idoxuridine
Indacaterol
Inosinic acid
Iodo-willardiine
Isoetharine
Isoproterenol
Labetalol
Lamivudine
Levodopa
Levonordefrin
L-tyrosinamide
L-tyrosine
Ly374571
Melphalan
Metaraminol
Methoxamine
Methyl 3-chloro-2-{3-[(2,5-dihydroxy-4-methoxyphenyl)amino]-3-oxopropyl}-4,6-dihydroxybenzoate
Methyldopa
Metoclopramide
Metyrosine
Midodrine
Mirabegron

Drug name
Moxalactam derivative
N-(1,4-dihydro-5h-tetrazol-5-ylidene)-9-oxo-9h-xanthene-2-sulfonamide
N-(1-adamantyl)-n'-(4-guanidinobenzyl)urea
N-(2-chloro-4-fluorobenzoyl)-n'-(5-hydroxy-2-methoxyphenyl)urea
N-(3,5-dimethoxyphenyl)imidodicarbonimidic diamide
N(4)-adenosyl-n(4)-methyl-2,4-diaminobutanoic acid
N-(4-aminobutanoyl)-s-(4-methoxybenzyl)-l-cysteinylglycine
N-(4-methoxybenzyl)-n'-(5-nitro-1,3-thiazol-2-yl)urea
N-(7-carbamimidoyl-naphthalen-1-yl)-3-hydroxy-2-methyl-benzamide
N-(cyclopropylmethyl)-4-(methyloxy)-3-({5-[3-(3-pyridinyl)phenyl]-1,3-oxazol-2-yl}amino)benzenesulfonamide
N-[(2r,3s)-3-amino-2-hydroxy-4-phenylbutyl]-4-methoxy-2,3,6-trimethylbenzenesulfonamide
N-[(4-methoxyphenyl)sulfonyl]-d-alanine
N-[[3-fluoro-4-ethoxy-pyrid-2-yl]ethyl]-n'-[5-chloro-pyridyl]-thiourea
N-[[3-fluoro-4-ethoxy-pyrid-2-yl]ethyl]-n'-[5-nitrilomethyl-pyridyl]-thiourea
N-[1-(aminomethyl)cyclopropyl]-3-(benzylsulfonyl)-n~2~-[(1s)-2,2,2-trifluoro-1-(4-hydroxyphenyl)ethyl]-l-alaninamide
N-[2-(5-methyl-4h-1,2,4-triazol-3-yl)phenyl]-7h-pyrrolo[2,3-d]pyrimidin-4-amine
N-[2-(carbamimidamidooxy)ethyl]-2-{6-cyano-3-[(2,2-difluoro-2-pyridin-2-ylethyl)amino]-2-fluorophenyl}acetamide
N-[3-(n'-hydroxycarboxamido)-2-(2-methylpropyl)-propanoyl]-o-tyrosine-n-methylamide
N-[4-({[5-(dimethylamino)-1-naphthyl]sulfonyl}amino)butyl]-3-sulfanylpropanamide
N-[5-(1,1-dioxidoisothiazolidin-2-yl)-1h-indazol-3-yl]-2-(4-piperidin-1-ylphenyl)acetamide
N-[amino(imino)methyl]-2-[2-(2-chlorophenyl)-4-(4-propoxyphenyl)-3-thienyl]acetamide
N-{[4-(but-2-yn-1-yloxy)phenyl]sulfonyl}-5-methyl-d-tryptophan
N-{3-[5-(6-amino-purin-9-yl)-3,4-dihydroxy-tetrahydro-furan-2-yl]-allyl}-2,3-dihydroxy-5-nitro-benzamide
N~2~-[(benzyloxy)carbonyl]-n-[(1s,2s)-2-hydroxy-1-(4-hydroxybenzyl)propyl]-l-leucinamide

Drug name
N~4~-methyl-n~4~-(3-methyl-1h-indazol-6-yl)-n~2~-(3,4,5-trimethoxyphenyl)pyrimidine-2,4-diamine
N6-isopentenyl-adenosine-5'-monophosphate
N7-methyl-guanosine-5'-monophosphate
N-acetyl-p-nitrophenylserinol
Naratriptan
Nelarabine
Neopterin
N-hydroxy 1n(4-methoxyphenyl)sulfonyl-4-(z,e-n-methoxyimino)pyrrolidine-2r-carboxamide
N-hydroxy-1-(4-methoxyphenyl)sulfonyl-4-benzyloxycarbonyl-piperazine-2-carboxamide
N-hydroxy-2(r)-[[(4-methoxyphenyl)sulfonyl](3-picolyl)amino]-3-methylbutanamide hydrochloride
N-hydroxy-4-({4-[4-(trifluoromethyl)phenoxy]phenyl}sulfonyl)tetrahydro-2h-pyran-4-carboxamide
N-hydroxy-4-(methyl{[5-(2-pyridinyl)-2-thienyl]sulfonyl}amino)benzamide
N-isobutyl-n-[4-methoxyphenylsulfonyl]glycyl hydroxamic acid
Nitrofurantoin
N'-l-seryl-3'-amino-(3'-deoxy)-adenosine
Norepinephrine
Orciprenaline
Orotidine-5'-monophosphate
P-aminophenyl-alpha-d-galactopyranoside
Pantoyl adenylate
Para-nitrobenzyl glutaryl glycinic acid
Pd173955
Phenylephrine
Phenyl-uridine-5'-diphosphate
Phosphomethylphosphonic acid adenosyl ester
Phosphomethylphosphonic acid guanosyl ester

Drug name
Phosphonotyrosine
Phosphoric acid mono-[3,4-dihydroxy-5-(5-hydroxy-benzoimidazol-1-yl)tetrahydro-furan-2-ylmethyl] ester
Phosphoric acid mono-[3-amino-5-(5-methyl-2,4-dioxo-3,4-dihydro-2h-pyrimidin-1-yl)-tetrahydro-furan-2-ylmethyl] ester
Phosporic acid mono-[3,4-dihydroxy-5-(5-methoxy-benzoimidazol-1-yl)-tetrahydro-furan-2-ylmethyl] ester
Pindolol
Pioglitazone
Pirbuterol
Procaine
Procaterol
Pseudouridine-5'-monophosphate
Puromycin
Puromycin aminonucleoside-5'-monophosphate
Rabeprazole
Regadenoson
Riboflavin
Riboflavin monophosphate
Ritodrine
Rosiglitazone
S-(p-nitrobenzyl)glutathione
S-adenosyl-1,8-diamino-3-thiooctane
S-adenosyl-l-homocysteine
S-adenosylmethionine
Sotalol
Sulfacytine
Sulfamerazine
Sulfamethazine
Sulfametopyrazine

Drug name
Sulfapyridine
Telbivudine
Terbutaline
Thymidine-5'- diphosphate
Thymidine-5'-(dithio)phosphate
Thymidine-5'-triphosphate
Triamterene
Trifluridine
Tubercidin
Tyrosinal
Uridine 5'-triphosphate
Uridine-5'-diphosphate
Uridine-5'-monophosphate
Valaciclovir
Valganciclovir
Vidarabine
Way-151693
Zalcitabine

Table 15.2 List of DrugBank molecules that match the toxicophore hypothesis as determined by the Pharmer program using a feature radii of 0.5Å.

Drug name
1-(2-hydroxyethyloxymethyl)-6-phenyl thiothymine
1-((2-hydroxyethoxy)methyl)-5-(phenylthio)pyrimidine-2,4(1h,3h)-dione
1-((2-hydroxyethoxy)methyl)-5-benzylpyrimidine-2,4(1h,3h)-dione
1-benzyl-3-(4-methoxy-benzenesulfonyl)-6-oxo-hexahydro-pyrimidine-4-carboxylic acid hydroxyamide
2'-5'dideoxyuridine
2'-deoxyguanosine-5'-diphosphate
2'-deoxyuridine
2-hydroxy-5-({1-[(2-naphthyloxy)methyl]-3-oxoprop-1-enyl}amino)tyrosine
2-hydroxy-5-({1-[(4-methylphenoxy)methyl]-3-oxoprop-1-enyl}amino)-l-tyrosine
3-(2-chlorophenyl)-1-(2-{[(1s)-2-hydroxy-1,2-dimethylpropyl]amino}pyrimidin-4-yl)-1-(4-methoxyphenyl)urea
3-amino-6-hydroxy-tyrosine
5--monophosphate-9-beta-d-ribofuranosyl xanthine
5-bromovinyldeoxyuridine
5-methyl-2'-deoxypseudouridine
5-methyluridine 5'-monophosphate
6-aza-ump
6-hydroxy-1,6-dihydro purine nucleoside
6-hydroxy-7,8-dihydro purine nucleoside
6-o-phosphoryl inosine monophosphate
7-methylguanosine
7n-methyl-8-hydroguanosine-5'-diphosphate
7n-methyl-8-hydroguanosine-5'-monophosphate
8-benzyl-2-hydroperoxy-2-(4-hydroxy-benzyl)-6-(4-hydroxy-phenyl)-2h-imidazo[1,2-a]pyrazin-3-one
9-deazainosine-2',3'-o-ethylidenephosphonate
(1r)-n,6-dihydroxy-7-methoxy-2-[(4-methoxyphenyl)sulfonyl]-1,2,3,4-tetrahydroisoquinoline-1-carboxamide

Drug name
(1n)-4-n-butoxyphenylsulfonyl-(2r)-n-hydroxycarboxamido-(4s)-methanesulfonylamino-pyrrolidine
(2e)-3-(3,4-dihydroxyphenyl)-2-iminopropanoic acid
(2r)-n-hydroxy-2-[(3s)-3-methyl-3-{4-[(2-methylquinolin-4-yl)methoxy]phenyl}-2-oxopyrrolidin-1-yl]propanamide
(2s)-2-amino-5-oxo-5-[(4-phenylmethoxyphenyl)amino]pentanoic acid
Aminophosphonic acid-guanylate ester
Amoxicillin
Benzoyl-tyrosine-alanine-methyl ketone
Balanol analog 1
Carbidopa
Cefprozil
Deoxythymidine
Dyclonine
Guanosine-2',3'-o-methylidenephosphonate
Guanosine
Guanosine-2'-monophosphate
Guanosine-3'-monophosphate
Guanosine-5'-diphosphate
Guanosine-5'-monophosphate
Indacaterol
Inosinic acid
Moxalactam (hydrolyzed)
N7-methyl-guanosine-5'-monophosphate
N-(sulfanylacetyl)tyrosylprolylmethioninamide
N-hydroxy 1n(4-methoxyphenyl)sulfonyl-4-(z,e-n-methoxyimino)pyrrolidine-2r-carboxamide
N-hydroxy-1-(4-methoxyphenyl)sulfonyl-4-benzyloxycarbonyl-piperazine-2-carboxamide
N-[1-(aminomethyl)cyclopropyl]-3-(benzylsulfonyl)-n~2~-[(1s)-2,2,2-trifluoro-1-(4-hydroxyphenyl)ethyl]-l-alaninamide

Drug name
N-[3-(n'-hydroxycarboxamido)-2-(2-methylpropyl)-propanoyl]-o-tyrosine-n-methylamide
Neopterin
Puromycin
Phenyl-uridine-5'-diphosphate
Phosphomethylphosphonic acid guanosyl ester
Riboflavin
Riboflavin monophosphate
Sulfasalazine
Uridine
Valganciclovir

Appendix 8: A549 Cell Culture

16.1 Preparation of Feeding Media

A549 FEEDING MEDIA: The human alveolar epithelial cell line (A549) was purchased from American Type Culture Collection (ATCC, Manassas, VA) and was cultured in Ham's F-12 medium (Invitrogen, Carlsbad, CA) supplemented with penicillin (100 U/ml), streptomycin (100 µg/ml), and fetal bovine serum to a final concentration of 10%. Prepare ~ 500 mL of A549 FEEDING MEDIA by adding 11 mL pencillin-streptomycin 50X liquid (Invitrogen, Carlsbad, CA: C/N 15070-063) and 55.5 mL of heat-inactivated (56□C for 30 minutes) fetal bovine serum (Interpath, VIC, Australia) to 500 mL of F-12K Medium ((Invitrogen: C/N 21127-022).

16.2 Thawing Cells

1. Retrieve vials from liquid nitrogen storage and hold in the 37oC water bath to thaw as quickly as possible.
2. Thoroughly clean the outside of the vial with 80% ethanol.
3. Add the ~ 1 mL of thawed cell suspension to 9 mL of A549 FEEDING MEDIA. Centrifuge at 1100 r.p.m. for 2 minutes.
4. Remove supernatant by suction and add 10 mL of A549 FEEDING MEDIA and add to a 10 cm dish
5. Incubate cells at 37oC, 5% CO2 overnight.
6. On the following day, aspirate the media and add fresh 10 mL A549 FEEDING MEDIA (to remove DMSO and cellular debris).
7. When cells are ready to split, ensure that you split at least 2 plates of the thawed culture, to refreeze therefore ensuring maintenance of stock cultures at low passage number.

16.3 Freezing down cells

To prepare stock cultures, plate cells so that they will be ~ 80% confluent on the day they will be frozen down.

1. For each 10 cm plate to be frozen down, prepare a cryovial as follows

Label each vial with cell line, initials, date and passage number

Add 100 µL of FBS

Add 100 µL of sterile DMSO

2. Trypsinize and centrifuge cells as in Appendix 4.
3. Resuspend cell pellet in 800 µL of A549 FEEDING MEDIA.
4. Transfer suspended cells to the pre-prepared cryo-vial and gently mix.
5. Place cryovials in a foam rack and cover with a second foam rack.
6. Transfer foam rack to the –80oC freezer for at least 24 hours.
7. Transfer samples from the –80oC freezer to the liquid nitrogen long term storage.

16.4 Splitting cells

N.B. Cells should be split 1/3 two times per week (e.g. Monday and Thursday or Tuesday and Friday).

1. To split cells, suction off media and wash 10 cm plates with 2 x 5 mL of sterile PBS (Sigma: C/N D-8537).
2. Suction off sterile PBS and replace with 2.5 mL of Trypsin-EDTA (Sigma: C/N T-3924) and incubate at 37oC for ~ 2 minutes. Check cell detachment microscopically and agitate to facilitate detachment, if necessary.
3. Add 2.5 mL of A549 FEEDING MEDIA and aspirate cells by gently pipetting (transfer solution to a 15 mL sterile centrifuge tube).
4. Centrifuge at 1100 r.p.m. for 2 minutes.
5. Remove supernatant by suction and resuspend cells in 3 mL of A549 FEEDING MEDIA.
6. Transfer 1 mL of cells to 9 mL A549 FEEDING MEDIA in new 10 cm dishes.

16.5 Plating Cells

1. To trypsinize 10 cm dishes, suction off media and wash with 2 x 5 mL of sterile PBS.
2. Suction off sterile PBS and replace with 2.5 mL of Trypsin-EDTA and incubate at 37oC for ~ 2 minutes. Check cell attachment microscopically and agitate to facilitate detachment, if necessary.

3. Add 2.5 mL of A549 FEEDING MEDIA and transfer solution to a 15 mL sterile centrifuge tube.
4. Centrifuge at 1100 r.p.m. for 2 minutes.
5. Remove supernatant by suction and resuspend cells in 5 mL of relevant FEEDING MEDIA.
6. Dilute 20 µL of this cell solution with 20 □L of trypan blue solution and count 5 squares on both sides of a haemocytometer. Average result, then multiply by 2 (dilution factor), then multiply by 104. This is the number of cells/mL. Use 10X magnification.
7. Plate cells according to experimental need, i.e. for Western blotting and RT-PCR in 6-wells (prepare 250,000 cells/mL in A549 FEEDING MEDIA so that when 2 mL is added to 6 well dishes 500,000 cells/well is achieved).

TYPE	PLATING DENSITY	MEDIA PER WELL
96-well	6,400 cells/well	0.1 mL
6-well	500,000 cells/well	2 mL